Max-Planck-Institut für Meteorologie

MAX-PLANCK-GESELLSCHAFT

NARVAL Campaign Report

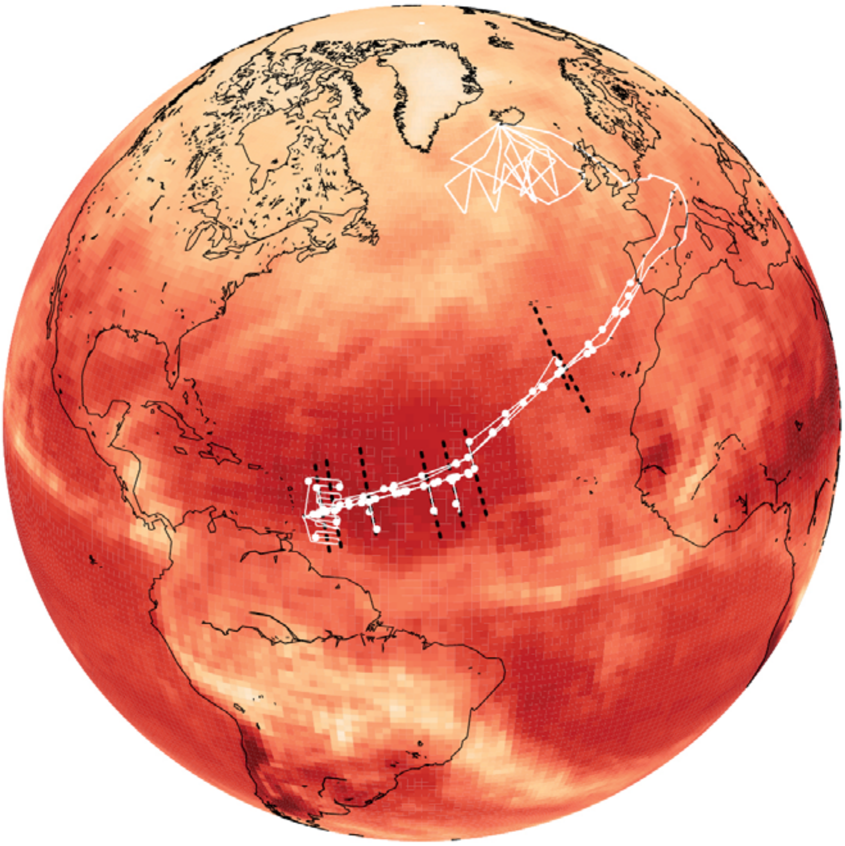

Christian Klepp, Felix Ament, Stephan Bakan, Lutz Hirsch, Bjorn Stevens

Hamburg 2014

Berichte zur Erdsystemforschung

Reports on Earth System Science

164

2014

Hinweis

Die Berichte zur Erdsystemforschung werden vom Max-Planck-Institut für Meteorologie in Hamburg in unregelmäßiger Abfolge herausgegeben.

Sie enthalten wissenschaftliche und technische Beiträge, inklusive Dissertationen.

Die Beiträge geben nicht notwendigerweise die Auffassung des Instituts wieder.

Die "Berichte zur Erdsystemforschung" führen die vorherigen Reihen "Reports" und "Examensarbeiten" weiter.

Notice

The Reports on Earth System Science are published by the Max Planck Institute for Meteorology in Hamburg. They appear in irregular intervals.

They contain scientific and technical contributions, including Ph. D. theses.

The Reports do not necessarily reflect the opinion of the Institute.

The "Reports on Earth System Science" continue the former "Reports" and "Examensarbeiten" of the Max Planck Institute.

Anschrift / Address

Max-Planck-Institut für Meteorologie
Bundesstrasse 53
20146 Hamburg
Deutschland

Tel./Phone: +49 (0)40 4 11 73 - 0
Fax: +49 (0)40 4 11 73 - 298

name.surname@mpimet.mpg.de
www.mpimet.mpg.de

Layout

Bettina Diallo and Norbert P. Noreiks
Communication

Copyright

The Next-generation Aircraft Remote sensing for VALidation Studies (NARVAL)
Campaign Flight Reports using the Research Aircraft HALO

NARVAL South 10-22 December 2013 (BGI, Barbados)
NARVAL North   7-22 January 2014 (KEF, Iceland)

Christian Klepp, Felix Ament, Stephan Bakan, Lutz Hirsch, Bjorn Stevens

Hamburg 2014

Lead Authors:
Christian Klepp, CliSAP/CEN, University of Hamburg, Germany
Felix Ament, University of Hamburg, Max Planck Institute for Meteorology, Germany
Stephan Bakan, Max Planck Institute for Meteorology, Hamburg, Germany
Lutz Hirsch, Max Planck Institute for Meteorology, Hamburg, Germany
Bjorn Stevens, Max Planck Institute for Meteorology, Hamburg, Germany

Contributing Authors:
Andreas Fix, Silke Groß, Martin Hagen, Andreas Schäfler, Martin Wirth
DLR, Oberpfaffenhofen, Germany

Friedhelm Jansen
Max Planck Institute for Meteorology, Hamburg, Germany

Akio Hansen, Heike Konow
University of Hamburg, Germany

Susanne Crewell, Mario Mech, Emiliano Orlandi
University of Cologne, Cologne, Germany

Tilman Hüneke, Marcel Reichert, Klaus Pfeilsticker
University of Heidelberg, Heidelberg, Germany

Manfred Wendisch, André Ehrlich, Frank Werner
University of Leipzig, Leipzig, Germany

Birger Bohn, Insa Lohse
Forschungszentrum Jülich, Jülich, Germany

Berichte zur Erdsystemforschung / Max-Planck-Institut für Meteorologie — 164
Reports on Earth System Science / Max Planck Institute for Meteorology — 2014

ISSN 1614-1199

Content

NARVAL campaign overview

1. Introduction

NARVAL (**N**ext-generation **A**ircraft **R**emote sensing for **Val**idation Studies) was conceived as a mission devoted to better understanding the prevalence and structure of clouds and precipitation from shallow convection in two large-scale regimes. The first being in the trade-wind regions of the North Atlantic (NARVAL South), the other in the cold sector of developing winter storms, over the mid-latitude stormtrack of the North Atlantic (NARVAL North). The main goal was to explore the use of the new German research airplane HALO (High Altitude and Long range research aircraft) as a remote sensing platform for retrieving the state of the atmosphere with particular attention on moist processes and composition. HALO serves the German Science Community and is based on a Gulfstream Aerospace G550 business jet. HALO is funded by a consortium of German research institutions with the support of the Federal Ministry of Education and Research. The aircraft is operated by the national aeronautics and space research center (DLR) at Oberpfaffenhofen (http://www.halo.dlr.de/).

In addition to exploring the particular science question on clouds and precipitation in shallow convective regimes, NARVAL sought to:

1. demonstrate the capability of a unique package of remote sensing instrumentation to provide insight into the atmosphere’s most important constituent, water, in all its phases;
2. testing the ability of using the aircraft in windows of opportunity out of the homebase Oberpfaffenhofen and investigating the advantages using remote airports on Barbados and Iceland;
3. exploit the long-range and high-altitude of the aircraft to make measurements of remote targets high above major systems in a way that is more difficult for other aircraft;
4. evaluation of satellite-based remote sensing data and products from the A-train CloudSat radar and the DMSP SSMIS (Defense Meteorological Satellite Program Special Sensor Microwave Imager Sounder) radiometers during collocated underflights with HALO. SSMIS is the backbone satellite of the Hamburg Ocean Atmosphere Parameters and fluxes from Satellite data (HOAPS) climatology (http://www.hoaps.org/).

NARVAL divided, by the turn of the year 2013/2014, in two parts: NARVAL South and NARVAL North. NARVAL South missions were flown first, in the period between 10 and 22 December 2013. NARVAL North took place in a second phase with a deployment of HALO out of Keflavik, Iceland (KEF), between 7 and 22 January 2014.

In total, 15 research flights were conducted over the North Atlantic. During NARVAL South, eight tropical tradewind flights were operated between Oberpfaffenhofen, Germany, (OBF) and Grantley Adams airport on Barbados (BGI) including local flights operated out of BGI. NARVAL North operated five research flights out of KEF airport over convective North Atlantic weather situations plus transfer flights from and to OBF. During these missions the airplane was equipped with a full array of state of the art remote sensing instrumentation (radiometers, radar, lidar, optical spectrometers), which was complemented by in-situ dropsonde sensors and additional instrumentation for evaluation purposes.

This publication documents the campaign activities through the collection of all 15 individual flight reports. These contain the description of the flight planning, large-scale weather conditions, approved flight tracks and in-flight events, photographic documentation of encountered cloud views, satellite imagery of the overall cloud situation, as well as a number of radiometer, radar, lidar, spectrometer and dropsonde quicklooks and preliminary results. Additionally, collocated CloudSat and SSMIS satellite underflights were performed.

A more detailed description of the originally planned campaign is provided in the NARVAL White Paper of 29.01.2010 (cf. Appendix).

2. NARVAL campaign synopsis

The measurement phase of NARVAL, the first cloud remote sensing mission of the new German research aircraft HALO, was a great success: the conditions were seemingly ideal, all of the NARVAL campaign instrumentation functioned without significant interruption, and the aircraft proved itself to be a tremendous platform for airborne research. The flexibility of DLR in dealing with last minute logistical issues was a key element of the successful deployment, as much as were the careful preparations of all those involved in the certification of NARVAL and preparation of the scientific payload. Preliminary analysis of the data demonstrates that

- the convection over the broader trades appears consistent with the long-term measurements at Barbados;
- convection in the trades rarely reaches a depth of 2 km without precipitation playing an important role in its life cycle and statistics;
- the trade-wind marine layer sharply delineates itself from a very dry free atmosphere over huge expanses of the tropical oceans;
- the postfrontal convection over the cold-season North Atlantic contains all types of shallow to mid-high convection with varying precipitation intensities including rain, snow and mixed-phase;
- postfrontal North Atlantic anvil-capped Cumulonimbus clouds are frequent with cloud tops between 4 and 6 km altitude;
- postfrontal cold-core spiral bands seem to suppress convection and hence contain fewer precipitation compared to the surrounding cellular convection;
- the HOAPS climatology is correctly indicating intense postfrontal convective precipitation.

2.1 HALO instrumentation and partners

HALO has special features which merit the definition of a standard remote sensing configuration of an aircraft. These include its long range, and its ability to fly at high altitude with a substantial payload. NARVAL carried a customized payload centered around remote sensing instrumentation mounted in the especially designed bellypod of the HALO aircraft. This instrumentation included a K-band radar and a suite of radiometers in three banks operating over more than a dozen wavelengths, called the HAlo Microwave Package (HAMP; Mech et al., 2014), and a DLR water-vapor dial lidar (WALES). In addition, key instrumentation included a 6 channel UV/vis/nearIR optical spectrometer for Limb and Nadir observations of trace gases and of all three phases of water provided by the University of

Heidelberg (mini-DOAS, Weidner er al., 2005; Kritten et al,. 2014), spectrally resolved short-wave radiation measurements by HALO-SR (FZ-Jülich and University of Leipzig), dropsondes, and the base BAHAMAS instrumentation, maintained as part of the standard HALO instrument package.

The radar MIRA-36, owned by University of Hamburg and manufactured by METEK, is a mono-static, pulsed, magnetron, Ka-band Doppler radar that operates at 35.5 GHz. The advantage of the Ka-band, as compared to the more common 94 GHz, or W-band, is in the reduced attenuation in the presence of condensate. Using this frequency is possible, because the HALO aircraft and its bellypod is sufficiently large to accommodate the relatively large antenna required at this frequency. The radar has two receivers to provide a co- and cross-polarization channel. The output parameters are the radar reflectivity Z, the Doppler spectra, the Doppler velocity or line of sight velocity of targets V, the spectral width, and the linear depolarization ratio LDR. An advantage of the mono-static, pulsed magnetron, is that it captures strong gradients in the reflectivity precisely. This is especially important to avoid problems with ground reflection in nadir looking instruments. The radar transmitter and receiver are initially calibrated using external sources. Internal reference sources are continually used to achieve a permanent calibration of the system.

The HAMP microwave radiometers are owned by the Max-Planck-Institute for Meteorology and were custom manufactured for HALO by Radiometer Physics GmbH (RPG). They are separated into three nadir pointing modules mounted in the bellypod underneath HALO.

The first module contains two independent packages with parallel antenna axis for the K- and V-bands (HALO-KV). Both units are direct detection filter bank receivers. The second module consists of two independent receiver packages (HALO-11990), one direct detection radiometer at a window channel at 90 GHz and one heterodyne receiver in double sideband mode with four channels along the 118.75 GHz O_2 line from ±1.4 to ±8.5 GHz. The third module (HALO-183) contains a single heterodyne receiver providing seven channels along the 183.31 GHz H_2O line (±0.6 to ±12.5 GHz, double side-band). The radiometers receive the upwelling microwave radiation through apertures in the bellypod, which are covered by window material with low microwave attenuation.

All frequency channels are continuously calibrated in-flight with two reference targets. Frequent injection of a calibrated noise source signal via a directional coupler is used for gain calibration while the receiver noise temperature (T_r) is adjusted by terminating the receiver input with a reference load either via a Dicke switch or, in case of the HALO-183 module, by quasi-optically switching the antenna beam to an internal ambient temperature target. In order to eliminate any losses, e.g., from windows or Dicke switches, a reference calibration with liquid nitrogen is performed before each take off and after landing using external calibration targets.

The lidar used during the NARVAL mission is the first and up to now only airborne four-wavelength water vapor DIAL. It was developed as an airborne demonstrator within the framework of the ESA Earth Explorer mission proposal "Water Vapor Lidar Experiment in Space" (WALES) to investigate the feasibility of operating an active profiling DIAL system in space. The WALES differential absorption lidar system consists of two transmitters, both based on an injection-seeded optical parametric oscillator (OPO) pumped by the second harmonic of a Q-switched, diode pumped Nd:YAG laser. Thus, WALES is capable of simultaneously emitting four wavelengths, three online and one offline, in the water vapor absorption band between 935 nm and 936 nm. The three online wavelengths achieve the necessary sensitivity needed for measurements over the whole range of tropospheric water vapor concentration. A complete water vapor profile of the troposphere is composed by using the information of the partly overlapping line contributions. The averaged pulse energy is 35 mJ with a repetition frequency rate of 2x100 Hz. The vertical resolution of the raw data is 15 m. In addition to the 935 nm channel, the receiver is equipped with polarization sensitive aerosol channels at 532 nm and 1064 nm, the first one with High Spectral Resolution capabilities using an iodine filter in the detection path (Esselborn et al., 2008). This allows for collocated measurements of humidity and optical depth, as well as studies of clouds and aerosol optical properties. For a detailed technical description see Wirth et al. (2009).

The HALO mini–DOAS instrument is a six–channel optical spectrometer for the 2-D detection of UV/visible/nearIR absorbing trace gases in Nadir and Limb scanning observation geometry. The 2-D detection of the targeted gases are via (a) differential optical absorption spectrometry (DOAS) of scattered skylight observed in different viewing directions, (b) forward modeling of the atmospheric radiative transport for each measurement, and finally (c) mathematical inversion of the measured slant column amounts into 2-D concentration profiles of the targeted gases (c.f., so called curtains of trace gas concentrations vs. height or vs time).

Spectral solar radiation was measured by HALO-SR, a collaboration between FZ-Jülich and University of Leipzig. Two optical inlets, one mounted at the top and one at the bottom of HALO, were used to derive the actinic flux density. Additionally, nadir radiance (field of view 2.1°) was measured by a third optics mounted on the same aperture plate as used for the downward-looking actinic optics (Fricke et al. 2014). Depending on flight speed and altitude, the sampling frequency of about 2 Hz provides radiance measurements with horizontal resolution of about 200-500 m. By grating spectrometers the actinic flux density was covered in a wavelength range between 280-650 nm with spectral resolution of about 1.8 nm and the nadir radiance between 350-2200 nm with spectral resolution varying from 2 nm for visible wavelength to 16 nm in the near infrared range. The combined measurements of both radiative quantities allow investigating the impact of cloud properties on photolysis processes. While photolysis frequencies are derived from the actinic flux densities, cloud properties such as cloud phase, cloud optical thickness and effective radius can be retrieved from the radiance measurements. In addition, the simultaneous microwave, radar and lidar cloud observations suit to validate and improve cloud retrieval algorithms applied to HALO-SR measurements as shown by Fricke et al. (2014).

The mission consisted of a mix of University (Hamburg, Cologne, Heidelberg, Leipzig) and extra-university partners (MPI-M, DLR, FZ-Jülich). Formally the MPI-M in Hamburg maintained the scientific lead and overall mission coordination, but in terms of scientific content the mission was co-led with the University of Hamburg and DFG taking most of the responsibility for NARVAL North and MPI-M leading NARVAL South, in close cooperation with DLR and the University of Cologne. The flight hours were split roughly 6:6:2 between the MPG, DFG and DLR. 75 dropsondes were released during NARVAL South, and 46 during NARVAL North.

Esselborn, M., M. Wirth, A. Fix, M. Tesche, and G. Ehret: Airborne high spectral resolution lidar for measuring aerosol extinction and backscatter coefficients, Appl. Opt., 47(3), 346-358, doi:10.1364/AO.47.000346, 2008.

Fricke, C., Ehrlich, A., Jäkel, E., Bohn, B., Wirth, M., and Wendisch, M.: Influence of local surface albedo variability and ice crystal shape on passive remote sensing of thin cirrus, Atmos. Chem. Phys., 14, 1943-1958, doi:10.5194/acp-14-1943-2014, 2014.

Kritten L., Butz, A., Chipperfield, M. P., Dorf, M., Dhomse, S., Hossaini, R., Oelhaf, H., Prados-Roman, C., Wetzel, G., and Pfeilsticker, K.: Constraining the N_2O_5 UV absorption cross-section from spectroscopic trace gas measurements in the tropical mid-stratosphere, Atmos. Chem. Phys. 14, 9555–9566, doi:10.5194/acp-14-9555-2014, 2014.

Mech, M., Orlandi, E., Crewell, S., Ament, F., Hirsch, L., Hagen, M., Peters, G., and Stevens, B, 2014: HAMP – the microwave package on the High Altitude and LOng range research aircraft (HALO), Atmos. Meas. Tech., 7, 4539-4553, doi:10.5194/amt-7-4539-2014.

Weidner, F., H. Bösch, H. Bovensmann, J. P. Burrows, A. Butz, C. Camy-Peyret, M. Dorf, K. Gerilowski, W. Gurlit, U. Platt, C. von Friedeburg, T. Wagner, and K. Pfeilsticker, Balloon-borne Limb profiling of UV/vis skylight radiances, O3, NO2, and BrO: Technical set-up and validation of the method, Atmos. Chem. Phys., 5, 1409–1422, 2005.

Wirth, M., A. Fix, P. Mahnke, H. Schwarzer, F. Schrandt, and G. Ehret: The airborne multi-wavelength H2O-DIAL WALES: system design and performance, Appl. Phys. B: Lasers Opt., 96(1), 201-213, doi:10.1007/s00340-009-3365-7, 2009.

2.2 NARVAL South

Science goals

The NARVAL South flights were intended to enable both in-situ sampling (dropsondes) and airborne remote sensing designed to relate the point measurements on Barbados to the broader tradewind region and the developing satellite record. In the context of NARVAL the in-situ sampling helped evaluating the capability of the remote sensing configuration of the aircraft to characterize the state and composition of the atmosphere.

The aim of NARVAL South was to fly above the northeast Atlantic trades to measure their evolution using the aircraft remote sensing instrumentation. The HALO mission pattern flown is illustrated in Fig. 1. Flights were performed between the HALO home base at OBF and BGI on Barbados, as well as long outward and return legs directly from BGI. HALO flew at flight levels exceeding 14 km altitude along an air-mass trajectory that intersected the A-Train satellites orbit for collocated underflights. The air-mass and cloud properties just upwind of the measurement site were measured during the descent into BGI and during local flights.

Campaign summary

NARVAL South originally was conceived to consist of five flights—two return trips from OBF to BGI, and one local flight. Each of the flights was to be coordinated with overpasses of the CloudSat and CALIPSO satellites. In light of the preparation delays, and the amount of overhead that went into the preparation it was decided to add an additional return trip (roughly 20 flight hours), bringing the number of planned research flights for NARVAL South to seven, with a total of 65-70 flight hours. Due to weather conditions in OBF, plans were changed during the course of operations and the second roundtrip from OBF to Barbados was cancelled in favor of four local flights out of BGI, resulting in nearly 70 flight hours and eight research flights (RF). Except for RF02, the local flights were local only in the sense that the aircraft took off and landed from the same airport, as RF03-RF05 averaged about seven hours each and spanned more than half the distance across the Atlantic (see e.g., the flight report from RF03). The change in deployment ensured that, during the period of the NARVAL South mission, HALO was used to its maximum potential given crew duty restrictions. Moreover, because of the lack of long stretches over land (two hours from OBF to Lisbon), more of the flight data served the scientific purposes of the mission. All flights, except for the second long track from OBF, flew a coordinated CloudSat overpass track. Fuel restrictions and unfavorable winds led to the inflight decision to abandon the overpass leg on RF07. Examples of the flight legs, the conditions encountered and preliminary quicklooks are provided in the flight reports for RF01-08.

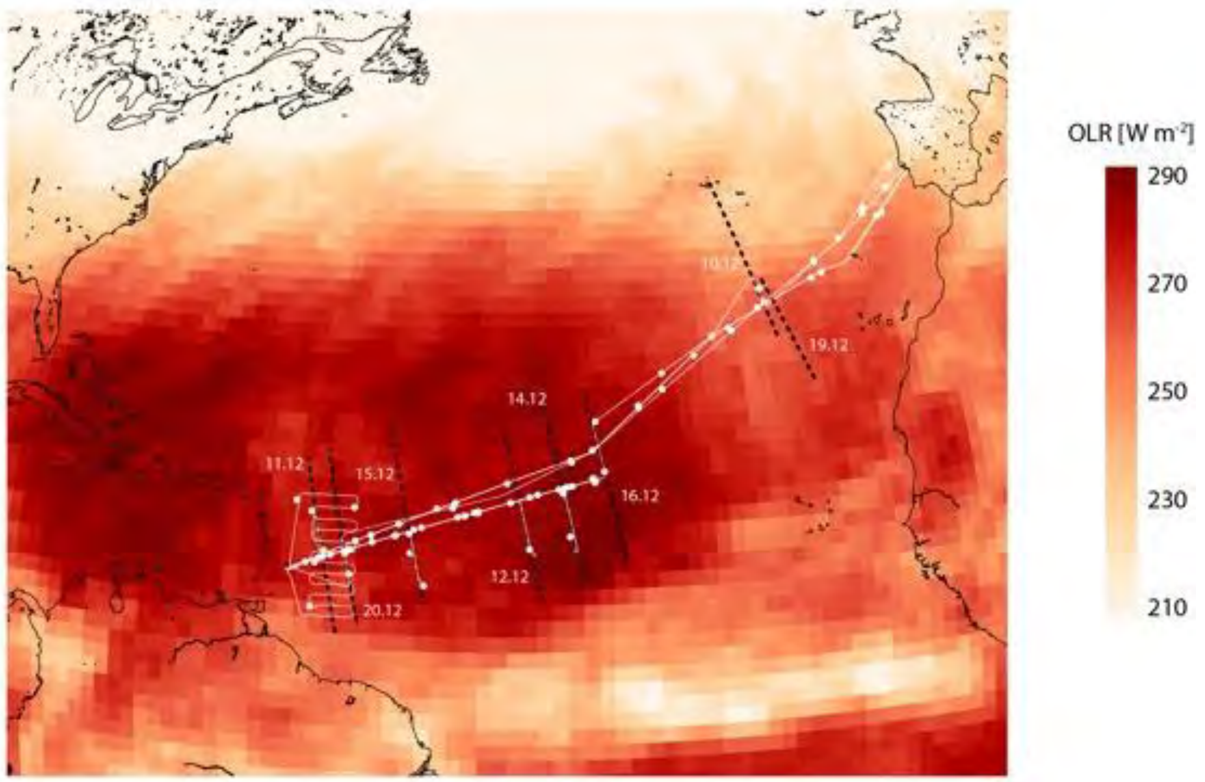

Fig. 1: The NARVAL South mission flight pattern over the North Atlantic tradewind region between Europe and Barbados. The individual research flights are illustrated by dates and white lines with dropsonde positions as white dots. Note the local flight mattress pattern out of BGI airport. The color-coding corresponds to the AIRS outgoing longwave radiation (OLR) in W/m^2.

2.3 NARVAL North

Science Goals

The main goal of NARVAL North was to collect high spatio-temporal resolution aircraft remote sensing data of convective postfrontal clouds and precipitation over the cold-season stormtrack of the North Atlantic. These data should help to better understand postfrontal convective phenomena and to investigate the accuracy of existing satellite precipitation climatologies. The measurements were complemented by in-situ sampling using dropsondes. Background of the scientific question are the large uncertainties associated with postfrontal precipitation in existing satellite climatologies as described by Klepp et al. (2003), Klepp et al. (2005) and Andersson et al. (2011). In contrast, HOAPS (Andersson et al., 2010) is the only satellite climatology that detects intense postfrontal precipitation in good agreement with voluntary observing ship weather reports. Hence, NARVAL data is ideally suited to uncover and validate the uncertainties in passive microwave based precipitation climatologies.

The frequencies used for the active and passive microwave instrumentation of NARVAL, as well as the visual wavelength of WALES, are identical to similar to those from the CloudSat radar and SSMIS radiometers, as well as the CALIPSO lidar. While SSMIS radiometers at about 800 km altitude have a surface resolution of approx. 50 km, the NARVAL radiometers at 8 km flight altitude reach 0.5 to 1 km resolution. Hence, it becomes possible to investigate the scale dependence of precipitation and to shed light into the beam-filling problematics of satellite climatologies. During the research flights the 1700 km broad swath of the SSMIS satellites passed 22 times over the target area. The SSMIS satellites are the mainstay of all passive microwave based global satellite climatologies (e.g. HOAPS, GPCP). CloudSat collocations were incorporated into the flight plans and were successfully flown in 4 cases. To achieve postfrontal aircraft remote sensing capabilities, it was a prerequisite to fly above all clouds at all times. Convective cloud tops reached 2 to 6 km altitude so that the flight altitude of 8 km (FL270, assigned by air traffic control) was ideally suited to obtain data in highest spatial resolution.

To cover the diversity of postfrontal cloud regimes we managed to fly 5 research flights over mesoscale postfrontal cyclones (PFL), spiral-shaped cold-core tiltback occlusions (TBO), enhanced cumulus with and without anvil-capped Cumulonimbus (ENC) as well as stratiform appearing shallow convection with cloud tops of 2 km altitude (SHC). The transfer flights between OBF and KEF were used to collect ground truth data over various European supersites (Fig. 2).

A. Andersson, K. Fennig, C. Klepp, S. Bakan, H. Graßl, and J. Schulz, 2010: The Hamburg Ocean Atmosphere Parameters and Fluxes from Satellite Data - HOAPS-3, *Earth Syst. Sci. Data*, **2**, 215-234, doi:10.5194/essd-2-215-2010.

A. Andersson, C. Klepp, K. Fennig, S. Bakan, H. Graßl, and J. Schulz, 2011: Evaluation of HOAPS-3 ocean surface freshwater flux components, *Journal of Applied Meteorology and Climatology*, **50**, 379-398, doi:10.1175/2010JAMC2341.1.

Klepp, C. P., S. Bakan, H. Graßl, 2003: Improvements of Satllite-Derived Cyclonic Rainfall over the North Atlantic., *Journal of Climate*, **16**, 657-669.

Klepp, C. P., S. Bakan, H. Graßl, 2005: Missing North Atlantic cyclonic precipitation in ECMWF numerical weather prediction and ERA-40 data detected through the satellite climatology HOAPS II., *Meteorologische Zeitschrift*, **14**, 809-821, doi:10.1127/0941-2948/2005/0088.

Campaign summary

HALO was transferred from OBF to KEF on 7 January 2014. During the transfer, HALO was overflying the measurement sites of Jülich (Germany), Cabauw (Netherlands) and Mace Head (Ireland) with the goal of obtaining ground reference data. The NARVAL North team arrived at KEF already between 3 and 6 January 2014 to establish all necessary contacts to the airport facilities and arrange for all logistic needs. Weather briefings were immediately started on a twice daily schedule to identify the targeted meteorological systems and to precisely forecast their position over the North Atlantic. This was crucial for NARVAL North, as Air Traffic Control (ATC) is handling flight pattern requests restrictively and does not allow for flight level changes in radar uncontrolled airspace. This restriction is applied due to dense civil and military air traffic in various flight levels of the area. Hence, ATC approval for HALO flight tracks required precise planning to limit the requested tied-up airspace in which mattress patterns would be flown. Finally, for all research flights HALO was approved to fly freely at flight level 270 within a pre-defined bounding box of tied-up airspace including clearance for dropsonde releases.

The large-scale atmospheric conditions were ideally suited for the investigation of postfrontal clouds and precipitation. The campaign started during a period of strong zonal flow over the North Altantic allowing two flights investigating a postfrontal low, embedded in a huge cold air outbreak through the Labrador Sea (RF10) and an exceptionally intense spiral-shaped cold-core tiltback occlusion (RF11). In the course of the campaign, the large-scale flow developed an intense blocking situation over Europe. This led to an accumulation of quasi-stationary fronts elongated in North-South direction between Europe and Iceland. Consequently, this allowed flying over a downstream development of cold air. RF12 began over the cloud-free area of a tip jet south of Greenland en-route to Ireland flying over progressively higher convection until Cumulonimbus clouds were reached. RF13 was flown over a cyclone with comparably weak cold-core convection. The postfrontal area of the most intense convection including Cumulonimbus was visually covered by a stratiform cloud deck aloft. RF14 was operated over a cyclone close to the blocking over Europe. The re-intensified cold air showed various stages of convection. All five research flights are summarized in Table 1 and visualized in Fig. 2.

The flight patterns were adapted individually to achieve maximum information content on postfrontal convection. As visualized in Fig. 2 the sizes of tied-up airspace target areas (mattress patterns) correspond to the area of the forecasted cold air activity. For the downstream development a large rectangle pattern was chosen for flying along the developing cold air convection. In total, about 36 hours of data from 5 research flights were successfully collected including 46 dropsondes (Table 1). All HALO bellypod and onboard instrumentation worked reliably. The transfer flight from KEF to OBF on 22 January 2014 was routed over the supersites of Chilbolton (UK) and Jülich (Germany).
Preliminary results reveal great detail of postfrontal clouds and precipitation and provide strong evidence that the HOAPS climatology is correctly detecting the observed variety of intense postfrontal convective precipitation over the cold-season North Atlantic Ocean. Overall, NARVAL North not only accomplished its main goal but additionally collected data of a broad variety of different cold air convective regimes in different development and intensity stages of wintertime North Atlantic cyclones.

Table 1: Overview on NARVAL North research flights during January 2014 and their objective.

Flt / Day	Objective	Duration	FL	Dropsonde	Cloudsat	SSMIS
RF10 09	Cold air outbreak, PFL	9:06 h	270	11	1	3
RF11 12	Tiltback occlusion	6:38 h	270	12	1	4
RF12 18	Downstream development	5:54 h	270/430	5	1	6
RF13 20	Weak cold core convection	8:30 h	270	11	-	6
RF14 21	Re-intensified cold air	6:12 h	270	7	1	3
total	All cold convective regimes	36:20 h		46	4	22

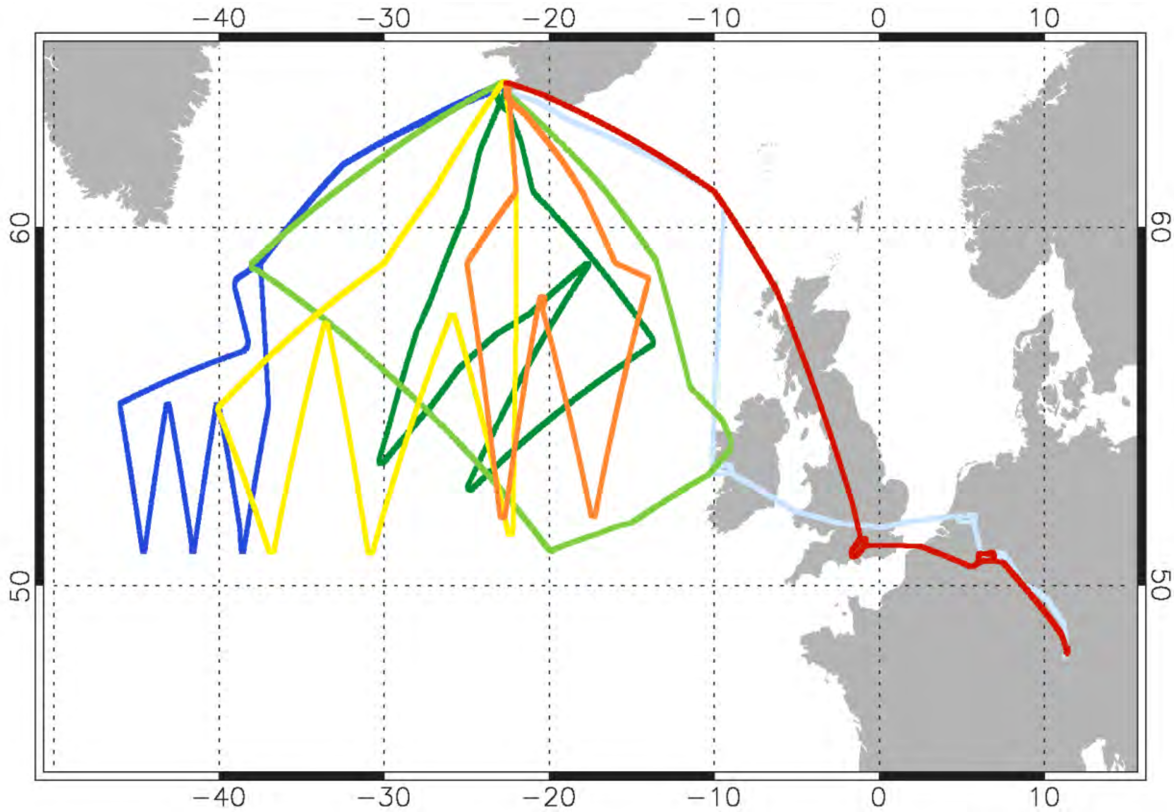

Fig. 2: The flight patterns of all five research flights (RF10 dark blue, RF11 dark green, RF12 light green, RF13 yellow and RF14 orange), and two transfer flights (TF9 light blue and TF15 red) between OBF and KEF. Note the supersite overpass patterns of TF9 over Jülich (Germany), Cabauw (Netherlands) and Mace Head (Ireland) and of TF15 in Chilbolton (UK) and Jülich (Germany). Additionally RF3 passed over Mace Head, (Ireland) at flight level 430 within radar controlled airspace.

3 Conclusions

The operational goals of NARVAL have been fully reached by collecting an extensive data set on a variety of subtropical North Atlantic tradewind precipitation clouds between 10 and 21 December 2013 and a diversity of different cold air convection regimes over the cold-season North Atlantic between 7 and 22 January 2014. In total, 15 flights (8 NARVAL South and 7 NARVAL North) have been carried out. The dedicated effort of all participants made it possible, that our instrumentation on HALO was reliably working during all flights. In addition to complex mattress flight patterns in the target areas we managed to launch a total of 121 dropsondes (75 NARVAL South and 46 NARVAL North) and to complete a total of 11 collocated CloudSat underflights (7 NARVAL South and 4 NARVAL North). Additionally, one collocated aircraft to aircraft flight with the French SAFIRE Falcon 20 (F-GBTM) was performed. Additionally, 22 SSMIS overpasses during NARVAL North flight missions were essential for the HOAPS evaluation. It is worthwhile to mention, that the NARVAL data set is complemented by three test and certification flights over Germany in summer 2013 named NARVAL-DE. NARVAL-DE consisted of little more than 10 flight hours with supersite overpasses over Jülich, Cabauw, Lindenberg and Munich as well as calibration patterns over the North Sea.

The successful operation out of OBF, BGI and KEF airport proved to be the right decision for the NARVAL campaign. Overall, basing the aircraft at an airport close to the target area turned out to be a major advantage to maximize the relevant data collection. With the invaluable understanding and help by the DLR personnel, restrictions issued by ATC due to the heavy air traffic in the North Atlantic sector were successfully overcome and turned into advantageous flight patterns.

Preliminary analysis of the data suggests that a standard configuration of HALO, consisting of HAMP, WALES and the mini-DOAS system, various imagers, and base instrumentation, can meaningfully constrain the composition of the underlying atmosphere (or surface). HALO, constituted as a remote sensing aircraft, with our standard and pre-certified set of sensors, can now be rapidly and flexibly deployed from its home base or remote airports, for follow-on NARVAL missions. So doing would complement the traditional, field deployment, use of research aircraft and optimize the usage of this unique resource.

In summary,

- HALO successfully accomplished 15 research flights during both phases of the NARVAL campaign with its remote sensing suite on-board.
- All instruments operated successfully and collected useful scientific data.
- Over 121 dropsondes were released.
- Supersite overpasses over Jülich (Germany), Cabauw (Netherlands), Mace Head (Ireland), Chilbolton (UK) and the Barbados cloud observatory - mainly during transfers from and to Germany - provide valuable ground truth data for remote sensing instrumentation validation.
- Flights were successfully collocated with about 11 CloudSat and 22 SSMIS overpasses.
- Preliminary results look promising. They reveal great detail of tropical as well as extra-tropical post-frontal convective clouds and precipitation. Especially the combination of different instruments (e.g. radar, lidar and passive microwave radiometers) holds great potential for new insight into cloud and precipitation processes.

- Data collected will be used for satellite retrieval validation and process studies.
- Water vapor, liquid- and ice water path and precipitation retrievals for the NARVAL radiometers and Z-R relationship investigation for the NARVAL radar are under development.

Further documents and data of the NARVAL campaign are provided and can be accessed through the ZMAW FTP server:

ftp://ftp-projects.zmaw.de/narval/NARVAL/

4 Overarching issues, recommendations and lessons learned:

In terms of access to HALO, from the perspective of the science steering board (WLA) perhaps the greatest realization during NARVAL and its preparation is that charging consortium partners based on flight hours makes no sense, and is in fact counterproductive as it hinders full usage of the aircraft. As an extreme but illustrative example, consider that the current formula implies that a mission that involves four weeks of dedicated access to the aircraft for preparation, two weeks of decommissioning time, but only flies a single hour to make a very important measurement, costs one tenth what it costs a mission that requires three days preparation, flies a ten hour mission, and takes one day to decommission the aircraft. The true cost of the missions is much better measured by the amount of dedicated access to the aircraft rather than the flight hours. The expense and time invested in preparing missions implies that the aircraft should be flown as often as possible once it is deployed. To make this possible the aircraft should not be divided based on a perceived number of possible flight hours per year, but rather based on days of dedicated access. For instance if the aircraft is available for consortium access for 40 weeks per year, the distribution of access should be based on fractions of this time. So if the one partner is entitled to 20% of the aircraft it should have eight weeks of dedicated access. Marginal costs during deployments, such as landing fees and fuel would then be covered in the same way as other incidentals.

Regarding the home base of HALO, an original idea of NARVAL was that there would be a great advantage of being able to fly based out of OBF. The thinking was that during gaps in usage the aircraft could be quickly configured for NARVAL and long remote sensing legs (for instance to Barbados and back) could be flown. This, it was thought, would optimize usage of the aircraft and be logistically simpler. In practice, even for a quick turn-around at the destination airport, logistical support was required. Hence, unless HALO were to depart and return to the OBF two ground crews would be necessary. During winter the possibility of fog at OBF adds great uncertainty to flight planning, something that we failed to consider in our original planning. Moreover, as far as NARVAL was concerned, the convenience of basing out of OBF came with the cost that it required an additional two hours per flight of ferry time, i.e., the time between takeoff and active measurements off-shore of Portugal. These considerations, the logistical overhead of preparing the aircraft for operations, and the development of a very dense schedule of flight planning and preparation for HALO as a whole, suggests that future NARVAL missions should be based as close to the measurement target as possible, preferably with take-off and landing at a single airport.

Lessons learned

a. The original idea to use the long-range capacity of HALO to reach the operation area from a logistically simple air base in Germany (OBF) turned out fairly unhandy. In contrast, external airport (BGI and KEF) usage including hangar capacity increases scientific data and campaign benefits. Being closer to the operation area limits transfer flight hours in favor of research flight time.
b. Cooperation and Communication with ATC were non-trivial in dense air traffic areas over the North Atlantic, especially for NARVAL North, and vertical level changes turned out being virtually impossible. After some initial irritations with ATC a satisfactory operational mode could be agreed in requesting tied-up airspace with dropsonde release allowances on a constant flight-level.
c. This agreement required HALO flying at FL270 (8 km) within a predefined and for other traffic blocked area for the postfrontal research flights. While not being considered optimal in the beginning, this agreement turned out fairly ideal as dropsondes could be launched and remote sensing was possible at all time because the postfrontal cloud tops were well below 8 km altitude. Only frontal cloud systems reached higher than 8 km so that HALO was within the clouds for the frontal passage times.
d. Initial concerns about freezing harm to the HAMP instrumentation during front passages due to wetting, icing or riming could not be supported and postfrontal data collection was not hampered. Similarly, flying over ice-capped Cumulonimbus anvils neither harmed the aircraft (lightning activity) nor influenced the measurements.
e. Radiometer calibration procedures and equipment should be improved to become more flexible and robust regarding external influences as e.g. high wind speed while the aircraft is parked on the apron, or tarmac icing conditions.
f. Online visualization of BAHAMAS data and near-real time satellite images at one or more info terminals in HALO would be welcome for scientist quicklook information (especially mission scientist). This would include the flight track, height and external conditions and maybe also the planned track. Also the online view of the downward looking camera would be much appreciated. A large clock in the cabin showing precise UTC time would be appreciated.
g. Occasionally missing GPS signal plagued several meteorological measurements, especially several dropsonde profiles. Data outages and data spikes in BAHAMAS data occurred occasionally for yet unknown reasons.
h. Data quicklooks during or soon after the flight are essential to identify problems and improve products already during the campaign.
i. NetCDF should be adopted as a common data format (BAHAMAS, Dropsondes). Standard radiation (IR, VIS) sensors and IR/VIS imaging should be part of the base instrumentation.
j. The data recording system of the radiometers needs to be improved to ensure high reliability and sampling at the nominal rate.
k. A mount for the headphones would be useful.
l. Catering, especially for demanding flight schedules, would be helpful and relieve the crew of additional and unnecessary preparation needs. A holder for coffee/drinks near

each seat may prevent spilling drinks. An Espresso (capsule coffee) might be better than the filter machine.

5 Acknowledgements

The authors of this campaign overview would like to take the opportunity to congratulate and thank everyone involved in NARVAL for making this campaign such a great success. We especially enjoyed a lot the great campaign spirit and working atmosphere among the team.

We are very grateful for the great and flexible support by the funding agencies (DFG, MPG, DLR and the various universities). The certification process was extremely complicated – a great thank to all, who contributed by extraordinary efforts, to succeed with this campaign –, by all: METEK, Radiometer Physics, Aerostructur, Leichtwerk, DLR-FX. Flight planning support by DLR-FX, the IPA of DLR and the pilots was tremendously helpful and important ingredient for the success of NARVAL. DLR-FX did a great job in solving all small and big technical issues during NARVAL campaign.

We gratefully thank the Caribbean Institute for Meteorology and Hydrology for their support at Grantley-Adams-International-Airport on Barbados during the campaign and especially for their very important support in the planning and preparation phase of flights and ground operations on and above the Island of Barbados.

Thanks go also to the Icelandic Met Office (IMO) for the provision of weather analysis and forecast products as well as quicklook satellite imagery for mission planning and documentation.

All figures provided in the reports are a group effort of the entire NARVAL Team including team members not present during the campaign. Nicole Albern (MPI-M) is thanked for her thorough proofreading of the NARVAL North reports. Rossita Puranaci is thanked for formatting the final document.

NARVAL demonstrated the great remote sensing potential of HALO which makes us very confident and optimistic for future NARVAL missions.

NARVAL South

Research Flight Reports

BJORN STEVENS

NARVAL South Team Oberpfaffenhofen and Barbados:
DLR: Axel Amediek, Christian Büdenbender, Andreas Fix, Steffen Gemsa, Silke Groß, Michael Großrubatscher, Martin Hagen, Andrea Hausold, Thomas Leder, Martin Wirth, Alexander Wolf, Ralph Zink
MPI-M: Lutz Hirsch, Friedhelm Jansen, Bjorn Stevens
University of Hamburg: Felix Ament, Akio Hansen, Heike Konow
University of Cologne: Susanne Crewell, Mario Mech, Emiliano Orlandi
University of Heidelberg: Tilman Hüneke, Klaus Pfeilsticker
University of Leipzig: Frank Werner, André Ehrlich
Forschungzentrum Jülich: Insa Lohse, Birger Bohn

NARVAL South Research Flight 01 (RF01), Flight Report
- 10 December 2013 -

BJORN STEVENS

Objective: North subtropical Atlantic cross section with coordinated CloudSat overpass.

Crew: Axel Amediek (WALES), Silke Gross (WALES), Steffen Gemsa (Pilot), Michael Grossrubatscher (Pilot), Lutz Hirsch (HAMP), Tilman Hüneke (mini-DOAS), Bjorn Stevens (Mission PI), Ralph Zink (Flight Tech)

TABLE 1. RF01 times: Overpass time is given at the beginning of the track shown on track map (Fig. 3). Flight times are between start and end of BAHAMAS record.

Event	UTC Time (since 1970)	UTC Time (since midnight)	Date
Takeoff	1386670434.45	1014	10.12.2013
Overpass	1386688020.00	1507	”
Landing	1386708093.45	2041	”

Overview: Good to seemingly typical trade wind conditions, over the central and west- central Atlantic, with a broad high-pressure zone and clear skies over Europe, and disturbed conditions offshore of Portugal in the Eastern Atlantic. The first sonde fell through a deep (5km) cirrus layer. Atmosphere above 800 hPa (2km) became progressively drier as the Atlantic was crossed. Coordinated overpass with CloudSat yielded a well-developed radar signature in the low-level cloud field showing precipitating cells with tops near 3 km.

Instruments: Thirteen dropsondes launched over the Atlantic. No major instrument problems. Radar sensitivity was less than expected, as signal appeared to fall off at about -25 dBZ; some dropouts in the radiometer data, and on approach to Grantley Adams (Barbados) we reduced flight levels to explore radar sensitivity, below flight level 280 the lidar had to be shutdown because its running temperature was to warm. Bahamas IGI system had some issues, and BAHAMAS data output is in a different format for this flight. All sondes appeared to function well. Initial indications were that miniDOAS and HALO SR functioned as intended. Photos on camera are UTC minus 4 hrs and 51 minutes.

Fig 1. Snapshots of cloud field. Left: shortly after leaving convective region (1430 UTC), about ninety minutes offshore of Portugal. Right: Image from 1500 UTC, near time of CloudSat overpass; note the tiers of convection, growing in steps progressively toward deep cumulonimbus in the very back left of image

Fig 2. More downstream cloud field. Left image looks like double (merging) cold pools with remnant stratus in the center, taken around 1800 UTC; Right image shows more closed cell structures taken (1900 UTC) near the end of the flight.

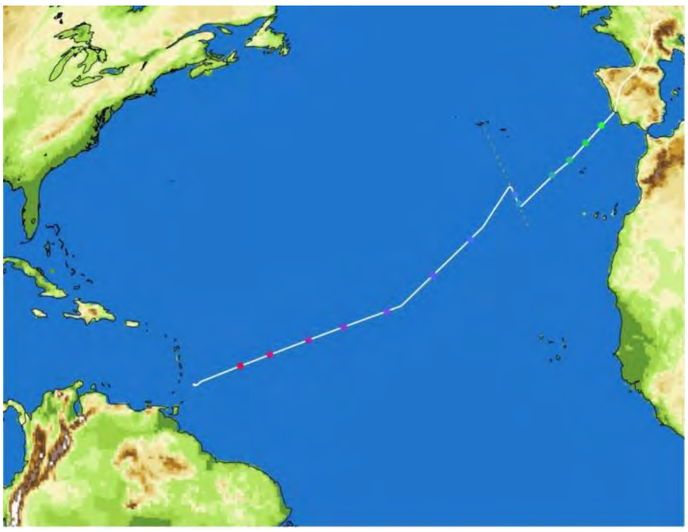

Fig. 3. Flight track showing positions of dropsondes and satellite overpass.

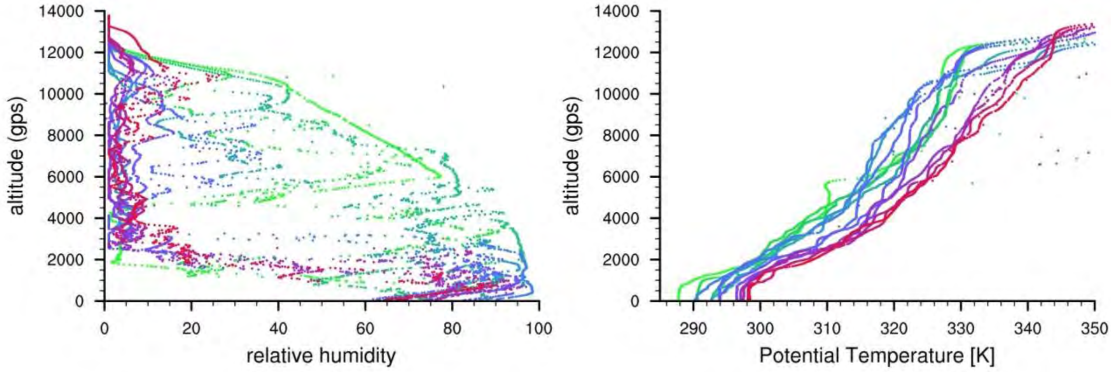

Fig. 4. Dropsonde humidity and potential temperature, colored following colors on track map.

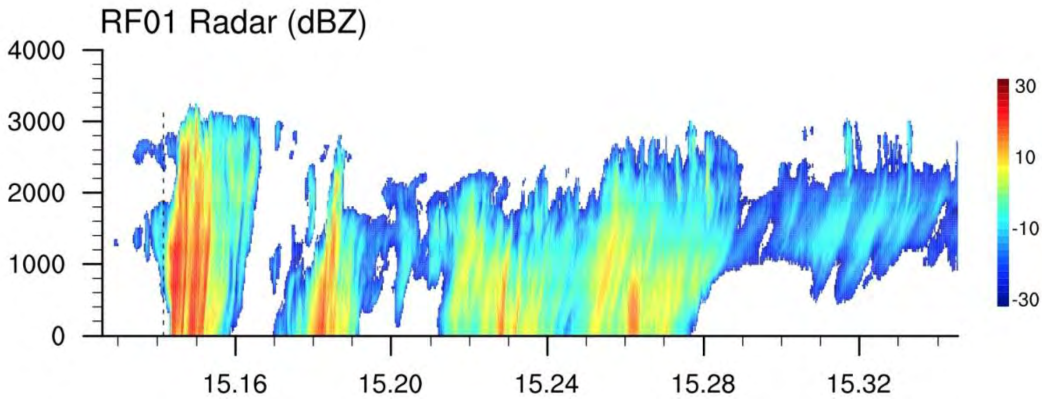

Fig. 5. Radar reflectivity during CloudSat overpass. Approximated overpass denoted by vertical dashed line.

Quicklooks RF01

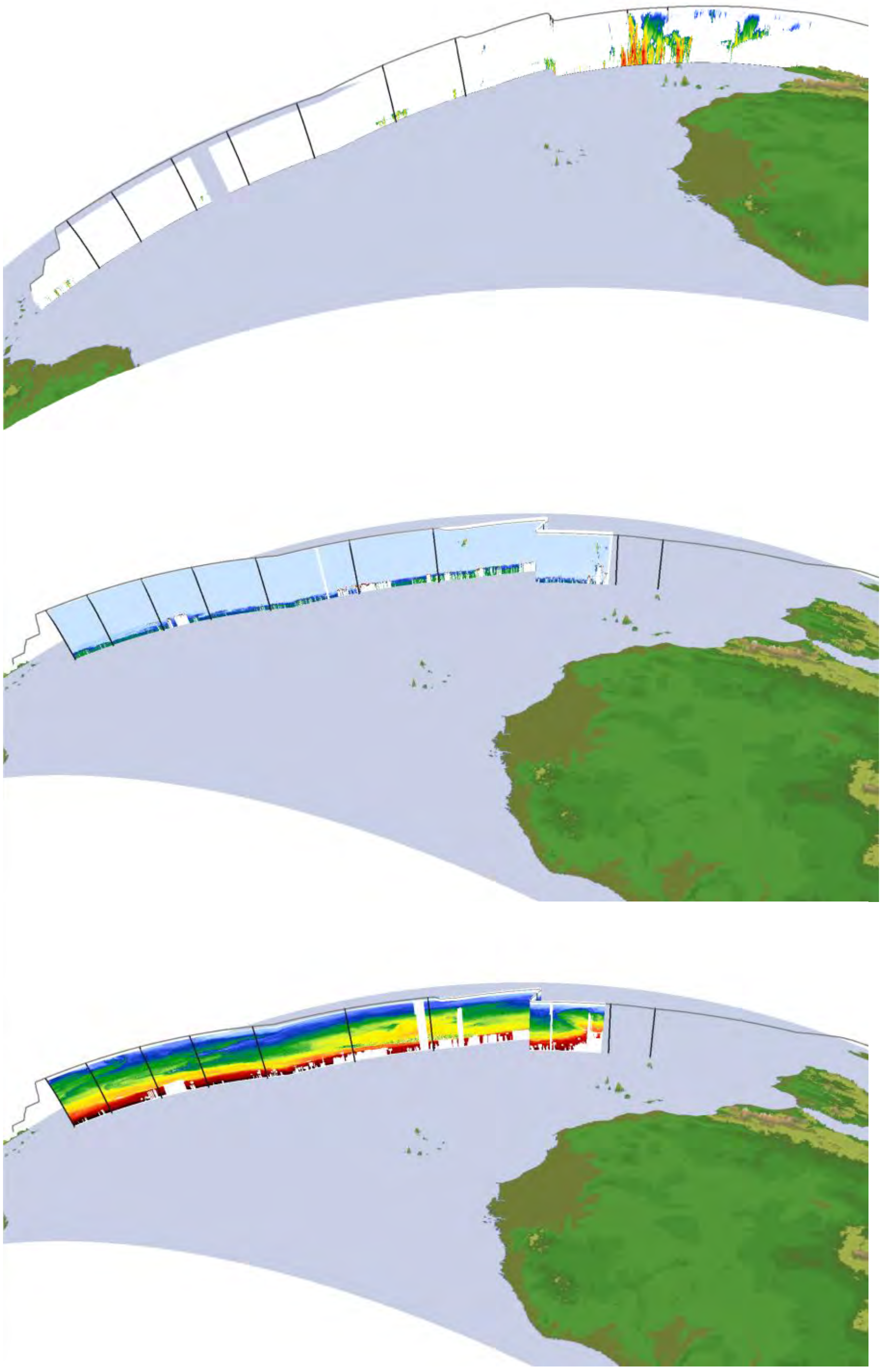

Fig.6: 3-D visualization of the radar backscattering (top panel), the lidar backscatter ratio (middle panel) and the derived water vapor mixing ratio (lower panel) along the entire flight track.

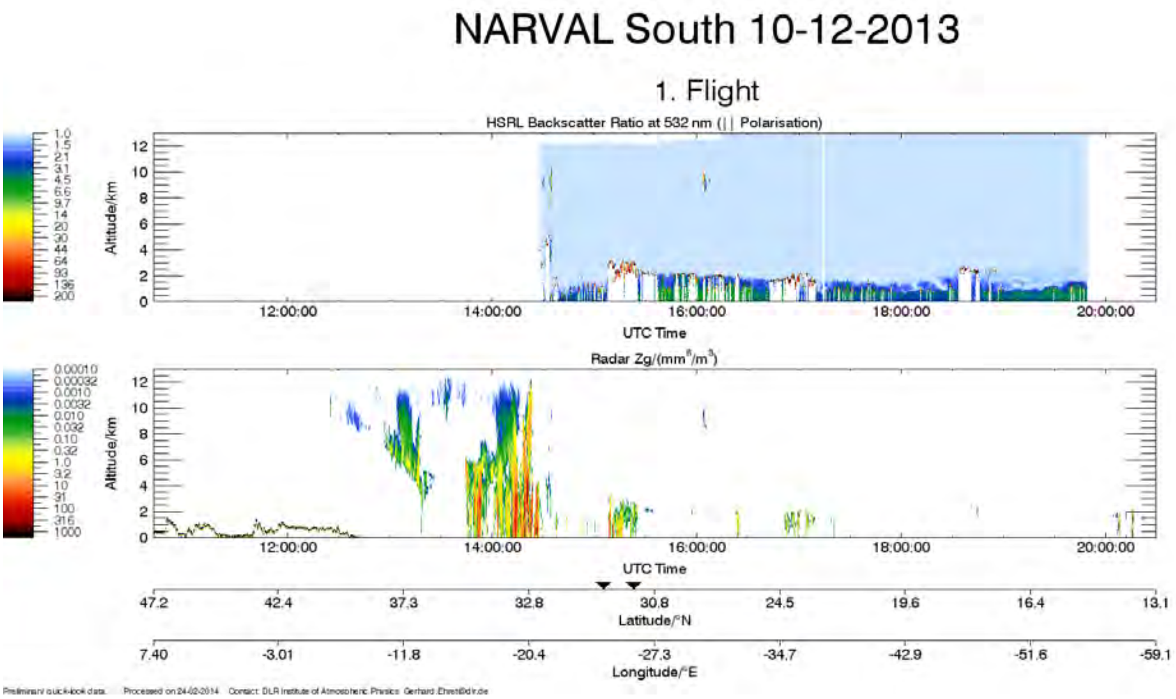

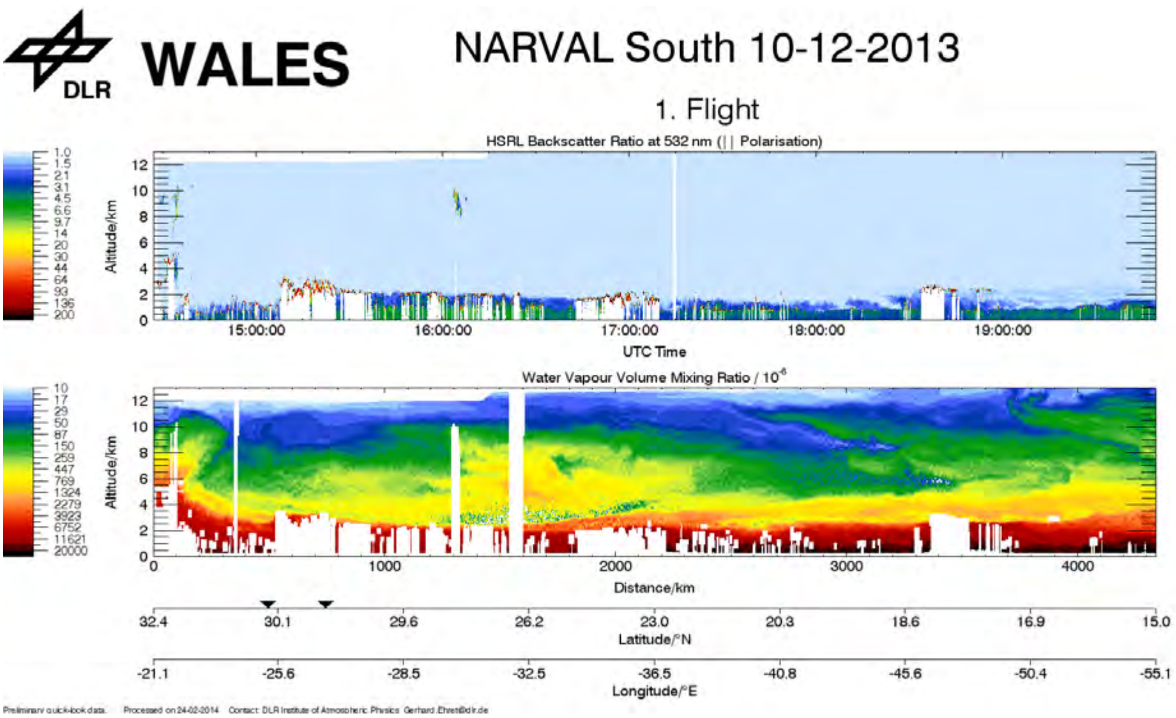

Fig.7: Time-height section of lidar backscattering vs. radar backscattering (upper panel) and lidar backscattering vs. water vapor volume mixing ratio (lower panel).

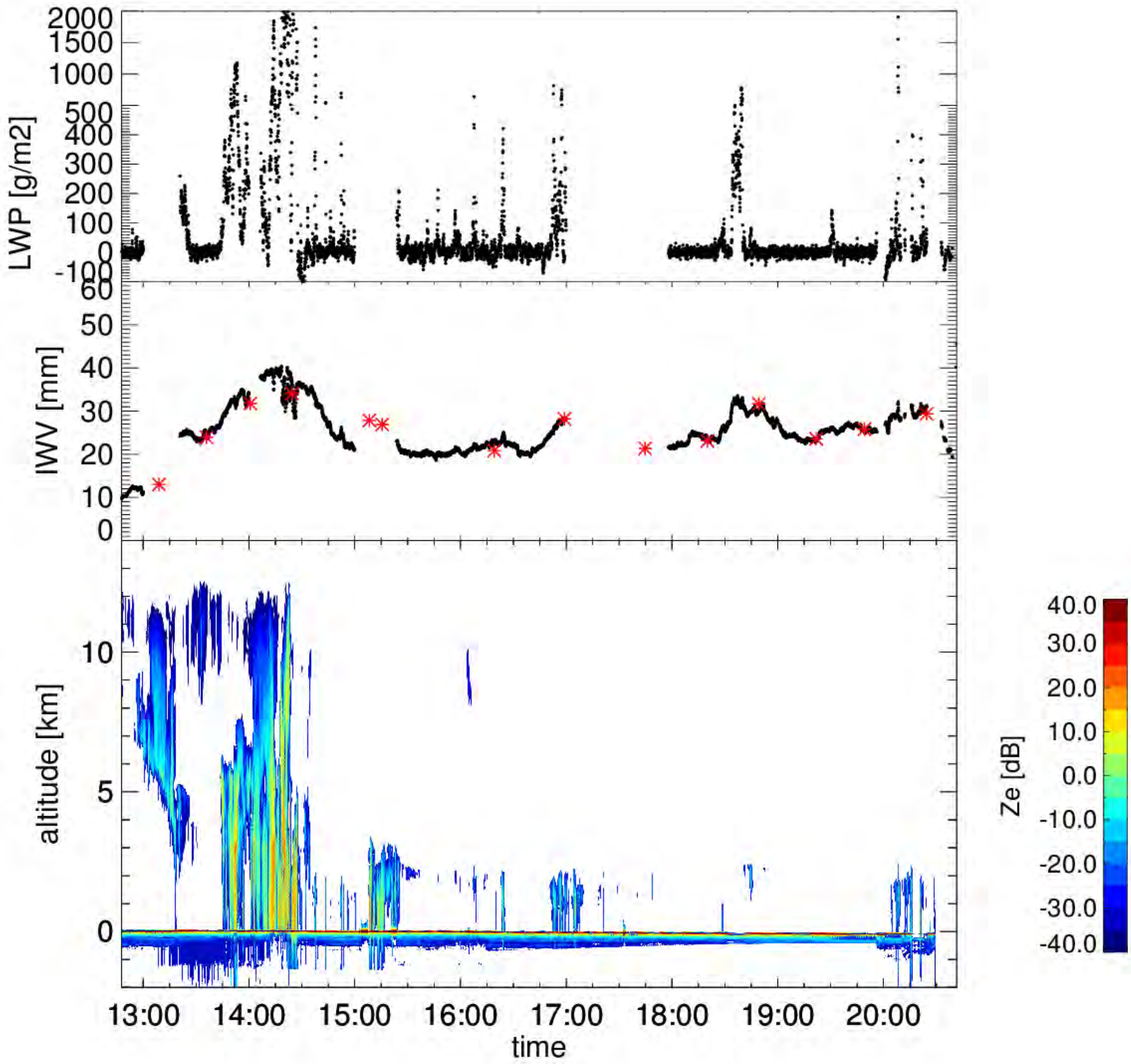

Fig.8: Time-height section of liquid water path (top panel) and integrated water vapor (middle panel) as derived from retrievals using the HAMP radiometer data vs. radar backscattering (lowest panel). Red stars in middle panel denote dropsonde derived integrated water vapor.

NARVAL South Research Flight 02 (RF02), Flight Report
- 11 December 2013 -

BJORN STEVENS

Objective: Local flight characterizing convective regimes upwind of Barbados, taking advantage of a CloudSat overpass near the Island.

Crew: Axel Amediek (WALES, Mission Coordinator), Silke Gross (WALES), Steffen Gemsa (Pilot), Michael Großrubatscher (Pilot), Lutz Hirsch (HAMP), Emiliano Orlandi (HAMP-Radiometers), Bjorn Stevens (Mission PI), Ralph Zink (Flight Tech)

TABLE 1. RF02 times: Overpass time is given at the beginning of the track shown on track map (Fig. 3). Flight times are between start and end of BAHAMAS record.

Event	UTC Time (since 1970)	UTC Time (since midnight)	Date
Takeoff	1386772131.45	1429	11.12.2013
Overpass	1386782640.00	1724	”
Landing	1386799096.45	2158	”

Overview: Typical conditions, convection to the south over the north-east coast of South America, was producing cirrus outflow over Barbados. There was a strong north south gradient between very dry trade-wind conditions and disturbed conditions. The flight pattern took a heating spiral form, sampling a north south cross section upwind of Barbados and the CloudSat overpass. The last sonde was let go in the midst of a deep convective system reached (by a slight detour) at the very end of the flight. Major difference was in the humidity structure of the atmosphere. Coordinated overpass with CloudSat early, to midway, through flight yielded a well-developed radar signature in the low-level cloud field showing precipitating cells with tops near 3 km.

Instruments: Six dropsondes launched over the Atlantic. Some initial problems with the network led to a delayed start. Radar had difficulty finding its oscillator, but eventually got started. Radiometer had no further dropouts and Bahamas IGI system function as intended. All sondes appeared to function well, last sonde fell through a region of deep convection. Initial indications were that miniDOAS and HALO SR functioned as intended.

Fig. 1. Snapshots of cloud field early in RF02. Shallow cumulus (left) at 15:45 (around takeoff) with cirrus overhead. Mixed shallow convection (right) with stratiform sheets near time of CloudSat overpass (17:00 UTC).

Fig. 2. Approaching region of deeper convection toward the southern region of the flight domain at 19:15 UTC (left) and 19:45 (UTC) right. Deeper convection was surprising by the development of the stratiform skirt delineated by a very sharp boundary toward more broken trade wind clouds.

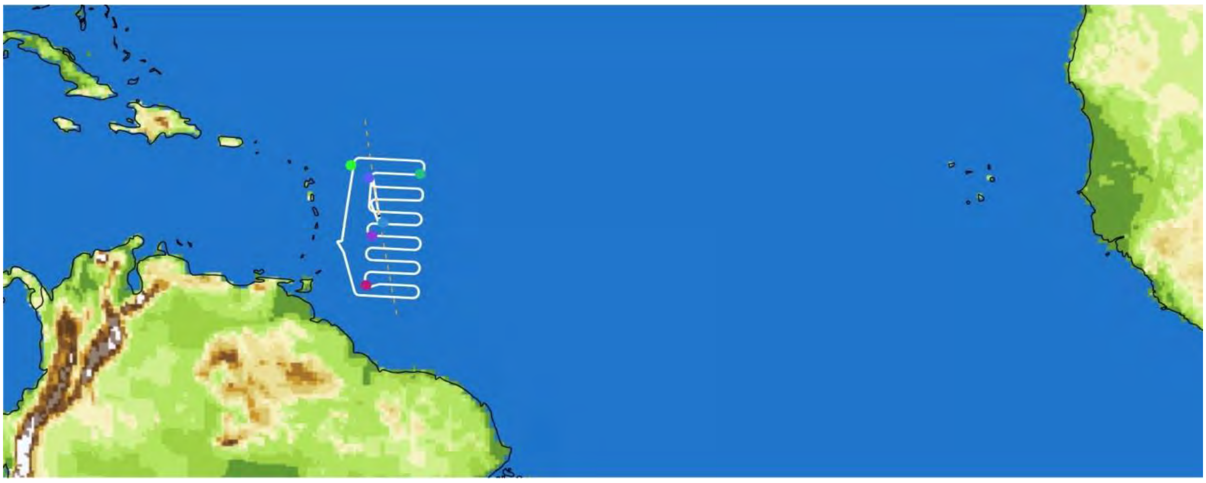

Fig. 3. Flight track showing positions of dropsondes and satellite overpass.

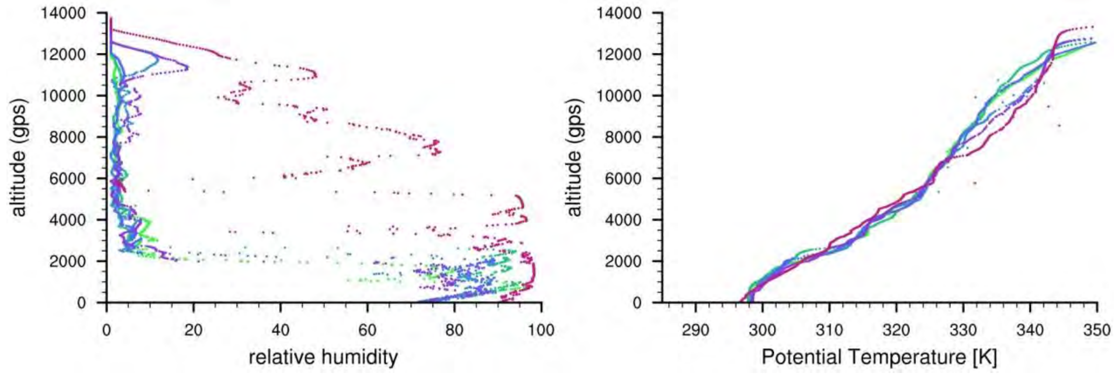

Fig. 4. Dropsonde humidity and potential temperature, colored following colors on track map.

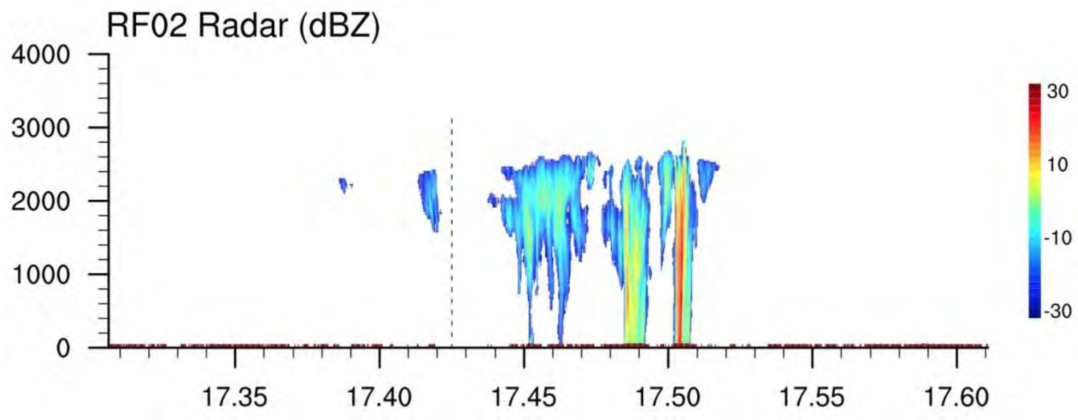

Fig. 5. Radar reflectivity during RF02 CloudSat overpass. Approximated overpass denoted by vertical dashed line.

Quicklooks RF02

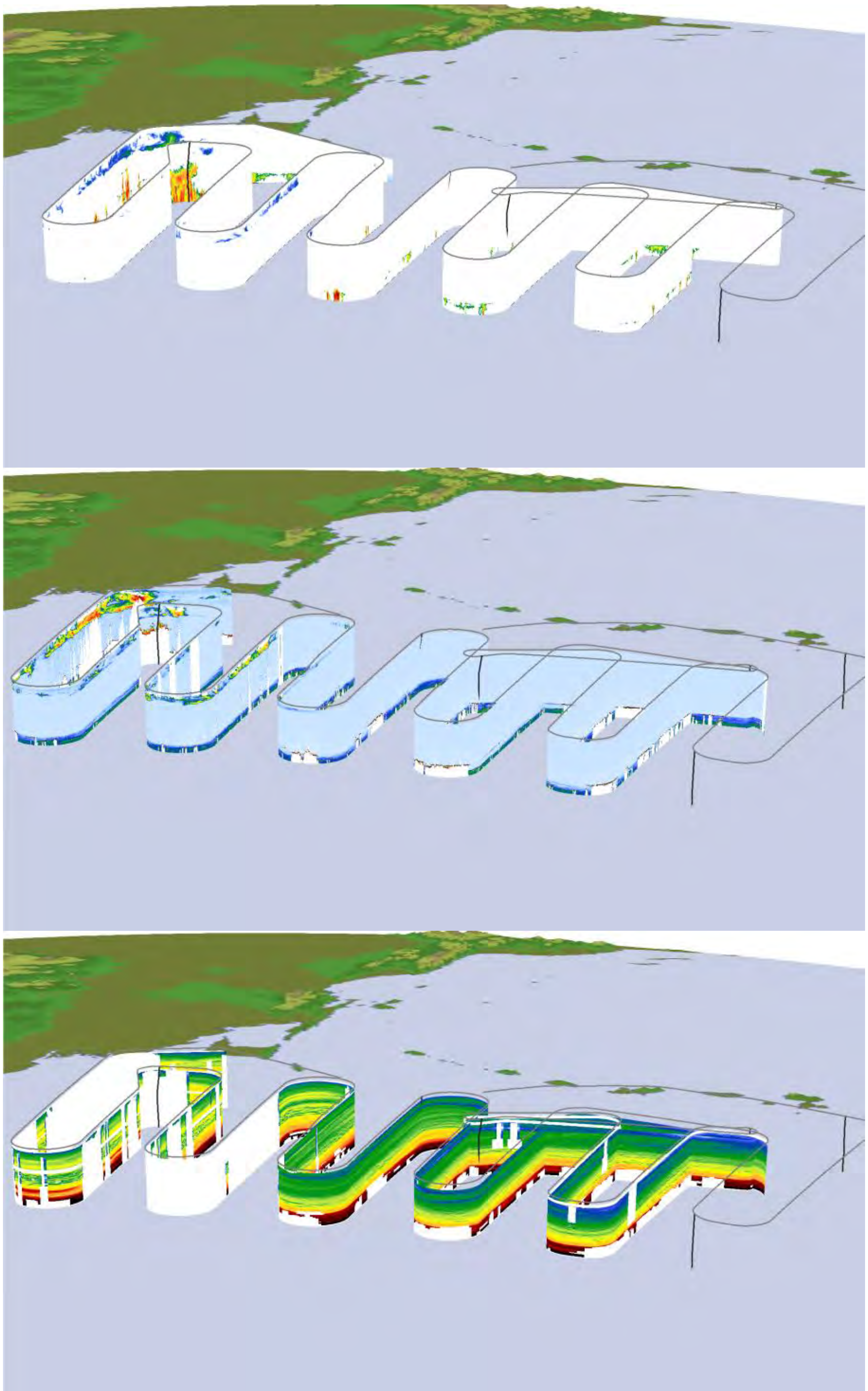

Fig.6: 3-D visualization of the radar backscattering (top panel), the lidar backscatter ratio (middle panel) and the derived water vapor mixing ratio (lower panel) along the entire flight track.

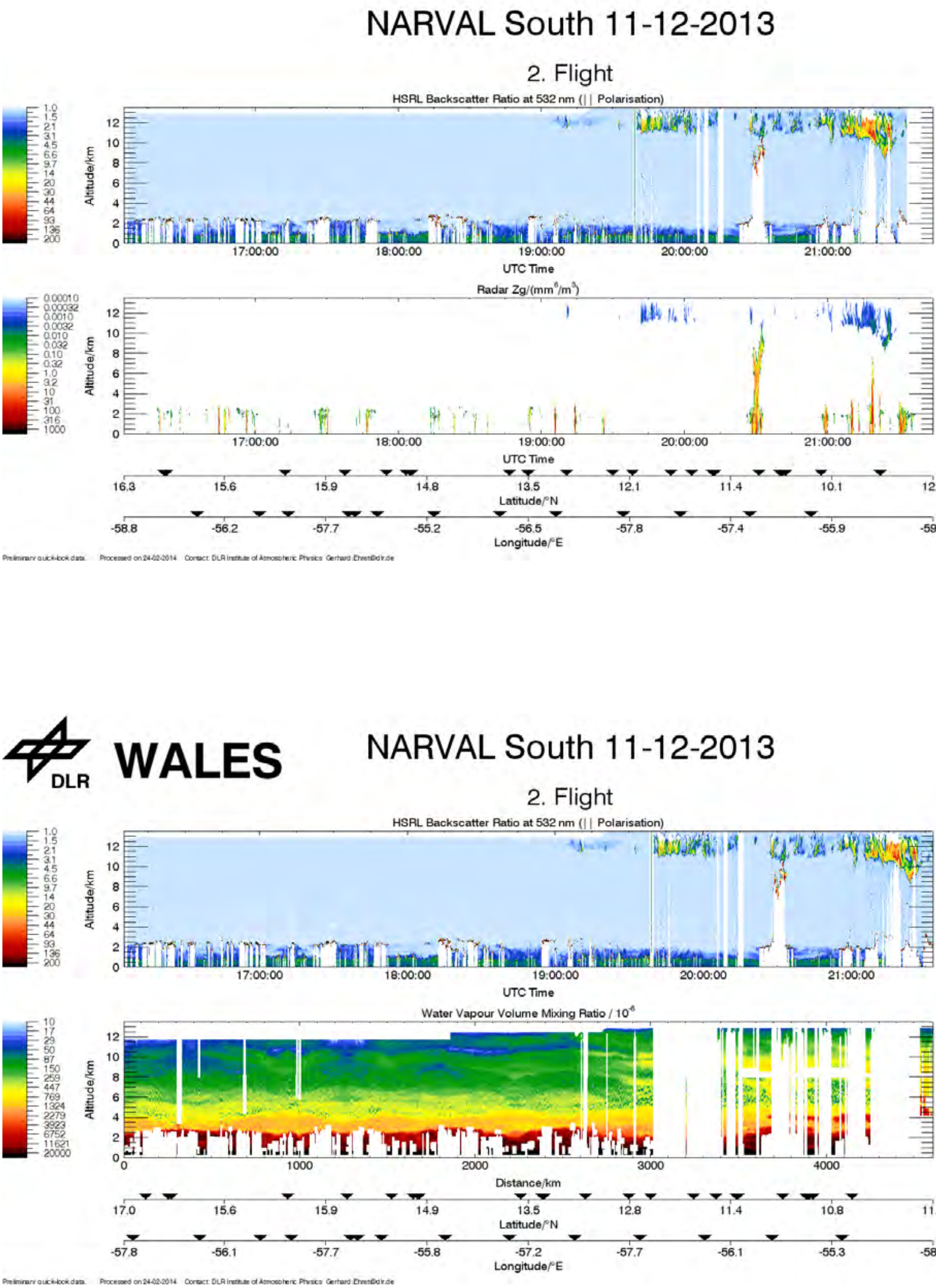

Fig.7: Time-height section of lidar backscattering vs. radar backscattering (upper panel) and lidar backscattering vs. water vapor volume mixing ratio (lower panel).

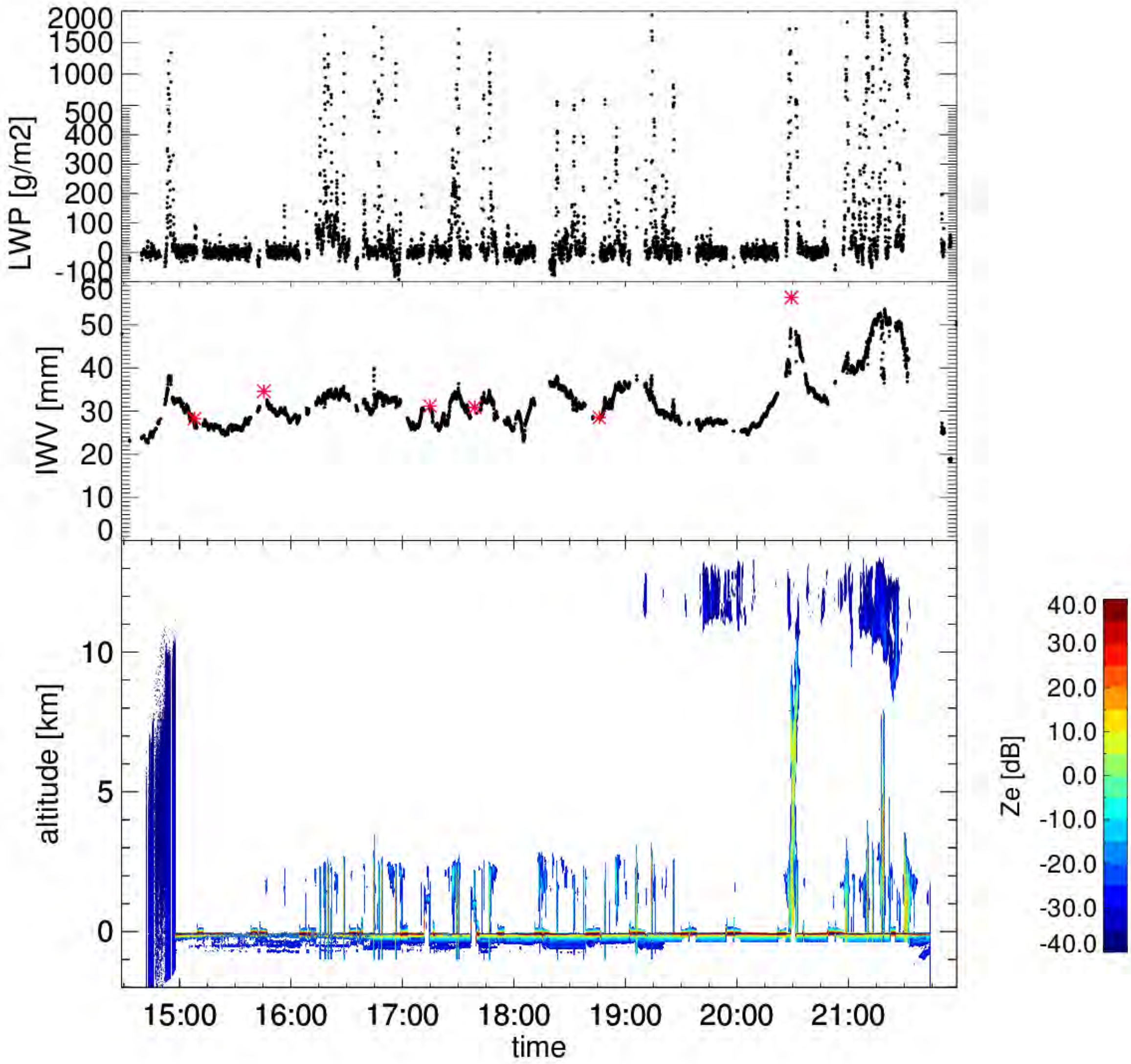

Fig.8: Time-height section of liquid water path (top panel) and integrated water vapor (middle panel) as derived from retrievals using the HAMP radiometer data vs. radar backscattering (lowest panel). Red stars in middle panel denote dropsonde derived integrated water vapor.

NARVAL South Research Flight 03 (RF03), Flight Report
- 12 December 2013 –

BJORN STEVENS

Objective: Mid-Atlantic cross section with CloudSat Overpass.

Crew: Steffen Gemsa (Pilot), Silke Gross (WALES), Michael Großrubatscher (Pilot), Lutz Hirsch (HAMP), Tilman Hünke(HAMP-Radiometers), Friedhelm Jansen (HAMP), Thomas Leder (Flight Tech; maiden flight), Bjorn Stevens (Mission PI)

TABLE 1. RF03 times: Overpass time is given at the beginning of the track shown on track map (Fig. 3). Flight times are between start and end of BAHAMAS record.

Event	UTC Time (since 1970)	UTC Time (since midnight)	Date
Takeoff	1386856190.45	1350	12.12.2013
Overpass	1386865740.00	1629	”
Landing	1386879614.45	2020	”

Overview: Typical conditions, convection continued to be present to the south with cirrus anvils blowing off eastward. Satellite imagery showed deep region of very dry air over flight region, with some cirrus blow-off. Flight stayed in dry conditions, with very homogeneous thermodynamic conditions, a continued very dry atmosphere, with a well-defined trade-wind layer below 2.5km, but diverse cloud patterns. The flight pattern had a police baton pattern with excursion for CloudSat overpass. On return leg the aircraft climbed to 45,000 ft, just beyond range of radar so that surface returns were eliminated. This pattern will be repeated for RF04 and RF05, but with different overpass points. CloudSat overpass showed a radar signature, despite considerable shallow convective systems in the vicinity (similar to previous days); the radar signature was more pronounced in the initial run through the track (CloudSat overpass was in outgoing run through track).

Instruments: Ten dropsondes launched, one (the sixth) launch did not appear to work as subsequent analysis showed no data, so only nine sondes processed. The first sonde had a period of data-overwrite due to a failure to shut off the sonde after termination, and no reset of the following sondes frequency. Otherwise no known instrumental issues.

Fig. 1. Snapshots of cloud field early in RF03. Some showers before take off. Mixed shallow convection (right) with stratiform sheets similar to previous days at near time of CloudSat overpass (16:00 UTC).

Fig. 2. Region of deeper convection west of Barbados as we approached for landing (left image, 19:00 UTC). Arc of shallow convective clouds at 19:15 (right).

Fig. 3. Flight track showing positions of dropsondes and satellite overpass.

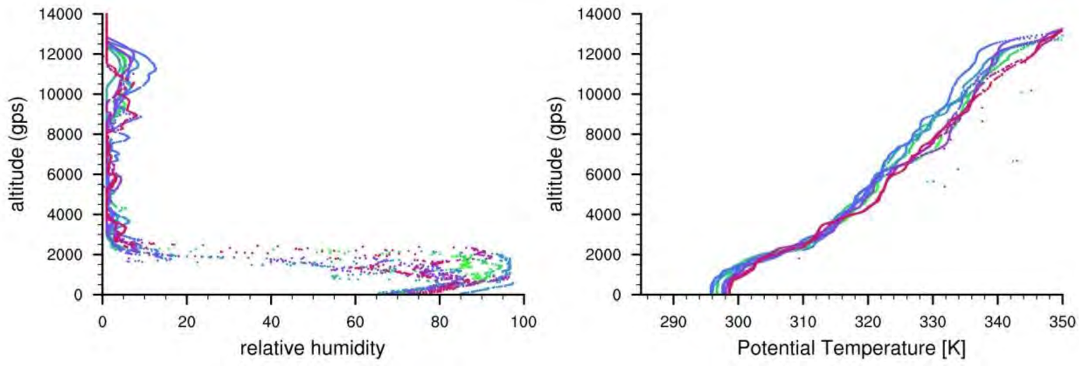

Fig. 4. Dropsonde humidity and potential temperature, colored following colors on track map.

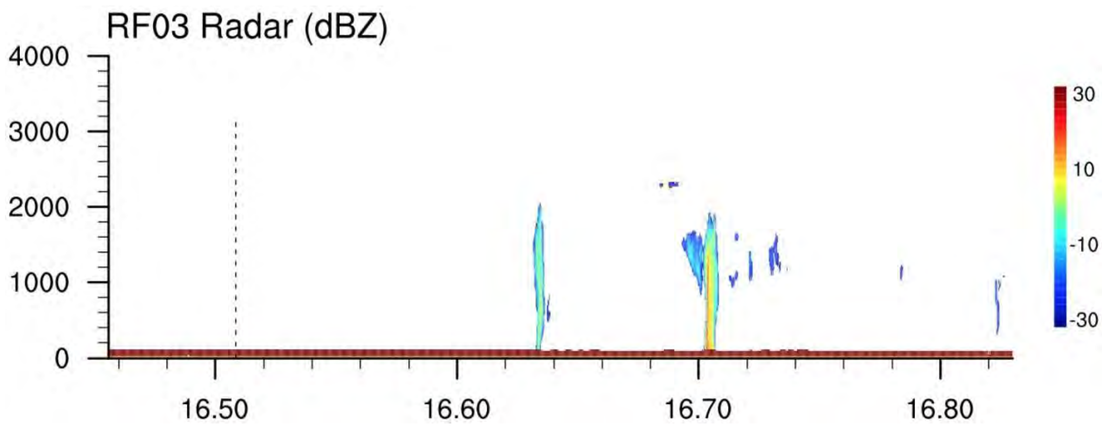

Fig. 5. Radar reflectivity during RF03 CloudSat overpass. Approximated overpass denoted by vertical dashed line.

Quicklooks RF03

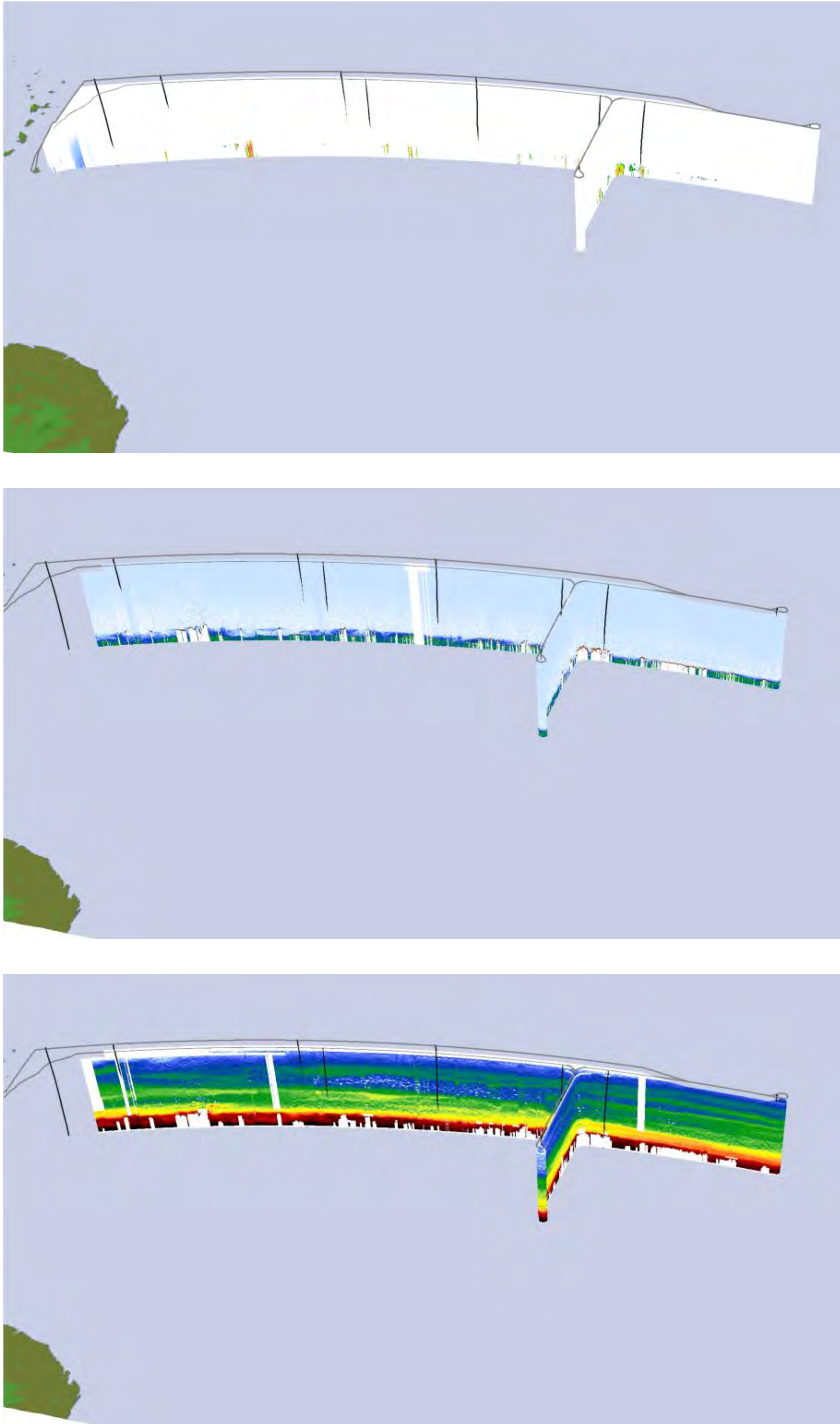

Fig.6: 3-D visualization of the radar backscattering (top panel), the lidar backscatter ratio (middle panel) and the derived water vapor mixing ratio (lower panel) along the entire flight track.

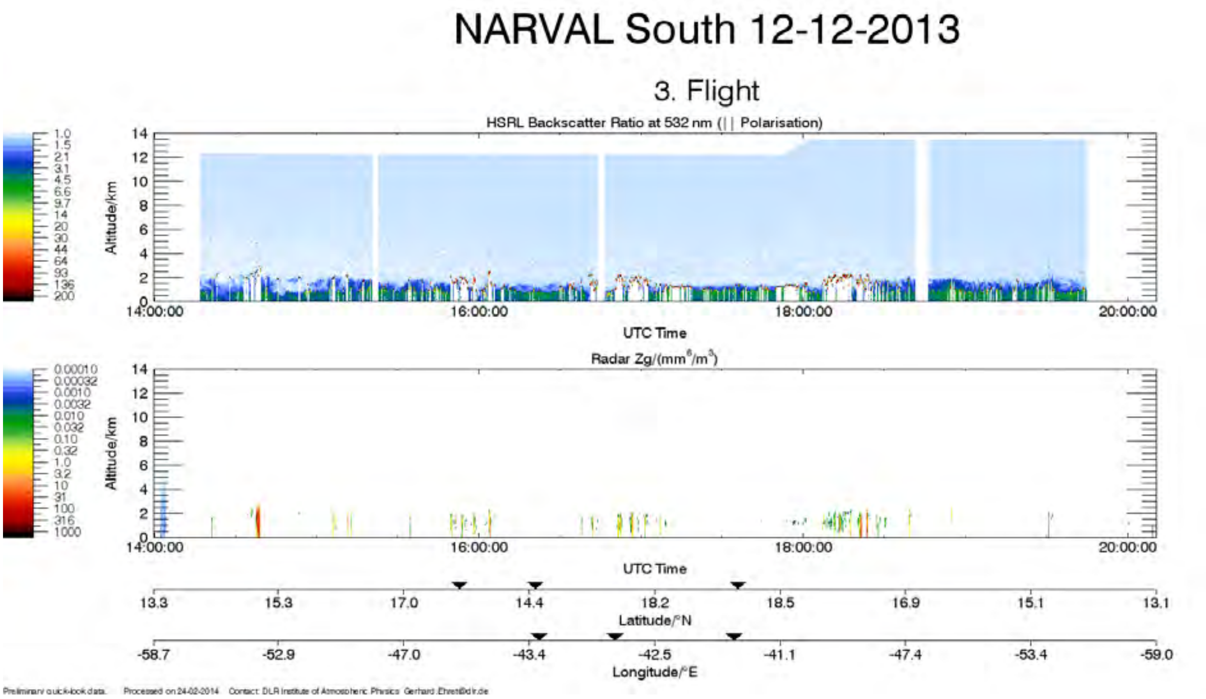

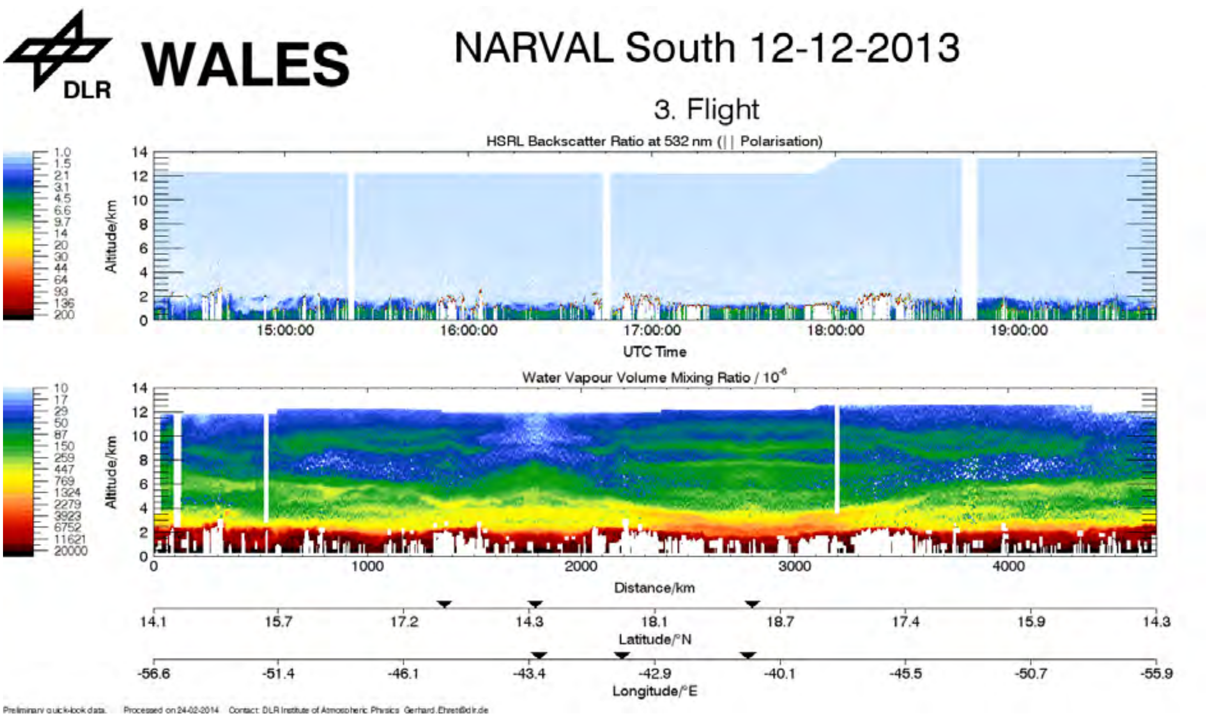

Fig.7: Time-height section of lidar backscattering vs. radar backscattering (upper panel) and lidar backscattering vs. water vapor volume mixing ratio (lower panel).

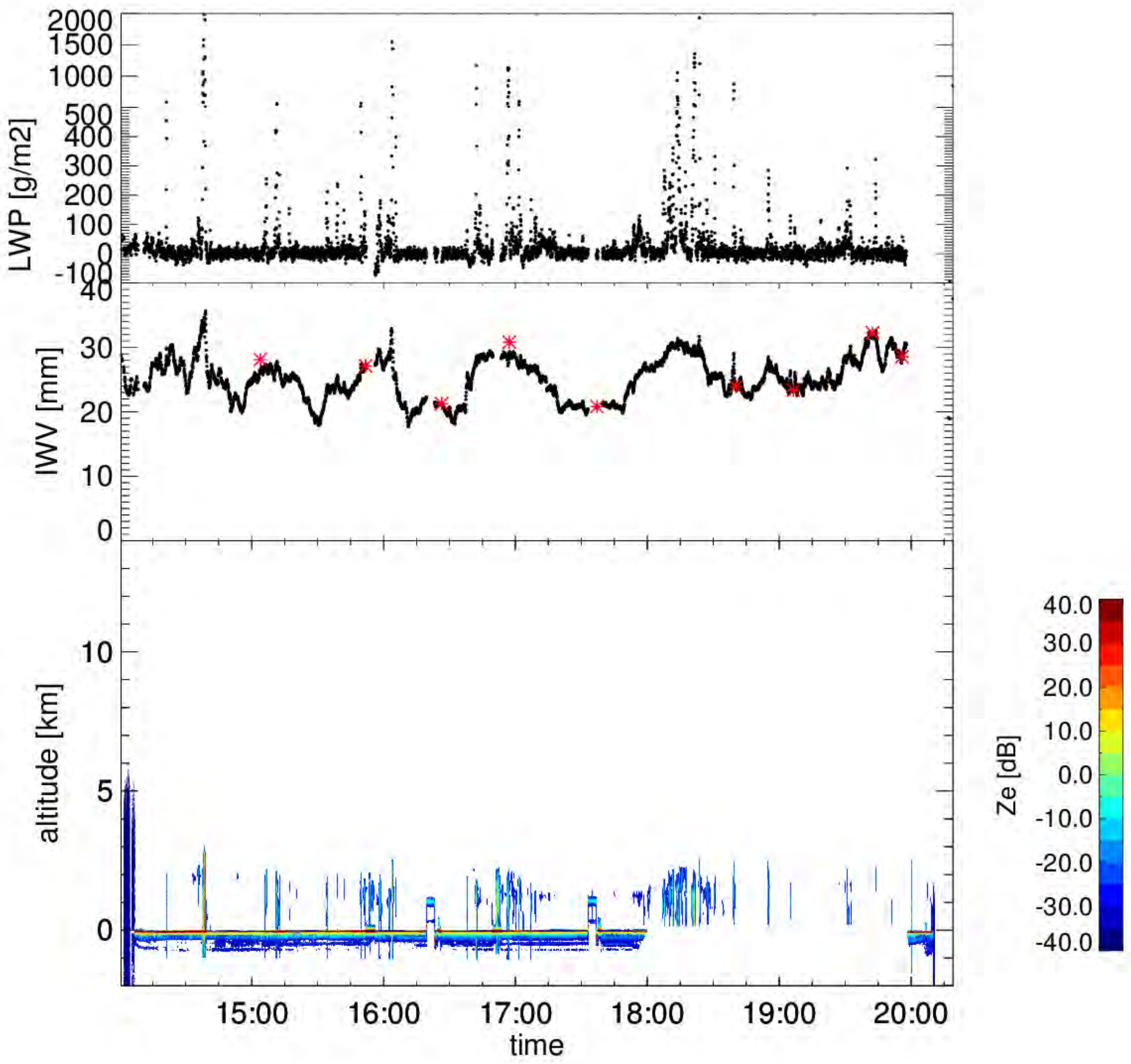

Fig.8: Time-height section of liquid water path (top panel) and integrated water vapor (middle panel) as derived from retrievals using the HAMP radiometer data vs. radar backscattering (lowest panel). Red stars in middle panel denote dropsonde derived integrated water vapor.

NARVAL South Research Flight 04 (RF04), Flight Report
- 14 December 2013 –

BJORN STEVENS

Objective: Mid-Atlantic cross section with CloudSat Overpass near terminal point.

Crew: Axel Amediek (WALES), Steffen Gemsa (Pilot), Michael Großrubatscher (Pilot), Friedhelm Jansen (HAMP), Bjorn Stevens (Mission PI), Ralph Zink (Flight Tech)

TABLE 1. RF04 times: Overpass time is given at the beginning of the track shown on track map (Fig. 3). Flight times are between start and end of BAHAMAS record.

Event	UTC Time (since 1970)	UTC Time (since midnight)	Date
Takeoff	1387028126.45	1335	14.12.2013
Overpass	1387037820.00	1629	”
Landing	1387052469.45	2021	”

Overview: Typical conditions prevailed. Convection to the south moved up into the western Caribbean with showers over Barbuda, some heavy, on and off during the day. Convection over eastern Atlantic fed an elevated layer of humidity for most of the flight; only over the central Atlantic did the atmosphere remain dry above 2 km. On return to Barbados more convective conditions prevailed and elevated humid layer became more pronounced throughout upper troposphere. CloudSat overpass was in a region that looked to be characterized by open cells, with a pronounced radar signature at time of overpass. Conditions over central Atlantic transitions to more closed cellular structures to the East. Similar to RF03, the flight level was increased from 41,000 to 45,000 ft at turn around.

Instruments: Eleven dropsondes launched all of which appeared to function well. The first sonde appeared to be carried by very strong upper level westerlies (25 m s^{-1}) to the east, which makes it appear off track. These strong westerlies were also evident in the satellite imagery, as cirrus blow off moved very rapidly eastward. Also evident in left panel of Fig. 1. One of the radiometer channels appeared to have difficulty remaining stable, although the drift between internal calibrations can be addressed in post-processing. Otherwise no known instrumental issues occurred.

Fig. 1. Convective blow off early in flight (left, 14:15 UTC) and convective conditions (right) upon return for landing (19:15 UTC). The last dropsonde was dropped near a more vigorous convective system near this (rightmost) image.

Fig. 2. Two images taken in succession (an hour apart) showing transition from open to closed convective structures. Left image of open cells taken at 16:28 UTC, coincident with CloudSat overpass, right image of closed cells taken an hour later at 17:30.

Fig. 3. Flight track showing positions of dropsondes and satellite overpass.

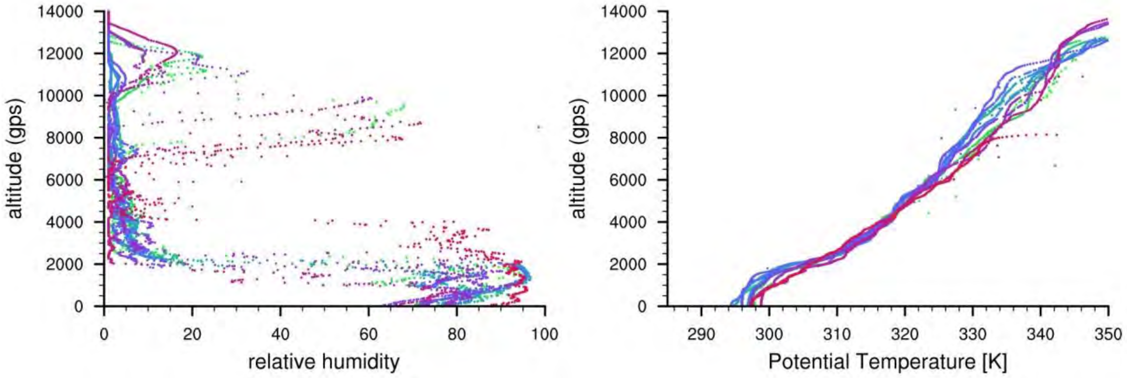

Fig 4. Dropsonde humidity and potential temperature, colored following colors on track map.

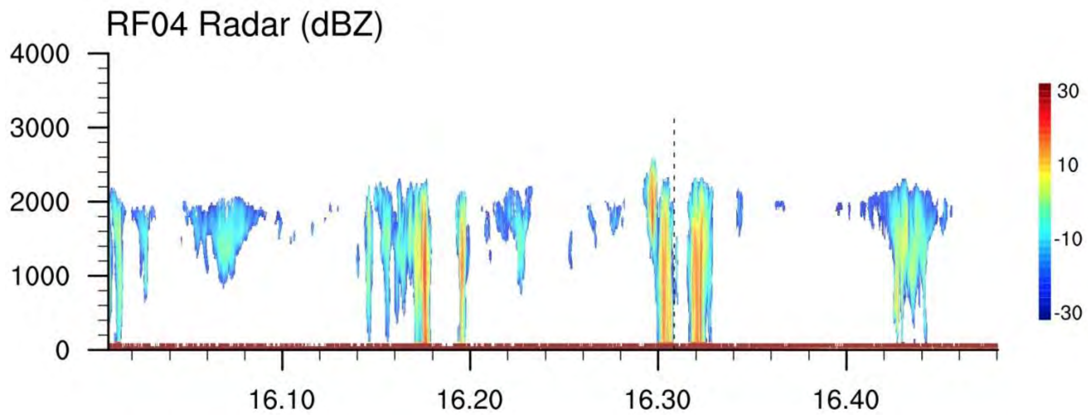

Fig. 5. Radar reflectivity during RF04 CloudSat overpass. Approximated overpass denoted by vertical dashed line.

Quicklooks RF04

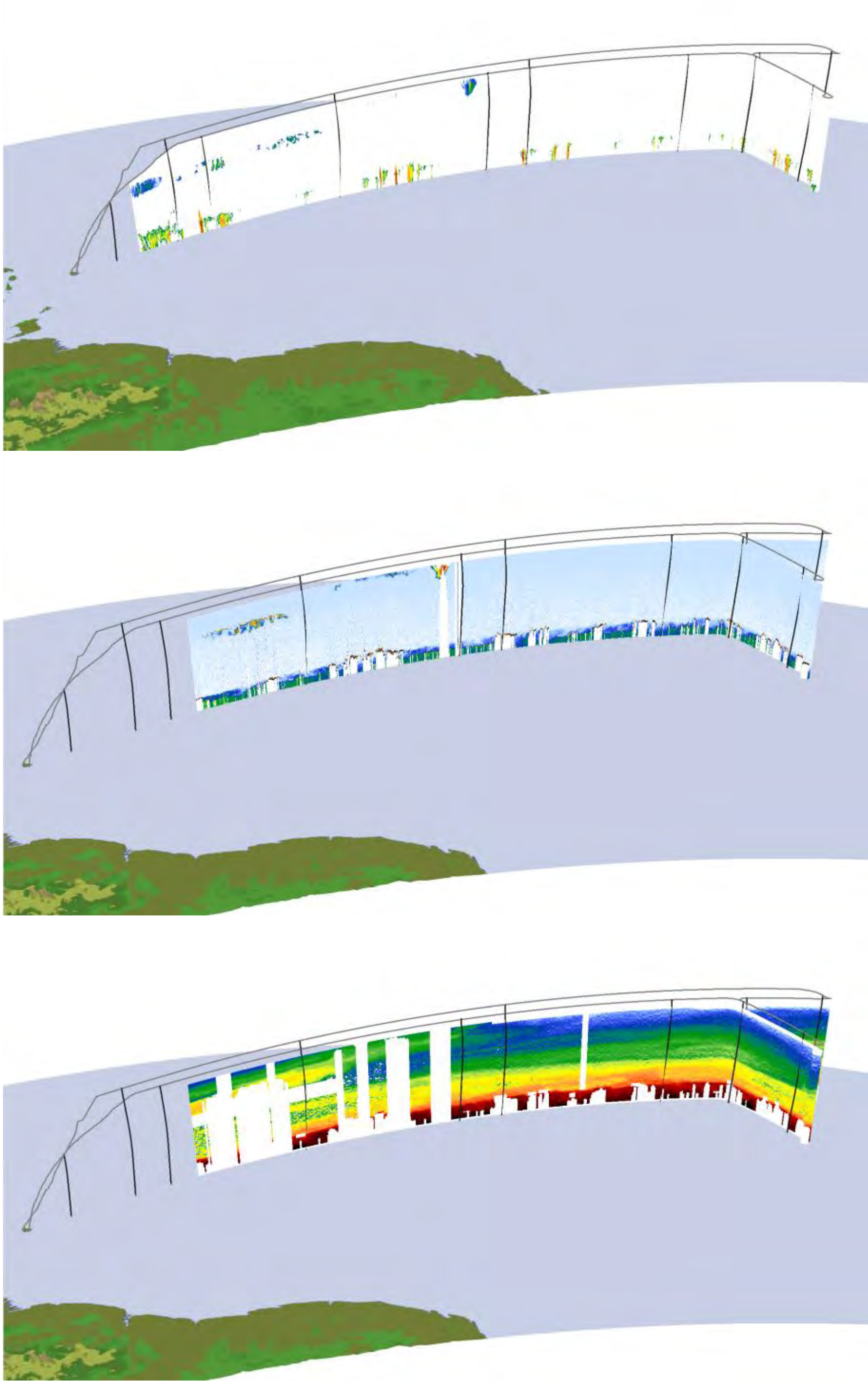

Fig.6: 3-D visualization of the radar backscattering (top panel), the lidar backscatter ratio (middle panel) and the derived water vapor mixing ratio (lower panel) along the entire flight track.

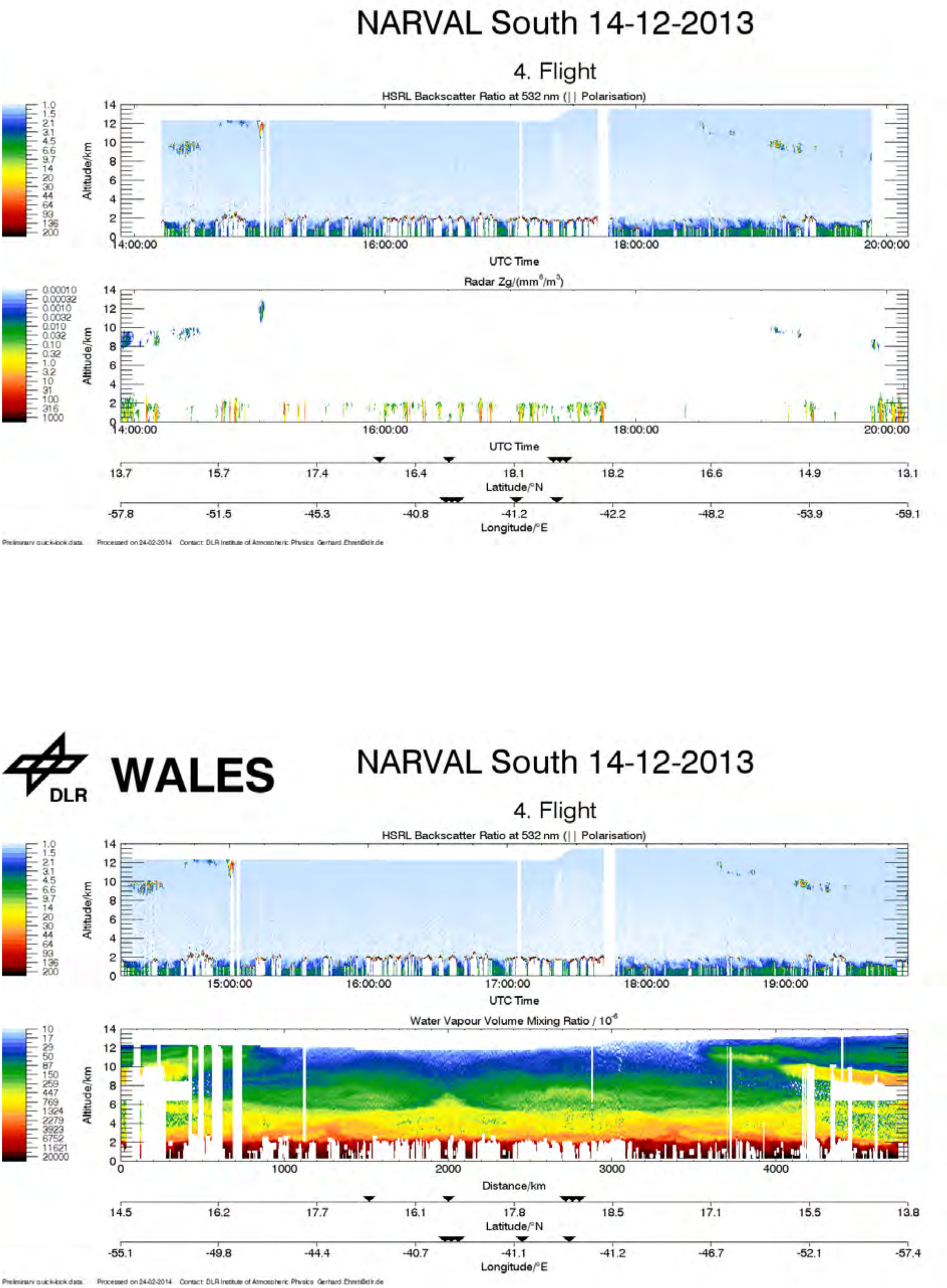

Fig.7: Time-height section of lidar backscattering vs. radar backscattering (upper panel) and lidar backscattering vs. water vapor volume mixing ratio (lower panel).

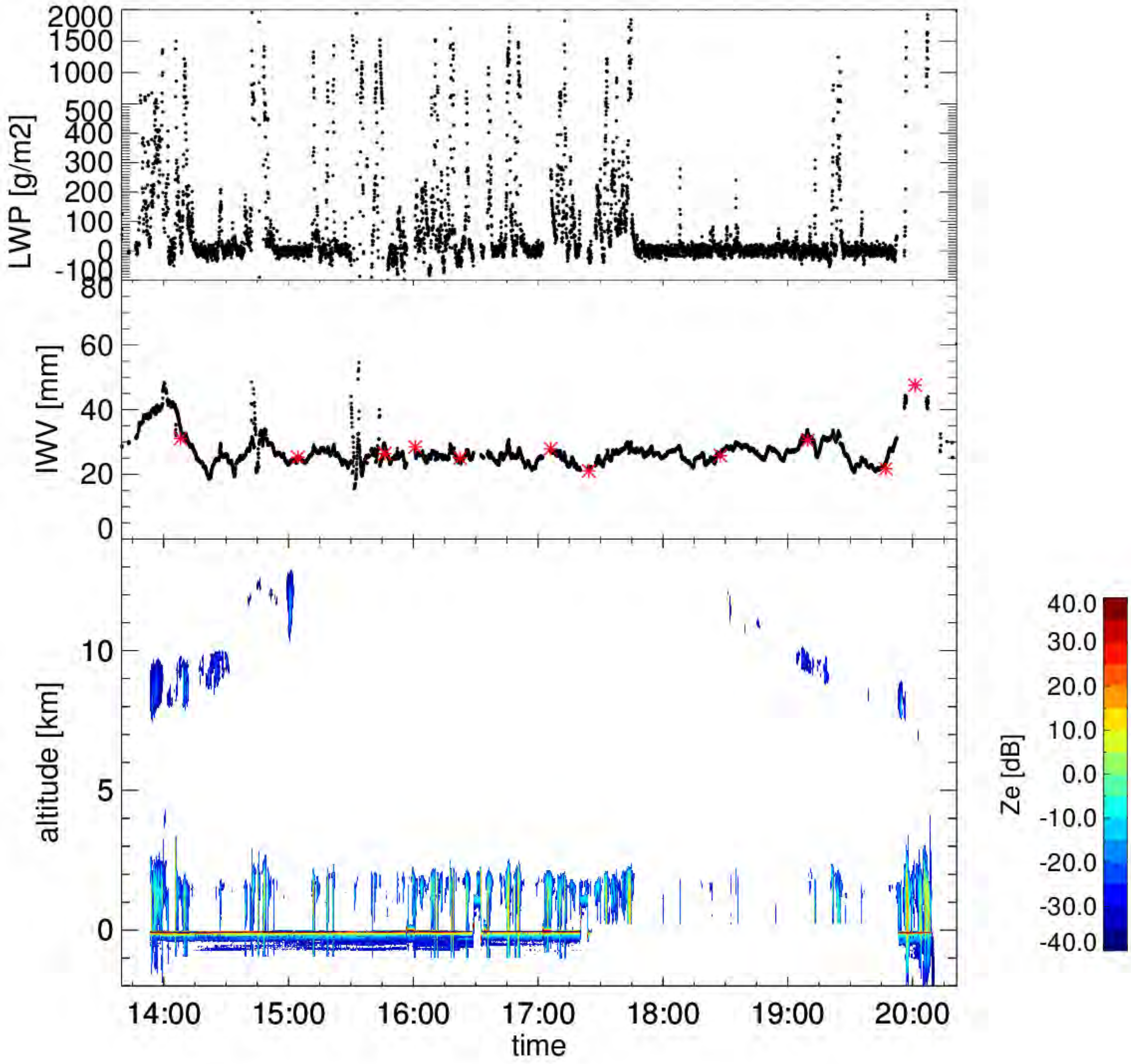

Fig.8: Time-height section of liquid water path (top panel) and integrated water vapor (middle panel) as derived from retrievals using the HAMP radiometer data vs. radar backscattering (lowest panel). Red stars in middle panel denote dropsonde derived integrated water vapor.

NARVAL South Research Flight 05 (RF05), Flight Report
- 15 December 2013 –

BJORN STEVENS

Objective: Mid-Atlantic cross section with CloudSat Overpass early during leg.

Crew: Steffen Gemsa (Pilot), Silke Gross (WALES, Birthday Girl), Michael Großrubatscher (Pilot), Lutz Hirsch (HAMP), Tilman Hüneke (miniDOAS), Emiliano Orlandi (HAMP-Radiometer and HALO-SR), Thomas Leder (Flight Tech), Bjorn Stevens (Mission PI)

TABLE 1. RF05 times: Overpass time is given at the beginning of the track shown on track map (Fig. 3). Flight times are between start and end of BAHAMAS record.

Event	UTC Time (since 1970)	UTC Time (since midnight)	Date
Takeoff	1387120508.45	1515	15.12.2013
Overpass	1387126800.00	1700	”
Landing	1387143957.45	2145	”

Overview: Typical conditions, as on previous flights, but less evidence of deep convection in the vicinity. There was some upper level cirrus toward end of flight but little sign of associated deep convection. Conditions appeared hazier at sunset, despite apparently very clean conditions. Flight pattern was identical to previous two flights, with an earlier CloudSat overpass. CloudSat was intersected on the return part of south-south-easterly oriented CloudSat leg, and there was very little sign of cloudiness; however on the outward part of the leg (see figure) there was a convective structure that was sampled, but apparently missed on the turn around. This could be because on the outward track we fly beyond the end point before turning, and return to the track at the end point, so the convective structure at the end of the track might have been on the CloudSat line, but missed on the return track because of how it is rejoined.

Instruments. Nine dropsondes launched all of which appeared to function well. Continuing stability issues with radiometer channel (183 GHz). Otherwise no known instrumental issues. In an attempt to provide calibration data for the downward looking instruments a series of three pitch and roll maneuvers were flown directly after the CloudSat leg (i.e., on the fourth leg). These consisted of continuously changing the pitch (up-down) and roll (right-left) this maneuver was repeated three times.

Fig. 1. Shallow convection (left) as seen from within cloud layer at takeoff (15:15 UT), mixed convective regimes toward end of leg at (18:15).

Fig. 2. Satellite images show pulses of convective lines, almost as if they are being spit out of West Africa. These images at 18:45, show convective structures that may be associated with the lines of convection, followed by clear patches seen in satellite imagery. On left the convection seems to be organized along a line of arcs with clear air behind and more stratiform clouds ahead (to left of line). Out the other window at the same time (one minute later) the more stratiform elements are evident.

Fig. 3. Flight track showing positions of dropsondes and satellite overpass.

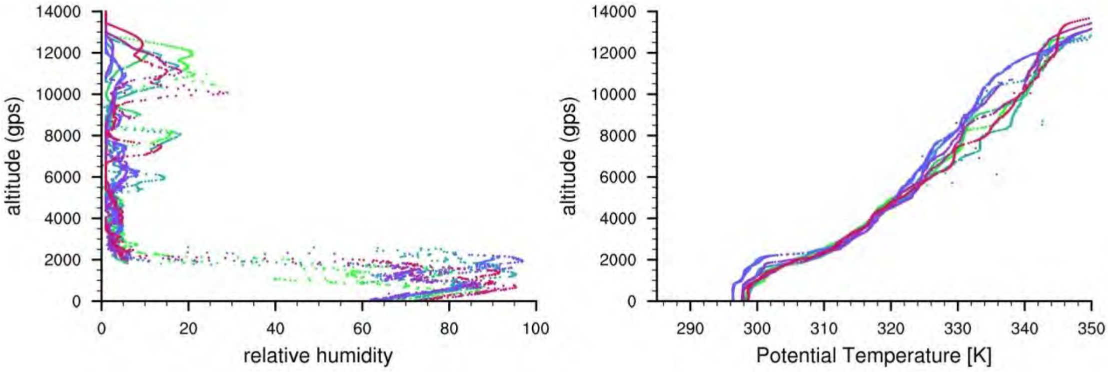

Fig. 4. Dropsonde humidity and potential temperature, colored following colors on track map.

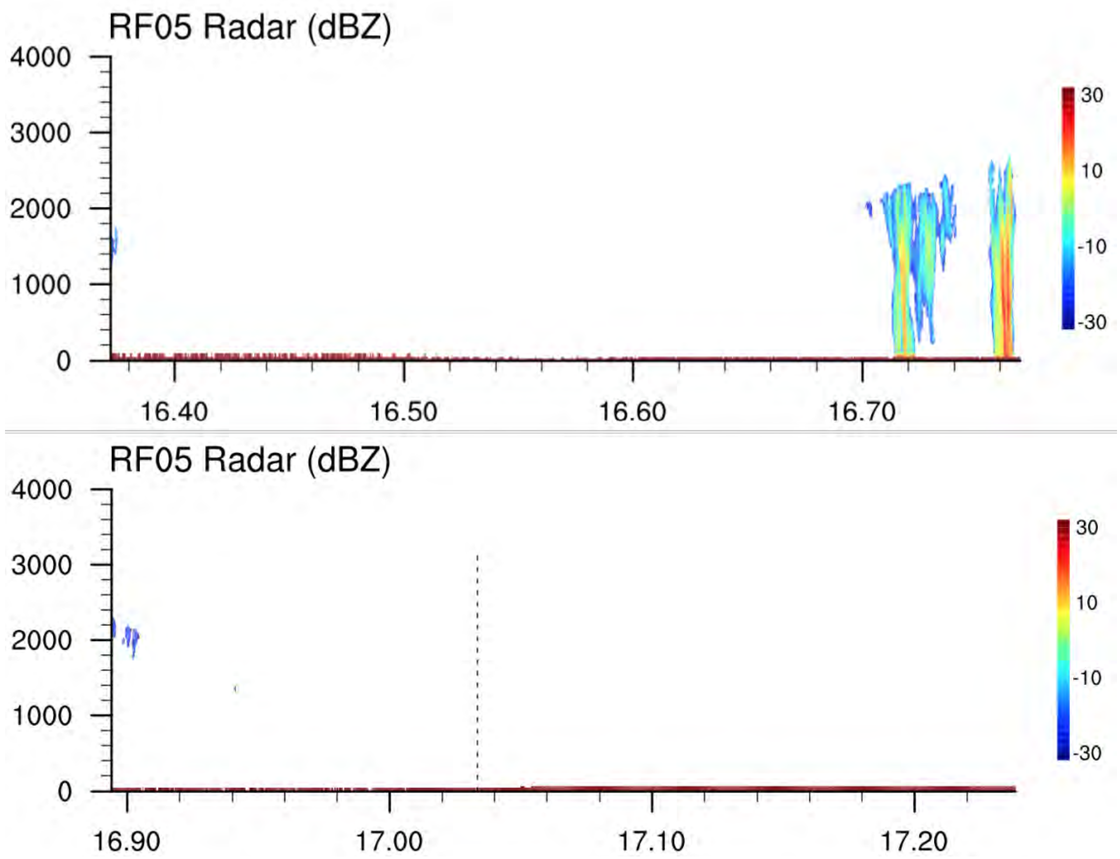

Fig. 5. Radar reflectivity during RF05 CloudSat overpass. Approximated overpass denoted by vertical dashed line on lower panel. Well-developed convective structure along line just before overpass, but after our turn and return it had vanished from the radar signature.

Fig. 6. NARVAL-South crew before takeoff of RF05

Quicklooks RF05

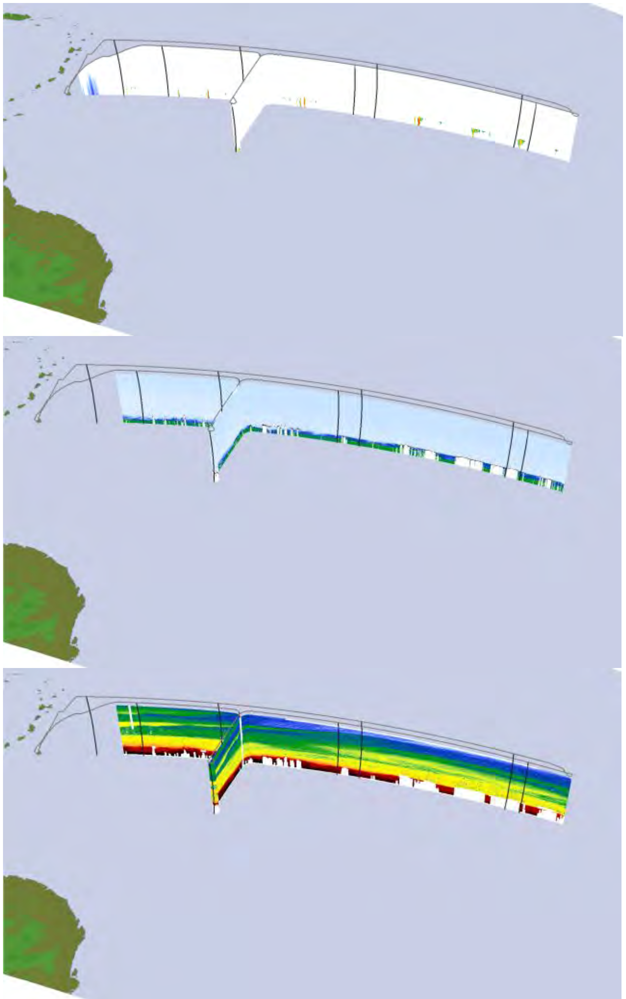

Fig.7: 3-D visualization of the radar backscattering (top panel), the lidar backscatter ratio (middle panel) and the derived water vapor mixing ratio (lower panel) along the entire flight track.

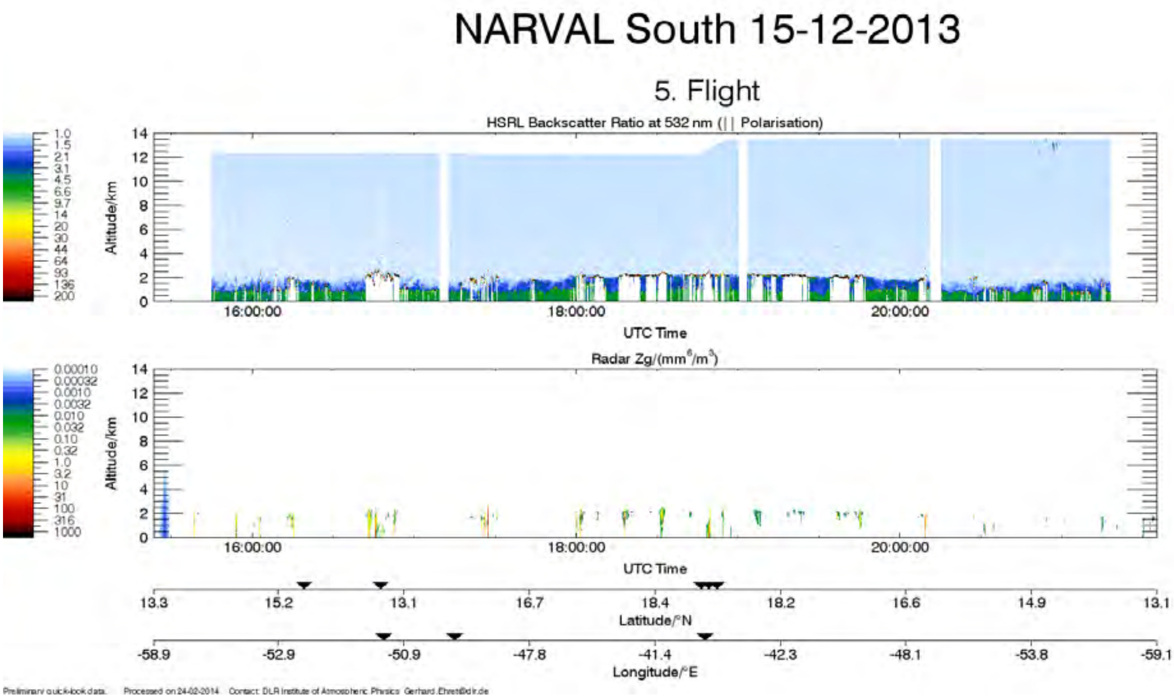

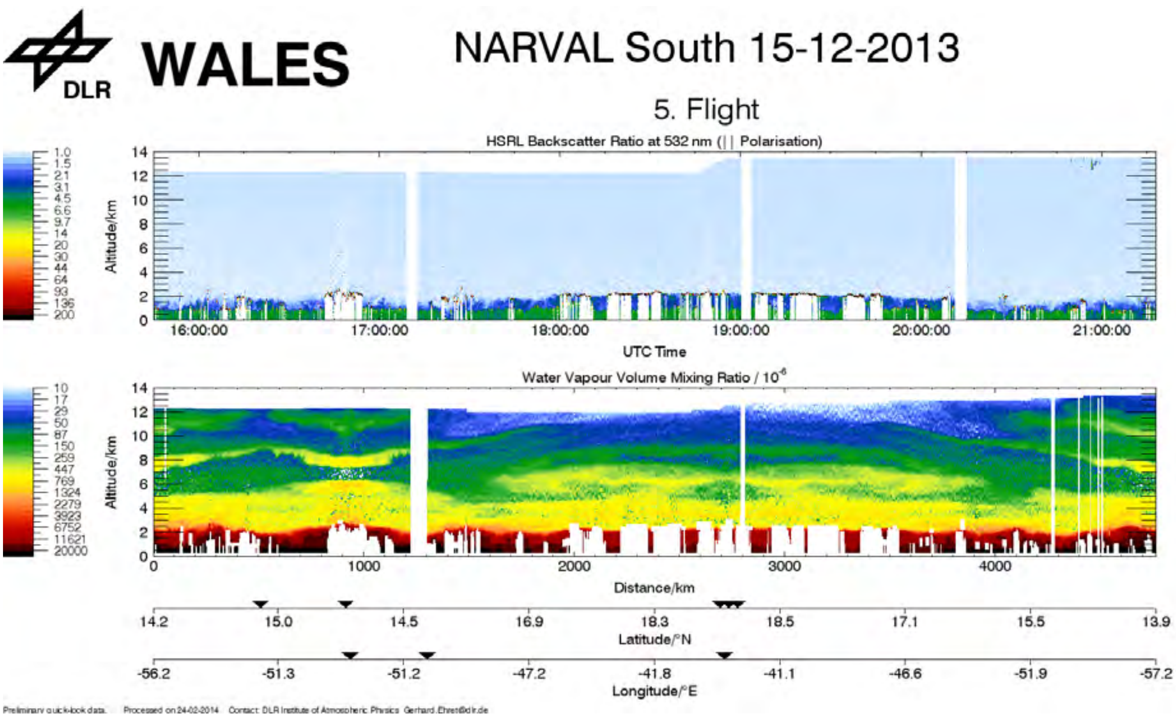

Fig.8: Time-height section of lidar backscattering vs. radar backscattering (upper panel) and lidar backscattering vs. water vapor volume mixing ratio (lower panel).

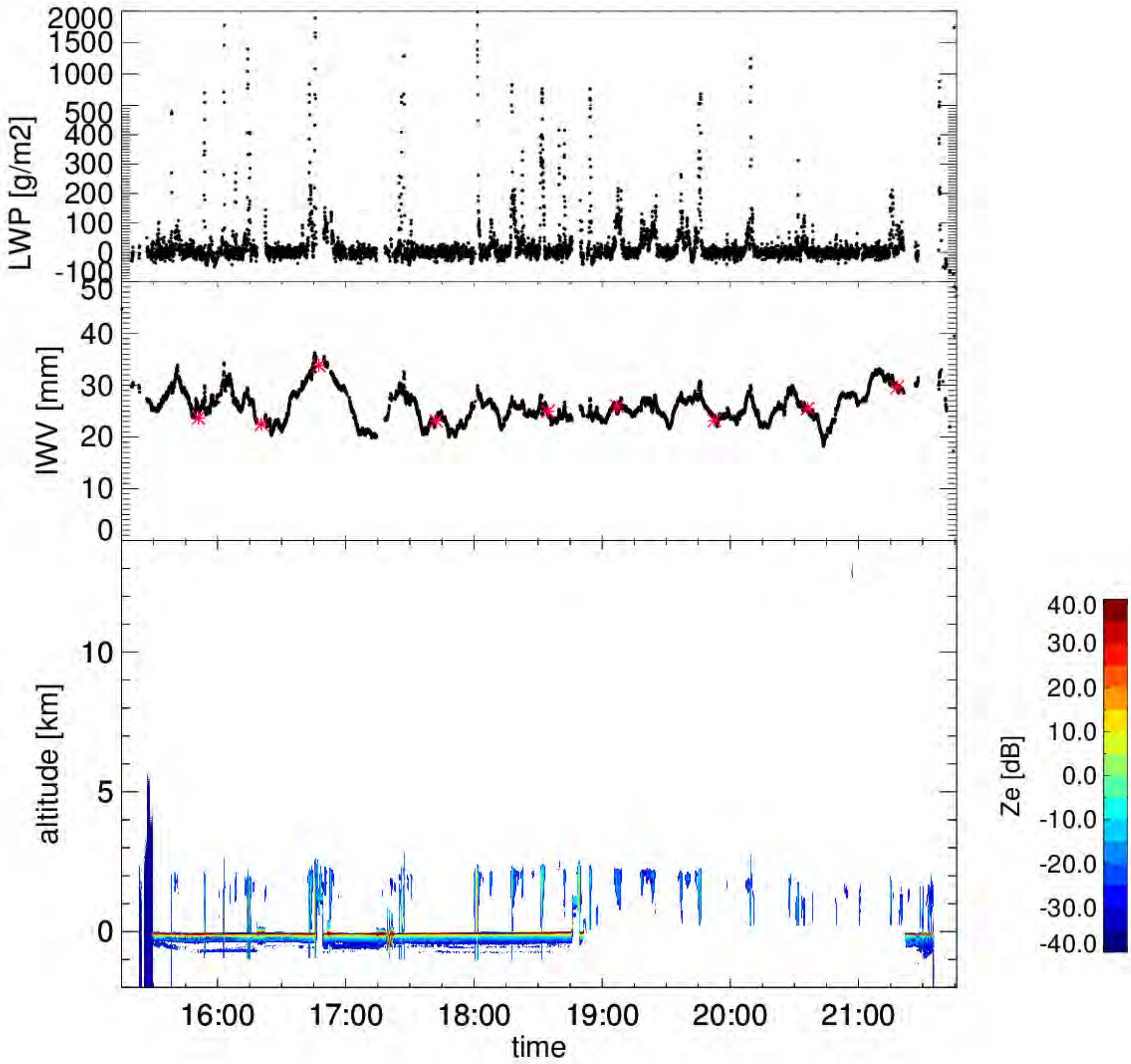

Fig.9: Time-height section of liquid water path (top panel) and integrated water vapor (middle panel) as derived from retrievals using the HAMP radiometer data vs. radar backscattering (lowest panel). Red stars in middle panel denote dropsonde derived integrated water vapor.

NARVAL South Research Flight 06 (RF06), Flight Report
- 16 December 2013 -

BJORN STEVENS

Objective: Return to Oberpfaffenhofen with a north subtropical Atlantic cross section with coordinated CloudSat overpass over mid Atlantic.

Crew: Axel Amediek (WALES), Silke Gross (WALES), Steffen Gemsa (Pilot), Michael Großrubatscher (Pilot), Lutz Hirsch (HAMP), Tilman Hüneke (miniDOAS and HALO- SR), Bjorn Stevens (Mission PI), Ralph Zink (Flight Tech)

TABLE 1. RF06 times: Overpass time is given at the beginning of the track shown on track map (Fig. 3). Flight times are between start and end of BAHAMAS record.

Event	UTC Time (since 1970)	UTC Time (since midnight)	Date
Takeoff	1387199457.45	1310	16.12.2013
Overpass	1387209900.00	1605	”
Landing	1387234784.45	2259	”

Overview: Well developed inversion and large bands of stratocumulus, fed by lines or arcs of underlying cumulus, under a deep (800 hPa) inversion were evident already at 14:30-15:00 UTC. Some of the stratocumulus (which was quite grey) was evident in the radar signal. Before meeting CloudSat orbit we flew through an unusually large batch of clear skies, upon meeting track and turning to north we passed over well-developed bands of shallow convection with large stratocumulus outflows under an 800 hPa inversion. Fourth sonde coincident with start of track. Fifth sonde at track end. Moderate to strong turbulence around 18 Z, strong side wind and CB in the distance. Attempted to throw the ninth sonde in the CB, resulting in a deep humid layer showing up on the sonde. Cirrus at 10 km on approach to Portugal coast.

Instruments: Ten dropsondes launched over the Atlantic. All sondes appeared to function well. Difficulties with the data from the IGI (new inertial navigation system) hence most aircraft state variables (pitch, roll, etc.) are provided by the old INS and position variables are taken from GPS. Other instruments appear to have functioned as intended. Photos of laptops for calibration of camera. Camera set to UTC time for subsequent flights.


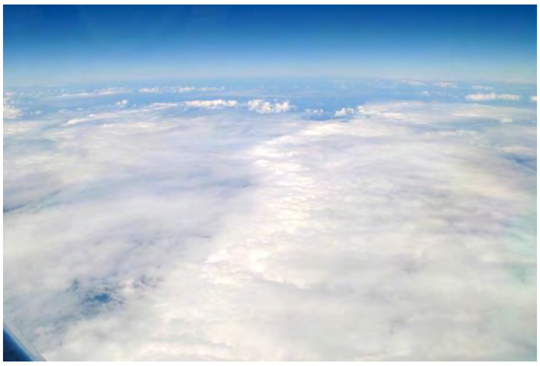

Fig. 1. Scattered chimney convection at take off, some with bibulous heads as shown on left (around 13:15 UTC). Large stratocumulus patched under a strong inversion around 15:00 UTC, here (on right) shown being fed by a line of cumulus convection.


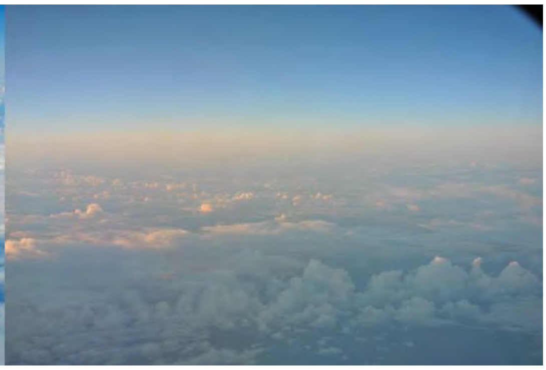

Fig. 2. Convective features at the beginning of the overpass leg just before 16:00 UTC (left). Deeper convective layer over colder oceans late in the day (18:30) UTC.

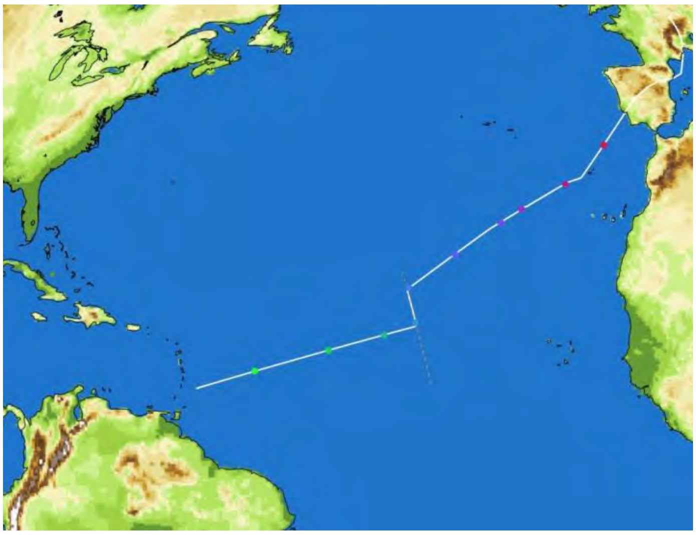

Fig. 3. Flight track showing positions of dropsondes and satellite overpass.

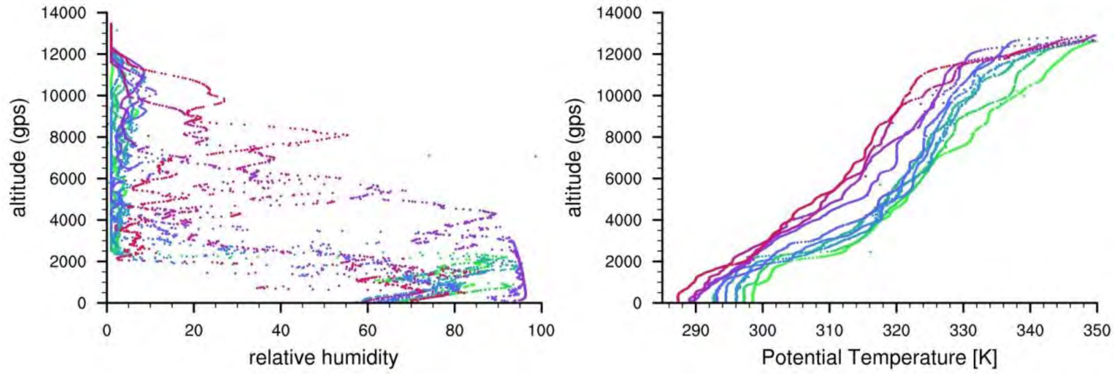

Fig. 4. Dropsonde humidity and potential temperature, colored following colors on track map.

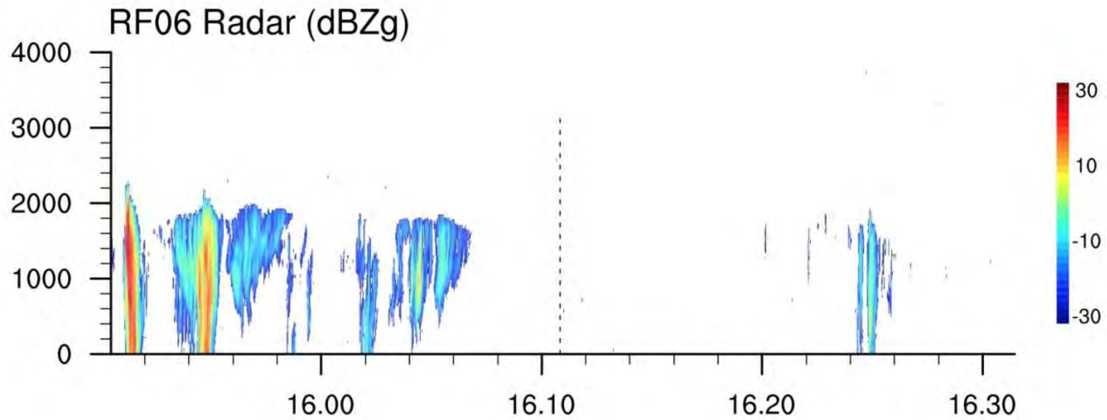

Fig. 5. Radar reflectivity during CloudSat overpass. Approximated overpass denoted by vertical dashed line.

Quicklooks RF06

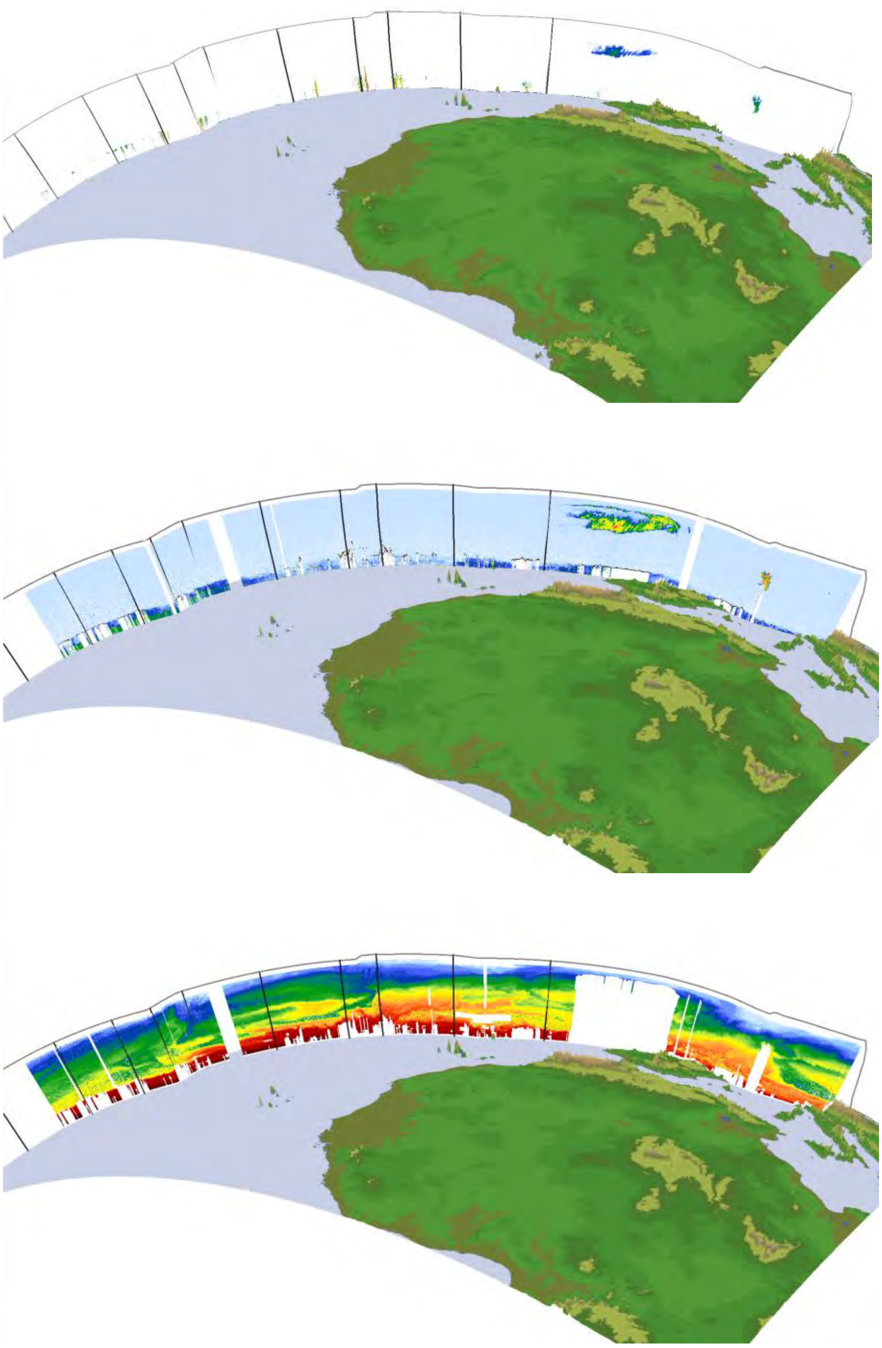

Fig.6: 3-D visualization of the radar backscattering (top panel), the lidar backscatter ratio (middle panel) and the derived water vapor mixing ratio (lower panel) along the entire flight track.

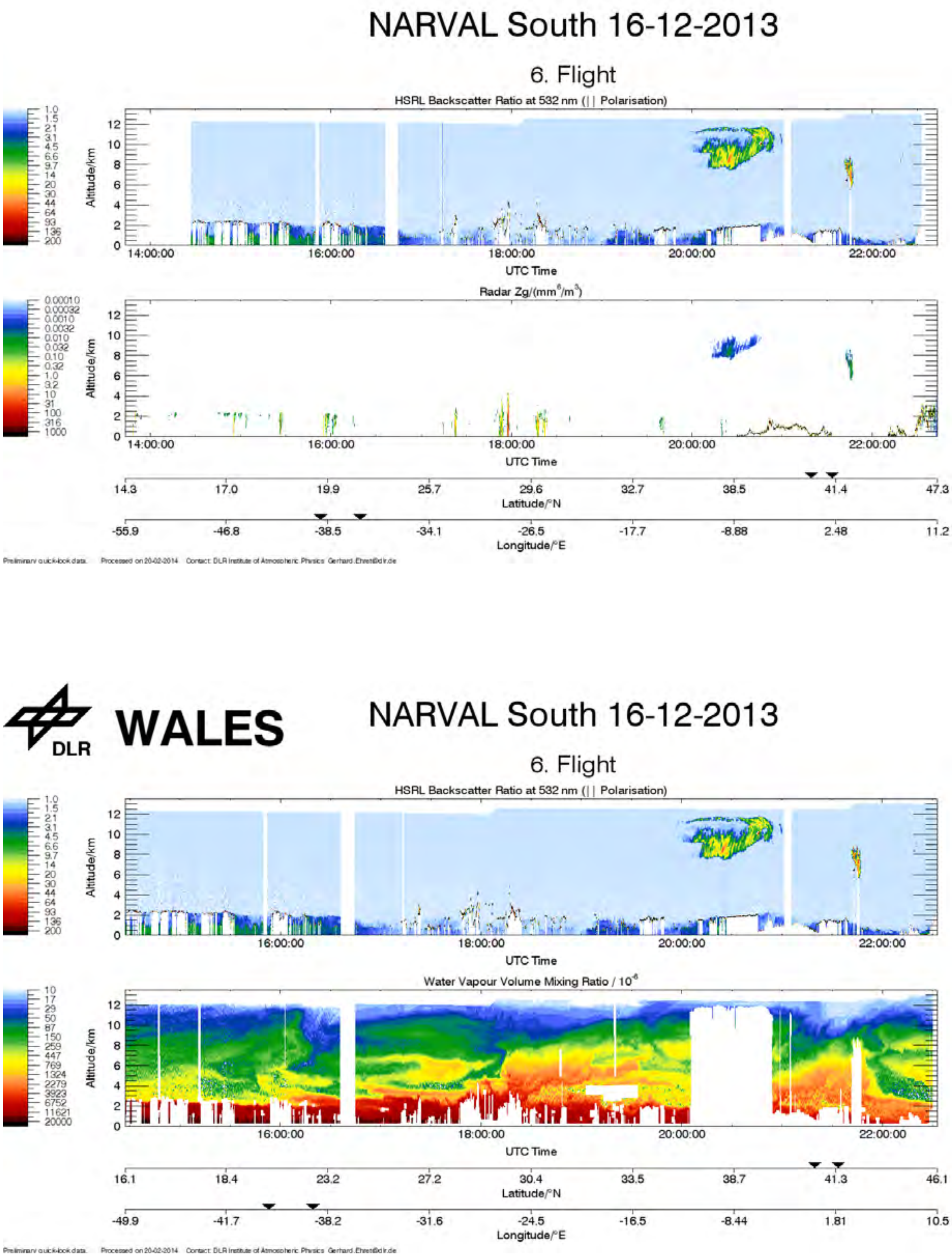

Fig.7: Time-height section of lidar backscattering vs. radar backscattering (upper panel) and lidar backscattering vs. water vapor volume mixing ratio (lower panel).

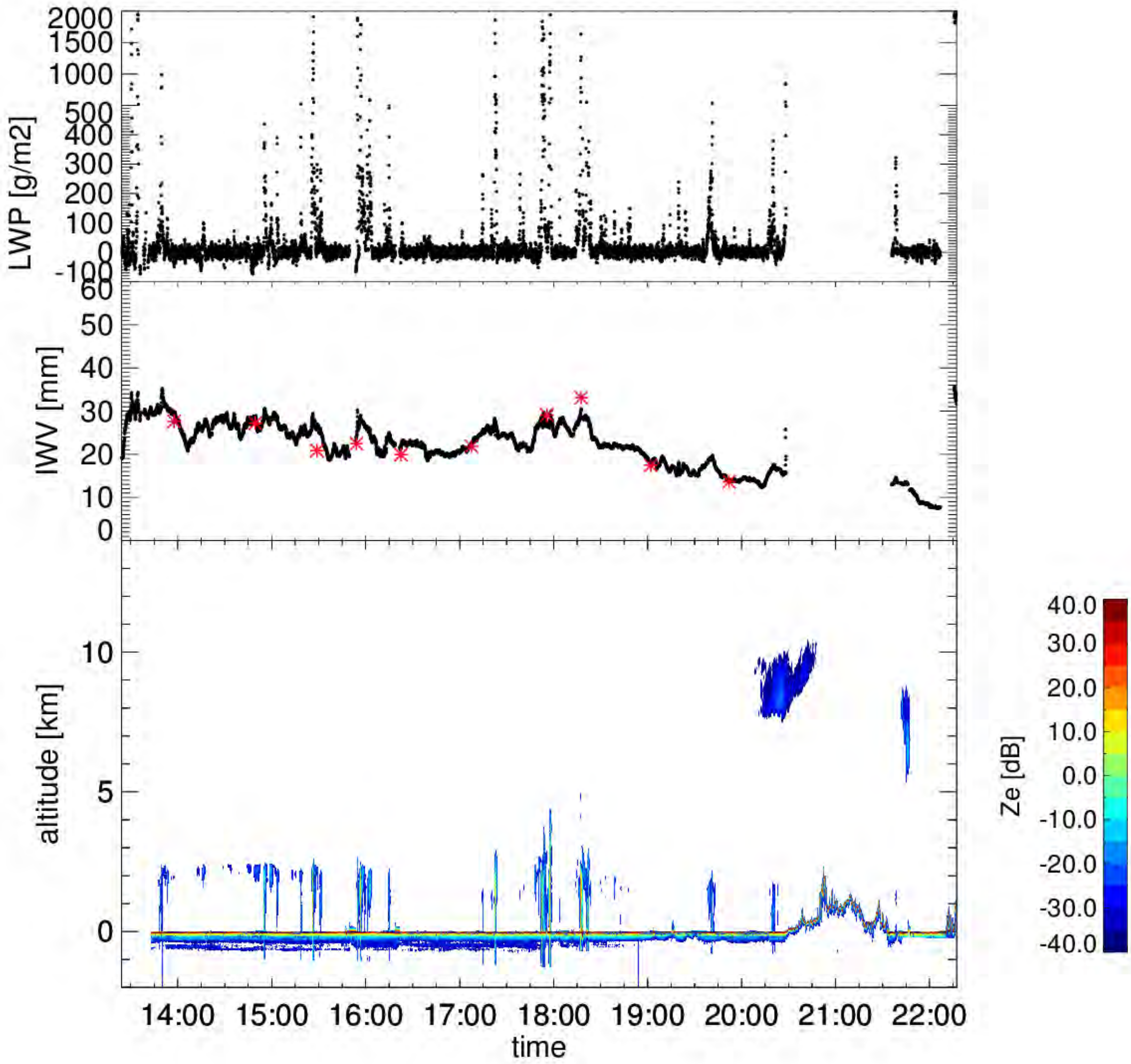

Fig.8: Time-height section of liquid water path (top panel) and integrated water vapor (middle panel) as derived from retrievals using the HAMP radiometer data vs. radar backscattering (lowest panel). Red stars in middle panel denote dropsonde derived integrated water vapor.

NARVAL South Research Flight 07 (RF07), Flight Report

- 19 December 2013 -

LUTZ HIRSCH

Crew: Steffen Gemsa (Pilot), Michael Großrubatscher(Pilot), Andreas Fix (WALES), Friedhelm Jansen (HAMP), Insa Lohse (HALO-SR), Christian Büdenbender (WALES), Alexander Wolf (DLR) , Lutz Hirsch (Flight PI)

Takeoff: 10:05 UT

Radar on: 10:15 UT
Radar operational: 10:40 UT (file_name: 20131219_1040.mmclx)

Rendezvous Falcon: approx. 11:00 UT - ca 11:37UT
(3 miles distance as of 11:10)

climb to FL 430
due to strong headwind: 11:45 UT
Portuguese Coast: approx. 12:35 UT Cam-Images DSC_688[5-7]
approx. 12:49 UT Cam-Images
Dropsonde 1: 12:55 UT Cam-Images
50 miles north of Pos.1(N37° 37‘ W 012° 43‘)

Fig. 1: 12:57 UT

Dropsonde 2: approx. 13:30 UT near Pos. 3 (N35° 02‘ W 16° 42‘)

Dropsonde 3: approx. 14:27 UT, on approx. N32° 34‘ W20° 48‘

skipped satellite overpass due to strong headwind

Dropsonde 4: 15:30 UT at N 28° W 28° on beginning of new cloud layer at approx.8000 m.

Fig. 2: 15:28 UT

Dropsonde 5: 16:20 UT at N 24° W 34° 30‘ end of upper cloud deck.

Dropsonde 6: 17:00 at N 20,87° W 39,28° near convective cells

No Dropsondes 17:10 - 18:20 UT due to airspace restrictions

Dropsonde 7: 18:24 UT at N 17.15 W 49.6

Dropsonde 8: 19:00 UT at approx. N 15.2° W 54°

Fig. 3: 19:04 UT

Dropsonde 9: 19:26 UT at approx. N 14.15° W 57°

TD: 19:57 UT at BGI

Performance of the measuring systems:

Radar: operation from 10:40 to 19:40
Radiometers: continuous operation, pre and post calibration performed
Lidar: continuous operation
HALO-SR: continuous operation
miniDOAS: continuous operation

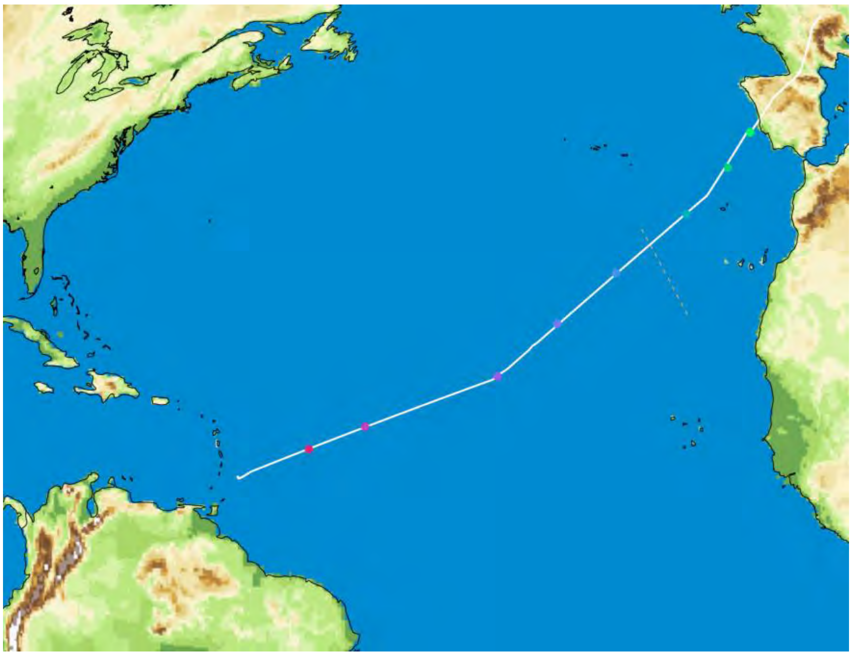

Fig. 4: Flight track showing positions of dropsondes and satellite overpass.

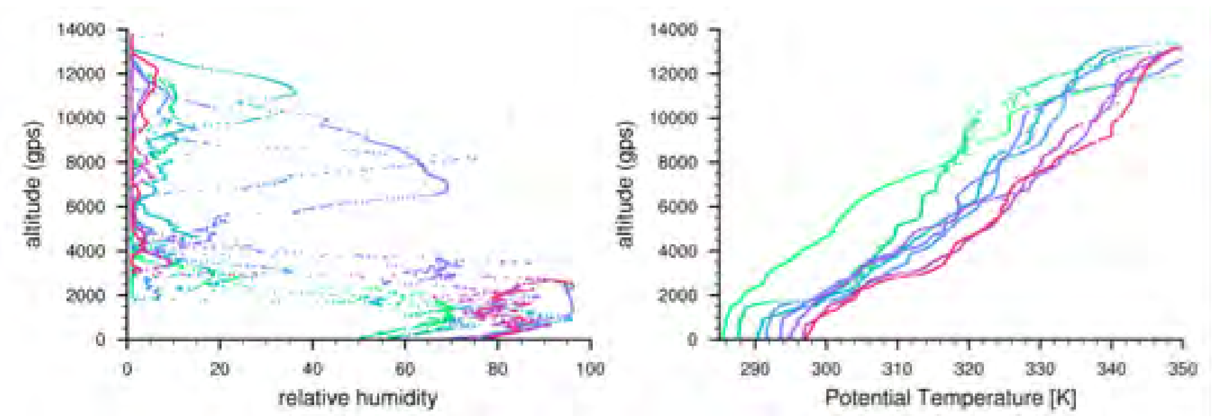

Fig. 5: Dropsonde humidity and potential temperature, colored following colors on track map.

Our observations of limb and Nadir scattered sunlight in the nearIR spectral range contain information on the radiative transfer, as well as of some optical (and microphysical) properties of aerosols and clouds. However, our current spectral retrieval tools (i.e., DOAS) are not yet well suited to perform a quantitative analysis for spectra containing saturated, i.e. non-linear with amount of absorber behaving absorption features (see Figure 6). Further, due to the lower solar irradiance as compared to the UV/vis range, the nearIR spectra have lower signal-to-noise ratios in general. This precludes a DOAS type approach for the spectral retrieval.

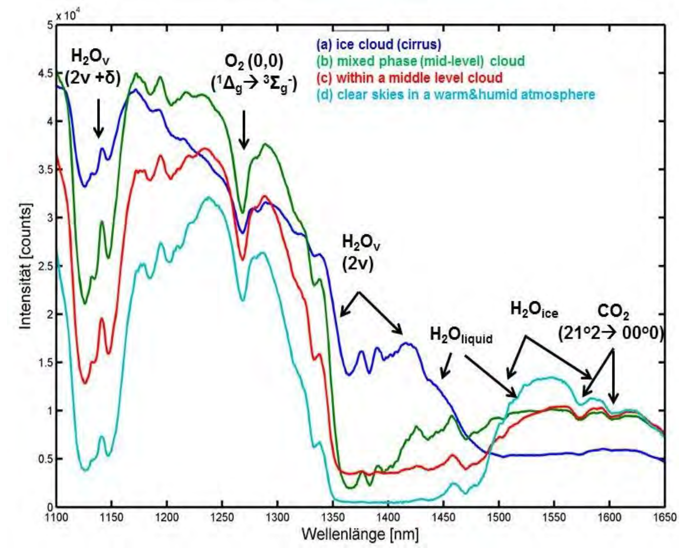

Fig. 6: Measured nearIR spectra during the NARVAL campaign flight from BGI to OBF on Dec. 19, 2013. The individual spectra were measured (a) during the presence of Cirrus cloud (first and fourth line from left in Figure 3), (b) mixed phased mid-level clouds (second line from left in Figure 3), (c) middle level cloud (third line from left in Figure 3), and (d) clear skies in a humid atmosphere (most right line in Figure 3). The spectra can be interpreted for liquid and ice water content, effective radius and cloud optical thickness using a refined Nakajima and King (1990) retrieval, which would use the information from the whole spectra rather than relative radiances of two wavelength bands (adopted Marcel Reichert, Diploma thesis, 2014).

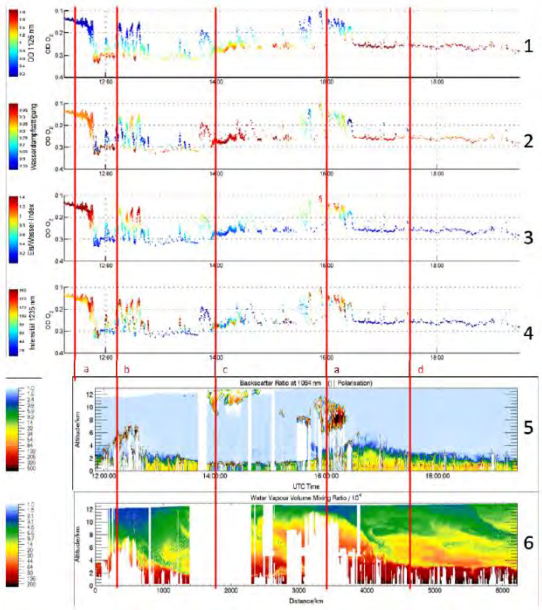

Fig. 7: *Inferred O_2 ODs at 1270 nm (vertical axis in panel 1 to 4) in Nadir direction during the HALO flight from BGI to OBF on Dec. 19, 2013 as a function of time with color scales of*

1. *OD of H_2O_v (2v+δ) absorption (panel 1)*
2. *Water saturation (panel 2)*
3. *Ice water index (panel 3)*
4. *Radiance at 1235 nm (panel 4)*
5. *Backscattering at 1064 nm from DLR-WALES (panel 5)*
6. *Inferred water vapor from DLR-WALES (panel 6)*

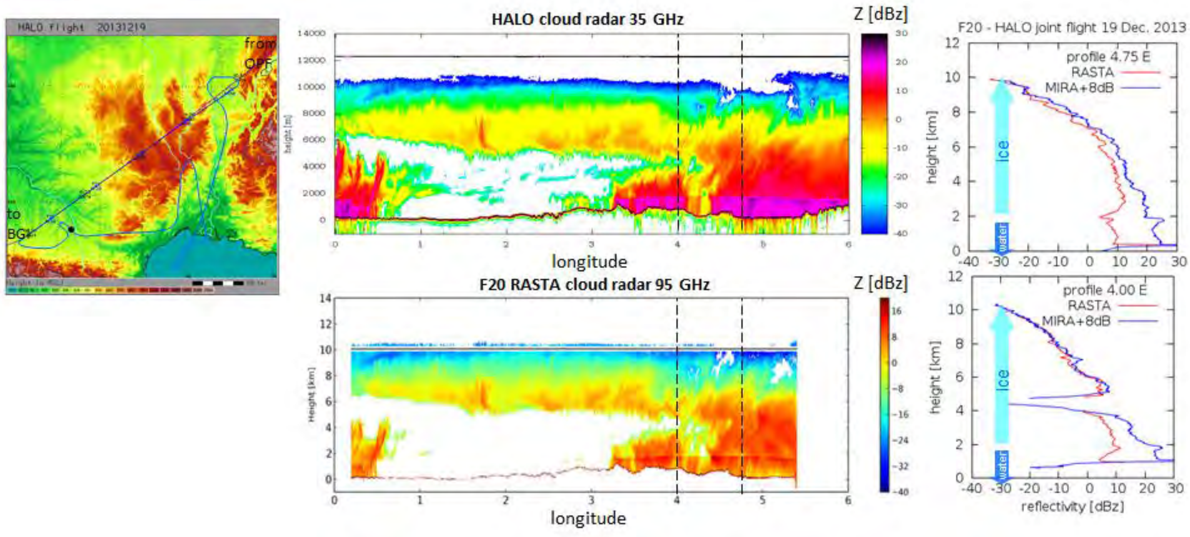

Fig. 8: HALO Cloud Radar (Ka-band) collocated flight with the French Falcon RASTA (W-band radar) on 19 Dec. 2013 during NARVAL South between Lyon and Tarbes. Differential attenuation (35 – 95 GHz) as measure for DSD and LWC.

Quicklooks RF07

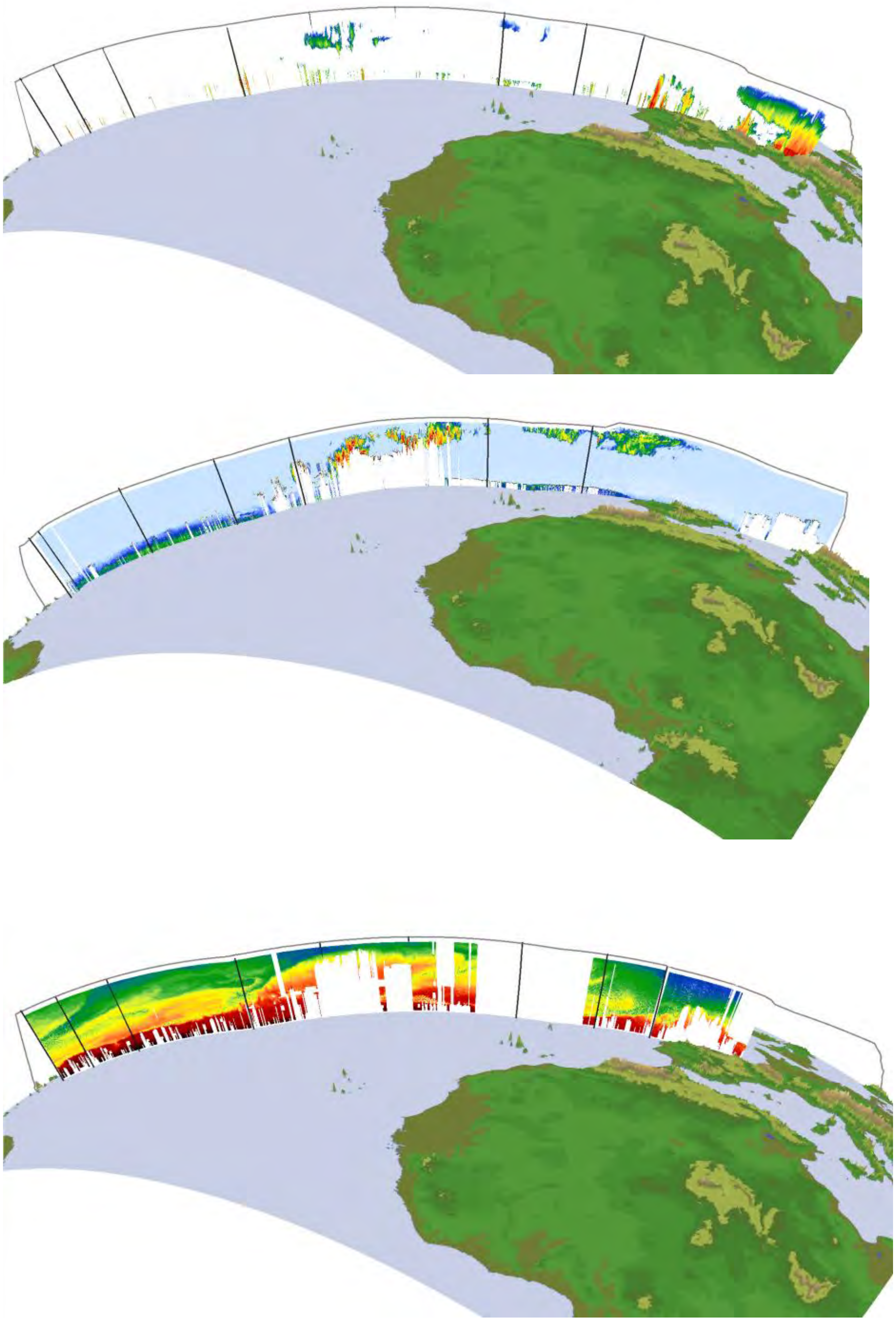

Fig.9: 3-D visualization of the radar backscattering (top panel), the lidar backscatter ratio (middle panel) and the derived water vapor mixing ratio (lower panel) along the entire flight track.

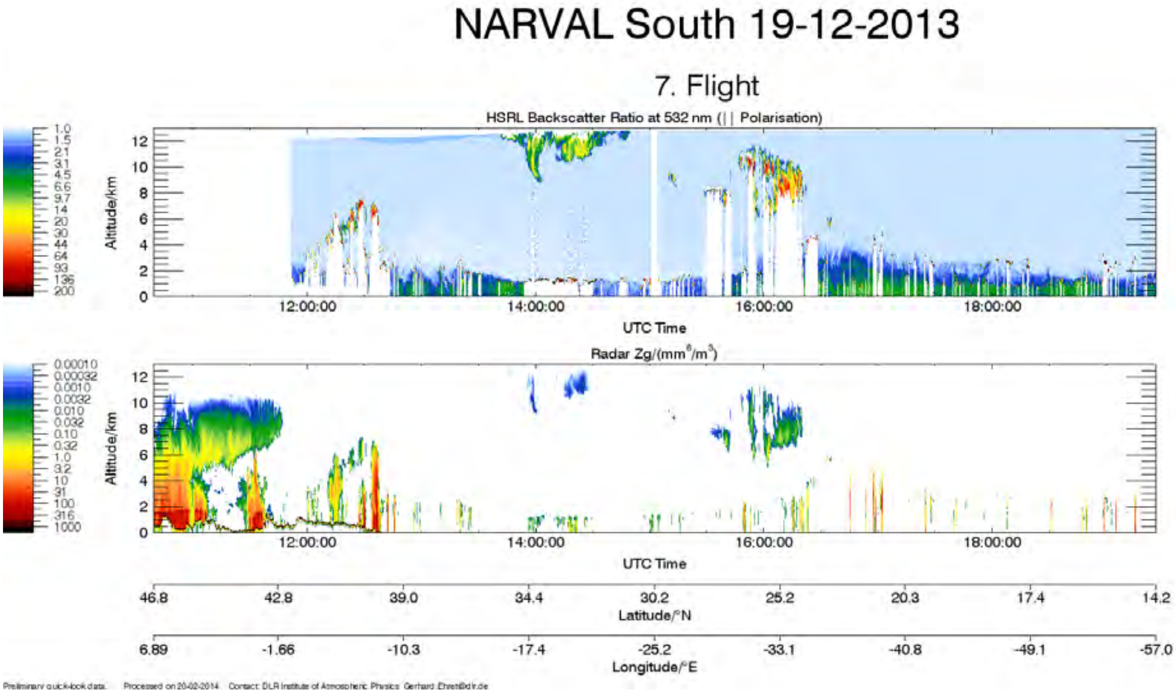

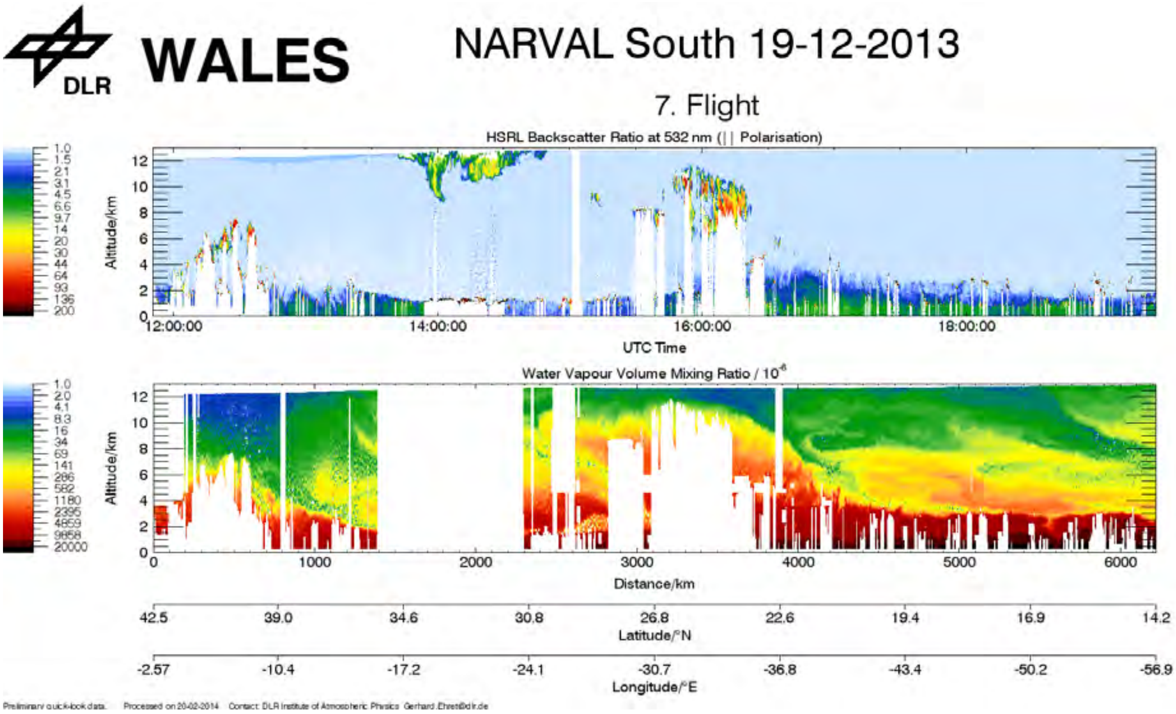

Fig.10: Time-height section of lidar backscattering vs. radar backscattering (upper panel) and lidar backscattering vs. water vapor volume mixing ratio (lower panel).

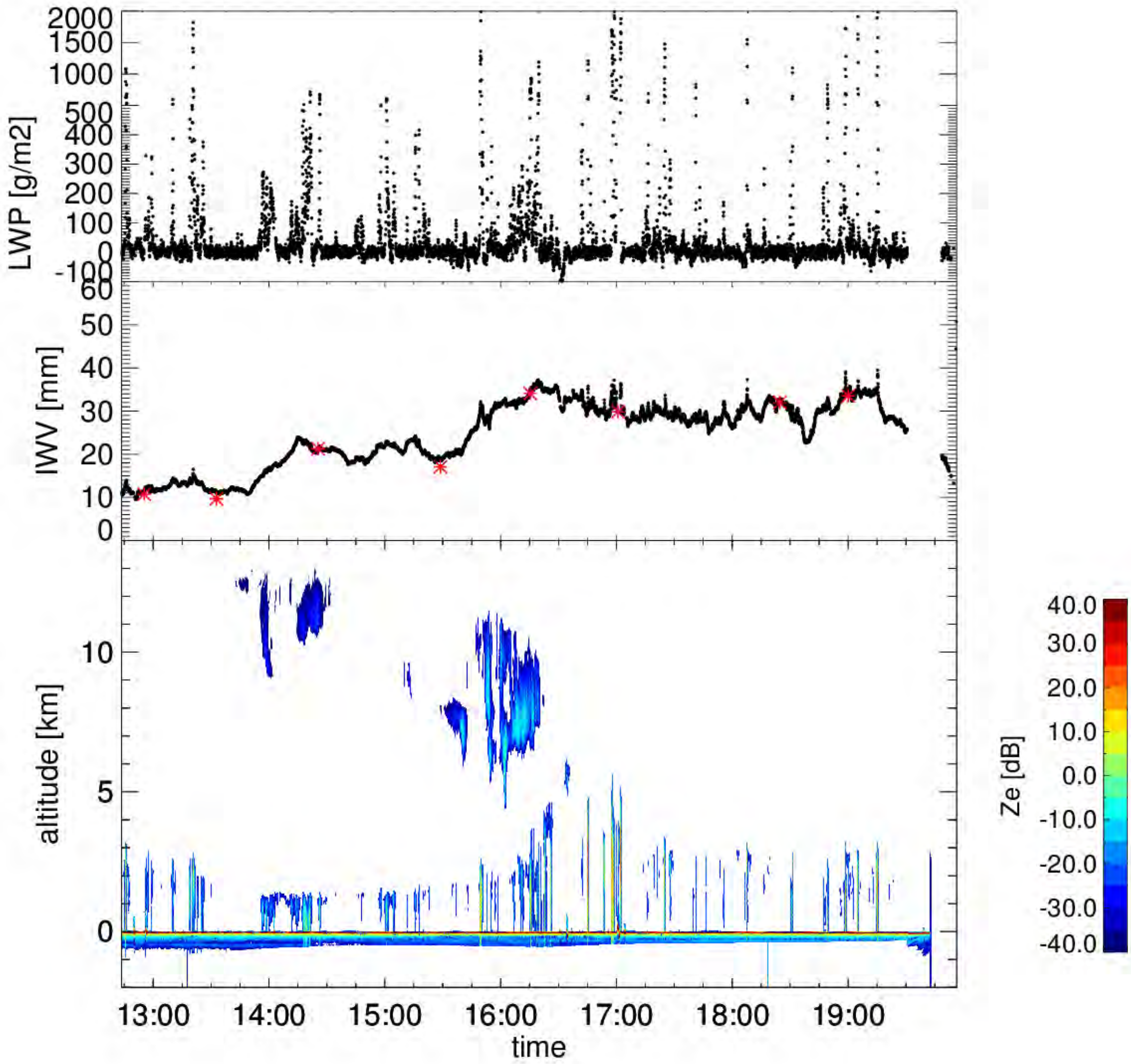

Fig.11: Time-height section of liquid water path (top panel) and integrated water vapor (middle panel) as derived from retrievals using the HAMP radiometer data vs. radar backscattering (lowest panel). Red stars in middle panel denote dropsonde derived integrated water vapor.

NARVAL South Research Flight 08 (RF08), Flight Report

- 20 December 2013 -

LUTZ HIRSCH

Crew: Steffen Gemsa (Pilot), Michael Großrubatscher(Pilot), Andreas Fix (WALES), Friedhelm Jansen (HAMP), Insa Lohse (HALO-SR) , Christian Büdenbender (WALES), Alexander Wolf (DLR) , Lutz Hirsch (Flight PI)

Takeoff:	16:20 UT	
Radar on:	16:40 UT	
Radar operational:	16:47 UT	(file_name: 20131215_1531.mmclx)
Lidar operational:	17:15 UT	
Dropsonde 1:	17:12 UT	at N 12.8° W 55.3° beginning of CloudSat underflight
Dropsonde 2:	17:23 UT	at N 14.2° W 55.7 middle of CloudSat underflight at overpass time
Dropsonde 3:	17:30 UT	at N 15.0° W 55.9° end of CloudSat underflight underflight dropsonde seems to be defect decision to drop another

Figures 1 - 5 (below): Cloud scenes during the CLOUDSAT overpass

Fig. 1:
16:58 UT

Fig. 2:
17:12 UT

Fig. 3:
17:22 UT

Fig.
4:17:31 U

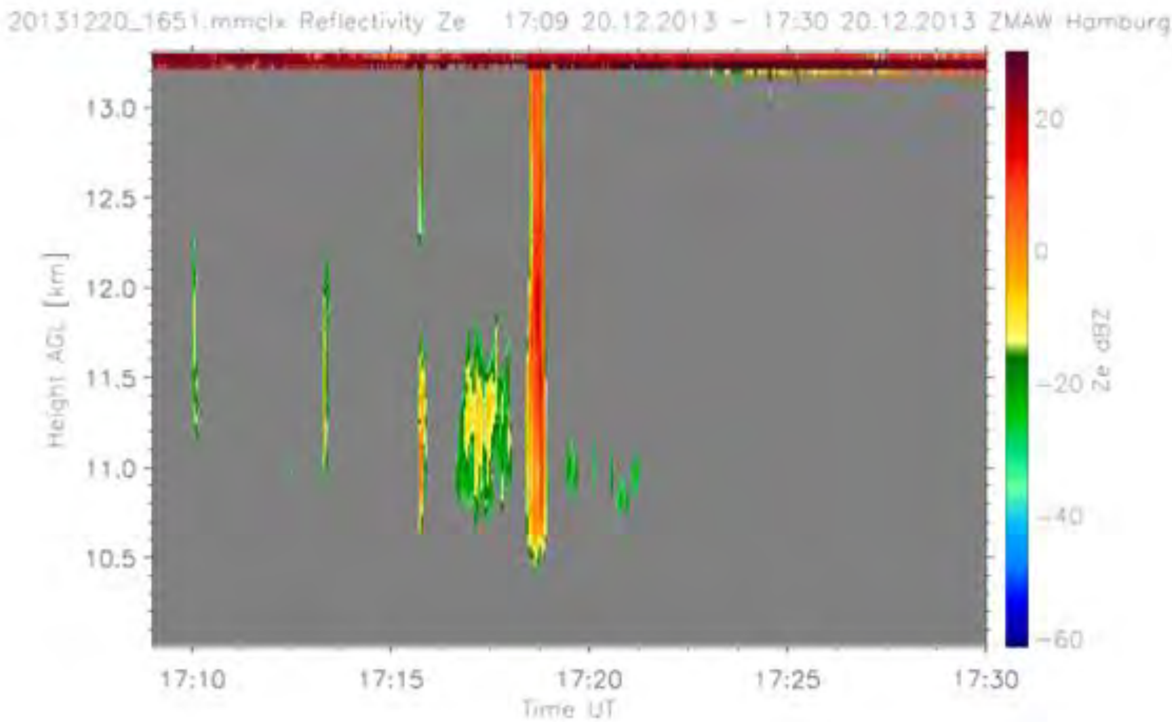

Fig. 5 (below): Quicklook of radar data during CloudSat overpass. Ground echo on top of the plot. Height describes distance from the aircraft, not AGL.

Dropsonde 4: 17:36 UT at N 15.5° W 55.2°

Dropsonde 5: 18:26 UT at N 13.3° W 48.0°

Dropsonde 6: 19:24 UT at N 20.0° W 40.7° Cam-Img DSC 7046/7047

Fig. 6: Cloud scene at 19:26 UT

Dropsonde 7: 20:10 UT at N 23.7° W 35.6°

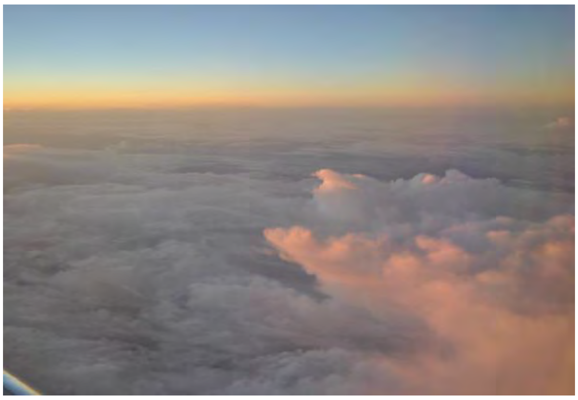

Fig. 7 Cloud scene at19:56 UT

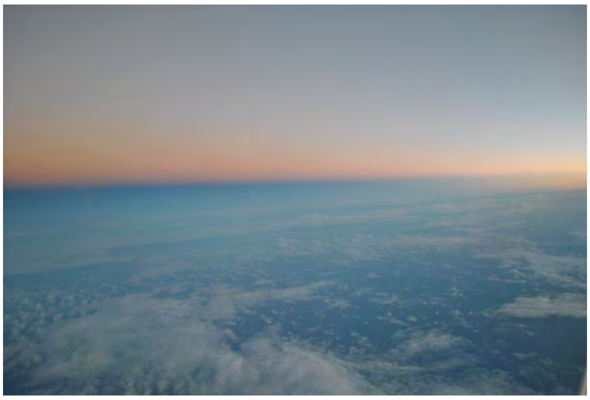

Fig. 8: Cloud scene at 20:00 UT

interesting cloud layers for radar and lidar between 20:30 UT and 21:00 UT

Dropsonde 8:	21:00 UT at N 28.0° W 29.8°
Dropsonde 9:	22:00 UT at N 31.6° W 21.0°
Dropsonde 10:	23:04 UT at N 35.6° W 13.2°
	23:10 UT climb to FL 450 to save some fuel.
	23:40 UT reaching Portuguese Coast
	02:35 UT TD in EDMO

Performance of the measuring systems:

Radar: operation from 16:47 UT to approx. 02:00 UT
Radiometers: continuous operation, pre and post calibration performed
Lidar: operation from 17:16 UT to 02:00 UT (5 min break at 19:15 UT)
HALO-SR: continuous operation
miniDOAS: continuous operation

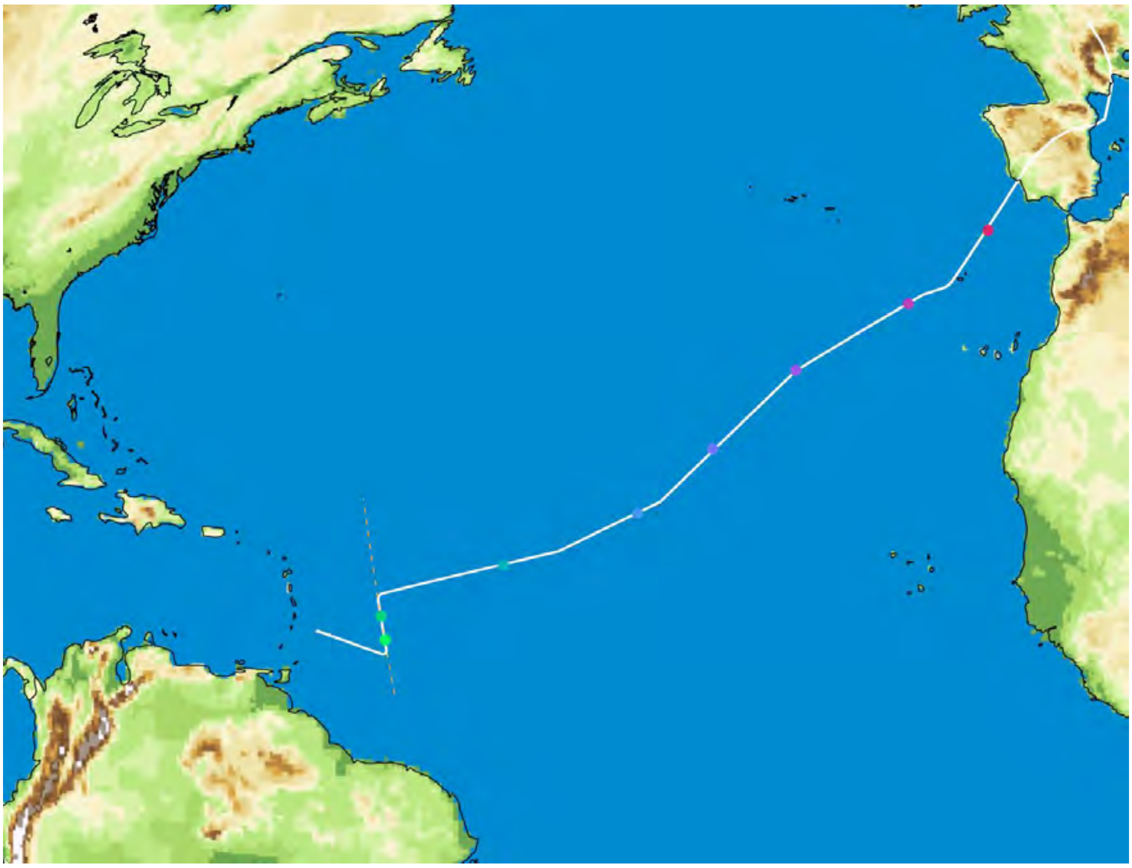

Fig. 9: Flight track showing positions of dropsondes and satellite overpass.

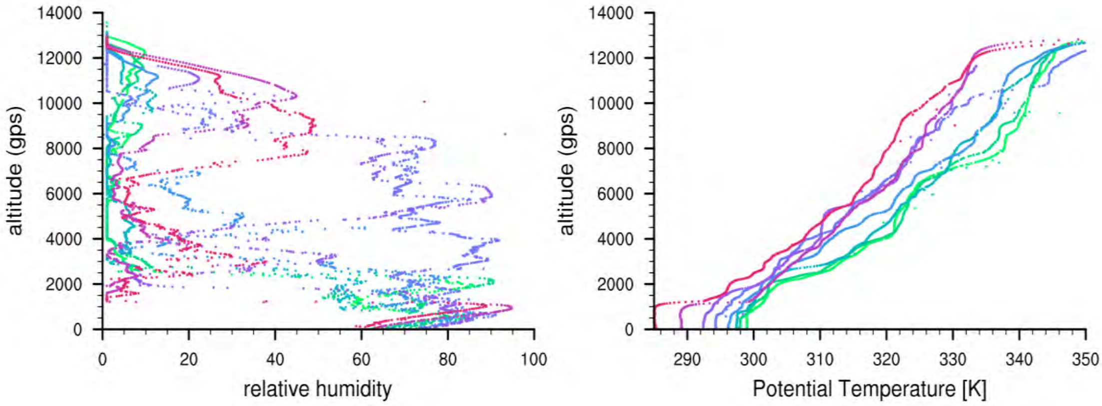

Fig. 10: Dropsonde humidity and potential temperature, colored following colors on track map.

Quicklooks RF08

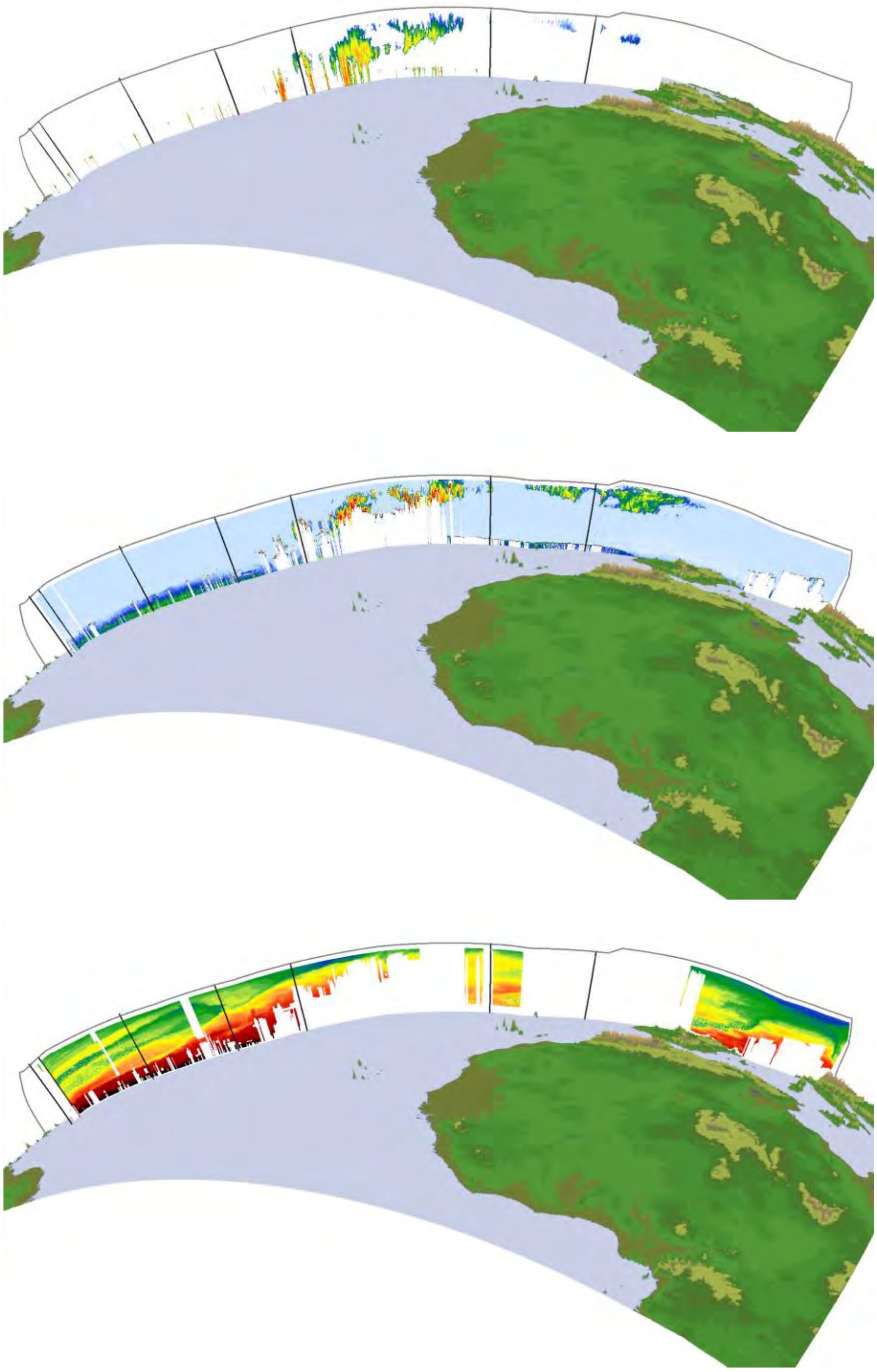

Fig.11: 3-D visualization of the radar backscattering (top panel), the lidar backscatter ratio (middle panel) and the derived water vapor mixing ratio (lower panel) along the entire flight track.

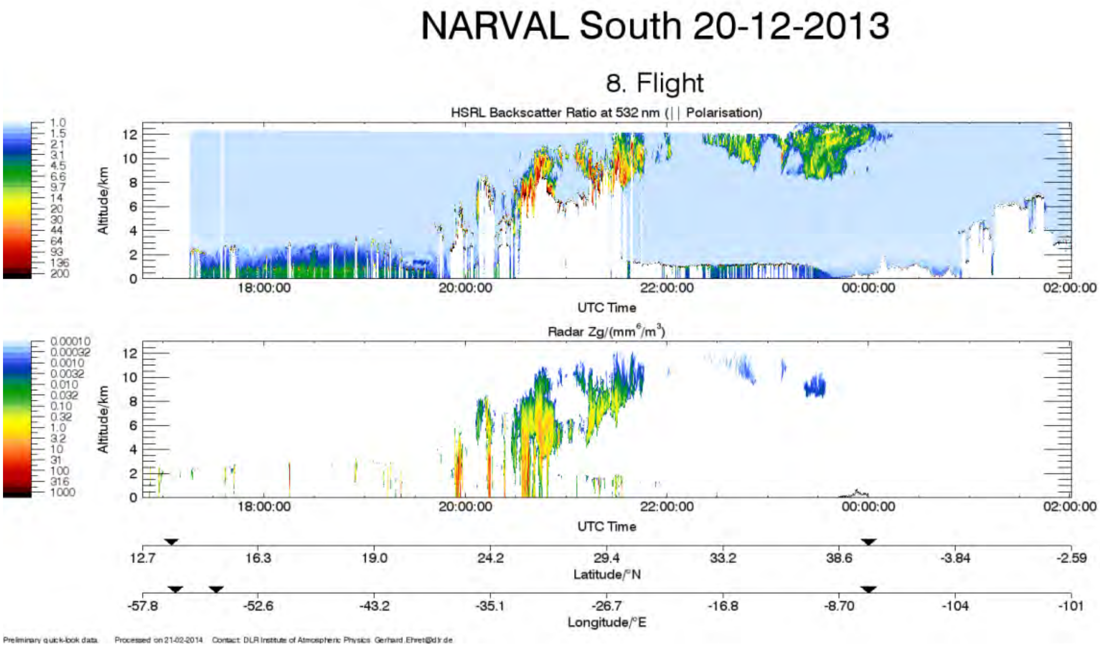

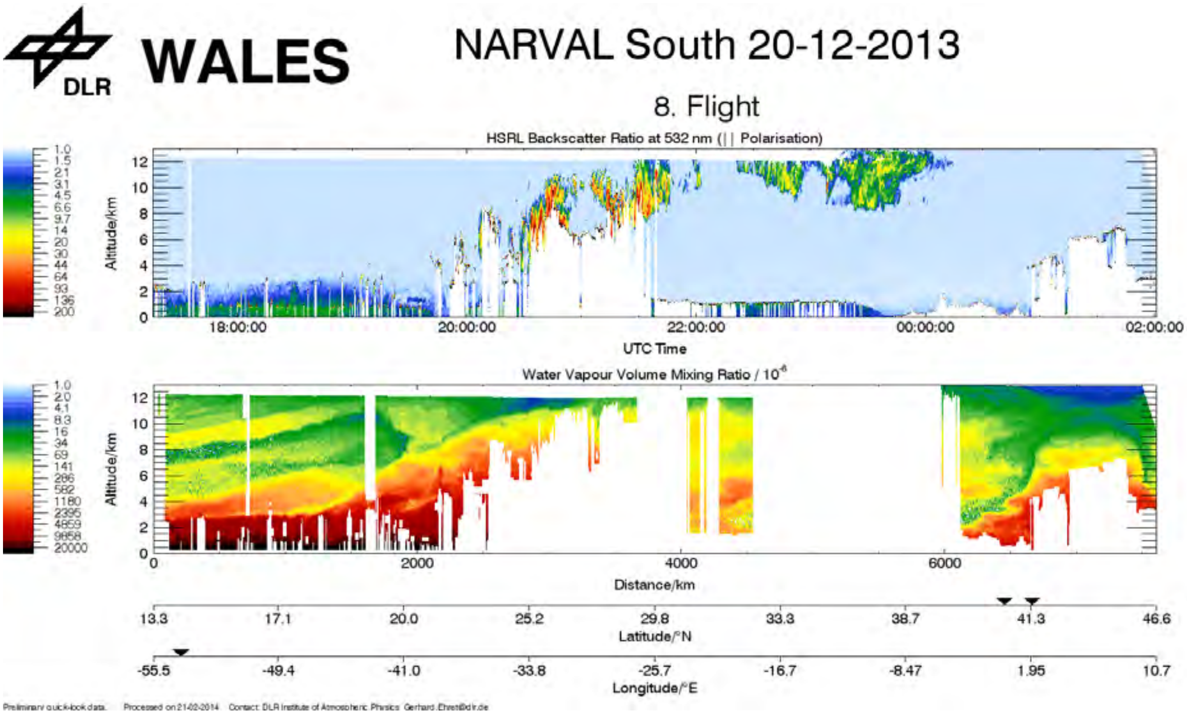

Fig.12: Time-height section of lidar backscattering vs. radar backscattering (upper panel) and lidar backscattering vs. water vapor volume mixing ratio (lower panel).

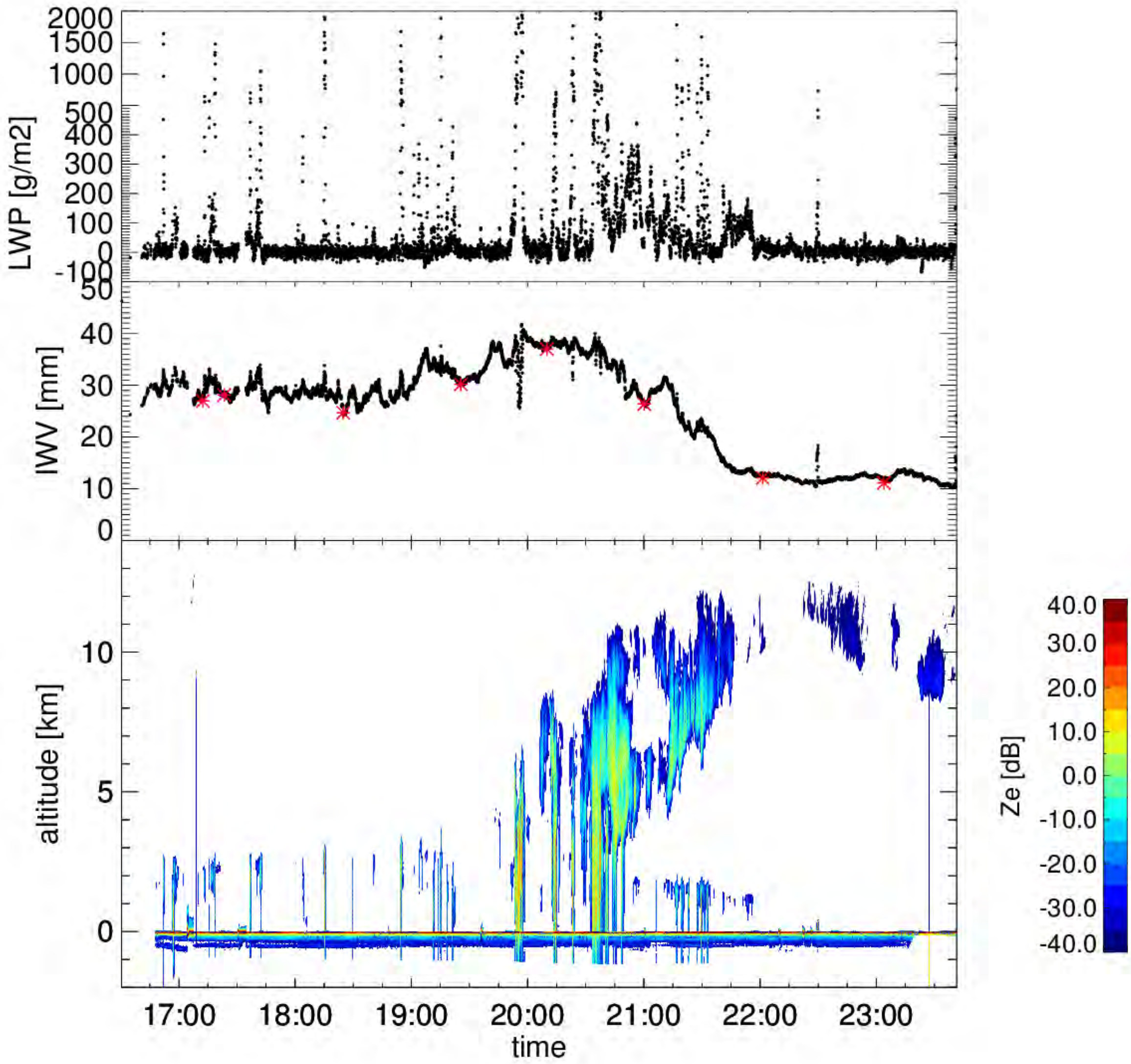

Fig.13: Time-height section of liquid water path (top panel) and integrated water vapor (middle panel) as derived from retrievals using the HAMP radiometer data vs. radar backscattering (lowest panel). Red stars in middle panel denote dropsonde derived integrated water vapor.

NARVAL North

Research Flight Reports

CHRISTIAN KLEPP

NARVAL North Team on Iceland:
DLR: Andreas Fix, Andreas Giez, Christoph Grad, Stefan Grillenbeck, Silke Groß, Martin Hagen, Andrea Hausold, Stefan Hempe, Andreas Schäfler, Roland Welser, Martin Wirth, Alexander Wolf
MPI-M: Stephan Bakan, Lutz Hirsch, Friedhelm Jansen
University of Hamburg: Felix Ament, Christian Klepp, Heike Konow
University of Cologne: Mario Mech, Emiliano Orlandi
University of Heidelberg: Marcel Reichert

NARVAL North Transfer Flight 09 (TF09), Flight Report

- 7 January 2014 -

LUTZ HIRSCH

Crew: Stefan Grillenbeck (Pilot), Roland Welser (Pilot), Andreas Fix (Wales), Silke Groß (Wales), Martin Hagen (HAMP), Marcel Reichart (HALO-SR). Lutz Hirsch (PI)

11:43 -11:52 (approx.) Warm (17.6°C) and Cold Target while on APU

12:08 UT TO EDMO

12:27 UT Radar operational (file_name:

12: 28 UT Lidar problem with stability

12:50 Lidar operational

12:55 UT - 13:15 (approx.) holding pattern Jülich

13:30 UT - 13:50 (approx.) holding pattern Cabouw

14:52 UT Windows computer 119/90 stalled -- > restarted

15:15 UT - 15:45 UT (approx.) holding pattern MaceHead

15:22 UT Radar: get_processing stalled -- > restarted 15:27

17:25 UT beginning approach Kef.

17:32 UT Lidar and Radar off at approx 8 km

17:50 Landing KEF

NARVAL North Research Flight 10 (RF10), Flight Report

- 9 January 2014 -

CHRISTIAN KLEPP

Crew: Roland Welser (Pilot), Stefan Grillenbeck (Pilot), Alexander Wolf (Flight engineer), Silke Groß (WALES, dropsondes), Andreas Fix (WALES), Marcel Reichert (HALO SR & MiniDOAS), Martin Hagen (HAMP), Felix Ament (HAMP & Mission scientist)

Objective: The scientific goal of the first research flight was to sample the cloud and precipitation fields of four different cold air regimes of a mature cyclone located over the North Atlantic. This comprised crossing the cold front on the transfer leg from KEF and the convective clouds embedded within the cold air outbreak. These were organized in enhanced cumulus cells that partly formed cloud streets, shallow more stratiform appearing convective cloud decks and the convective spiral cloud bands of the postfrontal low (PFL) located in the wake of the cold front and occlusion area (Fig. RF10.1). Furthermore, SSMIS and CloudSat underflights were performed and 11 dropsondes were released.

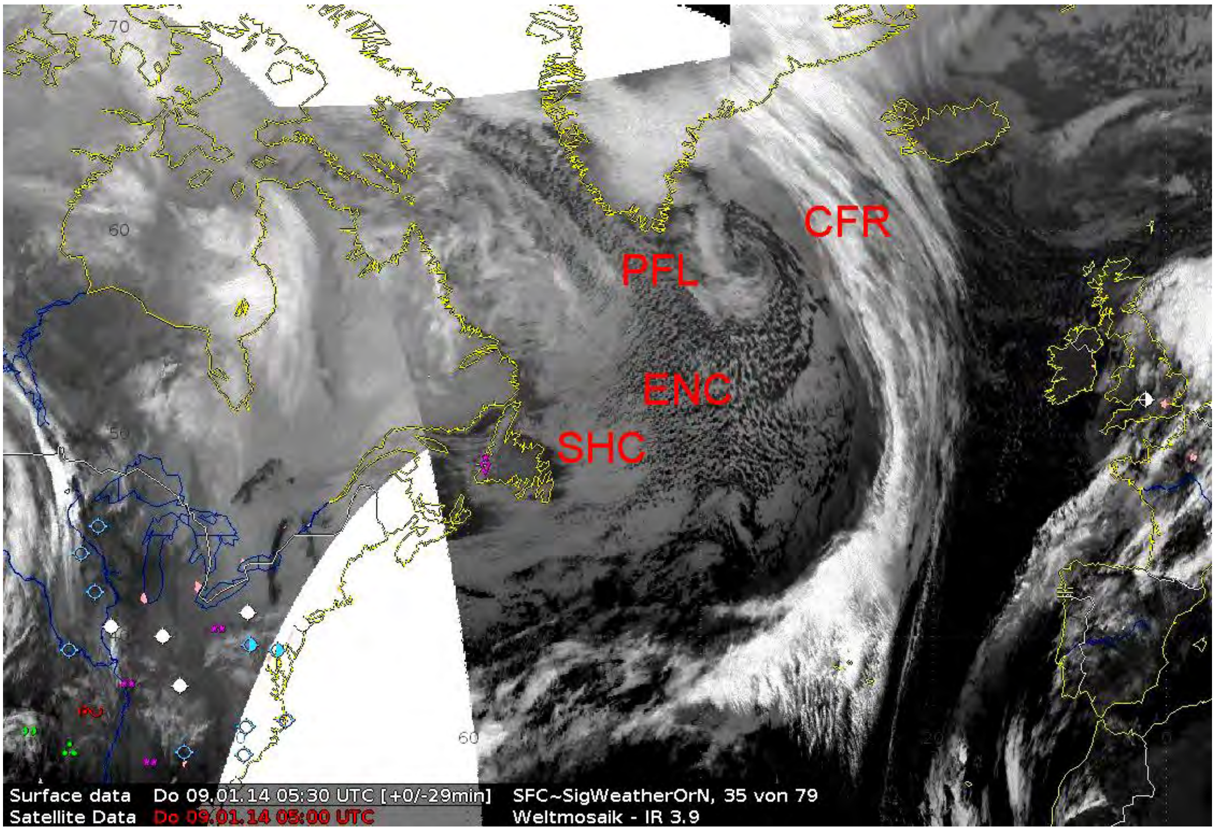

Fig. RF10.1: Infrared satellite mosaic of the North Atlantic from 09 Jan 2014, 05 UT showing the mature low pressure system of RF1 including four different cold air regimes with convective precipitation: Cold front (CFR), postfrontal low (PFL), enhanced cumulus (ENC), and shallow cumulus convection (SHC).

Overview: The North American cold wave was an extreme weather event extending from December 2013 to April 2014, and was also part of an unusually cold winter affecting parts of Canada and the Eastern United States. The event caused southward shifts of the North Polar Vortex. Record cold temperatures occurred and in contrast the European winter was unusually mild and characterized by intense and enduring blocking situations. On January 2, an Arctic cold front initially associated with a nor'easter, tracked across Canada and the United States, resulting in heavy snowfall. Temperatures fell to unprecedented levels, and low temperature records were broken across the United States. Sudden stratospheric warming led to the breakdown of the regular polar vortex and subsequent southward movement of tropospheric Arctic air. The jet stream deviated to the south bringing cold air with it as a result of unusual contrast between cold air in Canada and mild winter temperatures in the United States. Heavy snowfall and rainfall occurred on the leading edge of the weather pattern, which travelled from the American Plains and Canadian provinces to the East Coast. Strong winds prevailed throughout the freeze with temperature reaching record levels of -37 °C. On 8 January the frontal system reached the western North Atlantic Ocean.

On 9 January 2014 the cold front of the cyclone has moved to the west of Iceland, followed by a strong cold air outbreak from continental Canada into the NARVAL North target area off the coast of New Foundland and south of Greenland (Fig. RF10.2). Intense cold air convection developed following the occluded frontal system with an intense spiral shaped post frontal low (Fig. RF10.3). Cellular convection is intersected with fields of more stratiform appearing cloud decks and towards the American continent convection started to flatten out.

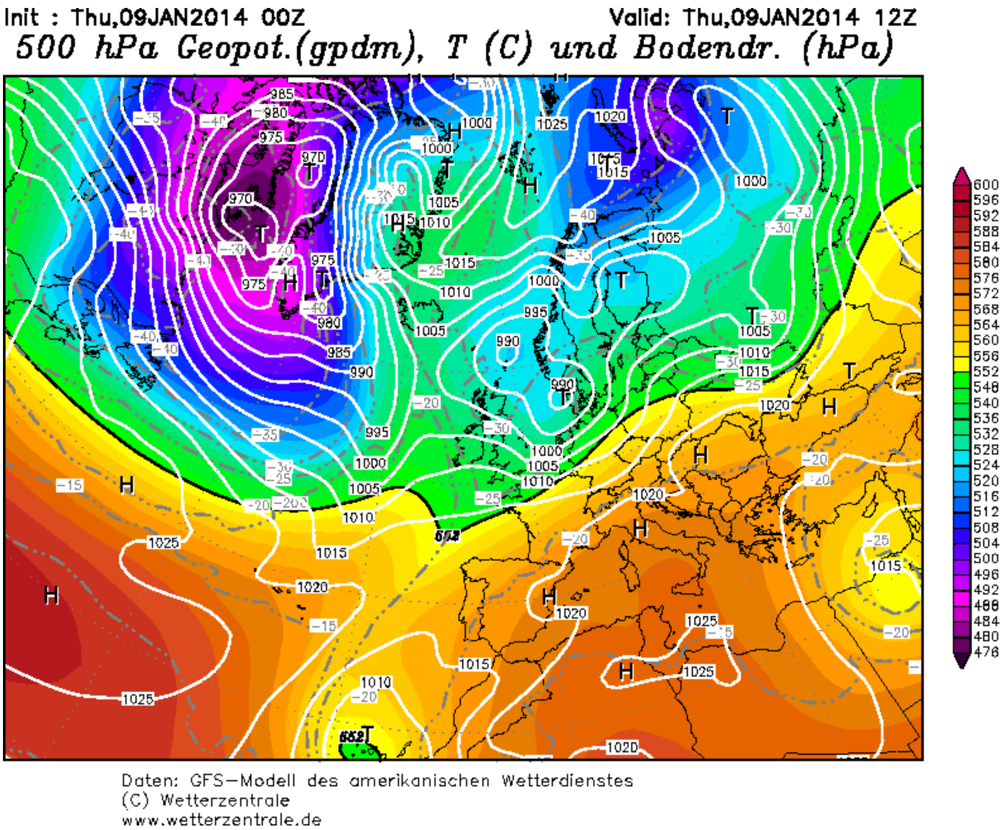

Fig. RF10.2: GFS 12 h forecast of surface pressure (white isolines), 500 hPa geopotential height (color, 552 dekameter isoline in black) and temperature (dot-dashed grey isolines and white boxes) in °C valid for Thu, 09 Jan 2014 12 UT.

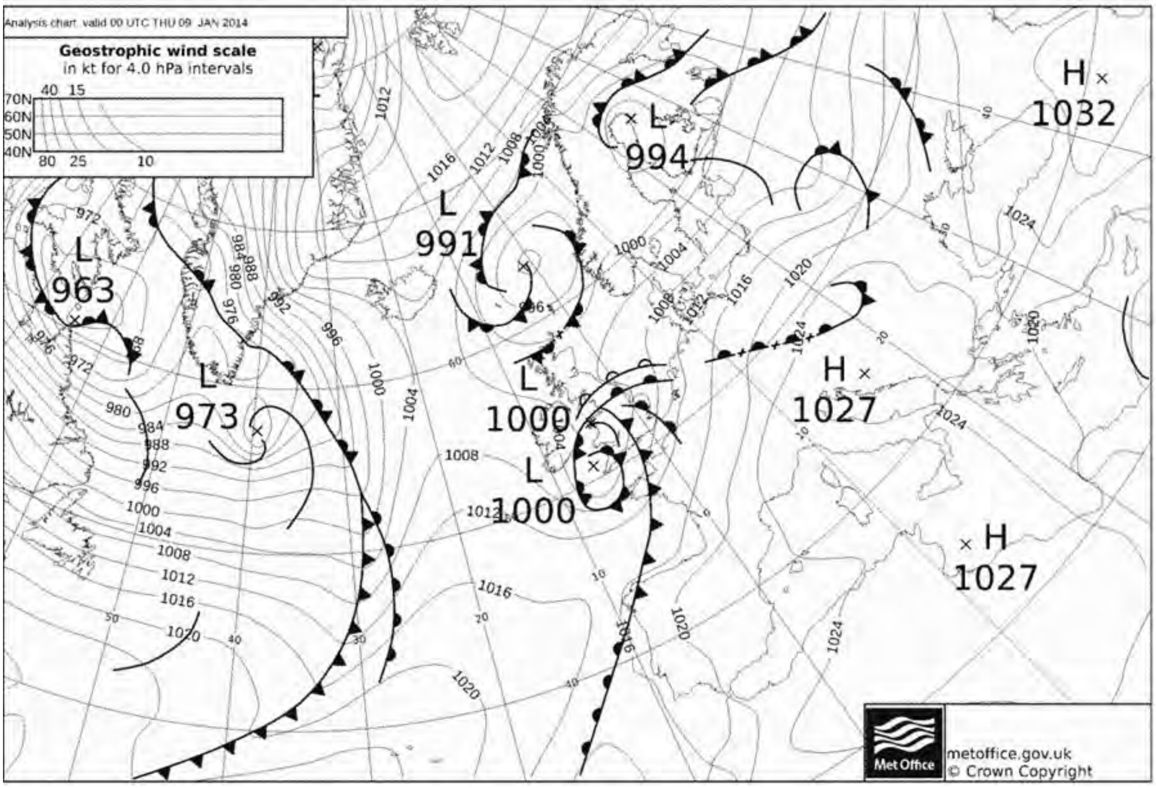

Fig. RF10.3: UK Met. Office analysis chart for 00 UTC on Thu 09 Jan 2014 with the target area of RF1around 55N/40W. The occlusion crossed Greenland and split into the cold and warm front at about 28W. The spiral shape PFL is located to the Southeast of Greenland including frontal structures as is also documented in the satellite mosaic of Fig. RF.1.1. The cold air outbreak from the American continent is well documented in the isobars being almost perfectly aligned longitudinally.

Flight Planning: After lengthy communication with the Air Traffic Control (ATC) and several iterations a restricted but acceptable flight plan needed to be finally approved 24 hours in advance. For dense air traffic controlled areas it is a challenging task for the briefing crew to hand in flight requests including exact research flight patterns 24 hours or more in advance. Thus two to three daily weather briefings were needed to specify the location of the target area for a potentially interesting meteorological situation. This required intense team work between the meteorologists, flight operation (FX), the pilots, and the ground crew. The flight was permitted at an altitude of FL270. Any altitude change requests were rejected due to the dense civil and military air traffic in this area. Finally, an airspace of about 1000 km diameter was tied up for HALO on flight level 260 (approx. 8 km height) for a time slot of 9 hours. This included the permission for free positioning and orientation of the intended mattress pattern together with dropsonde releases at any point within the approved bounding box (Fig. RF10.6). ATC assigned a predefined entry and exit point for the transfer from and to KEF as indicated in Fig. RF10.6.

For overall flight decisions large scale meteorological forecast maps (e.g. Fig. RF10.2 and Fig. RF10.3) were used. Additionally animated satellite image loops turned out to be useful (Fig. RF10.1) to predict the development of postfrontal convective activity. Precursors of postfrontal convection often initiates up to 12 hours in advance. For more detailed planning the ECMWF precipitation forecast (Fig. RF10.4) and the ECMWF data driven flight planning tool of DLR (Fig. RF10.5) proofed very useful. This allows visualizing the forecasted situation along the planned flight track. With this the position and height of cloud systems containing precipitation could be investigated in detail. This also eased the situation to comply with ATC regulations to fly on constant FL260 (about 8 km altitude) as the forecasted cloud altitude showed no significant postfrontal clouds above 500 hPa. The flight pattern flown with waypoint markers, dropsondes, positions and the CloudSat track is given in Fig. RF10.7 together with the underlying satellite composites from polar orbiting (AVHRR) and geostationary satellite IR data.

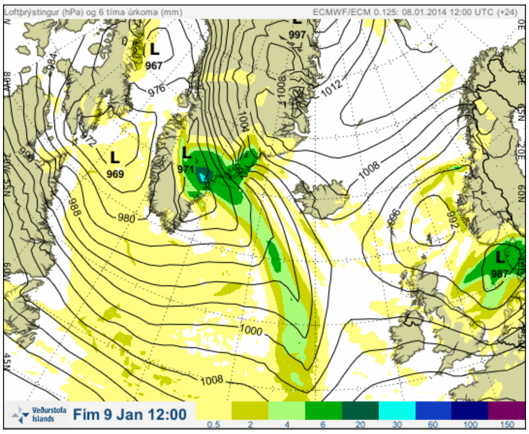

Fig. RF10.4: ECMWF forecast for 09 Jan 2014 12 UT for surface pressure isobars and precipitation amount accumulated over 6 hours (color). Despite the prominent frontal system enhanced precipitation patterns are embedded in the cold air outbreak region.

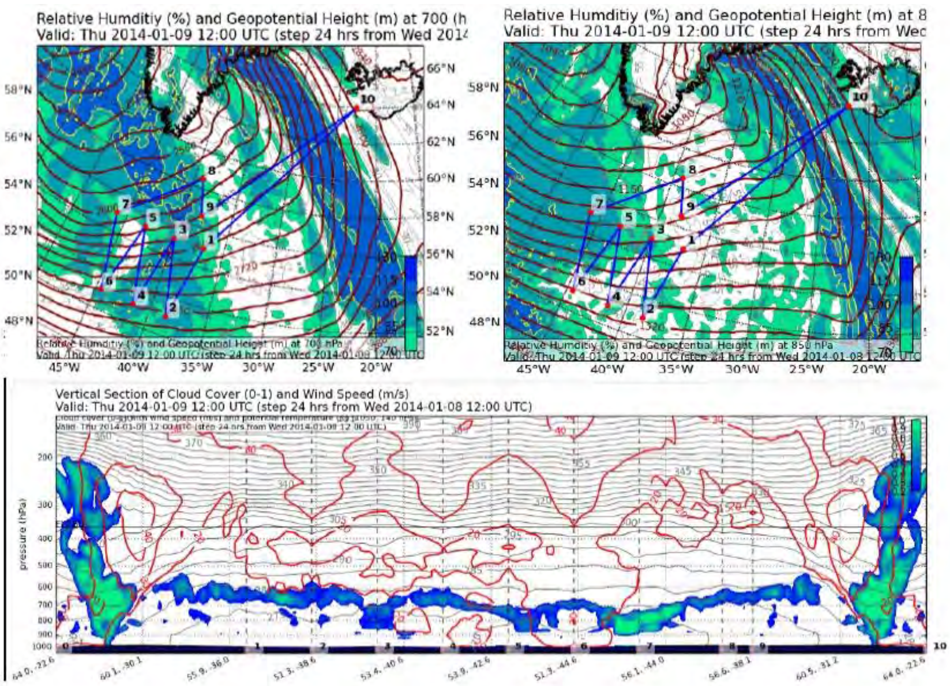

Fig. RF10.5: ECMWF based flight planning tool of DLR showing the relative humidity (color) and geopotential height (red isolines) for 700 hPa (left top panel) and 850 hPa (right top panel) for 09 Jan 2014, 12 UT including the flight pattern in blue and waypoints as red dots. The bottom panel shows the vertical section of cloud cover (color) and wind speed (m/s in red) along the flight track from left to right. The waypoints are listed on the x-axis. The constant flight altitude of FL260 is marked as a black line.

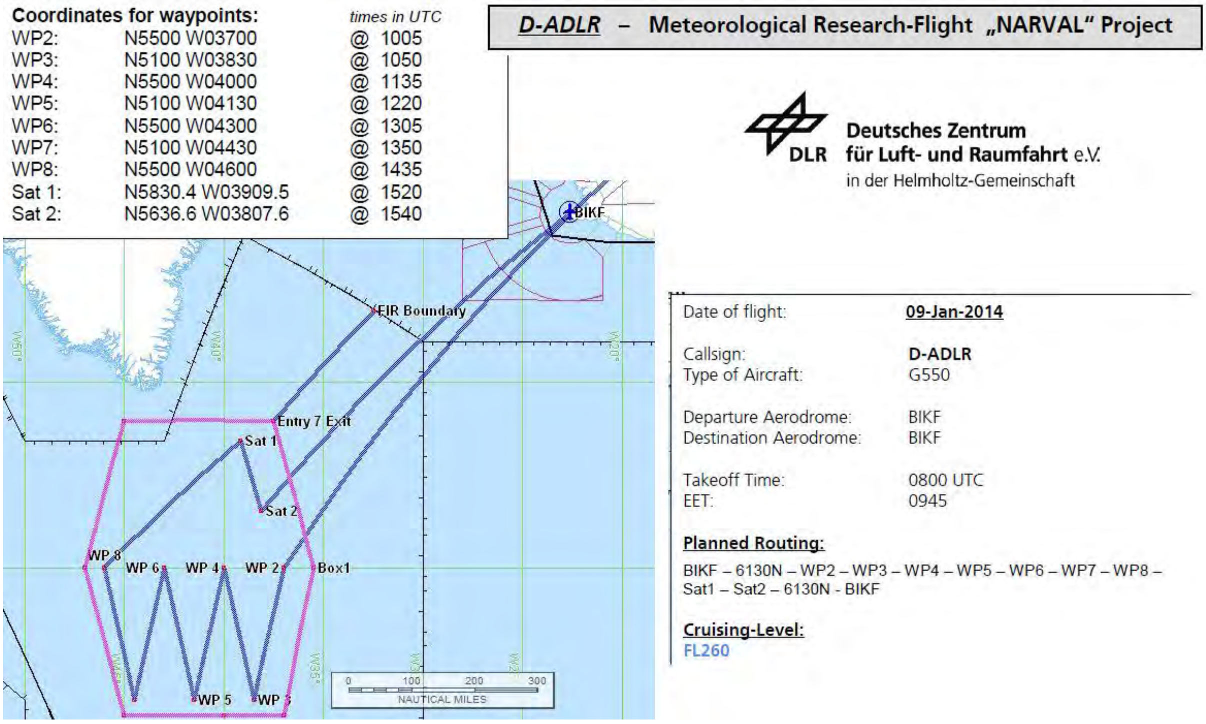

Fig. RF10.6: ATC requested and approved flight pattern for RF10. The violet bounding box contains the HALO tied up airspace at FL260 with dropsonde and flight pattern change clearance. The entry and exit point of the bounding are indicated. The actual flight pattern is shown in blue including the mattress waypoints (WP) and the CloudSat collocated underpath at 15:29 UT along SAT1 and SAT2. Coordinates of all points are listed in the upper left panel table.

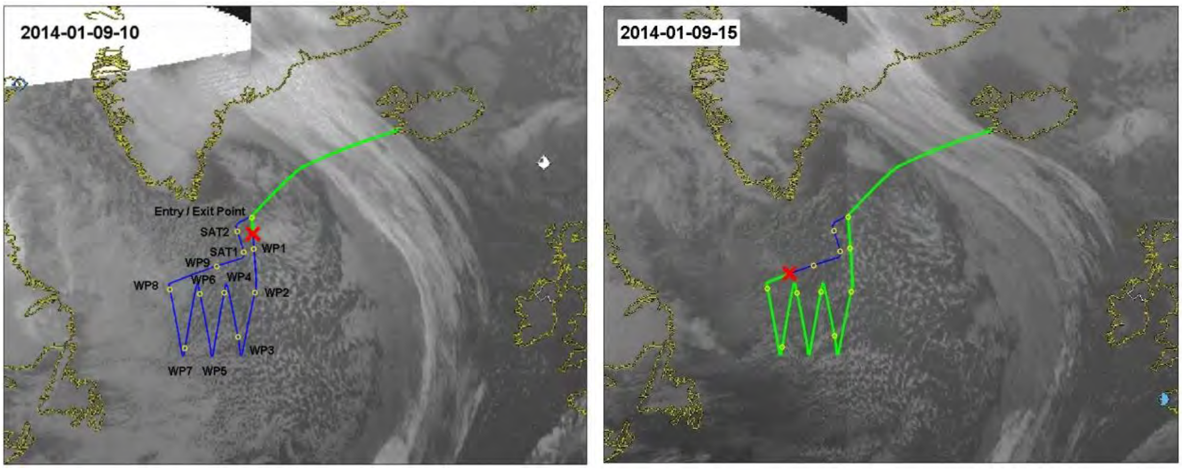

Fig. RF10.7: AVHRR and Meteosat composite of the 3.9 micrometer channel at 10 UTC (left) and at 15 UTC (right) with overlaid flight path: the red cross indicates the position of HALO at the respective time with the elapsed flight pattern as a green line. Release points of all 11 dropsondes are depicted by yellow circles. The waypoints (left) indicate the ATC entry and exit point of the pattern box from waypoint 1 to 8 and SAT marks the collocation line flown for the CloudSat underpass.

Flight Report: HALO was taking off from KEF at 8:14 UT and passed the cold front at FL260 within the clouds. After the frontal passage HALO remained well above all clouds and the tropopause for the remainder of the flight, except during the final descent into KEF. On the transfer to the box entry point HALO passed over a well-developed but decaying post frontal low which has passed the box area in its mature state during the night before. The mattress from waypoint 2 until waypoint 8 was designed to sample enhanced cumulus and shallow convection within the cold air outbreak. Two regimes of cumulus convection were encountered, with almost stratocumulus like convection in the most western part of the box (close to waypoints 6 and 8) and more active enhanced convection in the rest of the box. While HALO was within the mattress, collocations with three SSMIS overpasses (DMSP-F17 at 11:38 UT, and DMSP-F18 at 12:14 UT and 13:54 UT) were achieved. Such collocations are essential for validation and point-to-area investigation of the HOAPS passive microwave climatology precipitation and cloud liquid water parameters (www.hoaps.org). An underflight of the CloudSat satellite track at 15:29 UT was included between waypoints SAT1 and SAT2. The detailed protocol is listed below with all inflight meta data, cloud observations and data issues. Forced by ATC to perform the entire flight route on FL260 without height changes provided the knowledge that frontal passages within clouds are not affecting the performance of HAMP for long after the cloud passage.

The photos, taken during the flight through the airplane windows, illustrate differences in convective regimes (Fig. RF10.8) within the mattress. While randomly organized convective clouds including cumulonimbus prevailed in the east, cloud street patterns and more stratiform cloud decks were encountered further upstream. The left panel of Fig. RF10.9 shows towering cumulus congestus during the CloudSat overpass. In the right panel of Fig. RF10.9 the cold front can be seen to the very right of the image while the shielding cloud bands above the convection visualize the remains of the decaying PFL.

Fig. RF10.8: Cloud fields at waypoint 3 within the mattress show randomly organized cumulus convection up to 4 km height, party forming anvils of thin ice clouds (left). Widespread, almost stratiform cloud deck with cloud tops at 3 km height at waypoint 6 (right).

Fig. RF10.10 gives a comprehensive hourly overview on the cloud situation, the flight path, the aircraft position, and the elapsed flight track to provide a guideline for the detailed flight protocol.

Fig. RF10.9: Cloud field during the CloudSat overpass at 15:29 UTC close to waypoint SAT1 (left). Approaching the cold front on the way back to KEF the front can be seen in the far distance at the right edge of the image (right).

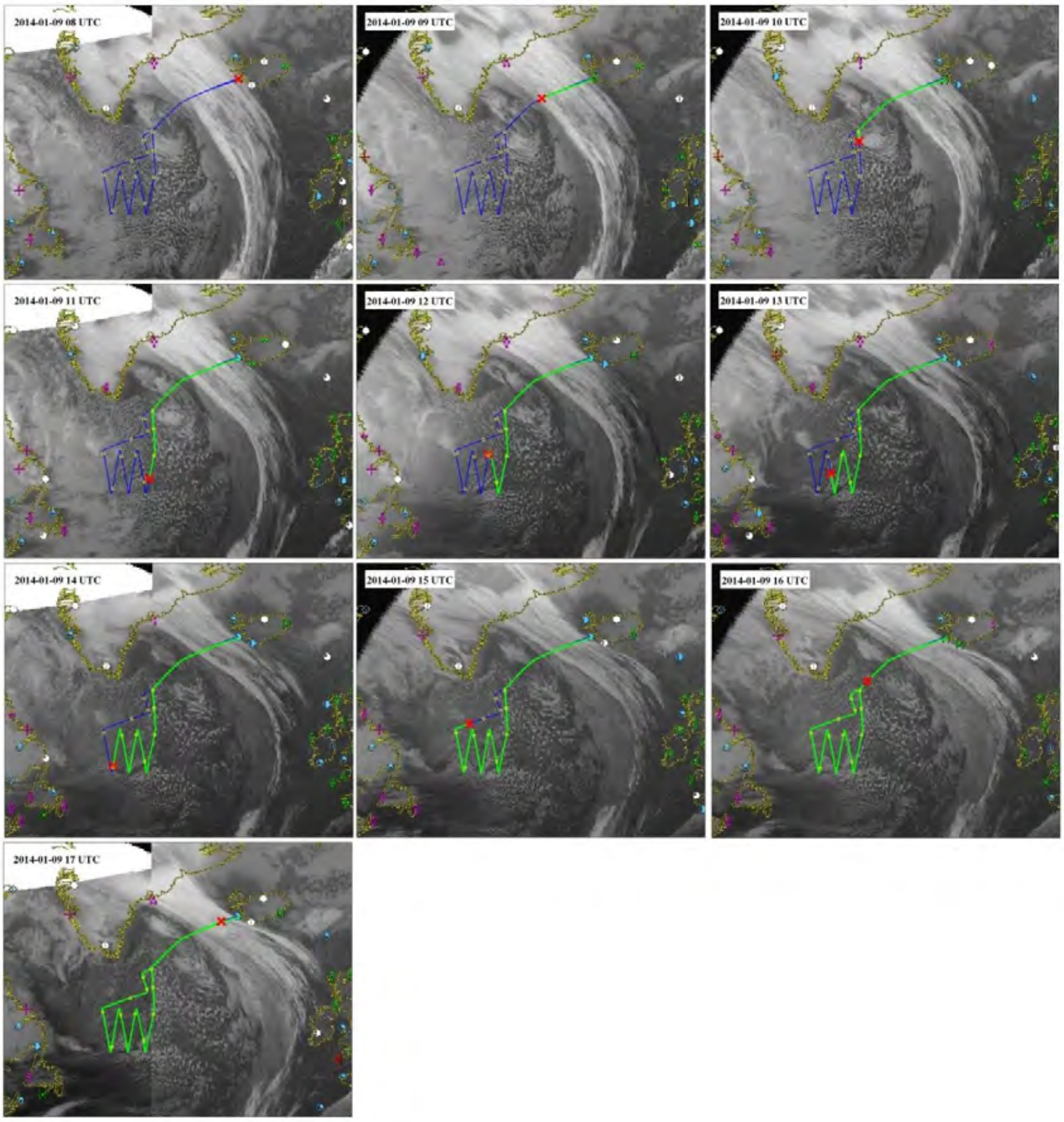

Fig. RF10.10: Hourly flight track composite in blue and infrared satellite data with elapsed flight time in green, current aircraft position as red cross and dropsondes positions as yellow circles. This composite is to be used as a reference for the flight protocol below.

Flight Protocol
All time in UT.
08:14 take off; drizzle at ground; low clouds during take off
08:21 stars above visible
08:26 7000 m reached; start to switch on Radar
08:29 radar is running
08:38 probably inside clouds, slight turbulence, 50 GHz frequencies are all almost similar indicating wet radiometer windows; however stars are still visible
09:02 leaving clouds - probably left the frontal system - still dark outside; radiometer seems to dry rather fast: 50 GHz brightness temperatures deviate again
09:09 first dawn
09:43 still rather dark: low, broken cloud decks (cumulus)
09:48 reaching the entry point
09:49 dropsonde 01 released
09:54 stratiform layer of mid-level clouds becomes visible
10:09 dropsonde 02 at the center between box entry point and WP1
10:30 WP2; dropsonde 03
10:35 sunrise
11:14 WP3 (begin of mattress); cloud top at 4000 m corresponding to a temperature inversion at about 650 hPa detected by dropsonde 03; variety of clouds visible: small shallow cumuli, organized high convective clouds and thin layers of ice at the top of the cloud layer resulting of anvils - decaying anvils are widespread and cover almost the entire sky
11:20 dropsonde 04
11:30 cloud field tends to become a little bit more organized into convective cells (reaching up to 4 km) associated with ice anvils on top and surrounded by areas with only very low or no clouds. Flying over such convective cells quite regularly with a period of about 7 min.
11:34 radar is down and rebooted
11:40 subsidence regions next to cells become more visible - more pronounced cloud free areas (except thin layer of ice on top of the cloud layer)
11:55 WP4
12:01 dropsonde 05
12:34 radar up again
12:35 WP5
12:37 dropsonde delayed due to water leakage in the baggage compartment
12:50 cloud field looks similar since sunrise: dominant are high (up to 4km) convective cells (randomly shaped) with ice clouds on top - sometimes fields of shallow cumulus
12:59 slight changes of roll angle to get water out of baggage compartment
13:06 dropsonde at the beginning of the leg skipped - postponed to the end of the leg
13:15 dropsonde 06
13:19 convective clouds appear to be little shallower with less intense convective activity, visible by lower cloud tops
13:22 WP6
13:30 cloud top height is lower: about 3 km, dropsonde indicates an inversion at about 720 hPa
14:02 dropsonde 07
14:04 again, more intense convection - but capped by the inversion
14:08 WP7
14:17 Lots of stratiform ice clouds below the inversion
14:28 Again, less intense convection (same as at 13:19 UTC)
14:43 dropsonde 08

14:50 WP8
14:53 less convection - development toward stratocumulus; probably structured in bands
15:12 dropsonde 09
15:28 reaching waypoint SAT1: alignment on satellite track finalized
15:29 dropsonde 10
15:39 dropsonde 11
15:41 waypoint SAT2
15:51 leaving the box area, exit point
15:51 less cloud cover, smaller cumulus clouds, less clustered
16:10 small cumulus clouds not visible with radar (but with lidar)
16:33 minimum cloud cover, almost cloud free
16:35 new cloud regime, more stratiform clouds, partly two layers, i.e. also midlevel clouds
16:38 passing by a band structure with first cirrus clouds
16:43 flying at the cloud top of stratiform cirrus - no cloud structure detectable - appears like fog
16:50 flying into clouds, slight turbulences
16:53 flying below a cirrus layer
17:01 descending
17:02 radar switched off
17:20 touch down KEF
17:26 parking position

Dropsondes
All time in UT. Fig. RF10.7 provides an overview on the dropsondes positions.

01 09:49 at entry point
02 10:09 at the center between box entry point and WP1
03 10:30
04 11:20
05 12:01
06 13:15
07 14:02
08 14:43
09 15:12
10 15:29
11 15:39

Instrument performance:
All instruments were up and running except one hour of downtime by the cloud radar (~11:30-12:30 UTC). The HAMP radiometer recovered quickly after the occlusion front cloud passage; strong signal of liquid water (K- and partial V-band), of ice (183 GHz channel) and precipitation (119 GHz channels). Data from the cloud passage needs to be excluded since the radome windows were wet. The radar reveals sinking brightband within the front and no postfrontal brightband indicating snowfall to the ground within the showers. Strong echoes of showers occurred behind the front. Mini-DOAS data is to be visualized after the campaign, but data was well recorded.

Preliminary HALO instrument data:

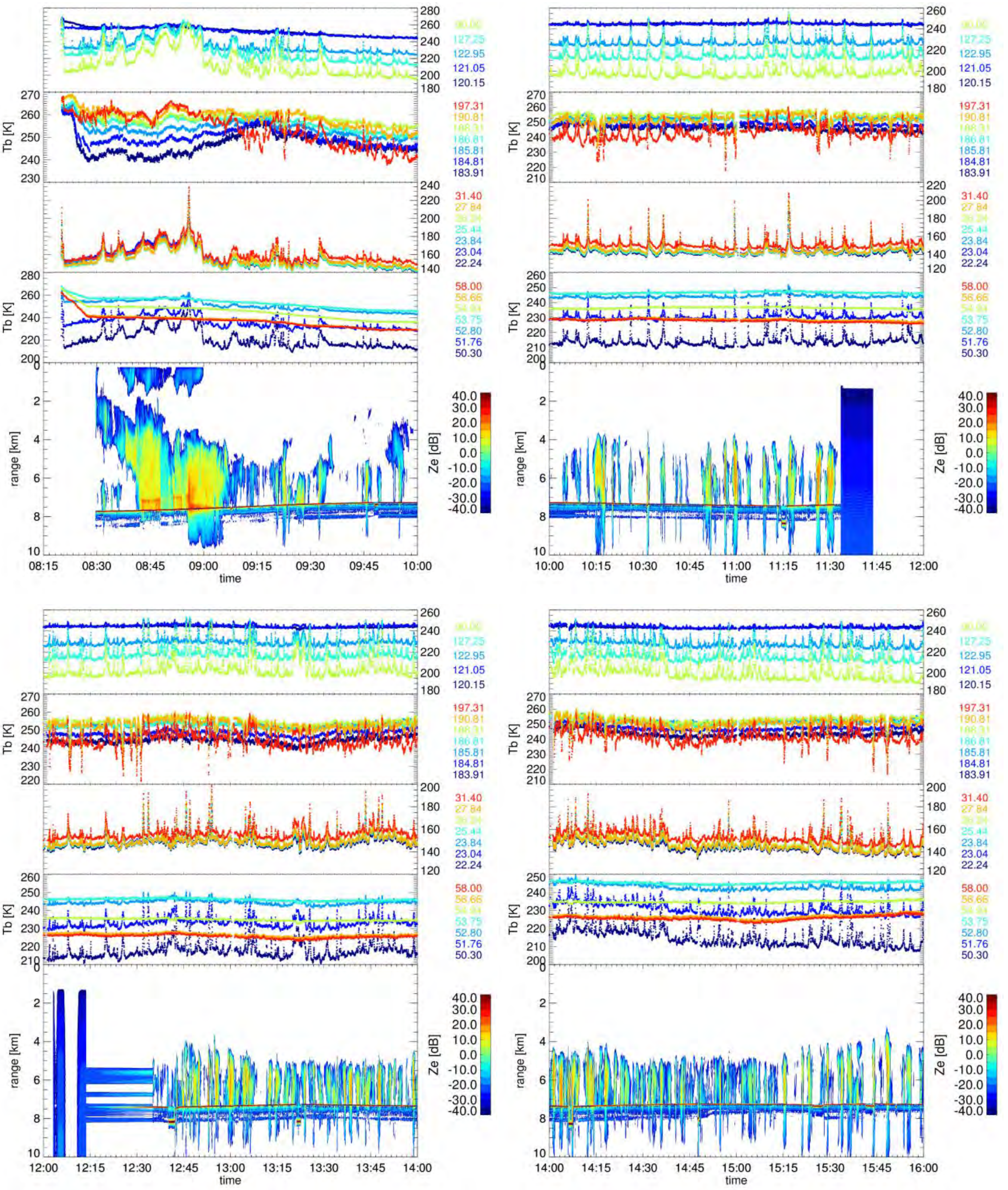

Fig. RF10.11: Time series in UT of microwave radiometer brightness temperatures and radar reflectivity profiles during the entire flight (in 4 panels with 2 hours length each) for the scattering channels (uppermost series in each panel), the sounding channels (second series from above in each panel), the emission channels (third series from above) and the 50 GHz channels (fourth series from above) and the range corrected radar reflectivity (lowest series in each panel). The raw data radar reflectivity profiles still include surface signals as well as multiple scatter signals at range gates beyond the surface. Between 8:30 and 09:05 UT the cold front was passed within the clouds followed by the postfrontal subsidence that is clearly identified by few midlevel clouds. At 09:25 to 09:35 UT the PFL was crossed above the clouds indicating strong convection with snowfall to the ground. Subsequently, numerous convective cells with cloud tops at about 4 km were measured.

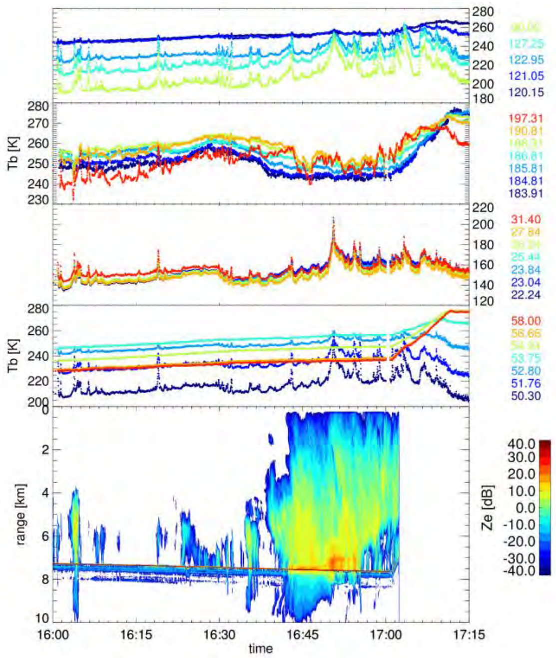

Fig. RF10.11: continued. The radiometers show signatures of both, supercooled liquid water as well as scattering by ice particles, and the radar indicates snowfall to the ground (no brightband). Towards the west the mattress pattern indicates a decrease in cloud height, convective activity and cloud tops at about 2 to 3 km height. The CloudSat underflight at 15:29 UT shows again increasing convective cell activity as also suggested by the cloud photography (Fig. RF10.9 left) and the CloudSat data (Fig. RF10.18). The postfrontal subsidence is clearly visible by the absence of clouds. Between 16:20 and 16:40 UT the decaying remains of the PFL were again crossed followed by the flight into the cold front.

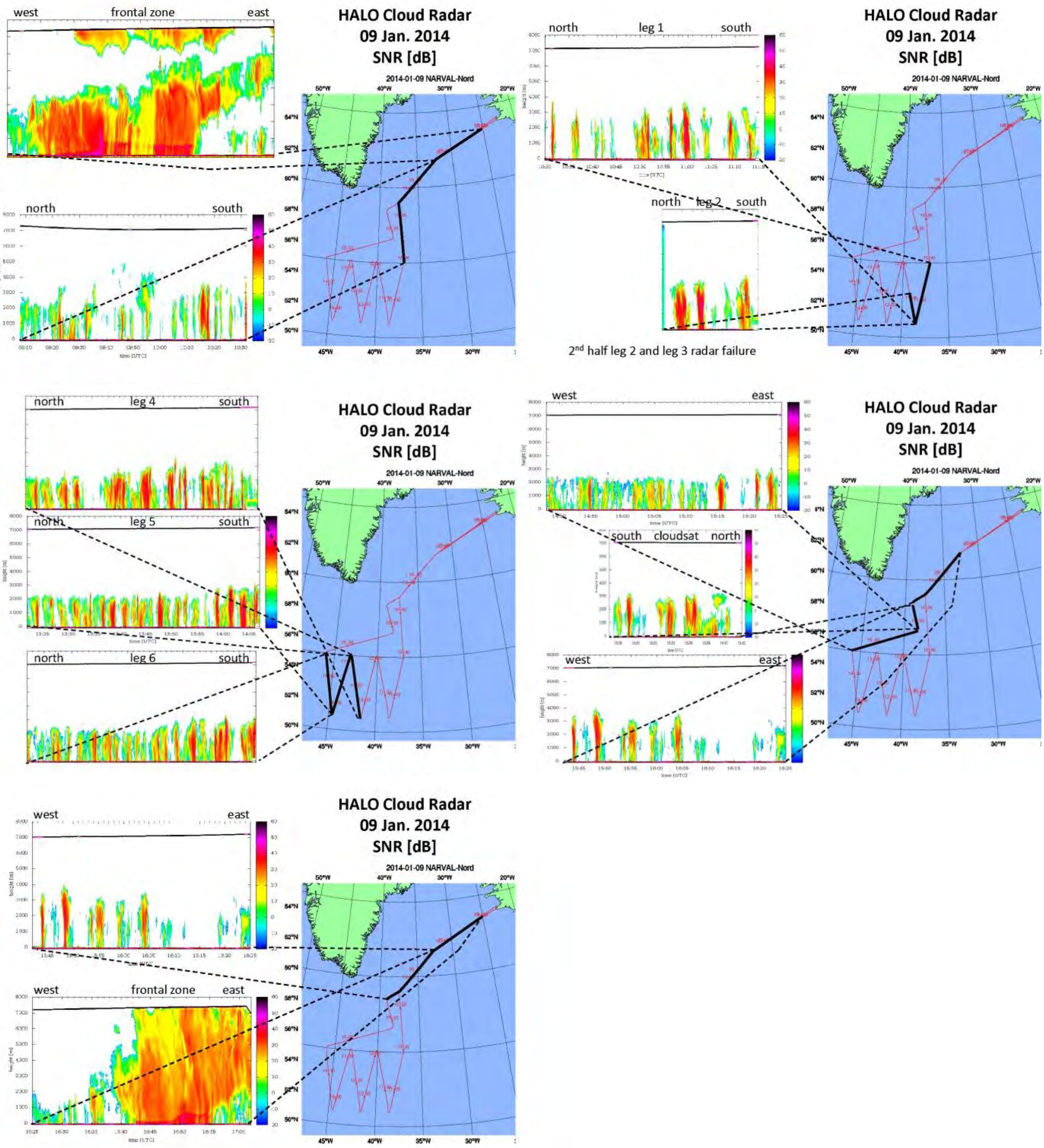

Fig. RF10.12: The radar reflectivity data for the entire flight of RF1 including the CloudSat underflight at 15:29 UT, and the return over the PFL. Note the varying cloud heights and absence of bright bands. Note that during leg 2 and 3 the radar was off for about one hour.

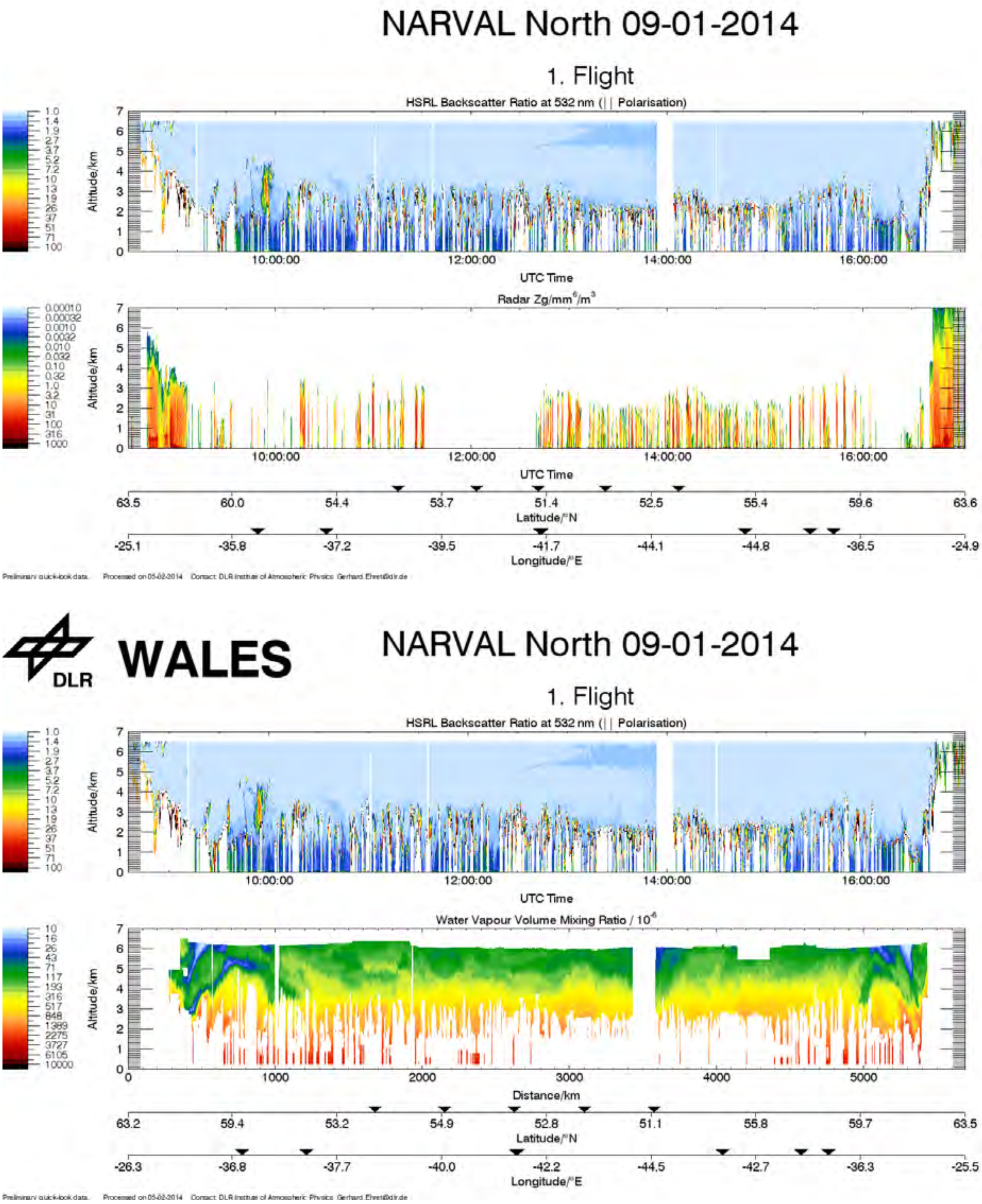

Fig. RF10.13: Entire time series of the WALES lidar backscatter ratio at 532 nm (top) compared to the radar data (top panel) and to the water vapor mixing ratio (bottom panel). In the top panel clear air is indicated by bluish colors while black and white colors denote strong extinction caused by optically thick cloud columns. In the lower panel yellow and green colors mark small water vapor mixing ratios as appear e.g. in dry intrusions. The numerous shower cells are seen as white columns of no data.

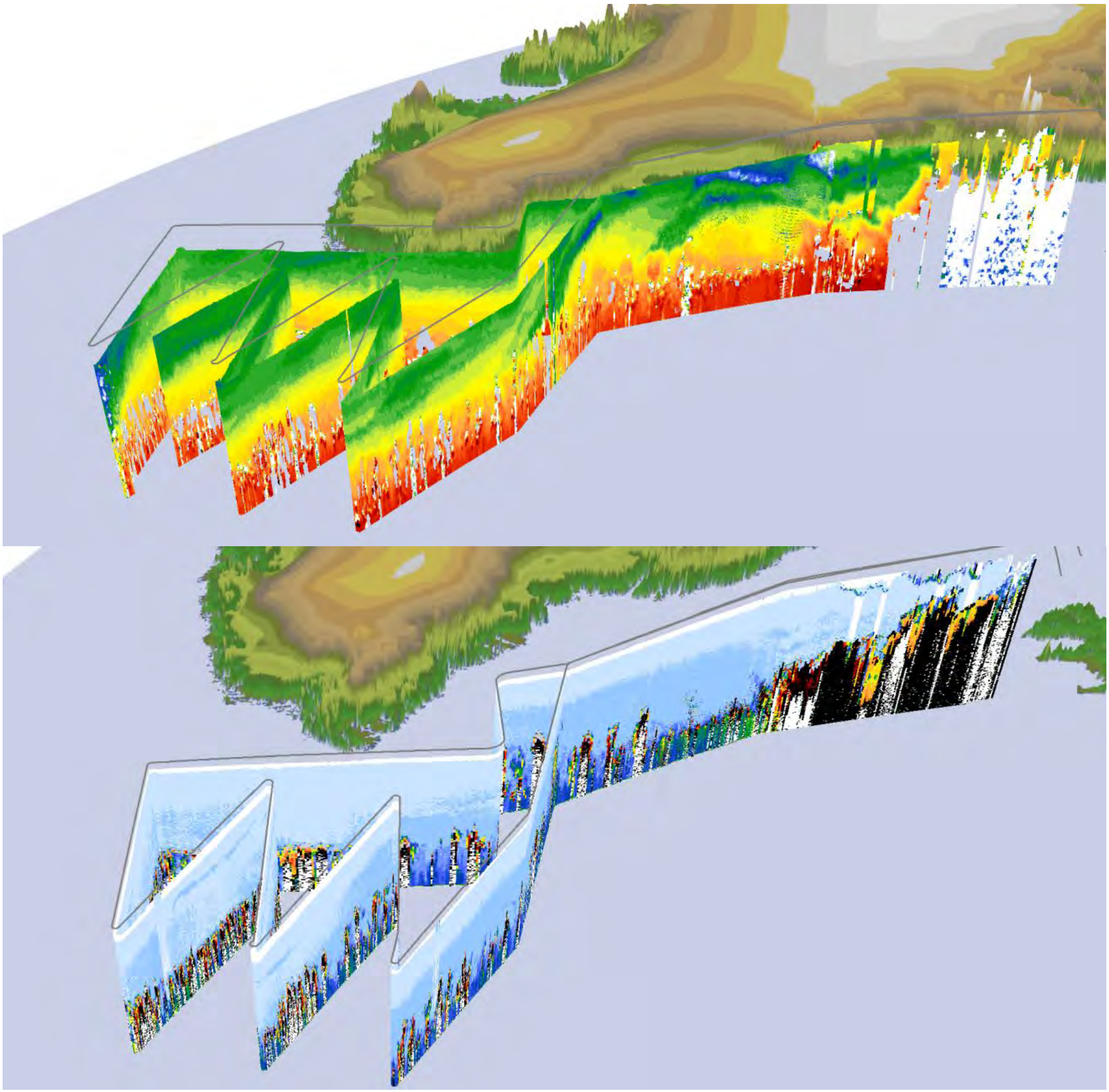

Fig. RF10.14: Time series of WALES lidar water vapor mixing ratio (top panel) and backscatter ratio (lower panel) in a 3-D view. The landmass in the background is southern Greenland. The thin grey line indicates the aircraft path at FL 260. Meaningful data are recorded from about 600 m below the aircraft down to the ground if atmospheric conditions allow. For better visualization the atmosphere is stretched by a factor of 70 to focus on the clouds.

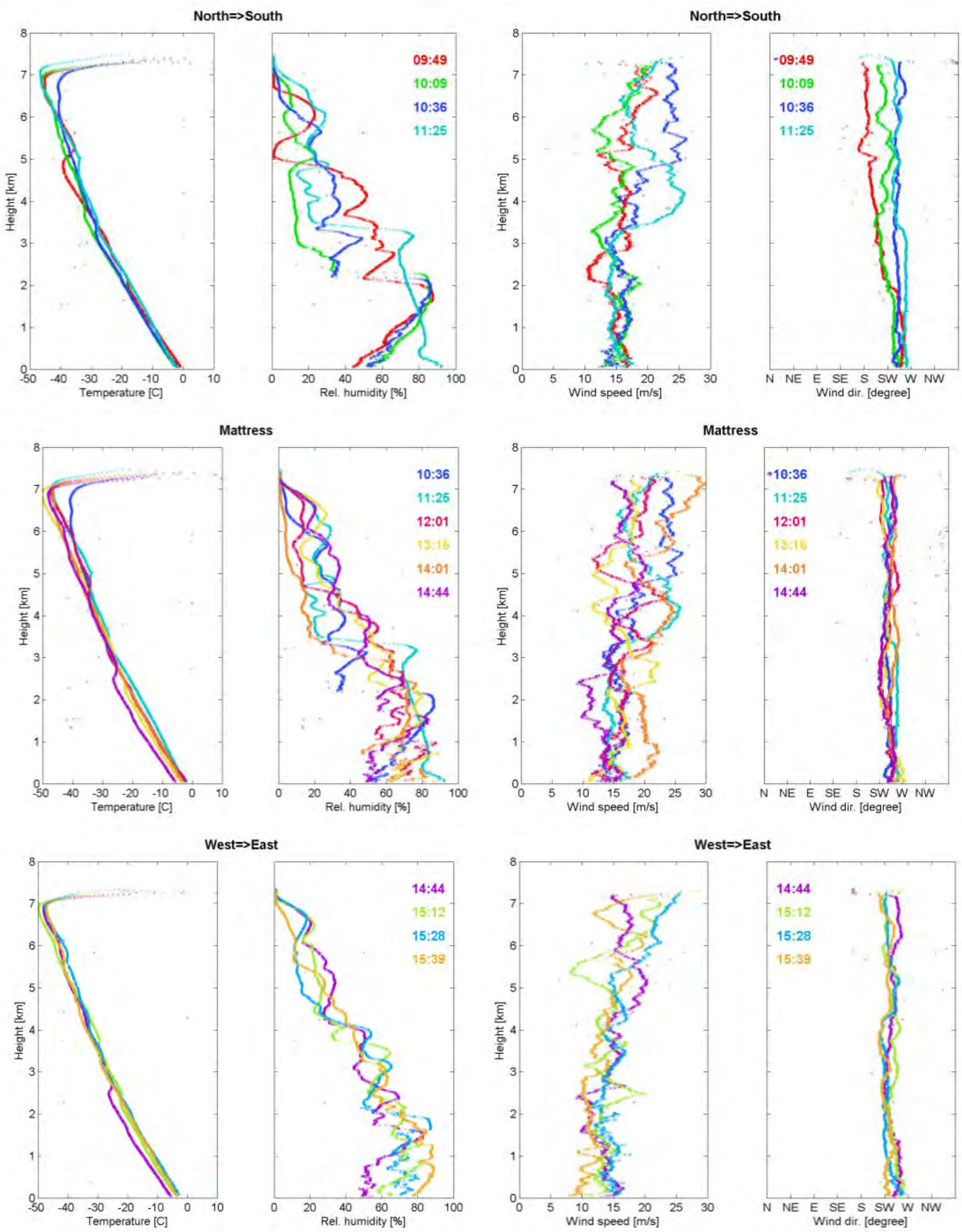

Fig. RF10.15: Quicklooks of the dropsonde profiles: Release of the eastern legs between the entry point and waypoint 3 (top), during the mattress (center) and between waypoint 7 and the box exit point including the CloudSat overpass (lower panel). Colors indicate the dropsonde release time and from left to right the parameters of air temperature (°C), relative humidity (%), wind speed (m/s), and wind direction (deg) are plotted. The apparently strong inversion at 7km height is an artifact of the temperature sensor shortly after the dropsonde release from the plane. The lower temperature inversions indicate cloud top heights in accordance with radar data. The convective cloud tops were lowest in the cold air being furthest away from the cyclone to the west with heights between 2 and 3 km. Surface temperatures were below freezing point at all times supporting the radar findings of snowfall down to the surface.

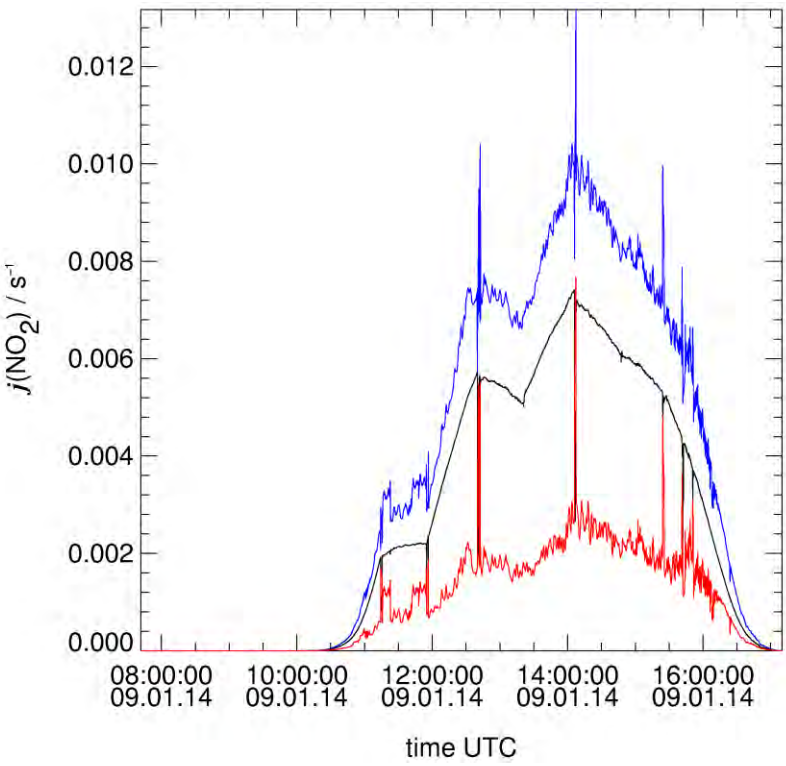

Fig. RF10.16: HALO-SR photolysis frequency $j(NO_2)$ from lower hemisphere (red), upper hemisphere (black) and combined (blue) measurements. Measurements reveal the latitudinal changes in the flight track. Strong peaks in nadir component correspond to higher aircraft roll angles while performing turns.

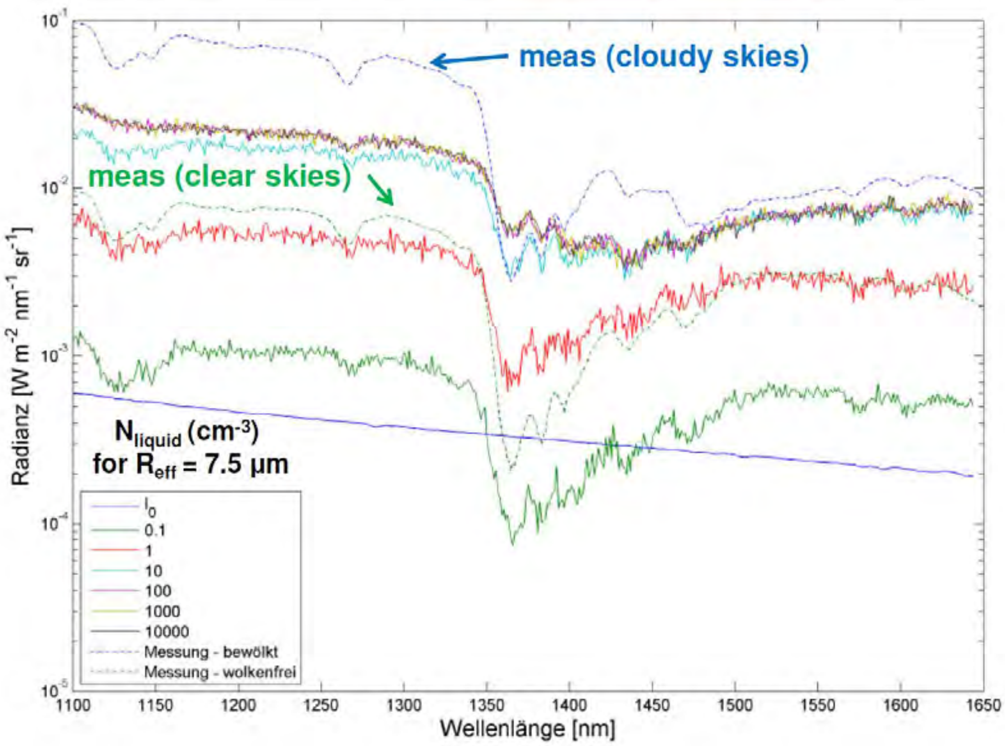

Fig. RF10.17: Mini-DOAS measured vs forward modelled near-IR nadir spectra for clear and cloudy skies.

The SSMIS and CloudSat perspective:

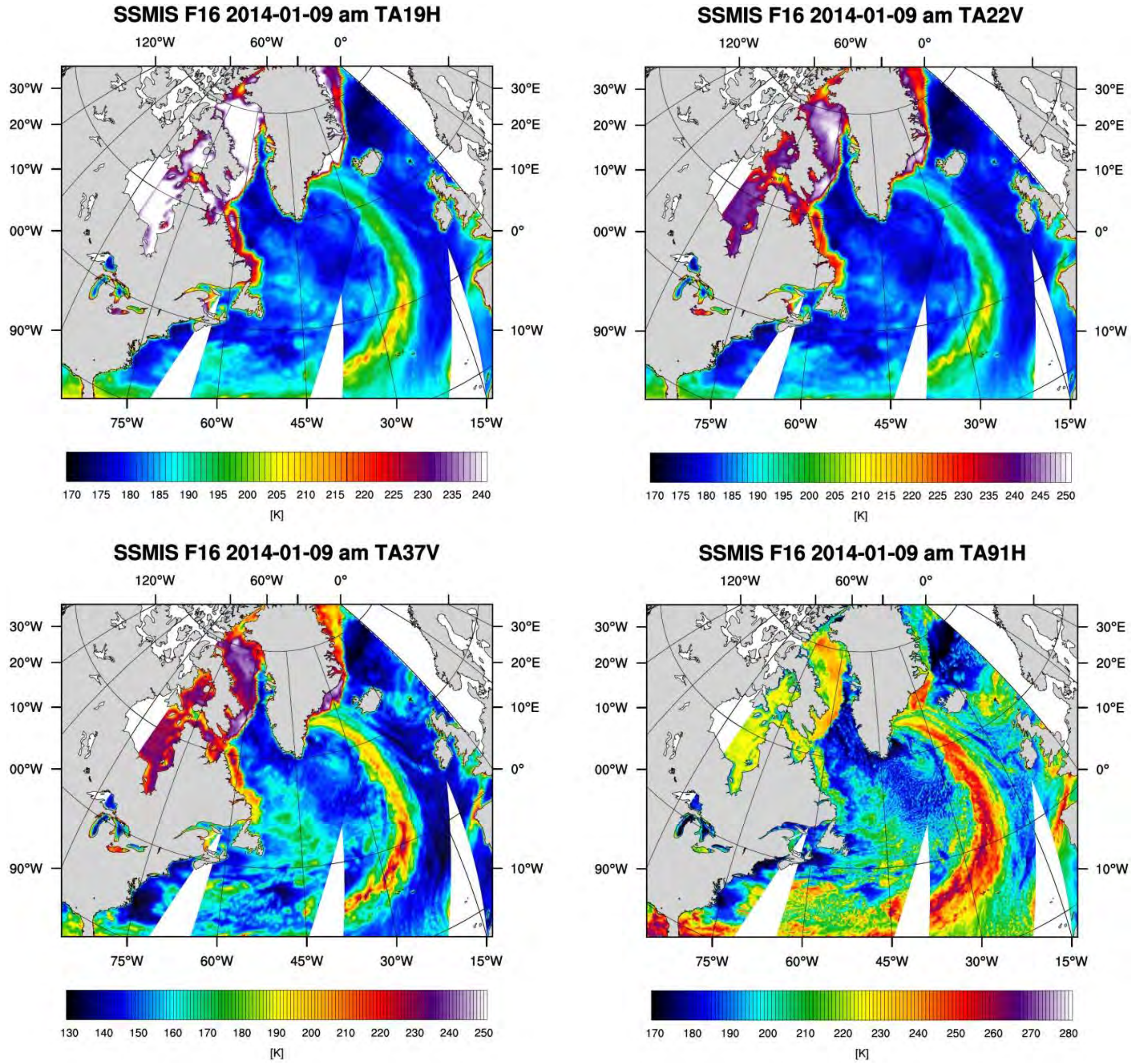

Fig. RF10.18: Preliminary HOAPS 4 fundamental climate data record (FCDR) antenna temperatures (TA) for DMSP-F16 SSMIS for the target area overpass at 11:38 UT. Shown are the environmental data record (EDR) emission channels 19 GHz H (sensitive to rain; top left), the water vapor channel 22 GHz V (top right), the 37 GHz V (lower left), and the 91 GHz H scattering channel (sensitive to ice; lower right) indicated for horizontal (H) and vertical (V) polarization. The cold front is easily recognized. The postfrontal precipitation regimes of enhanced cumulus containing rain are seen in light blue in the 19 and 22 GHz emission channels, green in the 37 GHz channels and green to yellow in the 91 GHz scattering channel. The scattering channel shows signatures of precipitating ice clouds in the enhanced cumulus region. It features also the postfrontal low in considerable detail suggesting that precipitation fell as snow which was also suggested by the absence of a radar brightband. Note the increase in resolution from the 19 GHz channel of about 50 km to the 91 GHz channel with 8 km. Collocations with three SSMIS overpasses (DMSP-F17 at 11:38 UT, and DMSP-F18 at 12:14 UT and 13:54 UT) were achieved.

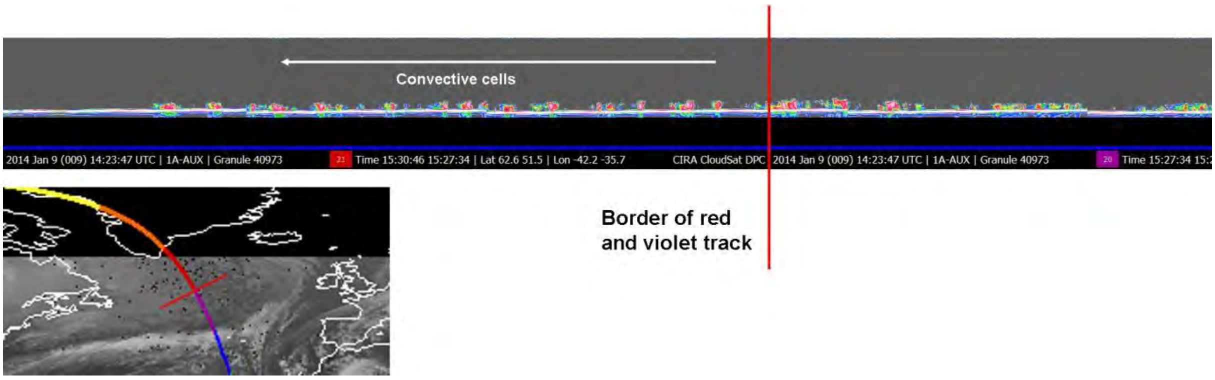

Fig. RF10.19: CloudSat granule 40973 track over the postfrontal region of the cyclone between 15:27 UT (violet section 20) and 15:30 UT (red section 21). The collocated HALO underflight was at 15:29 UT in the area marked with "convective cells". The northwestward flight direction of CloudSat is indicated by the white arrow. CloudSat passed over an area of convective cells.

15:28:00	52.8720	36.3296	343.88
15:29:00	56.4011	38.1301	342.81
15:30:00	59.9049	40.2455	341.42

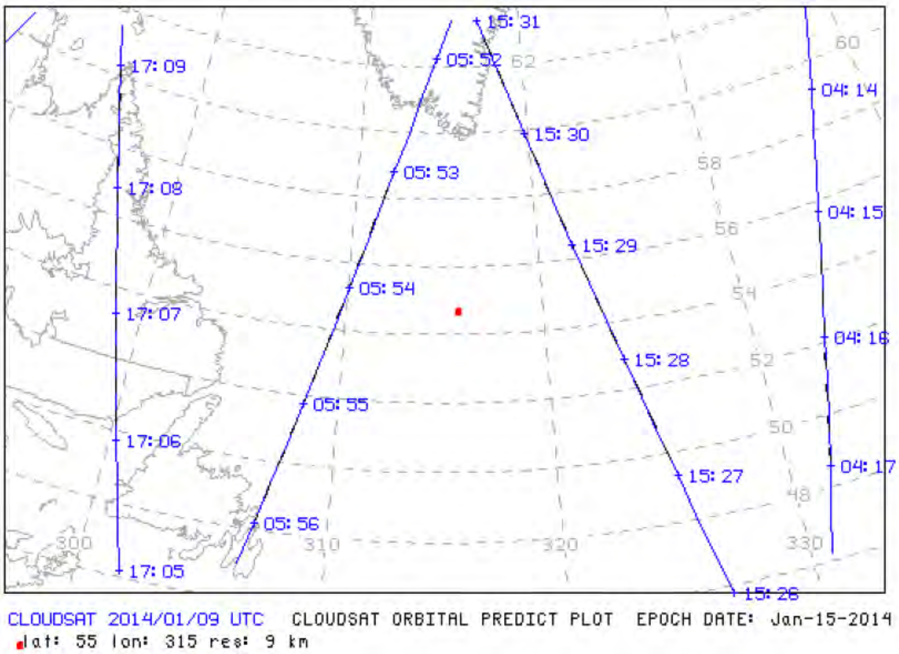

Fig. RF10.20: CloudSat ascending orbit track over the North Atlantic on 09 Jan 2014 between 15:26 UT and 15:31 UT. The collocated HALO underflight was at 15:29 UT in northwestward flight direction of CloudSat. Coordinates for 15:28 to 15:30 UT are given in the table above the figure.

NARVAL North Research Flight 11 (RF11), Flight Report

- 12 January 2014 -

CHRISTIAN KLEPP

Crew: Roland Welser (Pilot), Stefan Grillenbeck (Pilot), Alexander Wolf (Flight engineer), Andreas Schäfler (Dropsondes), Andreas Fix (WALES), Heike Konow (HALO SR & MiniDOAS), Friedhelm Jansen (HAMP), Christian Klepp (Mission PI & HAMP)

Objective: The scientific objective of the second research flight was to sample the convective core of a mature cyclone over the North Atlantic. The active tiltback occlusion (TBO) ruptured from the main frontal system of the cold front (CFR) and occlusion (OCC) and produced convective cloud bands (SCB) including cumulonimbus (CBs) spiraling towards the center of the cyclone. A total of 12 dropsondes were released. During operation time four SSMIS overpasses occurred. An originally planned CloudSat underflight had to be cancelled as gale force winds developing at KEF airport required an earlier return. Nonetheless, the CloudSat overpass revealed great insight into the convective system because the CloudSat satellite track followed an ascending path that cut through the entire cold core system and crossed the occlusion head of the cyclone. The temporal mismatch between HALO and the CloudSat overpass allows for investigating the temporal development of the system in great detail.

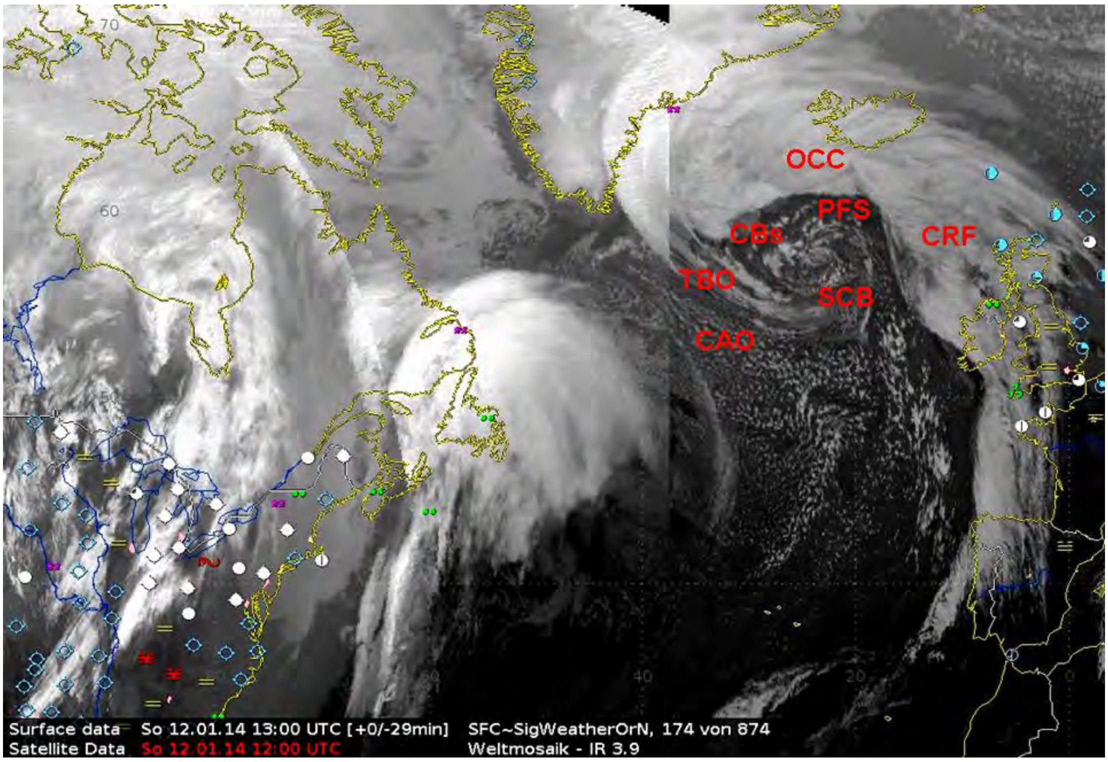

Fig. RF11.1: The mature low pressure system of the second research flight occupied a large fraction of the eastern North Atlantic Ocean. The flight aimed at measuring the entire suite of cold air regimes: The frontal occlusion (OCC), postfrontal subsidence (PFS), cold air convection with embedded Cumulonimbus (CBs), tiltback occlusion (TOC), cold air outbreak (CAO), convective spiral cloud bands (SCB), and the cold front (CFR).

Overview:

The cyclone of 12 January 2014 is the result of an explosive development from the previous day along the eastern side of a through located over the central North Atlantic bringing cold air far south to 40°N. This rapid development led to a postfrontal cold air outbreak that reached the northwestern coast of Portugal. Due to the blocking situation over Europe the entire low pressure system intensified without the usual eastward movement (Fig. RF11.2). The target area of the flight was located to the southwest of Iceland. The cyclone developed a strong tiltback occlusion that partly fractured from the cyclone head. The cold core system of the tiltback occlusion exhibited cloud bands spiraling into the cyclone center with a core pressure of 960 hPa (Fig. RF11.3).

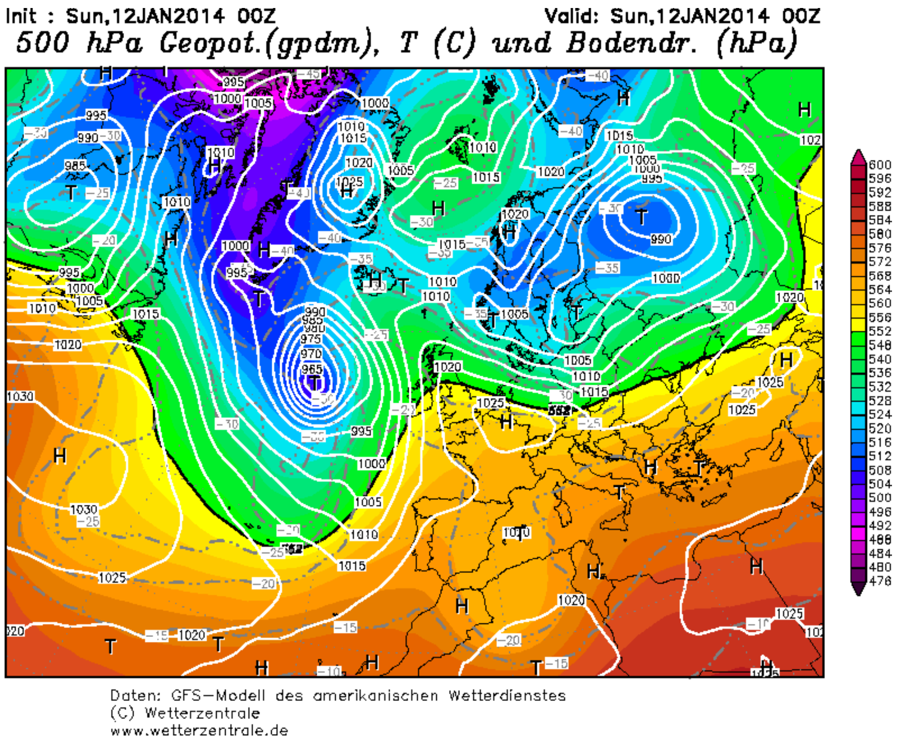

Fig. RF11.2: GFS analysis of surface pressure (white isolines), 500 hPa geopotential height (color, 552 dekameter isoline in black) and temperature (dot-dashed grey isolines with white boxes) in °C valid for Sun, 12 Jan 2014 00 UT showing the intense cyclone in place with a core pressure below 965 hPa.

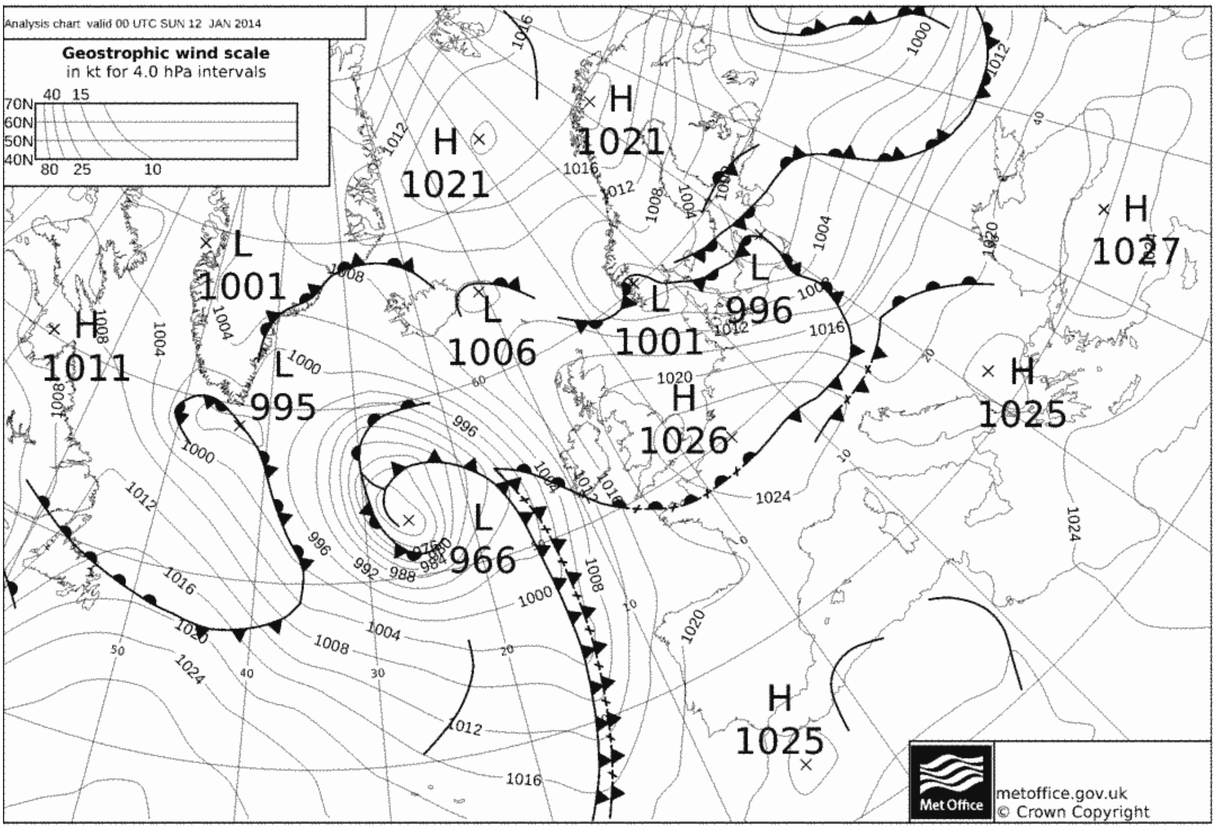

Fig. RF11.3: UK Met. Office analysis chart for 00 UTC on Sun 12 Jan 2014 with the target area being located in the area of the cyclone center of 53N/25W. The rapidly developing system shows the active cold front and the beginning of the tiltback occlusion fracture. The spiral shape of the cylone center documented in the satellite mosaic of Fig. RF.2.1 is in development.

Flight Planning: As ATC is not on duty during weekends the flight planning for a Sunday (12 Jan.) mission had to be finished by Friday (10 Jan.) noon. Of course it is a challenging task to foresee the required target area for airspace blocking 48 hours in advance with adequate accuracy from the available forecast material. The request for a flight on FL430 or FL450 to remain above the clouds at all times was rejected by ATC due to air traffic in the area. Finally, a block of airspace was tied up at FL 270 (approx. 8 km height) for HALO to the south of Iceland controlled by Irish air authorities and the allowance for dropsondes in this area was approved (Fig. RF11.7). On Saturday evening (11 January) the aviation weather forecast at KEF airport issued a wind warning of gale force for the flight day (12 January) from 12 UT on. Consequently, the originally planned flight pattern with 6 legs was shortened to only 2. In the morning shortly before take off the wind warning restrictions were eased allowing for a return at 15 UT and flying 4 legs. Nevertheless, the planned CloudSat underflight had to be cancelled in favor of a safe return to KEF. The available satellite images revealed however that 4 legs covered the entire center of action of the cold air activity. It was further planned to provide the HALO science crew with inflight satellite image updates from the surface crew in KEF. Several SSMIS overpasses were expected during the flight operations.

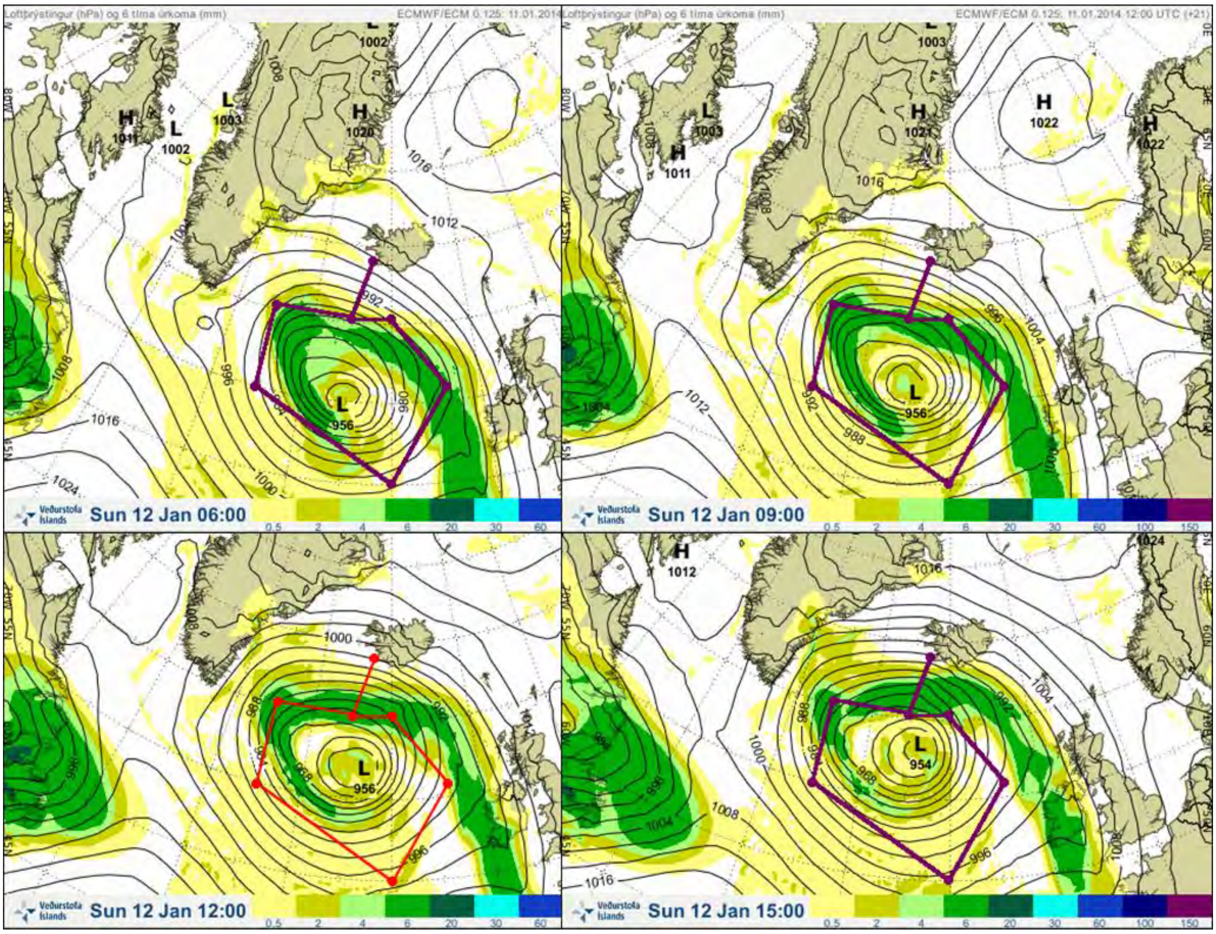

Fig. RF11.4: ECMWF forecast for 12 Jan 2014, 06, 09, 12, and 15 UT for surface pressure isobars and precipitation amount accumulated over 3 hours (color). The ATC approved flight bounding box is outlined. The cyclone shows significant frontal and postfrontal precipitation. The cloud bands spiraling towards the center are predominantly seen in the 12 and 15 UT forecast and exhibit patches of convectively enhanced precipitation.

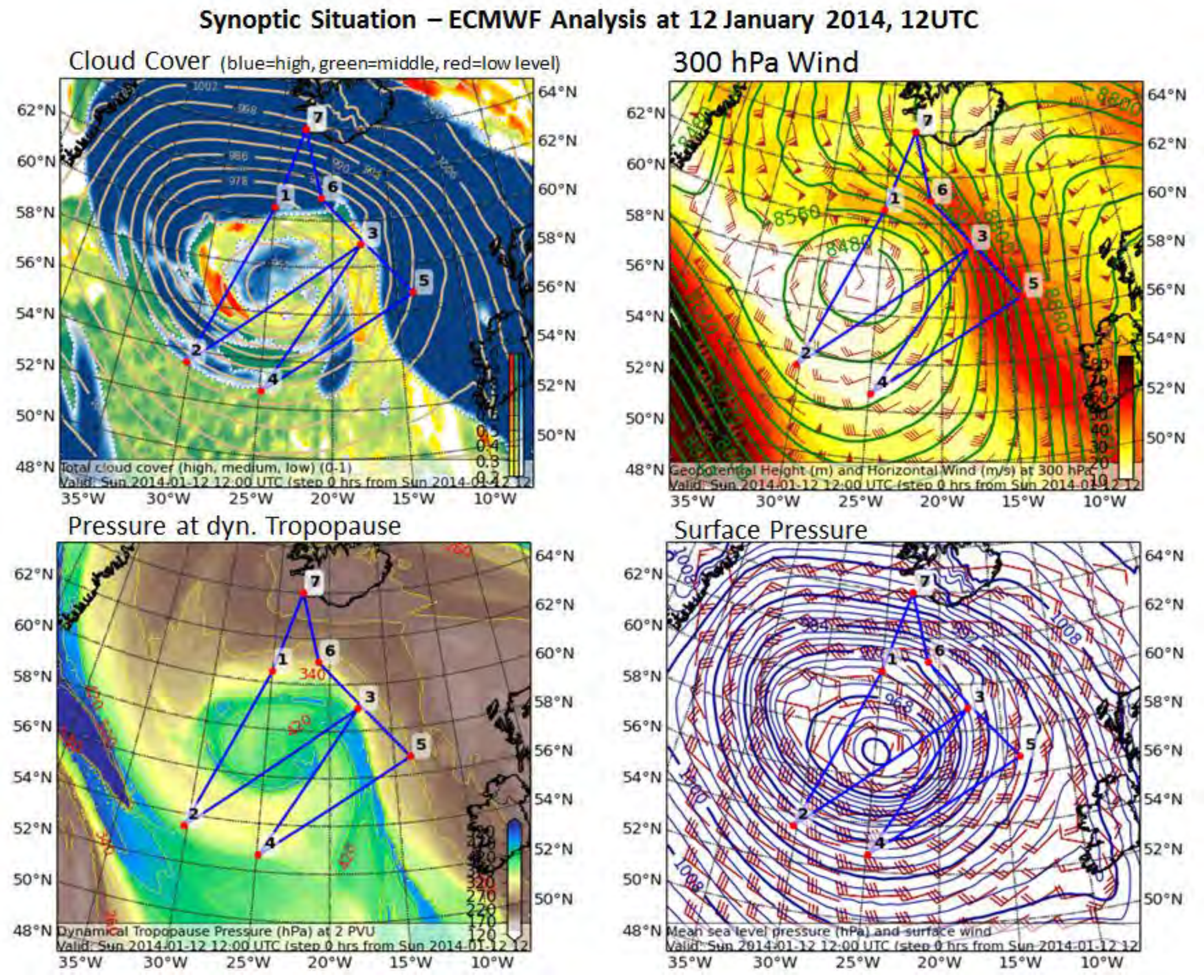

Fig. RF11.5: ECMWF based flight planning tool of DLR showing cloud cover (color) and surface pressure (isolines, top left panel), 300 hPa geopotential height (color) and wind speed (arrows, right top panel), dynamic tropopause pressure (color, lower left panel), and mean sea level pressure (isolines) and surface wind (arrows, lower right panel) for 12 Jan 2014, 12 UT, including the flight pattern in blue and numbered waypoints as red dots.

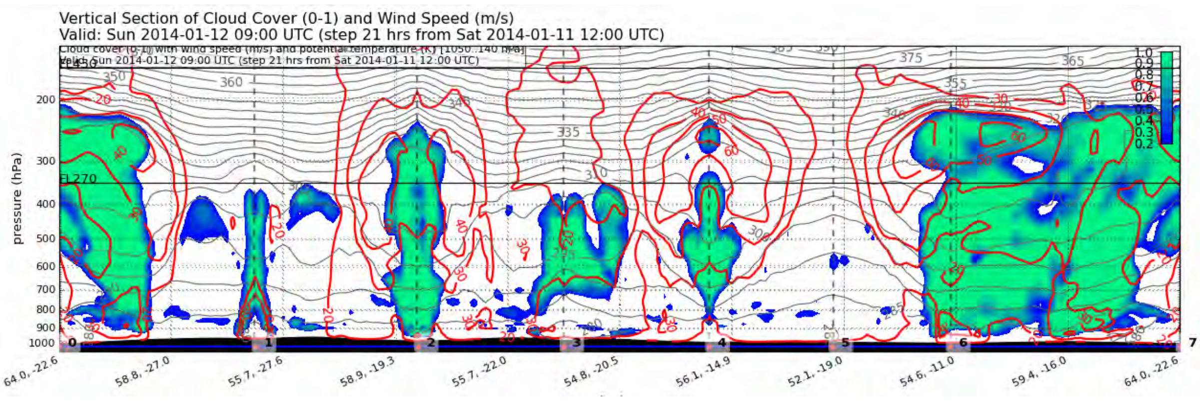

Fig. RF11.6: ECMWF based flight planning tool of DLR showing the vertical section of cloud cover (color) and wind speed (m/s in red) along the flight track from left to right. The waypoints are listed on the x-axis. The constant flight altitude of FL270 is marked as a black line.

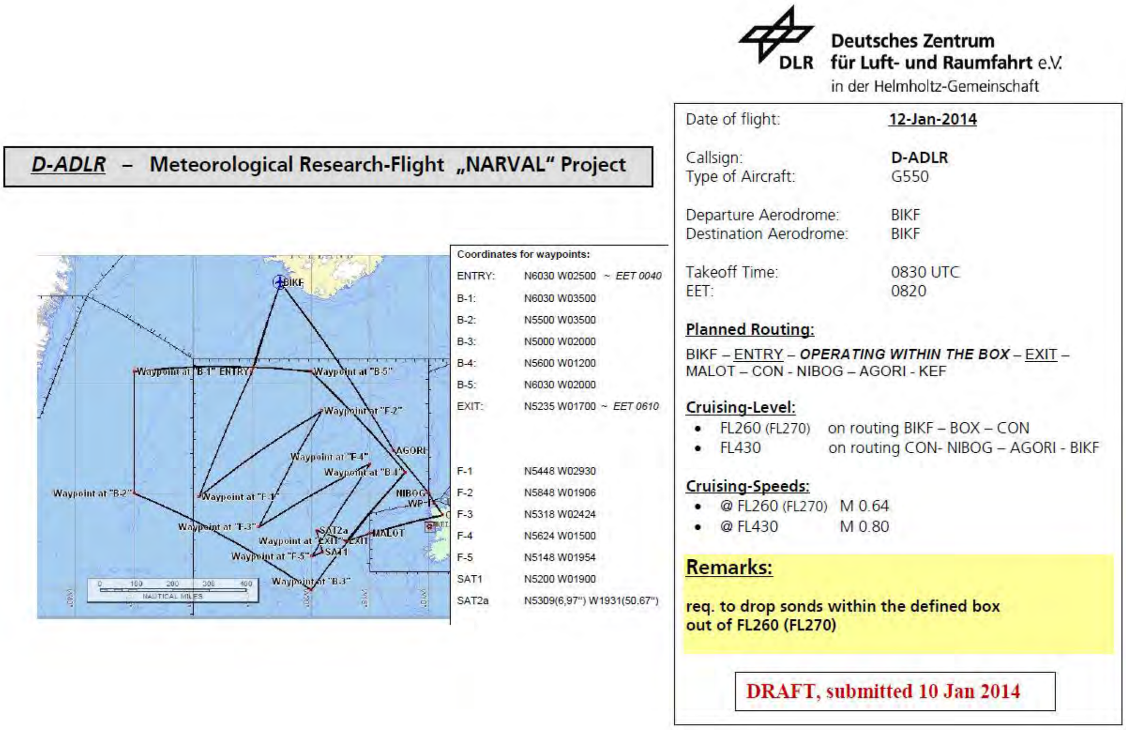

Fig. RF11.7: ATC requested and approved flight pattern for RF11. The black bounding box coordinates B-1 to B-5 contain the HALO tied up airspace at FL270 with dropsonde and flight pattern change clearance. The entry and exit point of the bounding are indicated at 60N/25W and 52N/17W. The actual flight pattern is shown in black including the mattress waypoints (WP F-1 to F-5) and the CloudSat collocated track SAT1 and SAT2. Coordinates of all points are listed in the panel table. The flight pattern was changed on short notice due to the wind warning at KEF, resulting in the cancellation beyond WP F-4. Consequently the flight returned on the direct way from F-4 to KEF (BIKF).

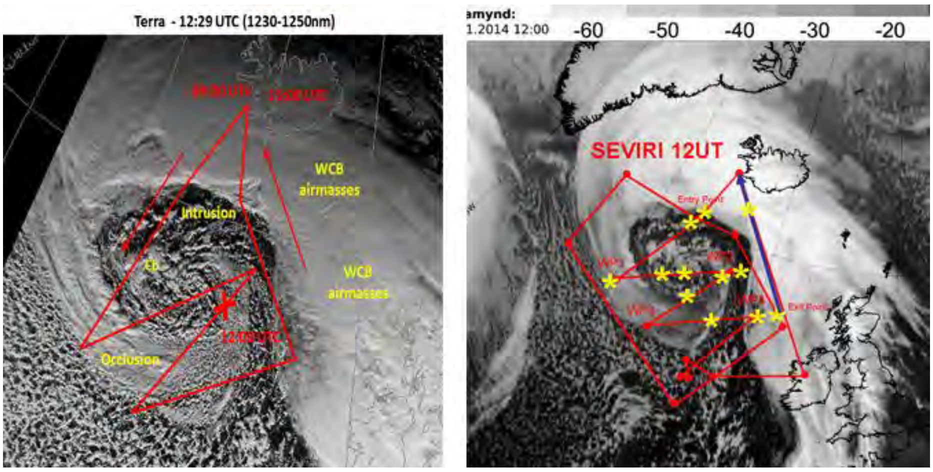

Figure RF11.8: Flight pattern on 12 January 2014 between 8:30 UT and 15:10 UT. The left image shows TERRA IR channels at 12:29 UT, the final flight pattern and documents the main air-masses included. The right image shows the same situation for the SEVIRI IR channels at 12 UT. The routing was from KEF to the FIR boundary entry point. From there the mattress pattern from waypoint WP1 to WP4 was flown. Dropsonde locations are given as yellow stars. Due to gale force winds in KEF the pattern was terminated at WP4 with a straight return flight into KEF.

Flight Report: HALO took off from KEF at 08:32 UT and reached the cruising altitude of FL270 in 13 minutes. At 08:54 UT the cloud base of the cold front / main occlusion was reached and HALO went into the frontal clouds. At 09:05 UT both radar and lidar were operational. The FIR boundary entry point of the tied up airspace was reached at 09:10 UT and flight leg 1 started. Fig. RF11.8 shows the bounding box, legs, waypoints, dropsondes positions and the satellite image for 12 UT for illustration of the flight track.

LEG1 (1:01 h duration)

At 60N the first dropsonde was released into the occlusion 5 minutes after passing the FIR boundary. At 09:16 UT HALO left the occlusion front. From this time on, the remainder of the flight stayed above all clouds; except for the transfer from WP4 en route to KEF and the final descent into KEF. The transition from the occlusion into the postfrontal subsidence was abrupt and the first light of dawn allowed seeing the sea surface through almost cloud-free conditions at 09:25 UT. Here, the second dropsonde was released. At 09:30 UT the cold air convection started with cloud tops of about 3 km height. Numerous cumulonimbus clouds with iced anvils protruded the convection up to 6 km height. Probing the deepest convective Cb with a dropsonde failed due to a short communication outage between the pilots, PI, and the dropsondes operator. At 10:00 UT the tiltback occlusion was reached and dropsonde 3 was released. By shifting waypoint 1 of the first leg to the ATC boundary box it was possible to entirely cross the tiltback occlusion and reach the cold air outbreak to the west. At waypoint 1 HALO turned at 10:16 UT for leg 2 (Fig. RF11.9).

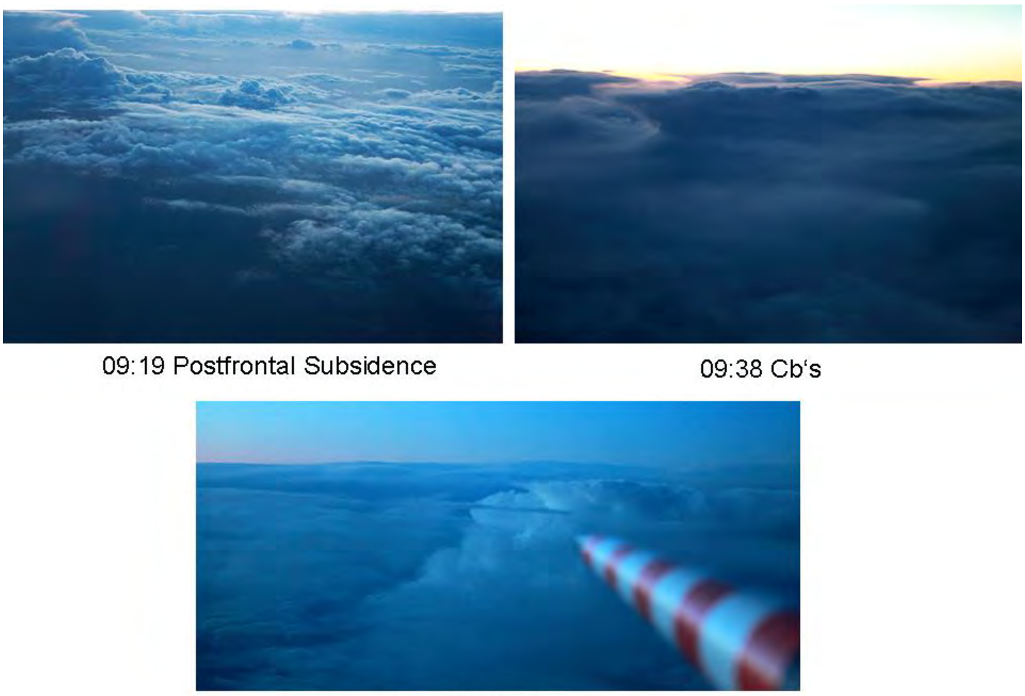

09:19 Postfrontal Subsidence

09:38 Cb's

09:37 Cb

Fig. RF11.9: Leg 1 inflight photo documentation of the cloud patterns showing the cloud-free postfrontal subsidence shortly before the convection starts at 09:19 UT (top left), the ice capped anvils of the cumulonimbus clouds at 09:38 UT (top right), and a cumulonimbus that HALO was overflying at 09:37 UT during a slight excursion from the leg path.

LEG2 (1:17 h duration)
HALO returned over the tiltback occlusion at 10:20 UT and reached the spiral convection bands towards the center of the cyclone at 10:42 UT. Dropsondes 4 and 5 were released at 10:49 and 11:13 UT over cumulonimbus clouds marking the center of the cyclone with a core pressure below 960 hPa. At 11:17 UT a prominent spiral cloud band was passed. As satellite images could successfully be received in flight it became possible to estimate the cloud patterns ahead. To some surprise, the cloud structure seen from the aircraft windows at 8 km height (Fig. RF11.10) was fully recognizable when compared to the satellites view. Dropsonde 6 was released into the postfrontal subsidence at 11:35 UT. At waypoint 2 (11:37 UT) the cold front was not fully reached due to the ATC bounding box limits. The view towards both the tiltback occlusions at the beginning of leg 2 and the cold front at waypoint 2 documents the wall of clouds adjacent to the almost cloud-free postfrontal subsidence (Fig. RF11.10).

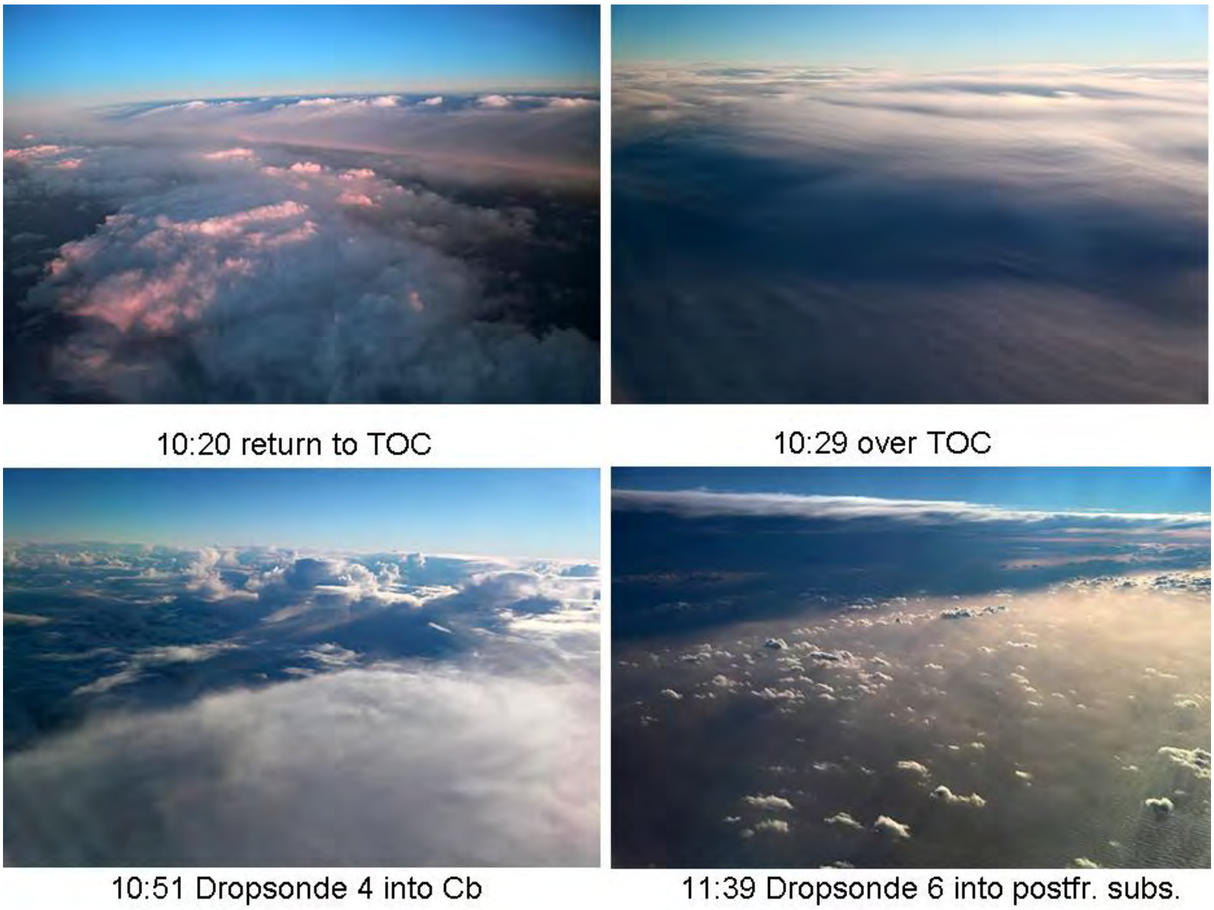

Fig. RF11.10: Leg 2 inflight photo documentation of the cloud patterns showing the cloud structures. HALO fully passed over the tiltback occlusion at the end of leg 1 and reached the cold air outbreak region to the west of the cyclone. The massive wall of clouds is seen on the upper left panel. At 10:29 UT HALO passed over the tiltback occlusion (upper right panel). The lower left image shows HALO right above a Cb with 6 km cloud top into which a dropsonde was released. The lower right image documents the subsidence region with Cumulus humilis and the wall of clouds belonging to the cold front at waypoint 2.

LEG3 (1:10 h duration)

Leg 3 started at 11:40 UT with the passage of Cumulus humilis over the subsidence regions and the convection picked up again at 11:50 UT with cloud tops reaching 1500 m height. At 11:54 UT dropsonde 7 was released into the spiral cloud band. The clouds grew further vertically into towering Cumulus congestus and altocumulus fields with convection reaching 4 km height at 12:09 UT. At 12:24 the convection height dropped significantly towards shallow cumulus reaching 2 km height and dropsonde 8 was released. Finally, the subsidence was again reached and the tiltback occlusion became fairly inactive with few high level clouds only and no precipitation (12:48 UT).

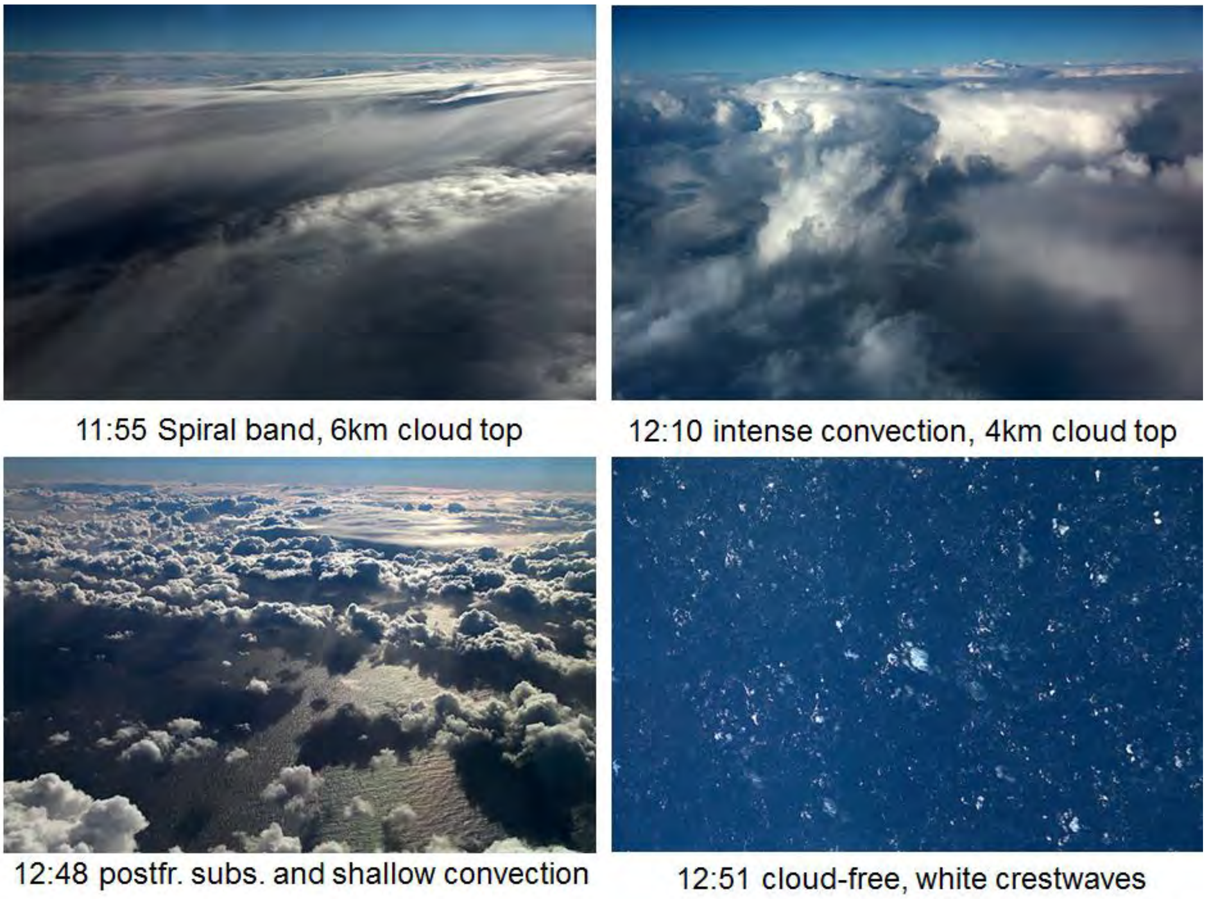

Fig. RF11.11: Leg 3 inflight photo documentation of the cloud patterns showing the crossing over one of the cold core spiral cloud bands at 11:55 reaching cloud heights up to 6 km. In between the spiral bands the intense convection grew to altitudes of 4 km including Cbs with overshooting iced anvils. Towards waypoint 3 the tiltback occlusion was again reached showing a significantly less pronounced activity compared to the previous legs. In contrast, the subsidence region was well expressed shallow convection dying out completely and giving view on the white crestwaves of the cloud-free ocean surface.

LEG4 (1:03 h duration)

Leg 4 started at 12:52 with few clouds. At 13:15 the convection started again and at 13:33 dropsonde 9 was released into the spiral cloud band. After the passage of the convective band a cloud-free area followed and virga snowfall was seen at 13:37 UT. At 13:40 the subsidence was reached and dropsonde 10 descended into a prominent cloud hole within the cold front at 13:46 UT. At 13:49 the cold front was reached and HALO flew into the high clouds to drop the sonde number 11 at 13:54. HALO turned back towards KEF at 13:55 after passing waypoint 4.

The transfer back took place within the cold front until at 14:06 UT the postfrontal air mass was again reached in the northeastern sector of the cyclone center. The exit point was reached at 14:36 at 61N, 21W. Wave structures were documented along the cold front and at 15:42 dropsonde 12 was released into the occlusion. Right after this the descent into KEF started. Radar and Lidar were switched off at 14:56 UT and HALO landed at 15:10 UT in gale force winds.

Fig. RF11.12: Leg 4 inflight photo documentation of the cloud patterns. Along leg 4 the cold air activity was less pronounced and the spiral bands suppressed the convection. By 13:50 the main cold front / occlusion were reached. The satellite image showed a pronounced cloud hole allowing vision down to the sea surface. From waypoint 4 HALO returned on a straight transfer leg towards KEF. Flying along the frontal structure revealed mostly thin cirrus-like clouds with repeated visibility down to the sea surface. By 14:23 the cold air was again reached. The flight parallel to the front allowed an unprecedented view on wave patterns within the front at 14:40.

In total 4 legs of approx. 1h duration each were flown with 2 transfer flights to and from the ATC bounding box. In total HALO was flying 6:45 h and 12 dropsondes were released. Four SSMIS collocation overpasses occurred during the mattress pattern by DMSP-F16 (14:50 UT), DMSP-F17 (09:17 UT), and DMSP-F18 (09:55 and 11:35 UT) (Fig. RF11.23).

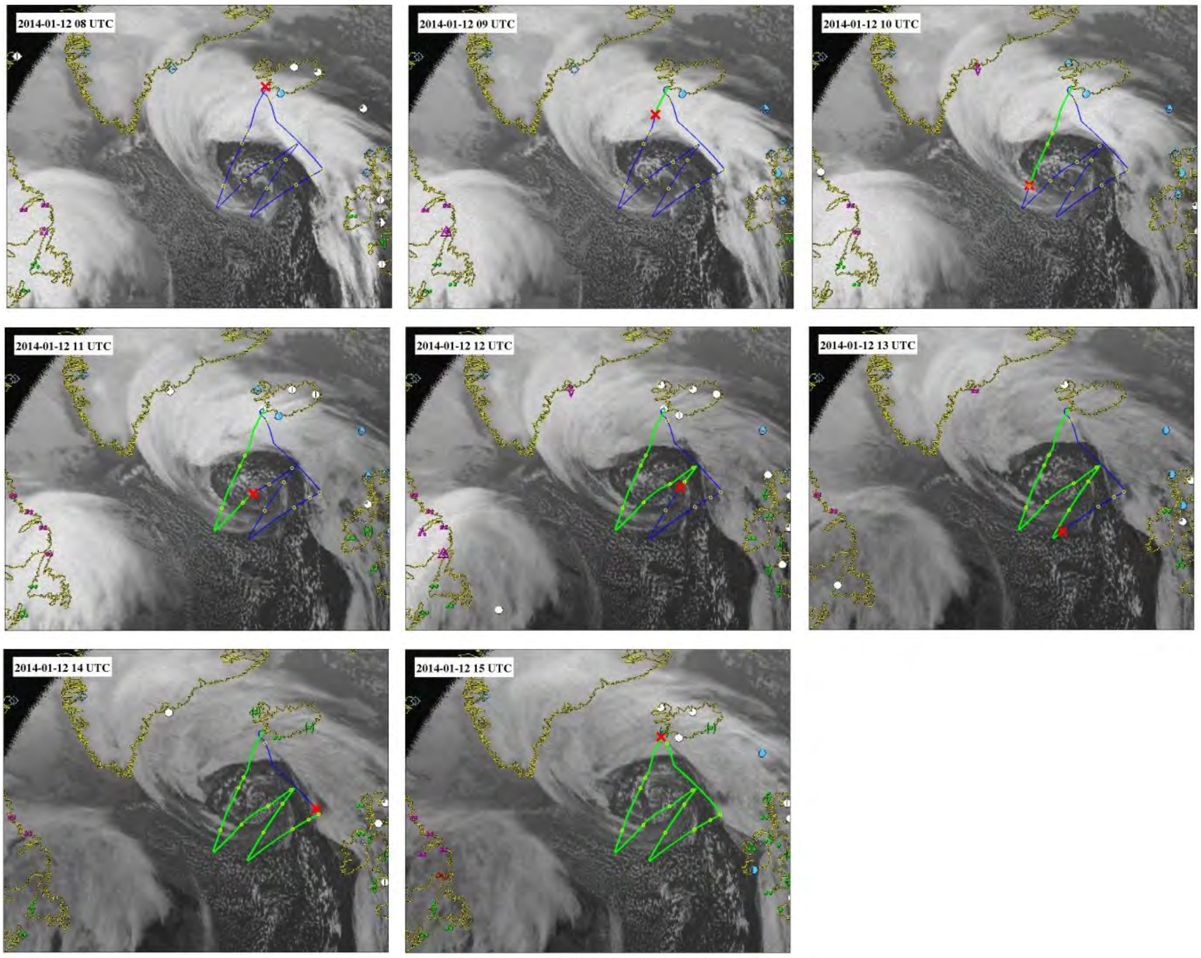

Fig. RF11.13: Hourly flight track composite in blue and infrared satellite data with elapsed flight time in green, current aircraft position as red cross and dropsondes positions as yellow circles. This composite is to be used as a reference for the flight protocol below.

Flight Protocol

All times in UT

No liquid nitrogen available, only warm target calibration

07:37 hangar rollout
08:10 radiometer operating stable
08:23 taxi to RWY 11
08:28 backtrack RWY 11
08:32 take off RWY 11
08:35 auto pilot on
08:36 10.000 ft altitude
08:43 8 km altitude
08:44 radar on
08:45 FL270 reached
08:49 radar reboot, radar not operating
08:54 first cloud contact
08:58 in clouds, light turbulences
08:59 lidar not operating yet
09:04 first dawn, flight along cloud top on FL270, few cirrus above

09:05 radar indicating clouds down to surface
09:08 flying into cold front / occlusion clouds
09:10 FIR boundary ENTRY 60.3N reached
09:15 dropsonde 01 at 60N into the cold front / occlusion
09:16 cold front / occlusion cloud top reached: from now on above all clouds, no high cirrus clouds
09:19 cloud top lowers significantly, still above all clouds
09:20 convective towering cumulus and Cbs to the east
09:25 above postfrontal subsidence, cloud-free down to the surface
09:25 dropsonde 02 into postfrontal subsidence
09:30 cold air convection reached, cloud tops significantly rising
09:32 sea surface partly visible, partly stratiform cloud decks, Cbs at the horizon
09:33 embedded towering convection without Cb anvils below
09:34 slight course correction to the right to reach a Cb centrally
09:38 image of the Cb below the plane taken from the cockpit
09:39 shallow convection and As fractus
09:40 Cb to the Southeast, photo taken from left window
09:41 slight course correction to the right to reach a Cb centrally
09:41 above Cb, dropsonde not released due to communication error
09:43 left course correction to get back to flight track
09:52 tiltback occlusion cloud wall ahead
09:53 clouds in two decks, Cu and As, Cbs at SE horizon
10:00 dropsonde 03 into tiltback occlusion front
10:08 sunrise
10:11 elongated cloud bands perpendicular to flight direction seen from cockpit indicating the end of the tiltback occlusion
10:13 ocean surface visible, end of tiltback occlusion, white crest waves seen, high wind speed
10:16 view along the tiltback occlusion cloud wall, flying further than initial WP1 until bounding box is reached
10:19 extended WP1 reached, turn left into leg 2
10:20 approaching the tiltback occlusion vertical cloud wall, impressive scenery documented by photos
10:23 above the tiltback occlusion
10:29 very homogeneous cloud top, appears like flying above cirrus
10:35 cockpit view shows cold air convection at the horizon in flight direction with towering Cc
10:38 slight course correction to the left to reach a Cb for dropsonde release into it
10:42 end of tiltback occlusion reached
10:47 Cb surrounded by cloud-free ring
10:49 dropsonde 04 into Cb, cloud top at 6 km
10:51 course correction back towards WP2
10:53 flying over ice-capped Cb's, center of the cyclone, core pressure 960 hPa
11:06 slight course correction to the right to fly over enhanced convection
11:08 photo from the cockpit towards convection cell to be probed by dropsonde 05
11:11 sea surface partly seen, shortly before dropsonde position over convective cell
11:13 dropsonde 05 released over Cb/Cc, in the center of leg 2 between WP1 and WP2
11:14 towering Cbs to the left (North)
11:16 slight course correction back towards WP2
11:17 more stratiform appearing cloud decks

11:25 open convective cells and sea surface visible
11:26 in flight direction the cold front / occlusion is seen as a broad cloud band across the flight direction
11:30 cockpit view shows significant flattening of the convection height towards the cold front / occlusion
11:35 dropsonde 06 within the postfrontal subsidence, almost cloud-free, appearance similar to Cu humilis in the trade wind zones
11:36 photo of cold front / occlusion with postfrontal subsidence and tradewind like cumuli
11:37 WP2 reached and right turn into leg 3 towards WP3; cold front / occlusion not fully reached but in sight
11:39 flight along the cold front / occlusion with postfrontal subsidence and Cu hum
11:43 shallow convection with 1500 m cloud tops
11:50 convection grows
11:51 high iced cloud band across flight direction is one cloud band of the inner cold core cloud spiral
11:54 dropsonde 07 into iced cloud band; cloud tops at 6km altitude, image 5601; low level bright band visible in radar
11:56 behind the cloud band reduced convection height, Cu and Ac, two-layer cloud decks
12:03 shallow Cu, few gaps allow seeing the sea surface
12:04 northward are Cbs visible
12:09 convection grows rapidly, Cbs below; intense convection; cloud tops at 4 km
12:12 intense convection and turbulences, convection has cloud-free rings around the cells, sea surface seen in the convective downdraft areas
12:15 end of intense convection reached, shallow closed convection, sea surface rarely seen
12:18 shallow convection, sea surface more often visible
12:24 dropsonde 08 in shallow convection, cloud tops at 2km; snow and rain to the ground
12:27 tiltback occlusion seen at the horizon in flight direction, southerly branch of the spiral cloud
12:47 postfrontal subsidence, sea surface largely seen, few Cu hum, tradewind cloud character, photo 5609+5610
12:50 WP3 reached, left turn into leg 4
12:52 leg 4
12:53 extreme white crestwaves, few shallow Cu hum
13:04 southerly tiltback occlusion part weakly developed compared to the northern branches, scattered Cu fields, sea surface mostly seen, sea surface has white streaked appearance due to crestwave foam
13:05 few precipitation in the radar data, no dropsondes released
13:13 thin cirrus band to the north seen as a comparably dark band, photo 5617
13:15 convection grows into scattered towers
13:29 close to fly over the next spiral band across the flight direction
13:33 dropsonde 09 released into the spiral cloud band, thin clouds, few precipitation
13:34 narrow cloud-free band after the passage of the spiral cloud band, suppressed convective area, photo 5621, followed by growing convection in cloud streets
13:37 scattered Cu with virga, photo 5622-5624
13:40 postfrontal subsidence and frontal / occlusion cloud wall in sight in flight direction
13:46 dropsonde 10 into prominent cloud hole within the frontal occlusion. Cloud hole seen in 12UT satellite image
13:49 reached the frontal occlusion clouds behind the cloud hole, cirrus at FL270, first cloud contact since start of leg 1
13:51 cold front / occlusion fully reached, clouds higher than FL270, HALO in clouds

13:54 dropsonde 11 into cold front / occlusion, sea surface again seen, few shallow Cu, high cirrus clouds
13:55 left curve at WP4 towards the EXIT point, flight northward along the cold front / occlusion, sea surface seen through in the warm conveyor belt area
14:02 sea surface out of sight, within thick cirrus
14:06 exiting cold front / occlusion again, scattered Cu, cold front / occlusion in sight to the right, photo 5627+5628, cloud-free postfrontal subsidence border in 12 UT satellite image
14:18 cold air convection reach again
14:21 cold front / occlusion in sight in flight direction, northern branch of the main occlusion, partly deeper convection within the cold air with showers indicated by the radar, photo 5629+5630
14:33 partly enhanced convection, occlusion ahead
14:36 EXIT point 61N 21W reached
14:38 postfrontal subsidence, cloud-free area behind the main occlusion, photo 5634
14:40 cloud wave structure along the main occlusion, photo 5635-5646
14:43 reaching the main occlusion, still above the clouds, turbulence
14:46 flight along the cloud top
14:50 within cirrus, additional cirrus layer aloft
14:52 dropsonde 12 into the main occlusion front outside the bounding box, requested and approved by KEF radar, 15 minutes prior to landing
14:56 lidar and radar off, descend into KEF
15:04 localizer KEF
15:08 cleared to land RWY 11, gear down
15:10 touch down RWY 11
15:12 taxi to park position
15:16 parking position

Dropsondes
All time in UT.

Entry Point 60.30 Nord
01 09:15 release into the front at 60°Nord
02 09:25 into postfrontal subsidence
03 10:00 into occlusion front
04 10:49 into Cb, cloud top at 6 km
05 11:13 released over Cb/Cc, in the center of leg 2 between WP1 and WP2
06 11:35 within the postfrontal subsidence, almost cloud-free, Cu humilis
07 11:54 into iced cloud spiral band; 6km cloud top, image 5601; low level brightband
08 12:24 in shallow convection, cloud tops at 2km; snow and rain to the ground
09 13:33 released into the spiral cloud band, thin clouds, few precipitation
10 13:46 into prominent cloud hole within the frontal occlusion, seen in 12UT satellite image
11 13:54 into cold front/occlusion, sea surface again seen, few shallow Cu, high cirrus clouds
12 14:52 into the main occlusion front outside bounding box, 15 minutes prior to landing

Preliminary HALO instrument data: All instruments onboard recorded data without significant gaps. Displayed below are selected preliminary results with the exception of MiniDOAS. This data will be analyzed after the campaign.

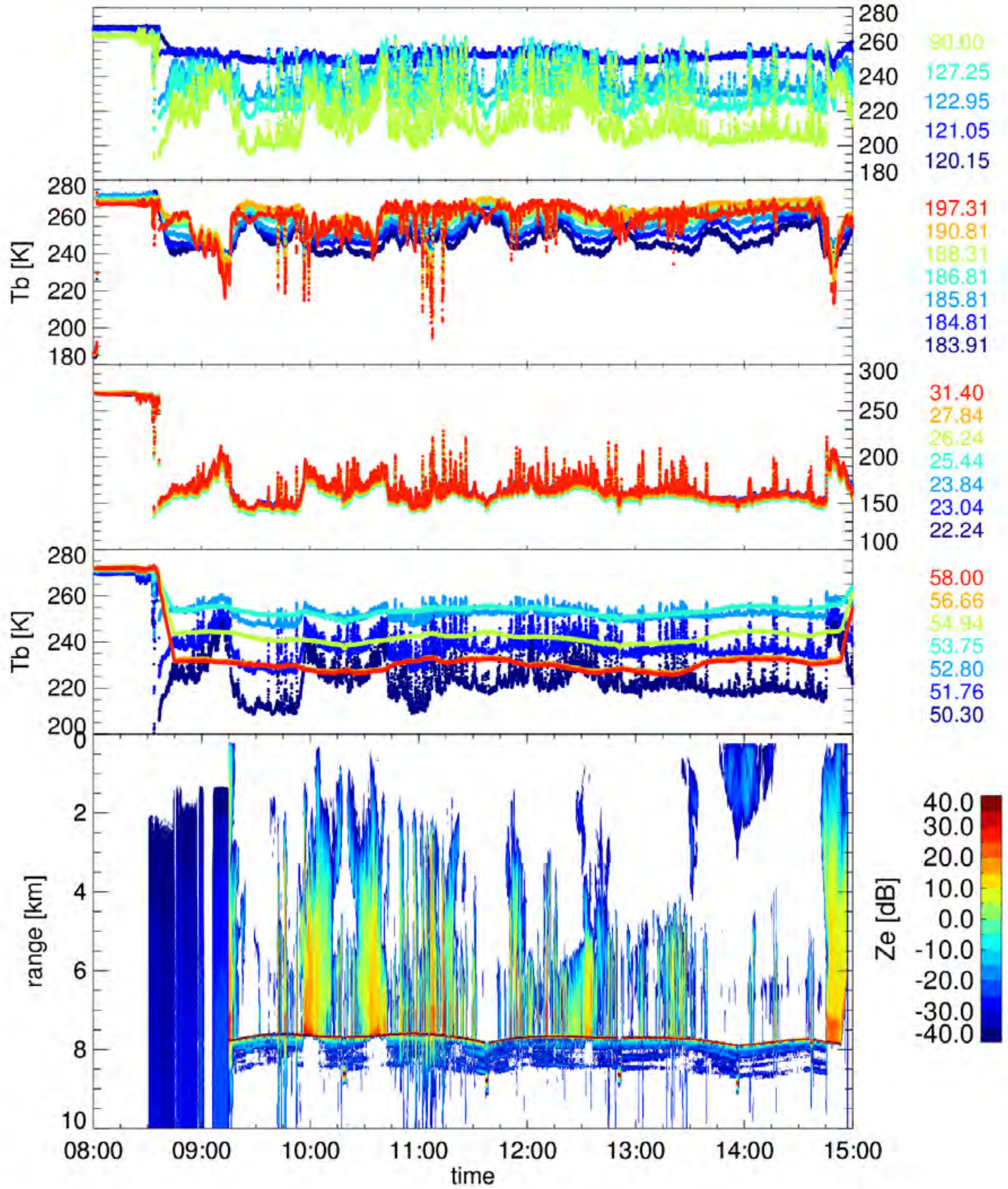

Fig. RF11.14: Complete (in UT) time series of the microwave radiometer brightness temperatures (top panels) and radar reflectivity profiles (lower panel) for the entire flight RF2 for the scattering channels (first panel), the sounding channels (second panel), the emission channels (third panel) and the 50 GHz channels (fourth panel) and the range corrected radar reflectivity (fifth panel). The raw data radar reflectivity profiles still include surface signals as well as multiple scatter signals at range gates beyond the surface. The time series starts and ends with flight within the frontal system. The remainder of the time HALO remained well above all clouds.

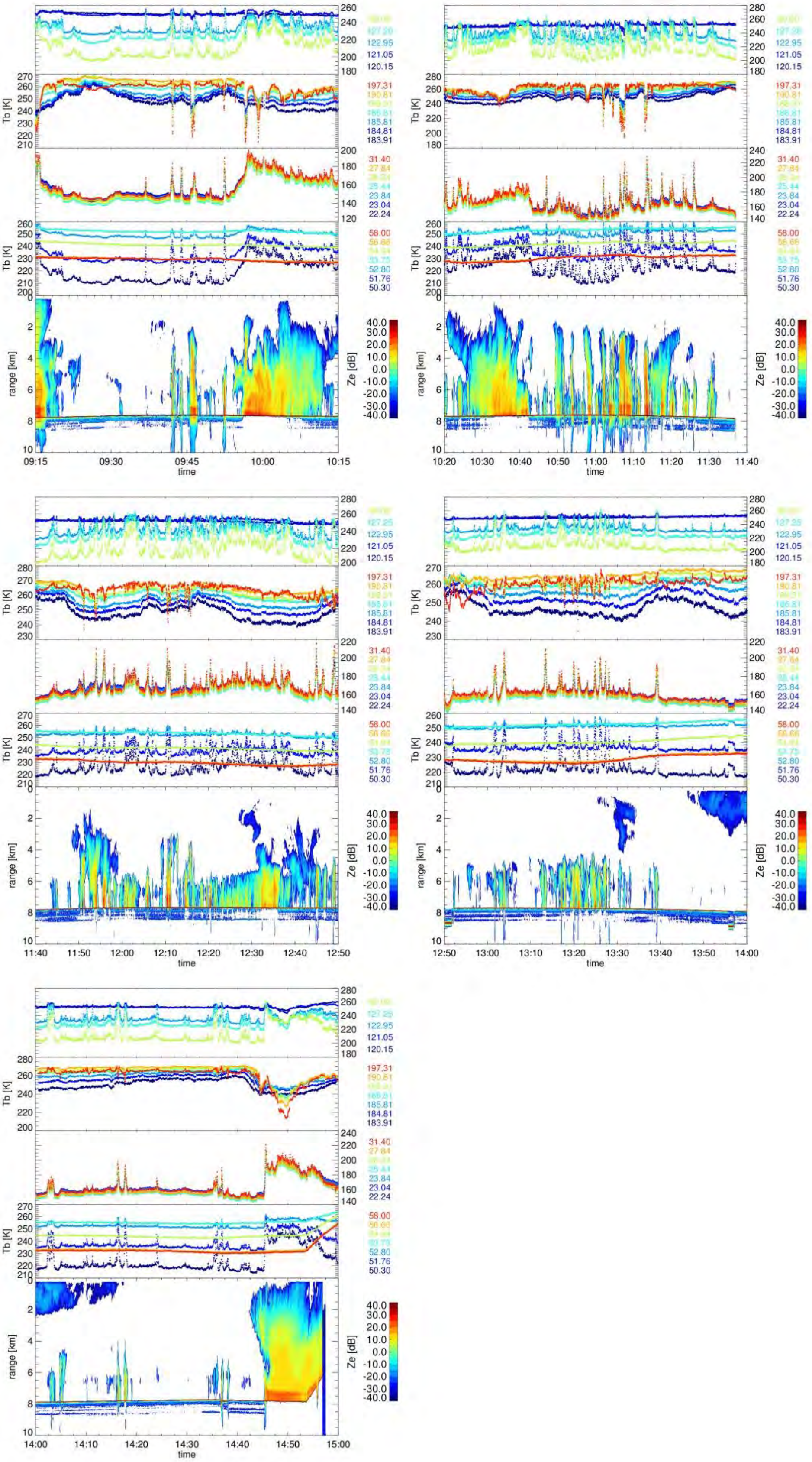

Fig. RF11.15: Time series as in RF11.11 but temporally higher resolved into 5 panels of approximately 1 hour interval length corresponding to legs 1 to 4 and the return to KEF.

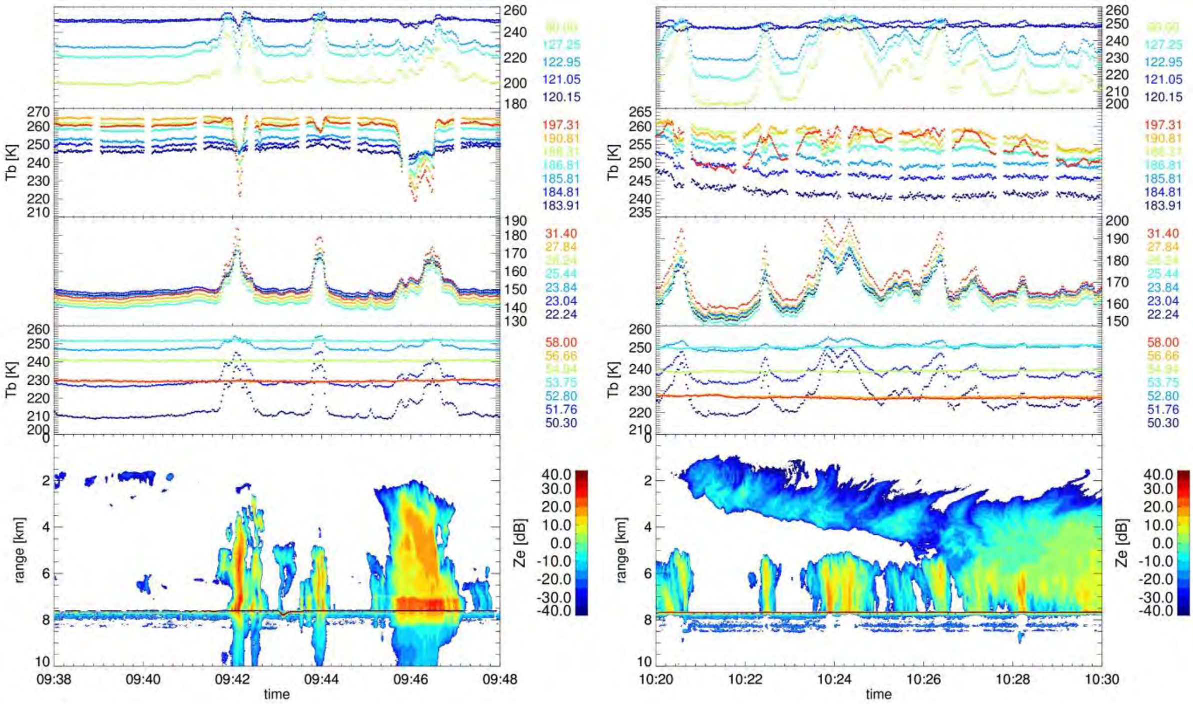

Fig. RF11.16: The radiometer and radar time series as in Fig. RF11.14 and 16 zoomed for the cumulonimbus overpass at 09:46 UT on leg 1 (left panel) and the flight over the tiltback occlusion at the beginning of leg 2 (right panel). The cockpit window picture in Fig. RF11.9 (lower panel) for 09:37 UT shows the distant cumulonimbus (Cb). The Cb exhibits broadly elevated liquid water values, shortly elevated ice values, and a strong brightband indicating intense rainfall with snowflakes aloft in the convective shaft of the system. The iced anvil is well seen and the cloud top is about 6 km height (left panel). The return over the tiltback occlusion between 10:20 and 10:30 UT shows first thin high clouds with comparably shallow convection below. At 10:30 the tiltback occlusion reaches the ground with embedded intense precipitation.

.

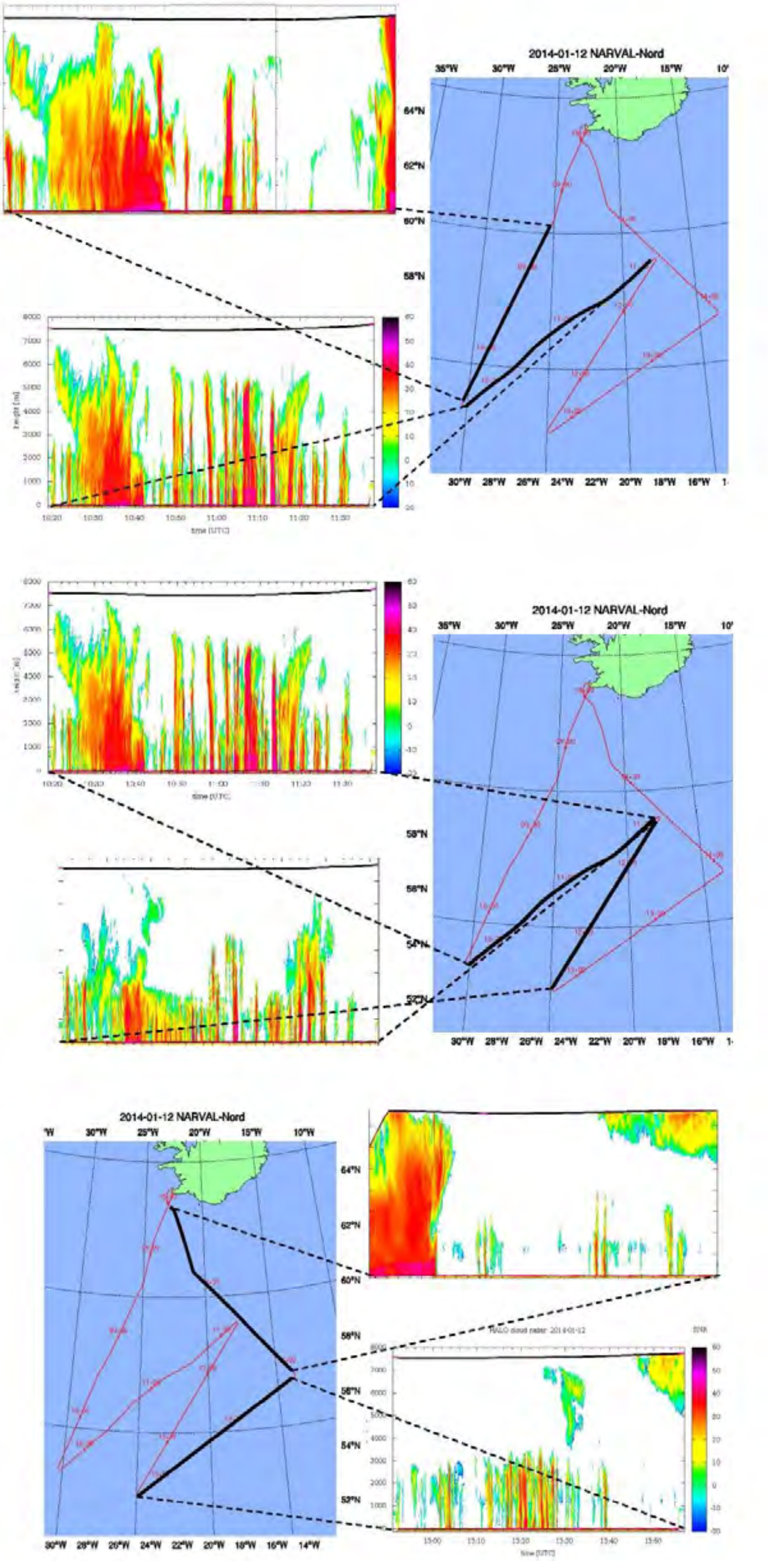

Fig. RF11.17: The complete RF2 MIRA-36 radar times series. Note the decreasing convective activity and convection height as the track moves further away from the active cyclone core to the South. The transfer from waypoint 4 to KEF exhibits the cirrus clouds of the cold front and documents that the sea surface was visible through the cirrus as no significant clouds are below. The transfer again reached the cold air in the subsidence region showing only few convective clouds. Finally HALO was flying into the frontal occlusion.

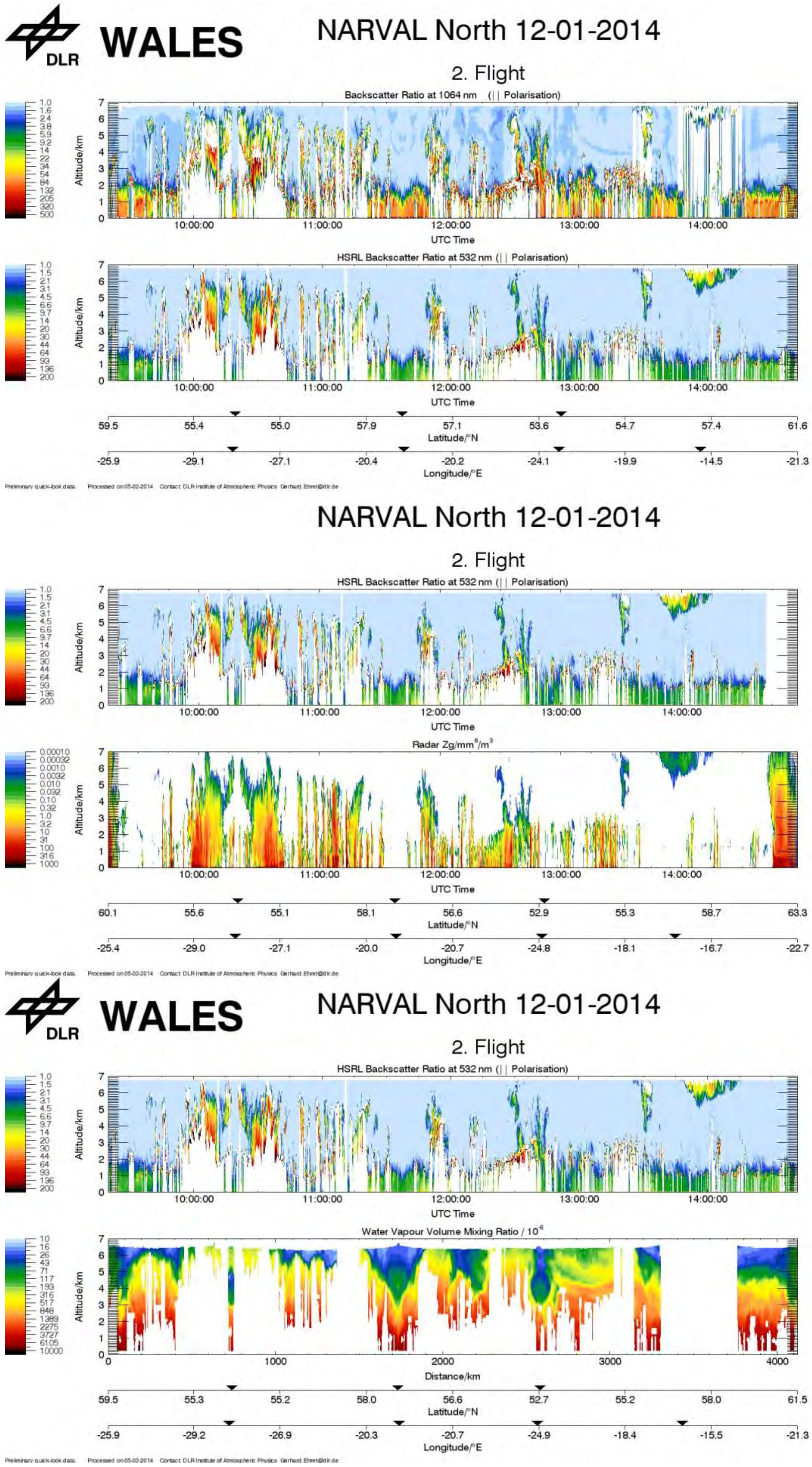

Fig. RF11.18: The top panel shows the WALES lidar backscatter ratio time series at 1064 and 532 nm compared to the MIRA36 radar data (middle panel) and the lidar water vapor mixing ration (bottom panel).

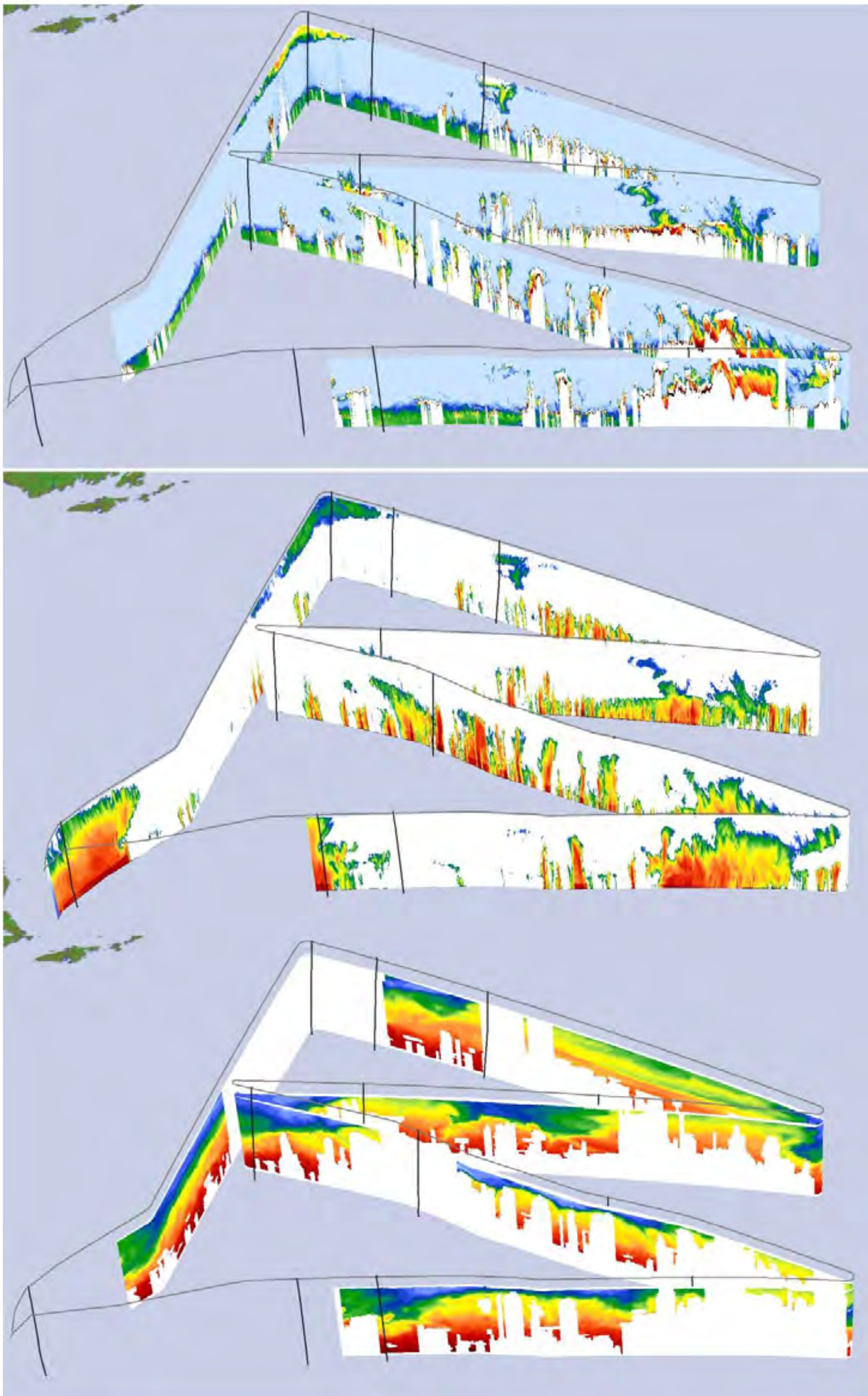

Fig. RF11.19: 3-D visualization of the lidar data for the backscatter ratio (top), the MIRA36 radar data (middle), and the water vapor mixing ratio (bottom) and along the entire flight track. Blue backscatter colors indicate clear air while white and black relate to strong extinction due to optically thick clouds. The water vapor mixing ratio exhibits dry air in green and the intrusions in yellow showing strong humidity gradients. For better visualization the atmosphere is stretched by a factor of 70 to focus on the clouds. The grey line is the plane position and data is recorded about 600 m below the aircraft down to the ground if atmospheric conditions allow. The vertical lines denote the dropsonde positions.

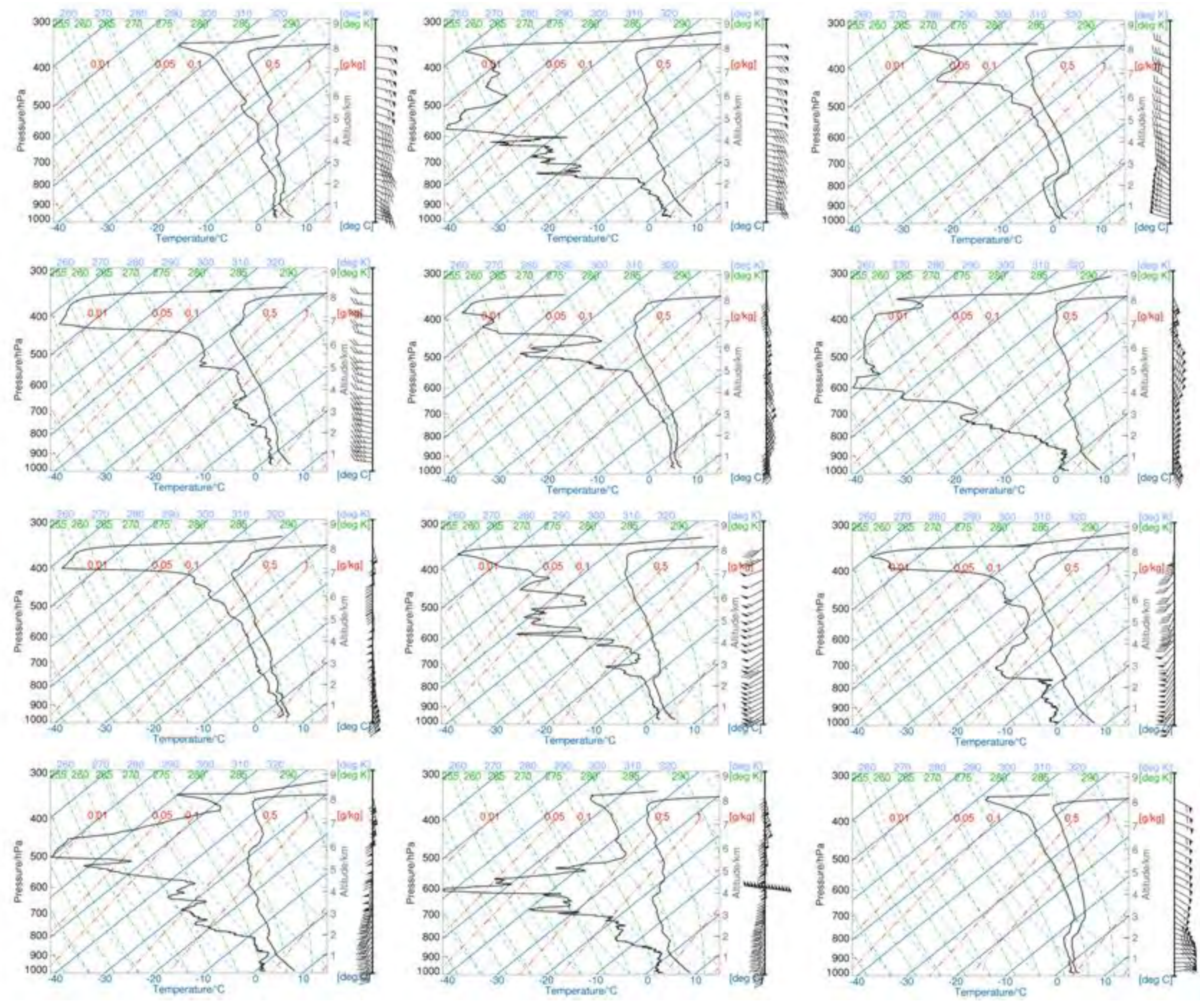

Fig. RF11.20: All 12 dropsonde profiles in chronological order from left to right released at 09:16, 09:24, 10:00 UT (first panel), 10:49, 11:13, 11:34 UT (second panel), 11:54, 12:24, 13:33 UT (third panel), and 13:46, 13:55, 14:53 UT (fourth panel).

The left graph in Fig. RF11.20 is the dewpoint temperature, the right graph the actual air temperature. If both graphs approach each other the atmosphere is saturated. If the graphs are far apart the air mass is very dry. The dropsondes fell with about 11m/s and required about 15 minutes to reach ground from FL270. The fifth dropsonde (second panel in the middle) was dropped in the center of the cyclone and shows low wind speeds and hence a more or less straight fall. The center pressure was approx. 960 hPa. The dropsondes were released at meteorologically specific places rather than in a regular pattern. Surface temperatures remained almost always above freezing point.

Dropsonde 1 (DS1) was dropped into the occlusion front and represents the moist air mass. DS2 was released into the dry slot with shallow convection of cumulus humilis near the surface. DS3 measured the humid air of the tiltback occlusion. D4 and D5 show moist adiabatic conditions where the cumulonimbus clouds were sampled with dry air aloft. D6 shows the dry slot with very dry air and a low level mixed layer with 1.5 km high shallow convective clouds. Note, how the wind speed and direction changes throughout the passage of the fronts and cyclone center. D10 shows low level shallow clouds and dry conditions above. D11 represents the cold front moist air at upper level with the ascending air warm conveyor belt, a dry layer around 600 hPa and low level moisture. D12 shows the strong winds associated with the occlusion front.

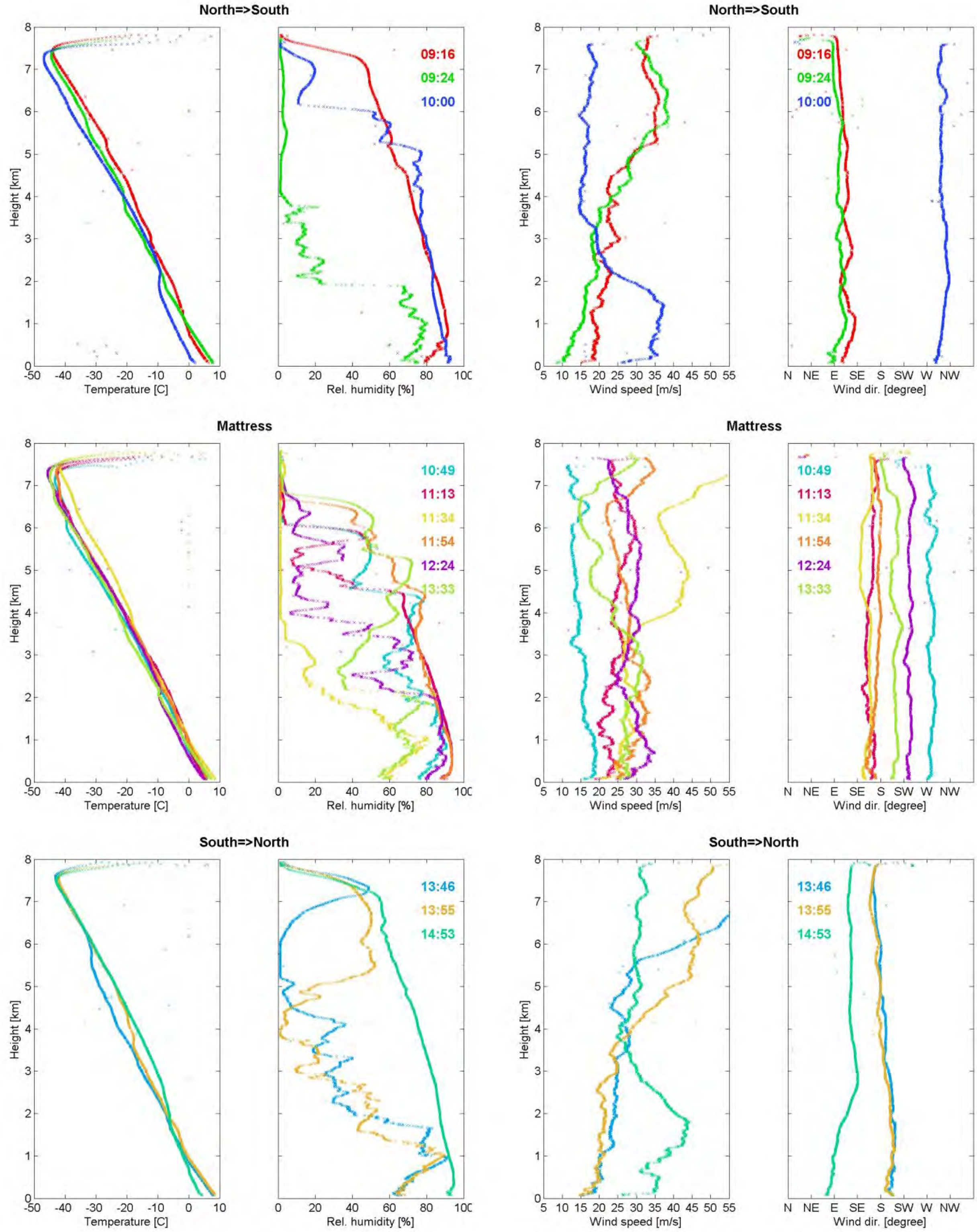

Fig. RF11.21: All 12 dropsonde profiles as in Fig. RF11.20 in chronological order from left to right released at 09:16, 09:24, 10:00 UT (top panel), 10:49, 11:13, 11:34 UT, 11:54, 12:24, 13:33 UT (middle panel), and 13:46, 13:55, 14:53 UT (bottom panel) plotted for height versus temperature (first column), humidity (second column), wind speed (third column) and wind direction (fourth column).

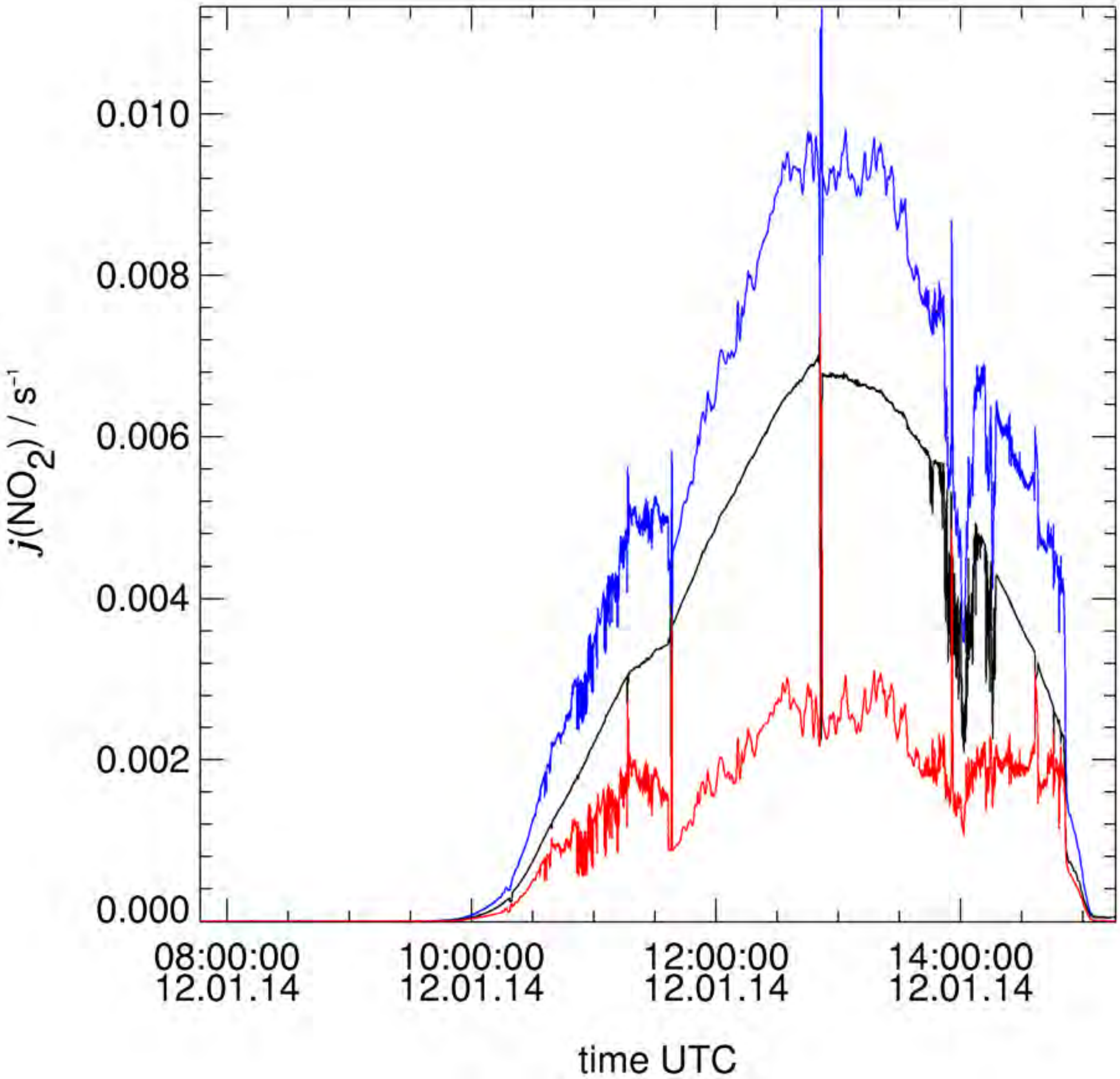

Fig. RF11.22: HALO-SR photolysis frequency $j(NO_2)$ from lower hemisphere (red), upper hemisphere (black) and combined (blue) measurements. Attenuation of radiation by clouds above the flight altitude is obvious around 14 UTC. Turning points in flight track correspond to peaks in nadir signal.

The SSMIS and CloudSat perspective:

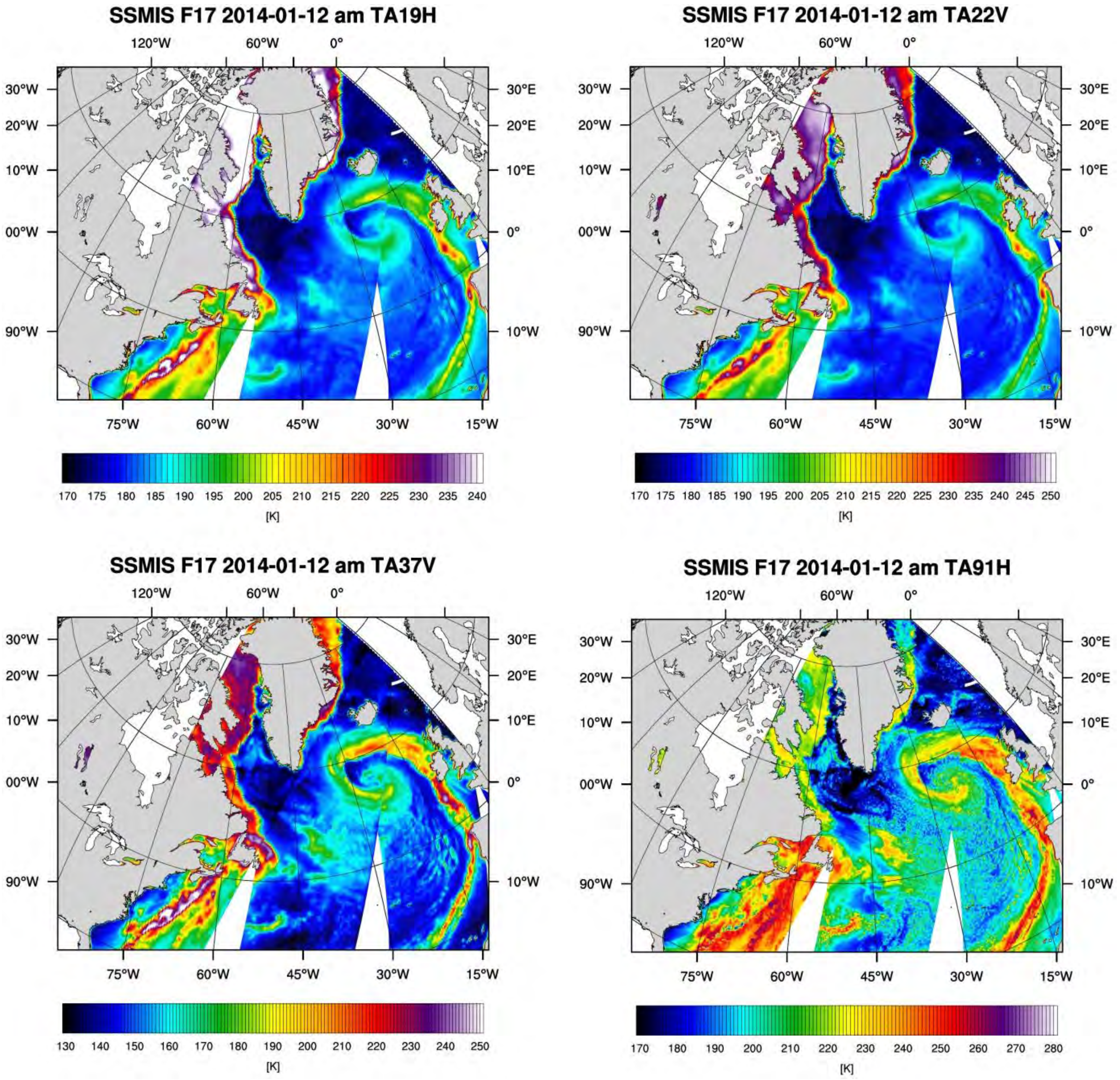

Fig. RF11.23: Preliminary HOAPS 4 fundamental climate data record (FCDR) antenna temperatures (TA) for DMSP-F17 SSMIS target area overpass at 09:17 UT. Shown are the environmental data record (EDR) emission channels 19 GHz H (sensitive to rain; top left), the water vapor channel 22 GHz V (top right), the 37 GHz V (lower left), and the 91 GHz H scattering channel (sensitive to ice; lower right) indicated for horizontal (H) and vertical (V) polarization. The main occlusion and cold front are easily recognized. The tiltback occlusion and spiral bands exhibit rainwater content in the 19 GHz emission channel and 22 GHz water vapor channel indicated by the light blue and green colors between 185 and 200 K. The scattering channel shows intense signatures of precipitating ice clouds, especially in the spiral bands with the embedded cumulonimbus clouds with values above 220 K. The great detail of the core structure in the antenna temperatures is promising for the forthcoming brightness temperature conversion followed by the precipitation rate retrieval. Note the resolution increase from the 50 km pixel size 19 GHz channel to the 8 km pixel size of the 91 GHz channel. 4 SSMIS overpasses occurred: DMSP-F16 (14:50 UT), DMSP-F17 (09:17 UT), and DMSP-F18 (09:55 and 11:35 UT).

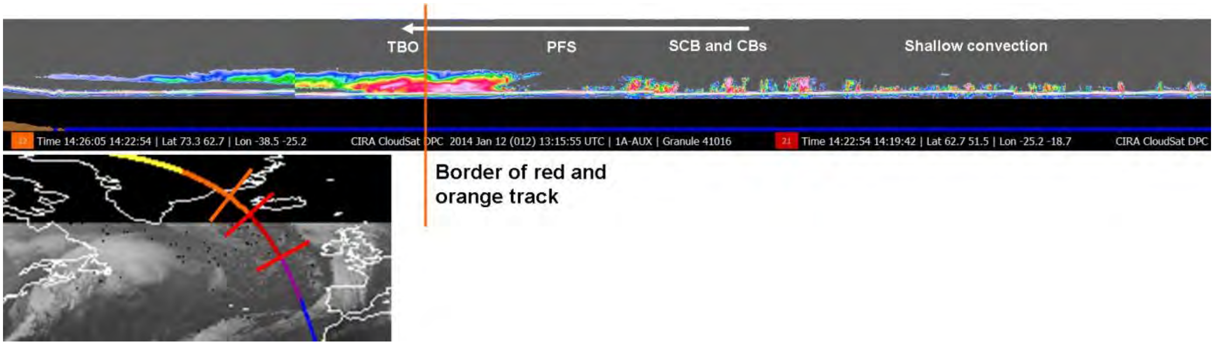

Fig. RF11.24: CloudSat quicklook track granule 41016 over the postfrontal region of the cyclone between 14:22 UT (red track) and 14:26 UT (orange track). The northwestward flight direction is indicated by the white arrow. CloudSat passed first over the shallow convection reaching far south and crossed the spiral cloud bands (SCB) of the cyclone center including cumulonimbus (CBs). The postfrontal subsidence (PFS) is well expressed showing almost no clouds. Finally, CloudSat crossed the tiltback occlusion (TBO) head of the cyclone. The CloudSat passage occurred 24 minutes after HALO left the target area. The collocation could not be achieved due to the wind warning from KEF flight control. As a result, the flight pattern was terminated at WP4.

NARVAL North Research Flight 12 (RF12), Flight Report

- 18 January 2014 -

CHRISTIAN KLEPP

Crew: Roland Welser (Pilot), Stefan Grillenbeck (Pilot), Alexander Wolf (Flight engineer), Silke Groß (Dropsondes), Andreas Fix (WALES), Emiliano Orlandi (HALO SR & MiniDOAS), Martin Hagen (HAMP), Christian Klepp (Mission scientist)

Objective: The scientific objective of the third research flight was to sample the downstream cold air convection development from cloud-free conditions to Cumulonimbus. This included the passage of several re-intensified occluded frontal systems moving in various directions, a dry slot within an occlusion center at 62N and 30W featuring a small-scale cyclone development with a tropopause funnel in the cyclone center, an almost cloud-free area southeast of the Greenland tip jet area (TIP) and the consequent downstream development of convection towards Ireland. The convection started as shallow and stratiform cloud decks (SHC) and developed into spiral-shaped cells with increasing cloud tops (ENC). Towards Ireland the convection grew into Cumulonimbus (CBS). Fig. RF12.1 shows the meteorological setting at 08 UT. Over radar controlled Ireland airspace the clearance to climb to FL430 was used to overpass Mace Head supersite. The flight towards KEF at FL430 reduced the instrument resolution to halve by virtually doubling the flight attitude to 14 km height. The flight from Ireland back to KEF crossed convective cells and cloud bands being part of several occluded systems. Along the waypoints SAT1 and SAT2 the flight path was adjusted to fly along the CloudSat track for a collocated underflight at 13:44 UT in convective cloud environment. During the HALO operation time six SSMIS overpasses occurred additionally. 5 dropsondes were released along FL270 while dropsondes were not permitted on FL430.

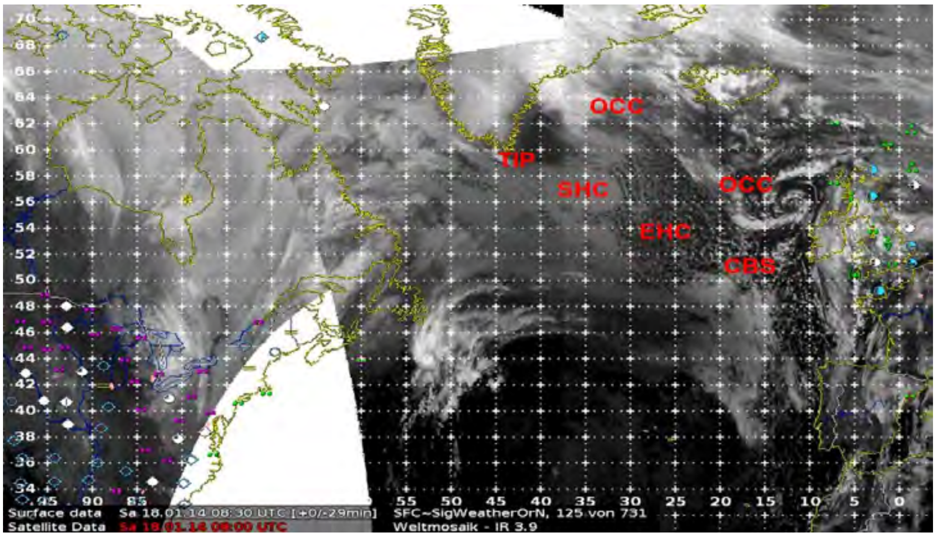

Fig. RF12.1: The occluded frontal systems (OCC) of the third research flight at 08 UT between Ireland and Iceland caused a cold air to flow out of the Denmark straight and partially from the Labrador Sea that orographically induced a tip jet (TIP) and consequent downstream convective development starting with shallow convection (SHC) and increasing to enhanced convection (EHC) and Cumulonimbus towards Ireland (CBS).

Overview:

A high pressure ridge moving in over the western North Atlantic narrowed the cold air trough that extended from Iceland over Ireland down to the Iberian Peninsula and into Northern Africa. The blocking situation over Europe continued. As a consequence the remains of the former low pressure systems stayed in place mostly over Iceland and the British Islands as quasi stationary occlusion fronts that moved in several directions (Fig. RF.3.2). Some of these occlusion fronts showed re-intensification into a complex low pressure system on 18 Jan 2014 00 UT with multiple cores of about 979 hPa in the area south of Iceland, 982 hPa over Iceland, and about 990 hPa between Iceland and Greenland with the formation of a dry slot (Fig. RF.3.3). The large scale flow favored cold air advection from both sides of Greenland towards the south, with the stronger cold air outbreak coming from the Denmark Straight. On the western side of these low pressure systems the cold air flow started southward with a cloud-free area in the wake of the southern tip of Greenland. The convection started south of 60°N as shallow and stratiform cumulus first and rapidly developed into enhanced cumumlus and Cumulonimbus offshore Ireland (Fig. RF.3.1).

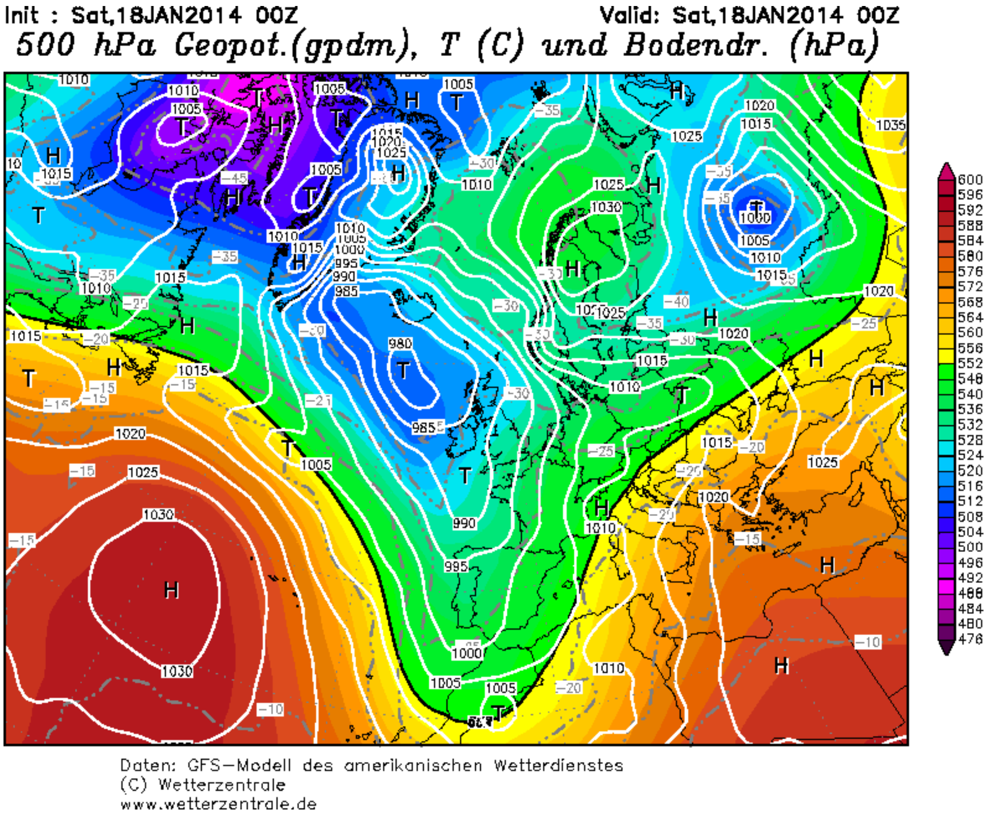

Fig. RF12.2: GFS analysis of surface pressure (white isolines), 500 hPa geopotential height (color, 552 dekameter isoline in black) and temperature (dot-dashed grey isolines and white boxes) in °C valid for Sat, 18 Jan 2014 00 UT showing the low pressure area between Ireland and Iceland with the cold air advection to the west. A high pressure ridge is moving in over the western North Atlantic and the blocking situation over Europe is still active. In between the narrow cold air trough reaches down to northern Africa.

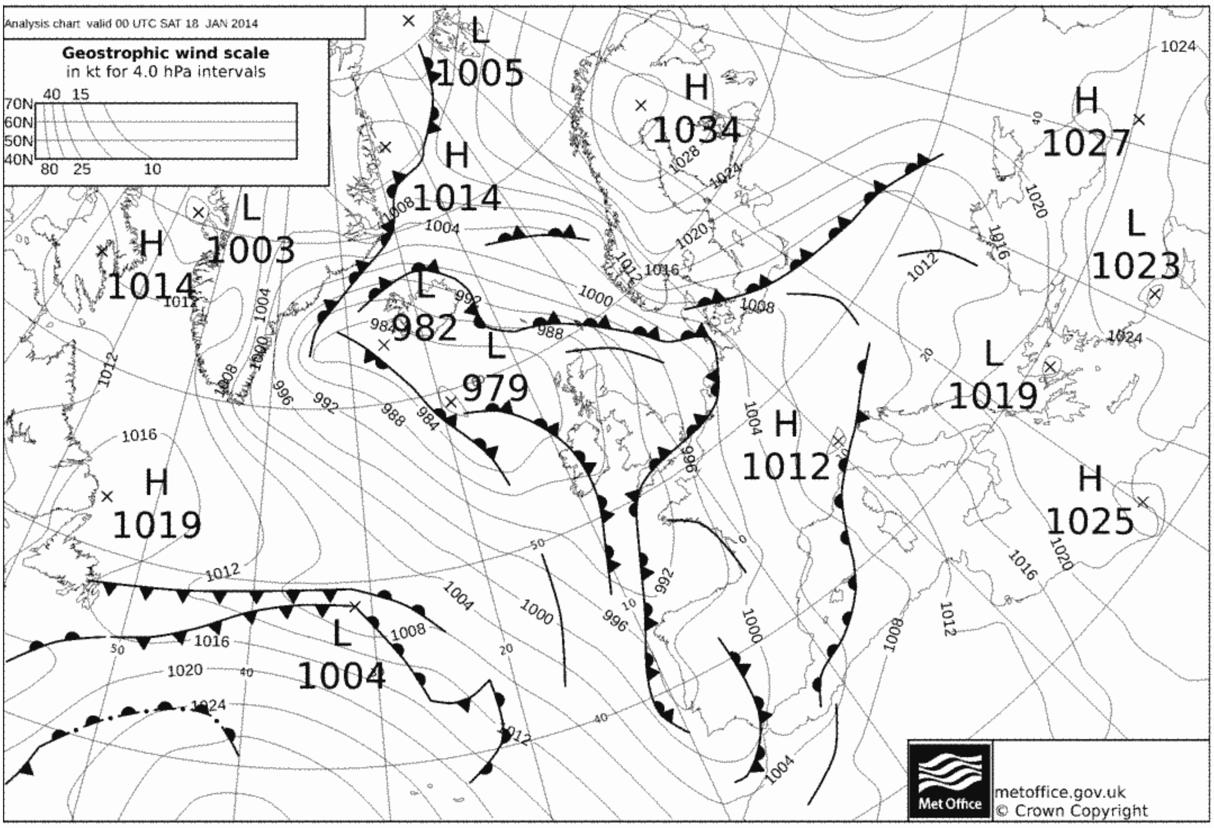

Fig. RF12.3: UK Met. Office analysis chart for 00 UTC on Sat 18 Jan 2014 with the target area being located between the southern tip of Greenland, Ireland and Iceland. Multiple occlusion fronts re-intensified into a low pressure system that developed a cold air outbreak from the Denmark Straight that is documented in the satellite mosaic of Fig. RF.3.1.

Flight Planning: The downstream convective development objective is best realized by flying a straight remote sensing leg along track the geostrophic wind. Hence, the mattress pattern was replaced in favor of a box pattern. For dropsonde allowance and ATC restriction reasons the flight altitude was requested for FL270 equivalent to approximately 8 km altitude. To reach the forecasted dry slot of the northerly low pressure center and the cloud-free tip jet area, the flight track was requested from KEF towards the southern tip of Greenland. The entry point was located at 61.3°N and 31.3°W and was shifted by ATC northward to 62°N during the flight. The westernmost waypoint 1 was located at 59°N and 38°W and marked the cloud-free beginning of the straight leg towards the coast of Ireland. Waypoint 3 at 50°N and 20°W marked the southernmost point and the left turn towards Ireland airspace. At 53°N and 10°W waypoint 4 was reached marking the entry into Irish radar controlled airspace. The request to climb gradually to FL430 was approved and FL430 was reached at waypoint CON over Ireland and Mace Head supersite was crossed at 53.2°N, 9.54°W. The altitude change was planned for two reasons. First, almost doubling the flight altitude would decrease the instruments resolution almost by half leading to conditions as originally planned to fly remote sensing at high altitudes. Second, FL430 allowed flying above all frontal clouds on the way back to KEF (Fig. RF12.6). The return leg to KEF was marked by crossing several frontal occlusion bands with high clouds reaching beyond FL270. With a left turn Irish radar controlled airspace was left at waypoint MOLAR (typo in Fig. RF12.7, reads MOLAK in error) and the planes routing was adjusted to reach the CloudSat track at waypoint SAT1. On the straight leg towards SAT2 CloudSat crossed at 13:44 UT. Another course correction to the right brought HALO on a straight leg to the exit point at 61°N, 16.35°W and consequently the descent into KEF began with a touch down time of 14:49 UT (Fig. RF12.7). Five dropsondes were released along FL270 and six SSMIS overpasses occurred during the flight operation time.

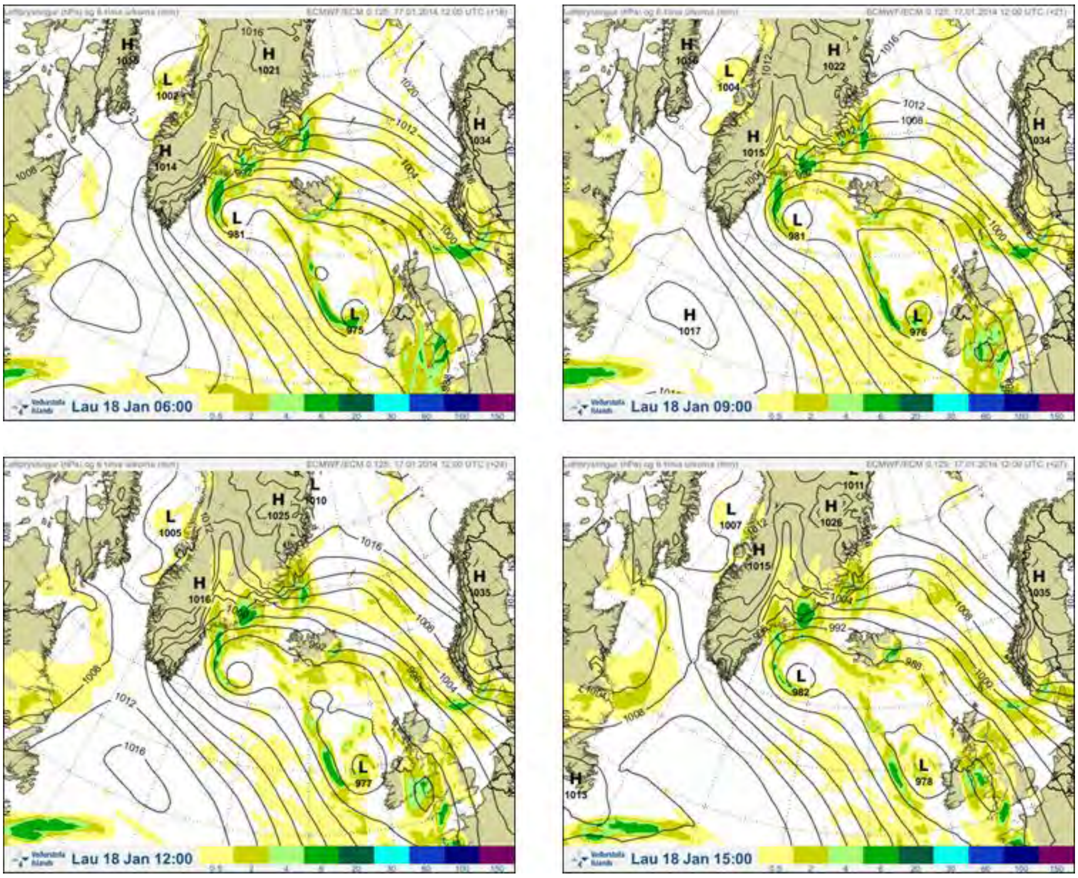

Fig. RF12.4: ECMWF forecast for 18 Jan 2014 06, 09, 12, and 15 UT for surface pressure isobars and precipitation amount accumulated over 3 hours (mm in color). The multiple core cyclone structure is well identified by both the pressure and precipitation fields. Also the forecast indicated the most intense precipitation within the northerly core that shows a well-developed dry interior resembling the dry slot and strong convective precipitation off the coast of Ireland, indicating Cb clouds.

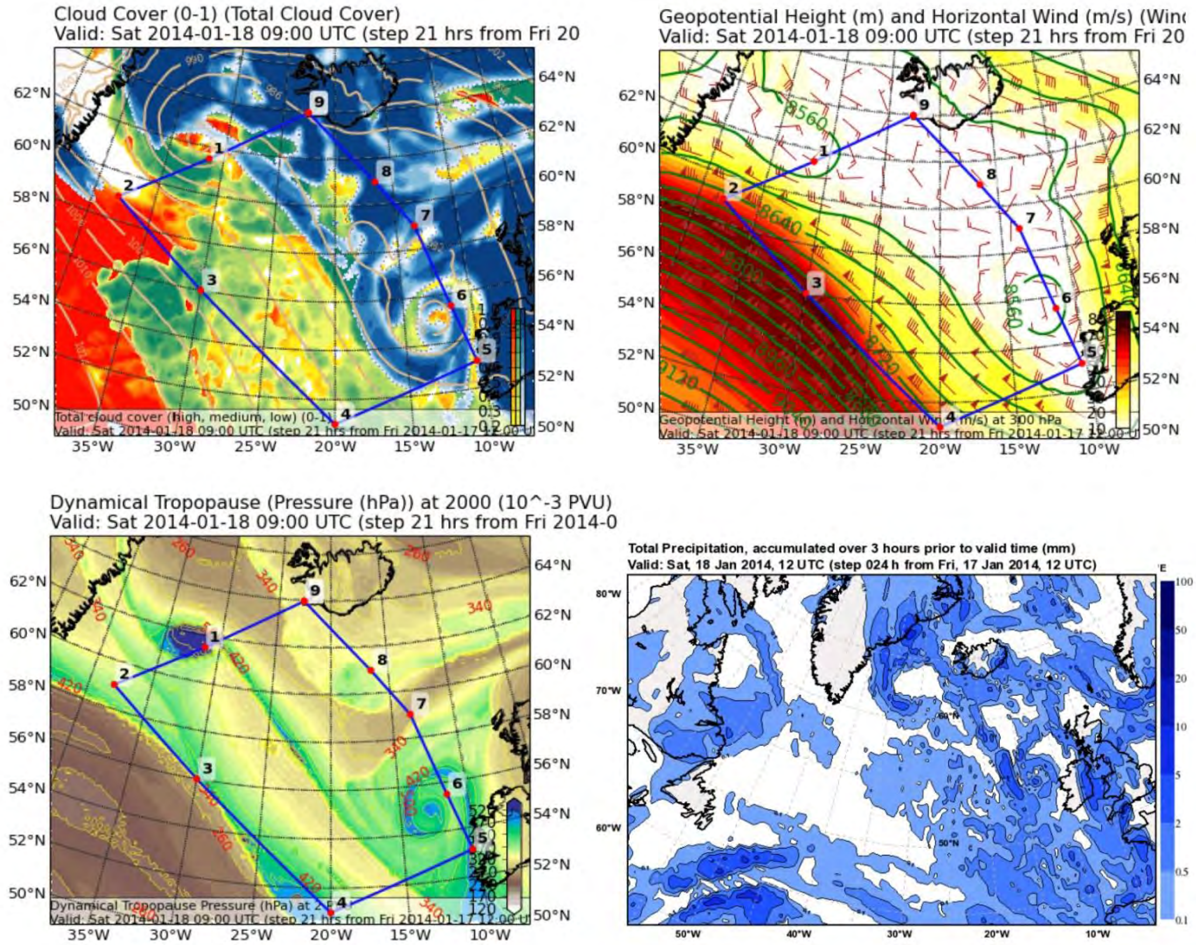

Fig. RF12.5: ECMWF based flight planning tool of DLR showing 18 Jan 2014, 09 UT forecast of cloud cover (high clouds in blue, mid-level clouds in green, low-level clouds in red) in the top left panel, the 300 hPa geopotential height (m, in color) and wind speed (arrows, right top panel), dynamic tropopause pressure (hPa, in color, lower left panel), and the accumulated 3-hourly precipitation forecast for 09 to 12 UT (mm, lower right panel) including the flight pattern in blue and numbered waypoints as red dots.

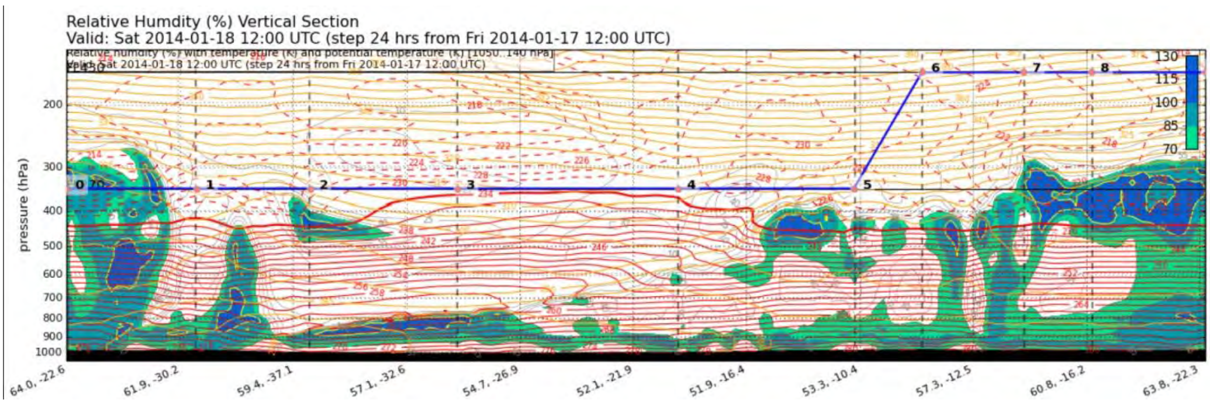

Fig. RF12.6: ECMWF based flight planning tool of DLR showing the vertical section of relative humidity (%, in color) and temperature (K, red lines) forecast at 18 Jan 2014, 12 UT along the flight track from left to right. The waypoints are listed as numbers along the blue lined flight altitude of FL270 and the altitude change at waypoint 5 to FL430. It is well recognized that from point 7 on HALO would have been within the occlusion clouds at FL270.

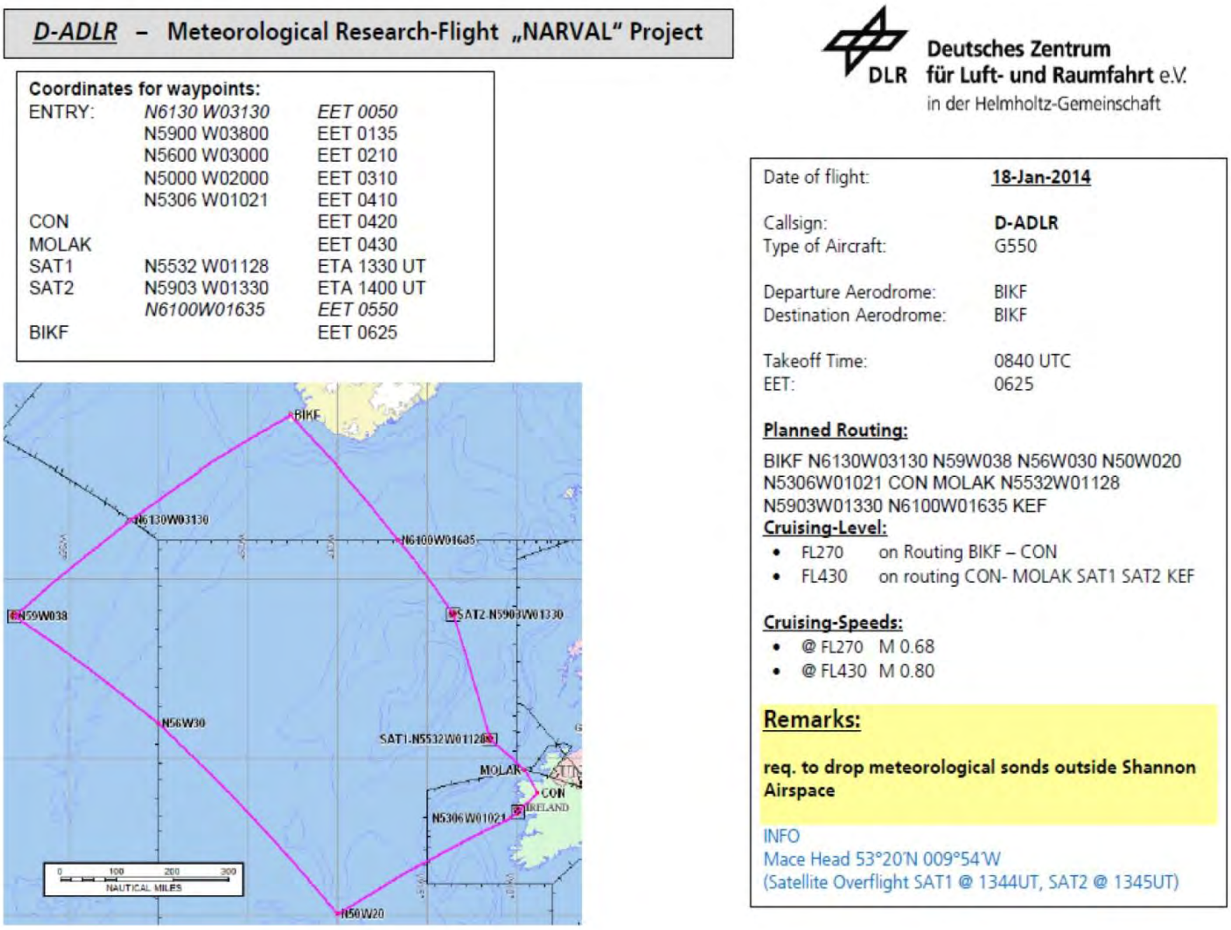

Fig. RF12.7: ATC requested and approved flight pattern for RF12. The magenta track sows the flight path at FL270 with dropsonde allowance from KEF to the entry point at 61.3° and 31.3°W, and the waypoints 1 to 3 along the straight leg towards Ireland. At waypoint 3 the left turn towards Irish radar controlled airspace began marked by the blue boundary pattern. At the boundary the climb was approved to FL430 and Ireland was crossed including Mace Head supersite at 53.2°N and 9.54°W. The CloudSat collocated track is located between the waypoints SAT1 and SAT2. The exit point is located at 61°N, 16.35°W followed by the descend into KEF. Coordinates of all points are listed in the panel table.

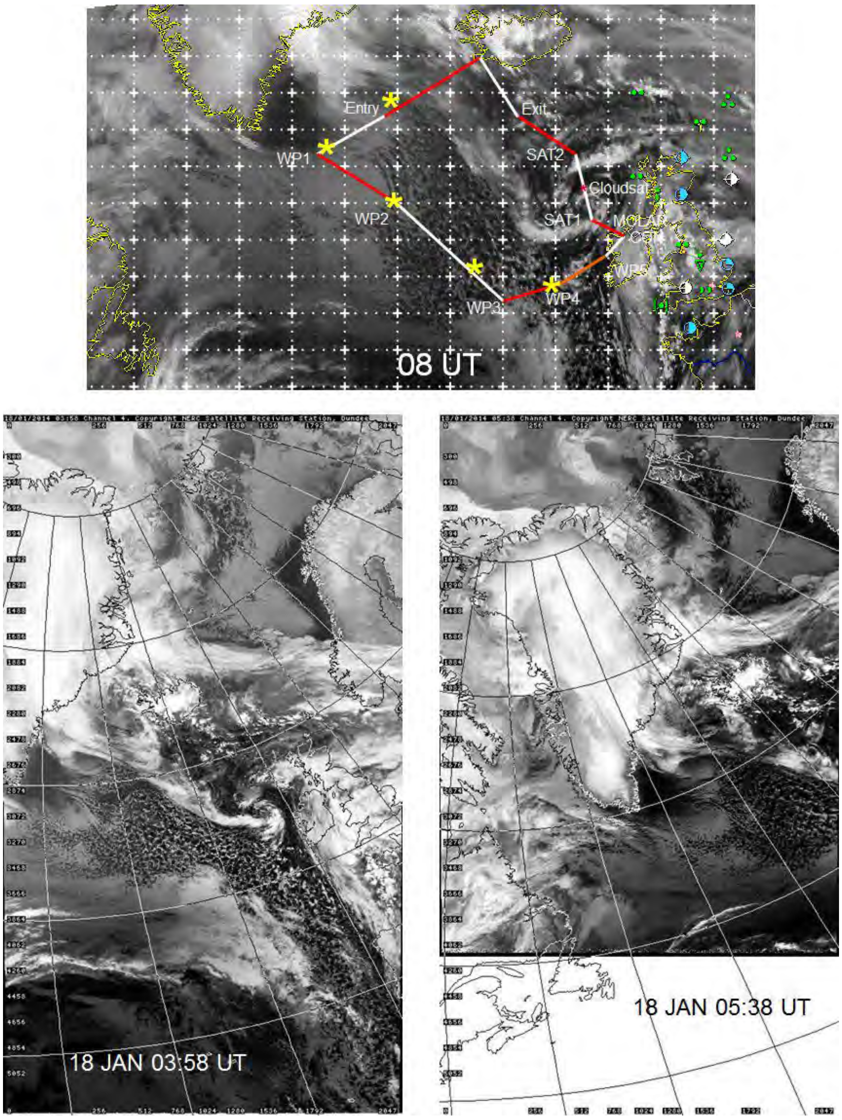

Figure RF12.8: Flight pattern on 18 January 2014 between 8:55 UT and 14:49 UT (top panel) including the waypoint tracks in different color coding and the dropsonde positions (yellow stars) with the satellite image of 08 UT. Note, that dropsonde positions off the flight track indicate inflight routing adaptations due to ATC or science requests. The bottom AVHRR satellite images show the weather development in the infrared channel 4 at 03:58 UT and 05:38 UT. Both the height difference in the cloud systems (white vs grey appearing clouds) and the convective activity and the tip jet are well expressed.

Flight Report: Photo numbers according to Canon RAW data files are given in brackets. HALO took off from KEF at 08:55 UT and had cloud base contact at 08:58 UT during the first dawn. At 09:04 UT HALO went into the convective high cloud band west of KEF with embedded Cbs. At 09:05 HALO was above all clouds for the remainder of the flight, except for the approach into KEF. Towering cumulus intersected with scattered cirrus fields at 09:06 UT belonging to the dissolving front seen in the satellite image. At 09:15 HALO reached FL270 and the radar and lidar were operational. Shallow convection dominated at 09:31 UT (5866) with bands of cirrus corresponding to the weak cyclone front at 29W. The flight path was shifted by ATC to 62N due to traffic (5867 and 5868). Fig. RF12.8 (top panel) shows the four flight legs separated into colored sections by waypoints, dropsondes positions with yellow stars and the satellite image for 08 UT for illustration of the cloud formations.

LEG1 (1:27 h duration)
At 09:36 UT the ATC shifted entry point was reached at 62°N, 30°W with broken shallow convection below. Cloud tops reached 1 km altitude and a few rain showers were recorded by the radar. The first dropsonde was released into the dry slot at 09:38 UT and photo 5869 was taken almost in darkness but documenting few clouds. By 09:44 UT the frontal occlusion head of the small scale cyclone was reached at 32°W and a single 4 km cloud top convective cells was passed indicating rainfall to the ground (5870, Fig. RF12.9 left panel). The cells were surrounded by shallow stratiform convection with 1 km cloud tops. At 09:49 UT the clouds appeared totally stratiform and belonged to the low-level tiltback occlusion at 32.2°W. At 09:52 UT the frontal zone was passed and almost cloud-free conditions prevailed by entering the tip jet area in the wake of the southern tip of Greenland. The lidar showed a significant dry intrusion and at 10:00 UT the southern border of the tip jet was reached (5872, Fig. RF12.9, right panel). Dropsonde 2 was released at 10:10 UT into the tip jet 10 minutes before reaching waypoint 1. At 10:16 UT the window view from the plane exactly resembled the satellites view with the cloud-free tip jet to the right (5874) and the shallow tiltback occlusion cumulus as a dark stratiform patch of clouds to the left. At 10:22 UT waypoint 1 was reached followed by a left curve heading south/southeast towards Ireland.

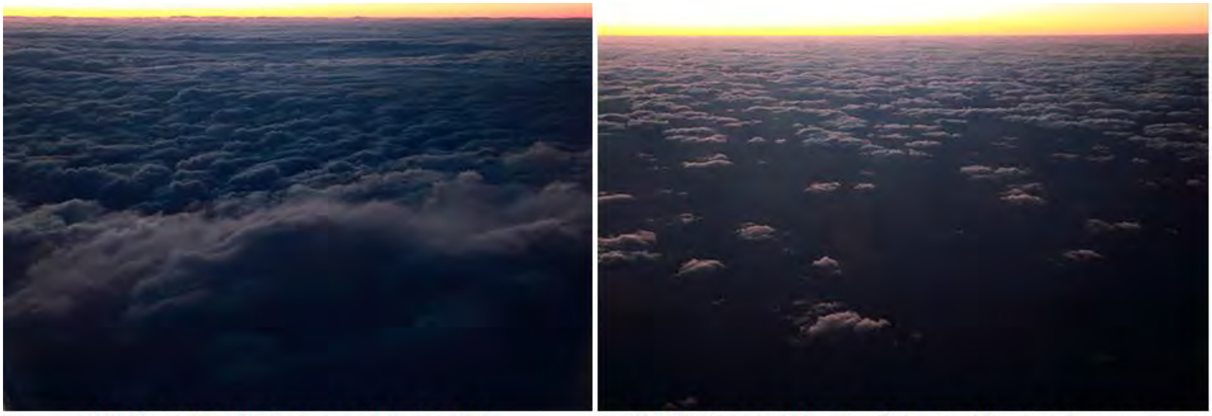

09:44 UT cyclone cold air slot, DS1, tow. Cu, 4 km, rain

10:06 UT DS2, stratiform / tip jet boundary Cu hum, 1 km, few rain

Fig. RF12.9: Leg 1 inflight photo documentation of the cloud patterns showing the tiltback occlusion stratiform clouds embedded by towering cumulus up to 4 km height at 09:44 UT (left panel) and the boundary between the stratiform tiltback occlusion and the tip jet area at 10:06 UT (right panel).

LEG2 (1:37 h duration)
With the turn at waypoint 1 the cloud-free tip jet area was immediately left and at 10:22 UT stratiform cloud decks prevailed with convective tops that showed no indication of precipitation in the radar (5876). The appearance of the clouds resembled Stratocumulus. At 10:45 UT the cloud appearance changed into remarkable stratiform spiral cloud structures with partial cloud gaps between them (Fig. RF12.10, top left panel). The cloud top was at 2 km and precipitation occurred with no brightband visible indicating snowfall. As no one on board was familiar with such cloud formations they were quickly dubbed “cinnamon roll

clouds". A dropsonde was prepared and released at 10:57 UT into these spiral clouds. The surface air temperature was at 3°C. At 10:58 UT waypoint 2 was reached. Gander airspace was left and Shanwick Irish controlled airspace was contacted following the clearance to continue towards waypoint 3 with a slight course correction to the left. Waypoint 2 also marked the boundary between the closed clouds decks and the beginning to higher reached open convection. At 11:06 UT the "cinnamon rolls" area ended (leaving behind a hungry crew) and broken higher convection came into sight (5894 and 5895). Open cellular convection prevailed at 11:08 UT with 2.5 km cloud tops and brightbands reaching the ground indicating mixed-phase precipitation. 150 kn tailwind was registered flying in the direction of the geostrophic flow. At 11:11 first scattered Cumulonimbus clouds came into sight with shallow thin anvils reaching up to 3 km altitude (5896 and 5897, Fig RF12.10, top right panel). Thin ice clouds with snow virga precipitation may indicate the decaying state of former Cbs at 11:23 UT. At 11:29 UT broken shallow convection intersected the flight route. From 11:38 UT on convection grew rapidly towards 4 km altitude and frequent Cbs with anvils and partially overshooting tops with snow virga in between dominated (Fig. RF12.10, lower panel). The Cbs totally dominated the convection with almost no clouds in between. Dropsonde 4 was released into the Cbs at 52.8°N and 21.56°W. At 11:59 UT waypoint 3 was reached being the southernmost point of the straight leg. With a left curve the plane turned towards the coast of Ireland.

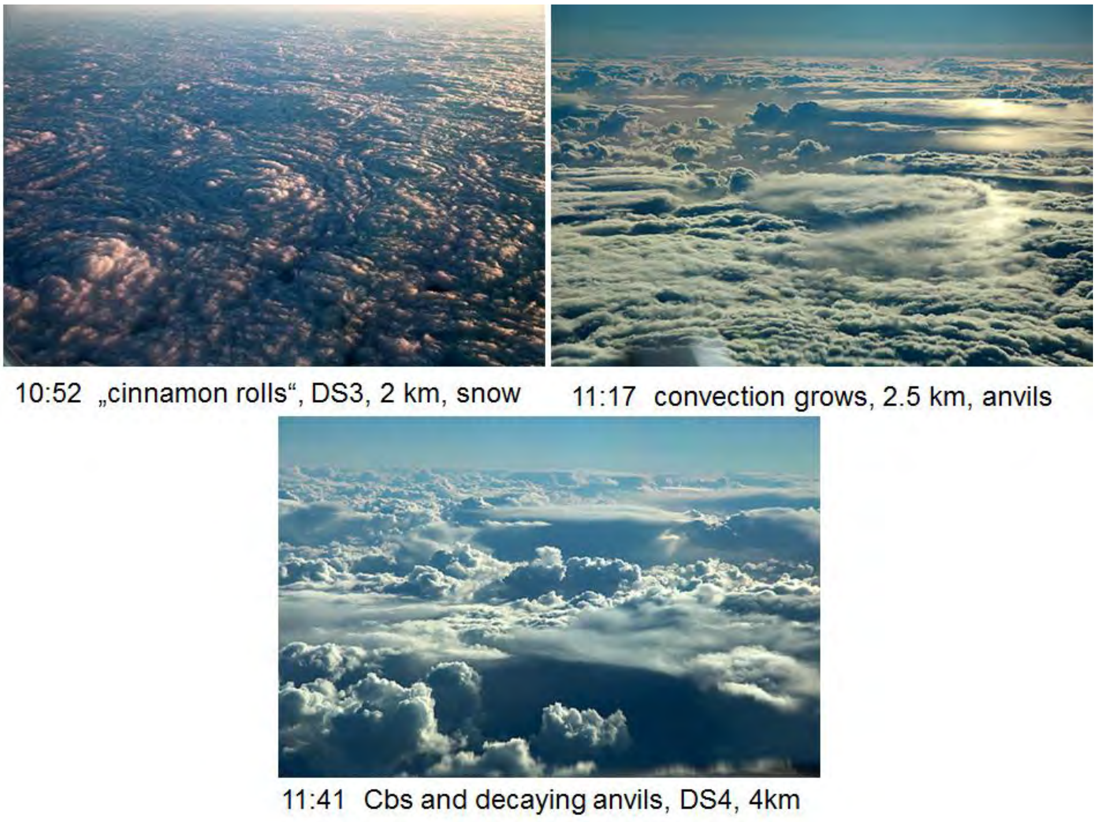

Fig. RF12.10: Leg 2 inflight photos of the cloud patterns document the gradual increase in convective height between waypoint 1 and waypoint 3. The top left panel shows the spiral shaped stratiform "cinnamon roll" clouds with 2 km clouds tops and snowfall at 10:52 UT. The top right panel documents the transition to open cellular convection reaching up to 3 km altitude and first iced anvils at 11:17 UT. At 11:41 UT the Cumulonimbus convection was reached with cloud tops of 4 km altitude with iced anvils and decaying virga snowfall (lower panel).

LEG3 (1:09 h duration)

Leg 3 continued in the Cb convective environment with partly iced anvils at 12:02 UT. Cloud tops were at 4 km and a clearly visible brightband indicated rainfall at the surface. At 12:22 UT a dropsonde was released into a Cb with overshooting cloud top at 51.39°N and 15.51°W with intense convection (Fig. RF12.11, left panel). At 12:28 UT waypoint 4 was reached and the first of the s-shaped occlusion bands came into sight at the horizon when viewed from the cockpit. Irish radar controlled airspace contact was established at 12:31 and climb to FL430 was requested and approved. At 12:32 UT HALO left FL270 and started the climb. Dropsondes were not permitted beyond this point as HALO entered the civil traffic corridor en route to Conway and KEF. Convective shafts of towering cumulus with partly open cellular convection was crossed at 12:39 UT. Elongated sheared anvil tops appeared at 12:43 UT (5923, 5924). At 12:45 a Cb was passed that showed the anvil signature in the radar data. Waypoint 5 and FL430 were reached at 12:43 UT together with the coast of Ireland. The coastline was marked by a dense frontal cirrus shield that due to the high flight altitude was passed above all clouds. The convection died out almost completely with the approach of the front (Fig. RF12.11, right panel). The window view of the cloud scenario changed completely at FL430 because the altitude allowed for a better overview and the stratospheric blue turned almost into a black sky. The frontal band showed no precipitation signature. At 12:55 Mace Head supersite in Ireland was passed with a few kilometers parallel offset to not interfere with the ground instruments. At 13:01 UT waypoint CON was passed and a left curve brought HALO on a northerly track back towards Iceland. At 13:06 UT the open ocean was again reached with dense cirrus below. Another left curve at waypoint MOLAR at 13:08 UT brought the plane into leg 4.

Fig. RF12.11: Leg 3 inflight photo documentation of the intense active Cumulonimbus convection at 12:29 UT intersected by decaying virga snowfall. Note, that the active cells suppress the convection around leaving rings of clear air (left panel). The right panel shows the approach of the Irish coast at FL430. The convection was strongly suppressed by the frontal cirrus clouds. Note the stratospheric blue color and increased overview on the meteorological setting at FL430.

LEG4 (1:33 h duration)

Leg 4 started at 13:08 UT over the ocean together with the end of the frontal cirrus shield. The suppressed convection influence of the front yielded large cloud-free patches. At 13:21 UT HALO turned into the CloudSat track to align with the overpass. The waypoint SAT1 was reached 10 minutes too early as a consequence of the strong tail wind along leg 2. Isolated decaying Cbs came into sight again to the west including cloud streets. At 13:30 UT a Cb was passed that formed mammatus clouds (5944 and 5945, Fig. RF12.12, top left panel). At 13:38 UT the next frontal s-shaped cyclone front became visible in flying direction (5946, Fig. RF12.12, top right panel). This frontal cloud band was reached at 13:39 UT flying along the CloudSat track. CloudSat passed over the alternating convective Cbs and frontal occlusions at 13:44 UT. The cloud situation at 13:44 UT is documented in Fig. RF12.12 in the lower panel. At 13:49 UT the towering iced convection reach cloud tops up to 6 km altitude (5952) with an aloft brightband indicating intense rainfall. At 13:50 UT waypoint SAT2 was reached and the CloudSat track was left in a left curve heading towards the exit point.

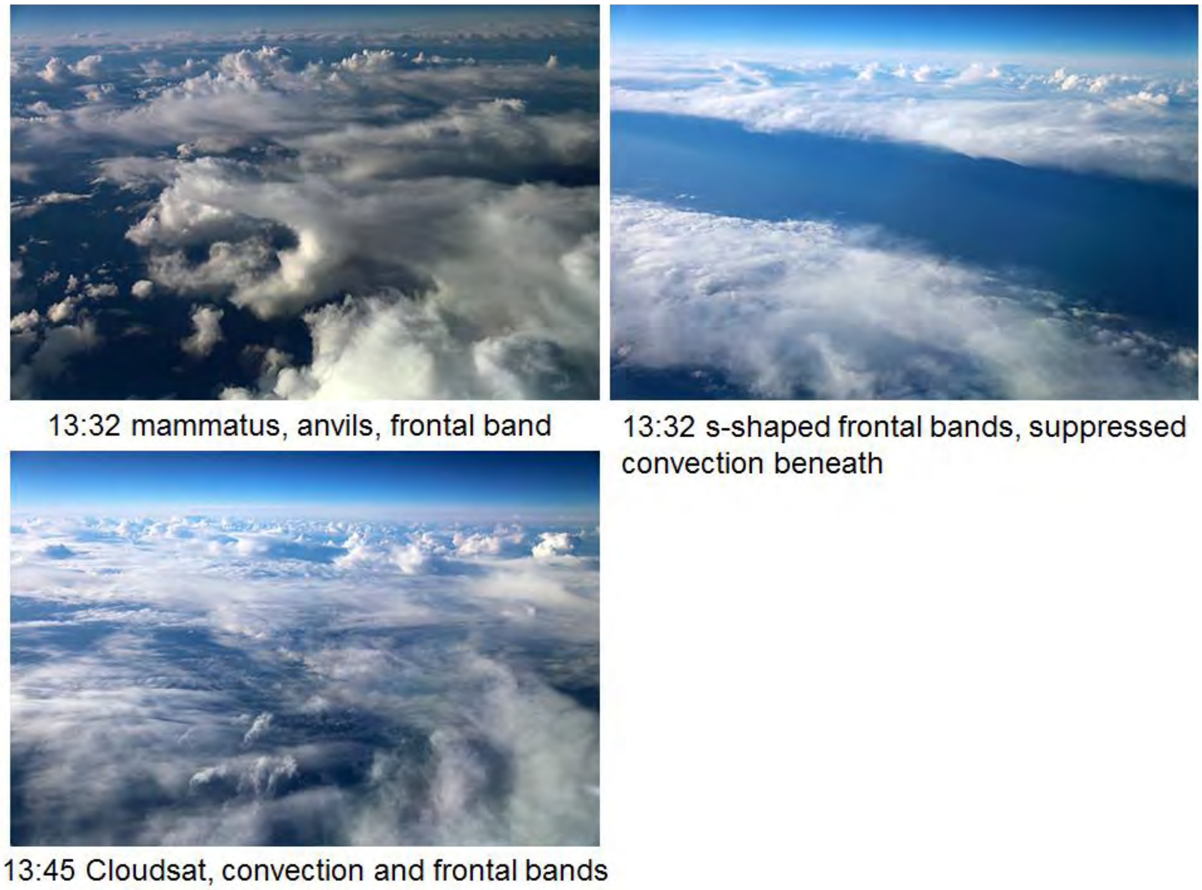

Fig. RF12.12: Leg 4 inflight photo documentation of the towering convection off the coast of Ireland in northerly flight direction (top left panel) at 13:32 UT. The anvils showed indications of mammatus downdrafts. In the remote distance one of the s-shaped occlusion bands is visible. The top right panel shows this occlusion band with the suppressed convection. Note, that the time should read 13:39 UT. The lower left panel shows the Cb convection with sheared of ice anvils and frontal bands during the CloudSat overpass at 13:45 UT.

Another occlusion cloud band was passed at 14:00 UT with rather thin cirrus and few convection below. At 14:10 UT towering cumulus with sheared off anvils dominated the cloud formations and ever more Stratocumulus decks intersected with active Cbs. The exit point was reached at 14:15 UT. Towering convection remained until 14:25 UT and is documented in photos 5956 to 5966. At 14:25 the descend into KEF started and FL430 was left consequently. At 14:28 UT HALO was close to the Cb anvil cloud tops at 6 to 7 km height and at 14:32 UT HALO flew into the Cb anvils which was the first cloud contact since the take off. The lidar was switched off. At 14:38 UT the final descend into KEF was approved. HALO flew through towering convection and established the localizer of runway 02 and received the cleared to land at 14:48 UT. The touch down on runway 02 was at 14:49 UT followed by taxiing to the parking position at 14:53 UT with engines shut down at 14:53 UT.

In total 4 legs of 1:27 h, 1:37 h, 1:09 h, and 1:33 h duration were flown including the transfer to the ATC entry and exit points. In total HALO was flying 5:49 h and 5 dropsondes were released at FL270. Six SSMIS collocation overpasses occurred during the box pattern (Fig. RF12.21) by DMSP-F16 (10:19 UT), DMSP-F17 (09:40, 11:19 UT) and DMSP-F18 (10:22, 12:03 and 13:42 UT).

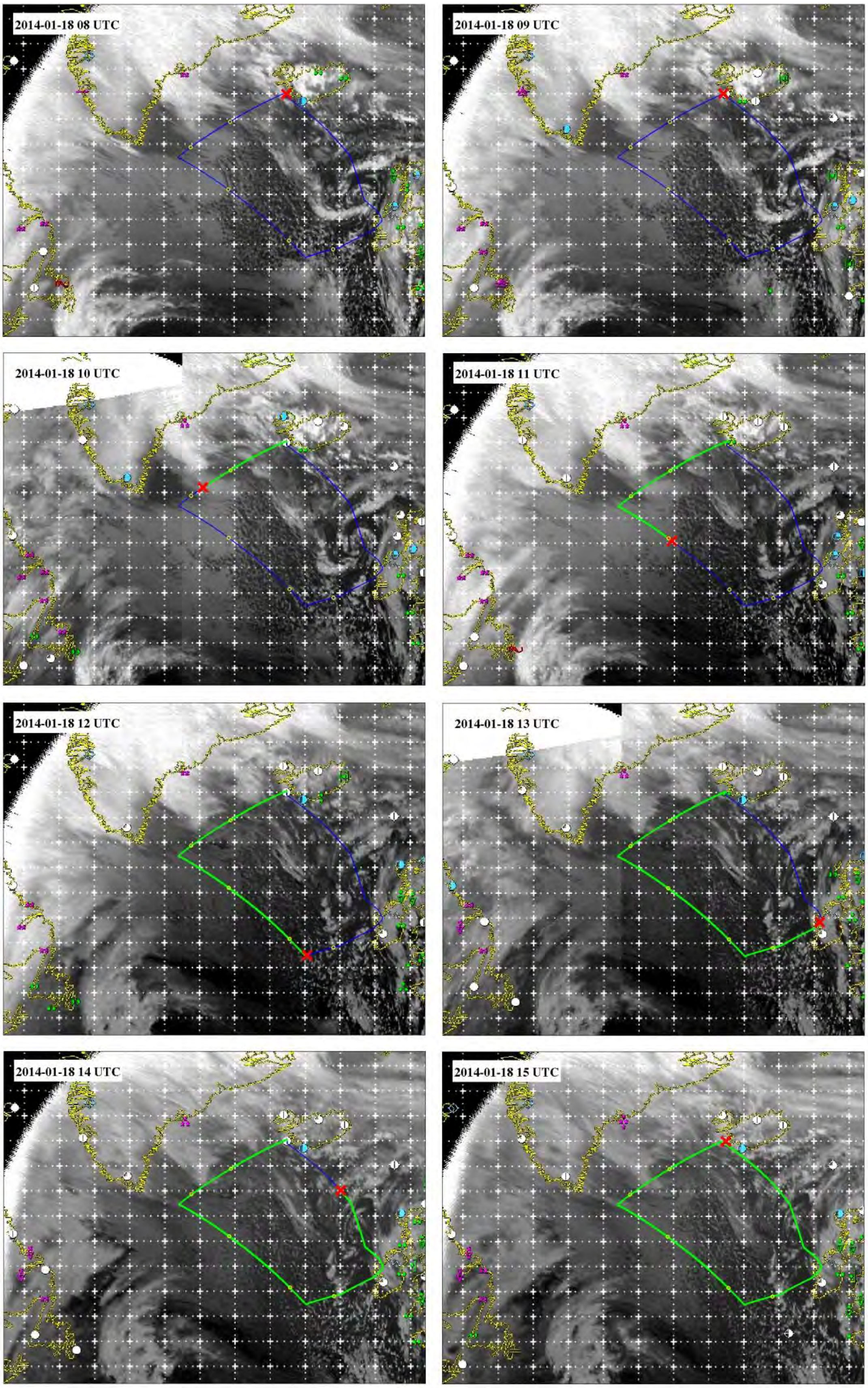

Fig. RF12.13: Hourly flight track composite in blue and infrared satellite data with elapsed flight time in green, current aircraft position as red cross and dropsondes positions as yellow circles. This composite is to be used as a reference for the flight protocol below.

Flight Protocol

All times in UT. Four digit numbers refer to Canon RAW file photo data.

08:00 hangar roll out
08:05 APU on
08:40 engines start up
08:51 taxi
08:55 take off
08:58 cloud base contact
08:59 dawn at horizon
09:03 into clouds, convection before looked like scattered Cbs but too dark to evaluate
09:04 crossing the high cloud band west of KEF
09:05 above all clouds from now on
09:06 above clouds, towering cumulus, scattered cirrus, the sector before passing the thin high clouds of dissolving front
09:15 FL270, radar on, lidar on
09:31 shallow convection 5866
09:31 bands of cirrus above corresponding to weak cyclone front at 29W, flight path shifted by ATC to 62N, 5867+5868
09:36 62N 30W entry point, no cirrus and broken shallow convection, 1 km cloud top, few rain showers
09:38 dropsonde 1 into cold slot, 5869, broken shallow convection with few rain showers
09:44 32W flying over single 4 km cloud top convective cell with rain, brightband shallow, 5870, surrounding shallow convection of 1 km cloud tops
09:49 32.2W stratiform convection of 1 km height, almost no gaps to surface, corresponding to stratiform cloud patch south of occlusion in satellite image, 5871, cloud tops 3 km with scattered showers
09:52 lidar shows dry intrusion (yellow greenish colors) reaching down
09:55 slight turbulence
10:00 almost cloud-free, southern border of the tip jet area, 5872
10:10 dropsonde 2 into almost cloud-free tip jet area 10 minutes before WP1, 5873 few more clouds to SE, no clouds to NW
10:16 situation as in satellite image, to the right cloud free (tip jet, 5874), to the left shallow cumulus is dark stratiform cloud patch between WP1 and WP2, 5875
10:22 waypoint 1, turn left, 5876, turning into region of stratiform convection, no precipitation, looks almost like Sc
10:31 still uniform shallow convection with almost no precipitation, 5877
10:45 "cinnamon rolls" of 2 km cloud top precipitating stratiform cloud deck with no gaps, no brightband, probably snow
10:52 photos of "cinnamon rolls" 5886 to 5893
10:57 dropsonde 3 into cinnamon rolls at 56.22N 30.55W, 3°C at the ground, shortly before the boundary on satellite image between closed and open convection
10:58 waypoint 2, exit gander, calling Shanwick ATC
11:06 boundary between cinnamon rolls and broken higher convection, 5894+5895
11:08 150 kn tail wind, open cellular convection reached with 2.5 km cloud tops, brightband reaches ground, snow, mixed-phase precipitation
11:11 scattered Cbs visible with very shallow anvils, probably 3 km high, 5896+5897
11:15 5899-5911 convective clouds from the cockpit window
11:23 thin ice clouds below with snow virga, 5912
11:29 5913 broken shallow convection

11:38 Cbs and convection 5914, dropsonde 4 52.8N 21.56W, Cb anvils with almost no convection below, 5914-16, virga
11:38 dropsonde 4 while crossing 53N 25W
11:59 waypoint 3
12:02 broken convection, partly anvils of ice, 5917, flying over cell with anvil, 4 km cloud top, brightband suggests rain
12:22 dropsonde 5 into Cb with overshooting top, 51.39N 15.51W, strong convection, 5919 shows situation aside, convection below plane
12:28 waypoint 4
12:29 s-shaped front visible at horizon
12:30 5920+5921 Cb cloud with anvil to the right, not overflown, but typical for situation
12:31 entered Shannon air space for climb
12:32 exit FL270 climb into FL430, no dropsonde permissions anymore
12:38 5922 convection shafts
12:39 partly open, partly closed cloud cover with embedded towering cumulus
12:40 elongated sheared anvils tops of convection, 5923+5924
12:45 flying over Cb that shows anvil in the radar
12:43 waypoint 5, FL430 reached, reached Ireland, cirrus shield follows coastline of Ireland
12:52 approaching dense frontal cirrus cloud field, 5925-5928, radar shows no precipitation below, only high level clouds
12:55 Mace Head fly by
13:01 waypoint CON, left curve
13:06 over ocean again, dense cirrus
13:08 left curve into waypoint MOLAR
13:16 cirrus shield ended, over oceanic convection again, large gaps between clouds
13:21 waypoint SAT1, 10 minutes early, isolated decaying Cbs to the west, cloud streets to the east, 5940-5943
13:30 Cb with mammatus 5944+5945
13:38 5946 Cb in foreground with spiral frontal s-shaped cyclone in the distance, first two bands in satellite 08 UT image may be drifted out of flight path
13:39 frontal cloud band 5947-5950
13:44 CloudSat overpass, 5951 above the northern s-shaped spiral cyclone, embedded towering convection
13:49 5952 towering iced convection, 6 km cloud tops, high brightband, rain
13:50 waypoint SAT2, left curve
14:00 another cloud band passage, rather thin cirrus with few convection below, 59.38N
14.23 W, 5953+5954
14:10 towering cumulus, sheared of anvils with almost no cloud below and Sc decks intersected with active Cbs
14:15 exit point, towering convection, 5956
14:25 5966 towering convection, descend
14:28 5967 Cbs and flown over, in descend anvil tops just below plane, cloud height 6 to 7 km, radar shows isolated anvil and convective rain shafts below
14:32 flying into the Cb anvils, first cloud contact, lidar switched off
14:38 descend into KEF, flying through the towering convection
14:44 established ILS KEF
14:48 cleared to land RWY 02
14:49 touch down
14:50 taxi to parking position
14:53 parking position

14:53 engines off
Dropsondes
01 09:38 62.5N 32.0W cold air slot of cyclone
02 10:10 in cloud-free tip jet area 10 minutes before waypoint 1
03 10:57 into cinnamon rolls at 56.22N 30.55W, 3°C surface temperature, snowfall
04 11:38 52.8N 21.56W, Cb anvils with almost few convection below
05 12:22 dropped into Cb with overshooting top, 51.39N 15.51W, strong convection

Preliminary HALO instrument data: All instruments onboard recorded data without significant gaps. Displayed below are selected preliminary results with the exception of MiniDOAS. This data will be analyzed after the campaign.

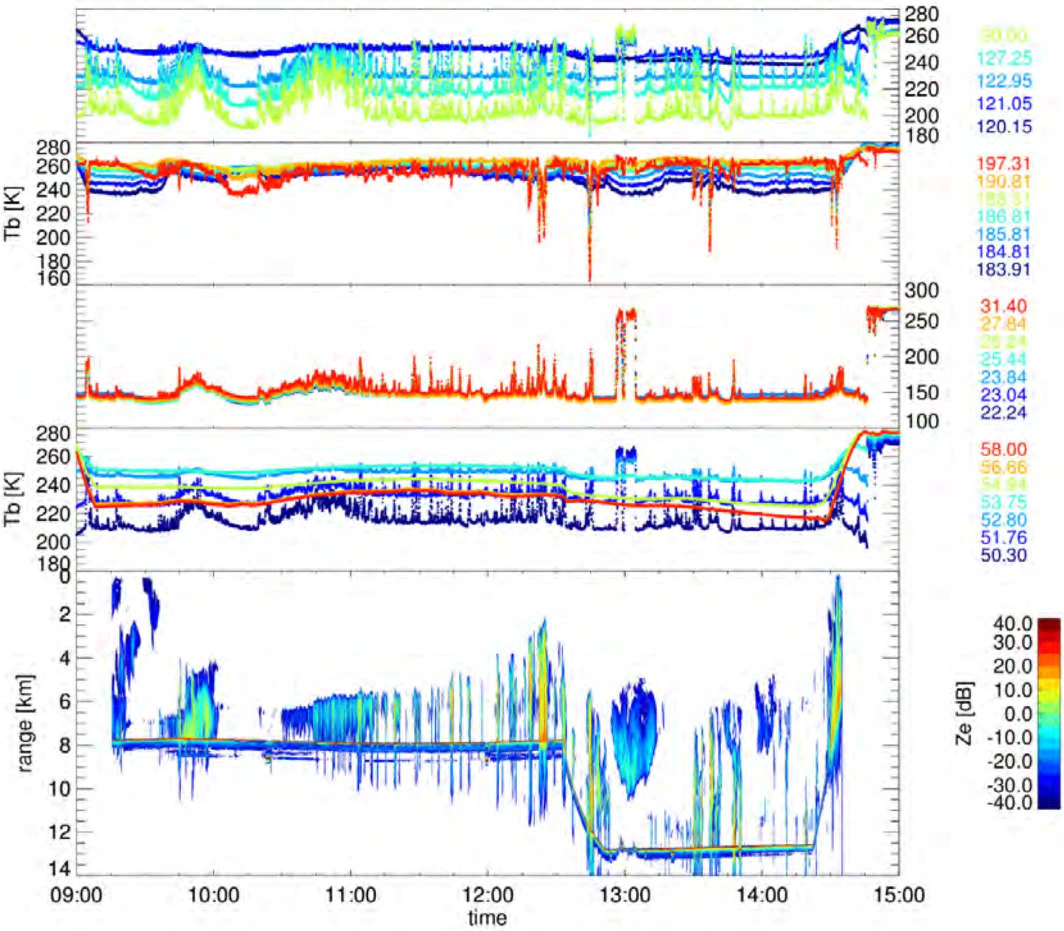

Fig. RF12.14: Time series (in UT) of the microwave radiometer brightness temperatures (top four panels) and radar reflectivity profiles (lower panel) for the entire flight RF3 for the scattering channels (first panel), the sounding channels (second panel), the emission channels (third panel) and the 50 GHz channels (fourth panel) and the range corrected radar reflectivity (lowest panel). The raw data radar reflectivity profiles still include surface signals as well as multiple scatter signals at range gates beyond the surface. Flights through clouds only occurred at take off and landing. Note the remarkable increase in convective height from cloud-free conditions at 10:00 UT to stratiform clouds, the "cinnamon roll" clouds at 11:00 UT, the open cellular convection at 11:30 UT and Cbs at 12:30 UT at the end of leg 2. The fight level change to FL430 is visible as is the non-raining cloud over Ireland and the convection and occlusions of the CloudSat overpass time at 13:45 UT.

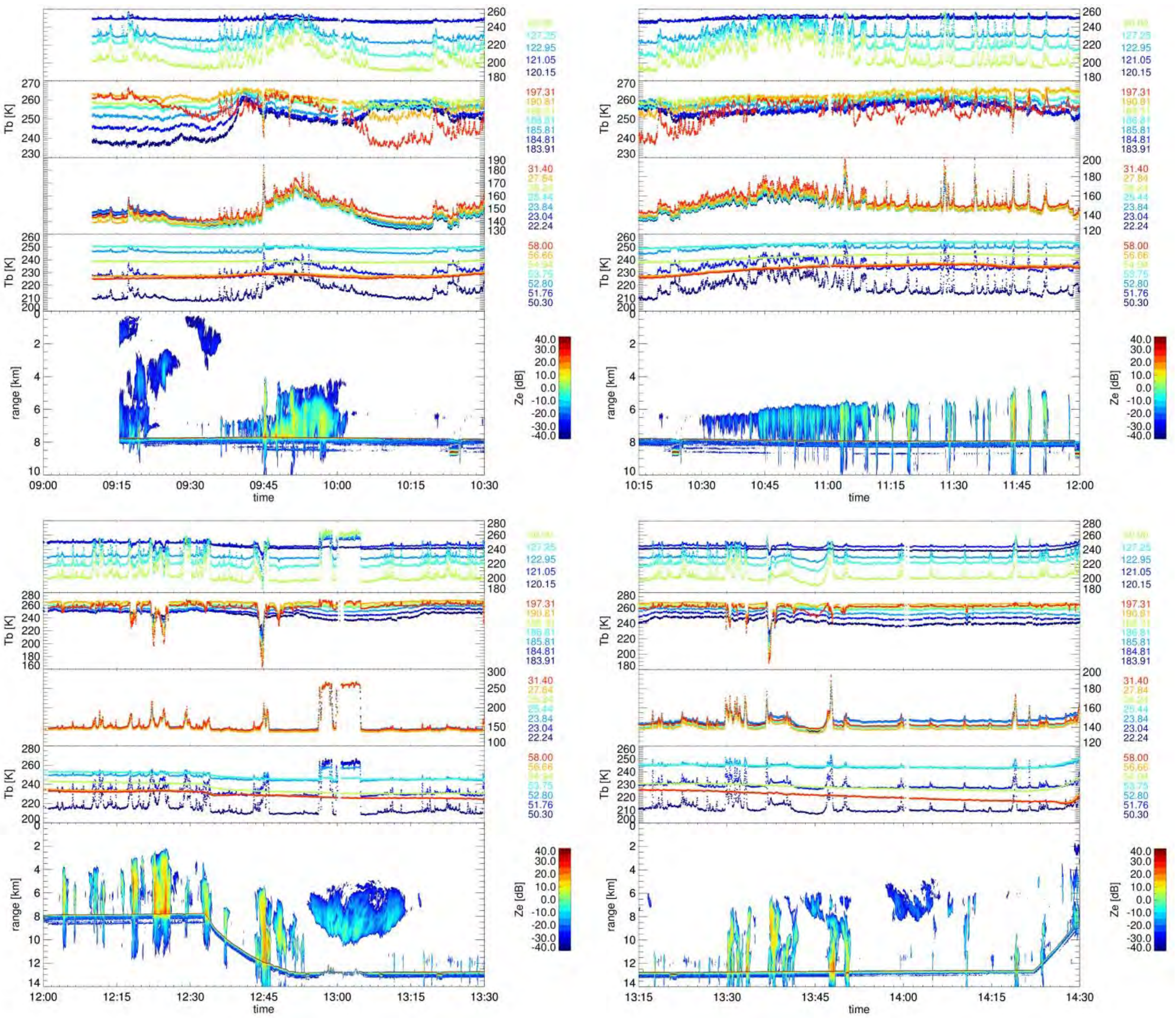

Fig. RF12.15: Time series as in RF12.14 but temporally higher resolved into 4 panels of approximately 1.5 hour interval length corresponding to legs 1 to 4 and the return to KEF. The top left panel contains the take off, the passage over the occlusion, the dry slot, the 4 km convective tower embedded into frontal convection and the abrupt cloud-free tip jet area south of Greenland. The top right panel continues with the tip jet and the turn into the southerly leg, beginning with shallow stratiform clouds and the spiral-shaped "cinnamon rolls" from 10:45 UT on. Note, how the convection cells open around 11:15 UT. The lower left panel documents the growing convection into Cb clouds and the flight level change to FL430. Also the cloud field over Ireland is well seen. HALO was over Ireland between 12:43 UT and 13:06 UT and FL270 was left at 12:32 UT and FL430 was reached at 12:43 UT. The Mace Head overpass was at 12:55 UT. The lower right panel documents the flight leg 4 towards KEF and the convection intersected by the s-shaped occlusion bands with the CloudSat overpass at 13:45 UT. From 14:20 UT the descend into KEF began.

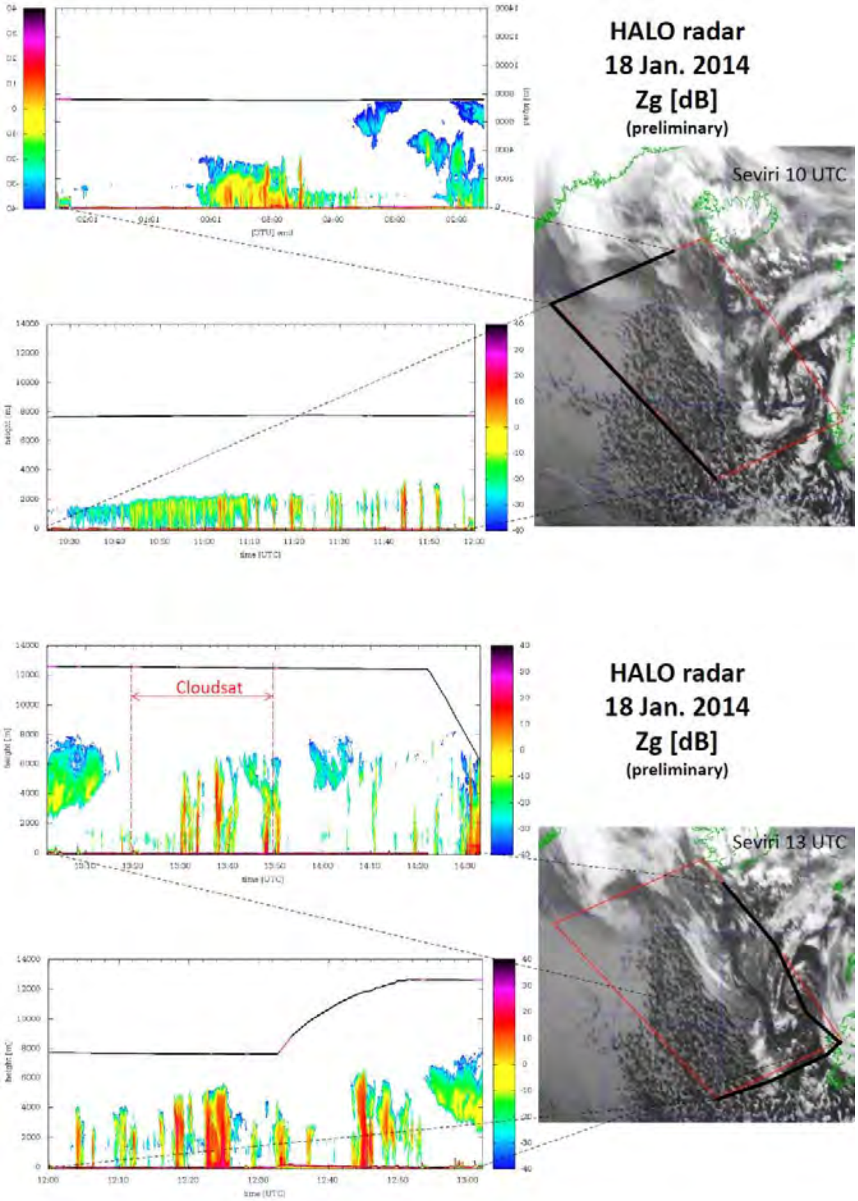

Fig. RF12.16: The complete RF3 MIRA-36 radar times series. Zg is the range gate corrected reflectivity with eliminated signals below the surface and the vertical axis is flipped to the one in Fig. RF12.14 and RF12.15. At 12:45 UT a Cb with a prominent anvil was passed reaching about 6 km altitude. The radar legs locations are visualized by the satellite images. The first panel contains the passage over the occlusion, the dry slot, the 4 km convective tower embedded into frontal convection, and the abrupt cloud-free tip jet area south of Greenland. The second panel continues with the tip jet and the turn into the southerly leg, beginning with shallow stratiform clouds and the spiral-shaped "cinnamon rolls" from 10:45 UT on. Note, how the convection cells open around 11:15 UT. The third panel documents the flight leg 4 towards KEF and the convection intersected by the s-shaped occlusion bands with the CloudSat overpass at 13:45 UT. From 14:20 UT the descend into KEF began. The fourth panel documents the growing convection into Cb clouds and the flight level change to FL430. Also the cloud field over Ireland is well seen. HALO was over Ireland between 12:43 UT and 13:06 UT and FL270 was left at 12:32 UT and FL430 was reached at 12:43 UT. The Mace Head overpass was at 12:55 UT.

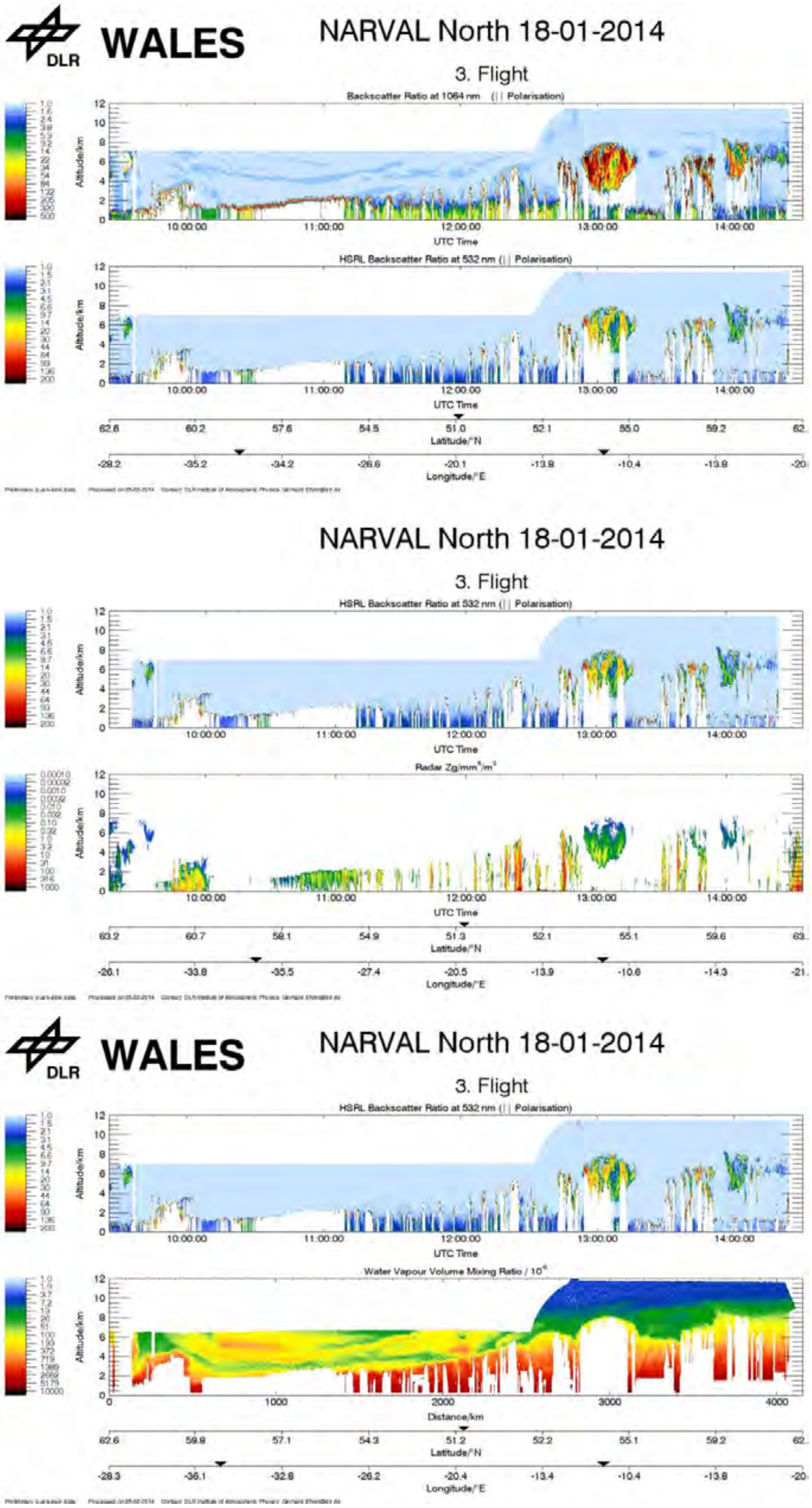

Fig. RF12.17: The top panel shows the WALES lidar backscatter ratio time series at 1064 and 532 nm compared to the MIRA36 radar data (middle panel) and the lidar water vapor mixing ration (bottom panel).

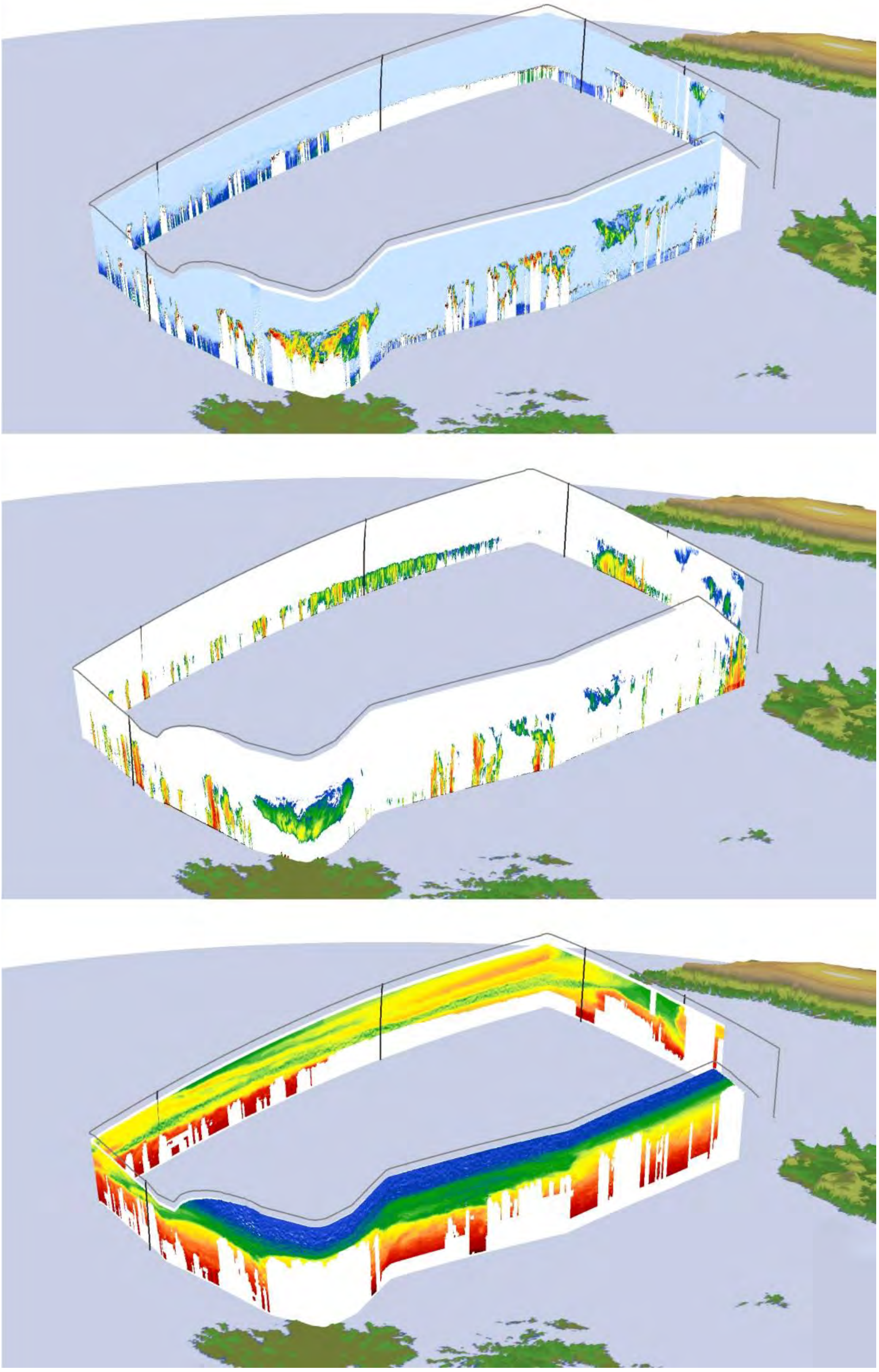

Fig. RF12.18: 3-D visualization of the lidar data for the backscatter ratio (top), the MIRA36 radar data (middle) and the water vapor mixing ratio (bottom) along the entire flight track. Blue backscatter colors indicate clear air while white and black relate to strong extinction due to optically thick clouds. The water vapor mixing ratio exhibits dry air in green and the intrusions in yellow showing strong humidity gradients. For better visualization the atmosphere is stretched by a factor of 70 to focus on the clouds. The grey line is the plane position and data is recorded about 600 m below the aircraft down to the ground if atmospheric conditions allow. Fig. RF12.16 discusses the meteorology being valid for this viewgraph also. The downstream convective growth is nicely documented in the 3-D panels.

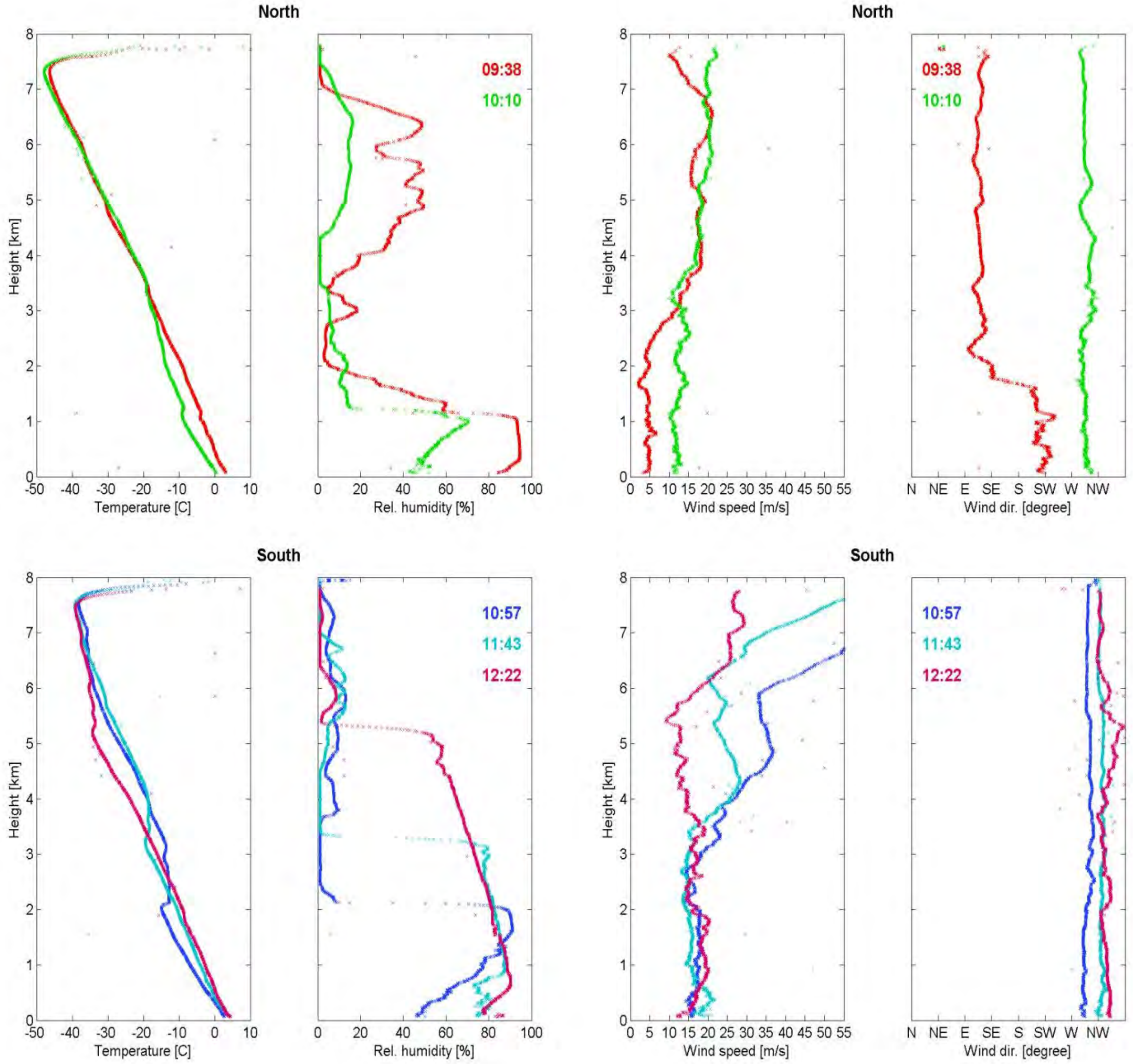

Fig. RF12.19: All 5 dropsonde profiles in chronological order released at 09:38 UT, 10:10 UT (upper panel), and 10:57 UT, 11:43 UT, and 12:22 UT (lower panel), plotted for height versus temperature (first column), humidity (second column), wind speed (third column) and wind direction (fourth column). Dropsonde 1 was located in the dry slot of the northerly cyclone center. Dropsondes 2 to 5 document the downstream convective development from cloud-free conditions in the tip jet (2), the spiral-shaped "cinnamon roll" clouds (3) and the Cb clouds (4 and 5). Note, that the dropsonde at 11:43 UT is marked 11:38 UT in the flight protocol.

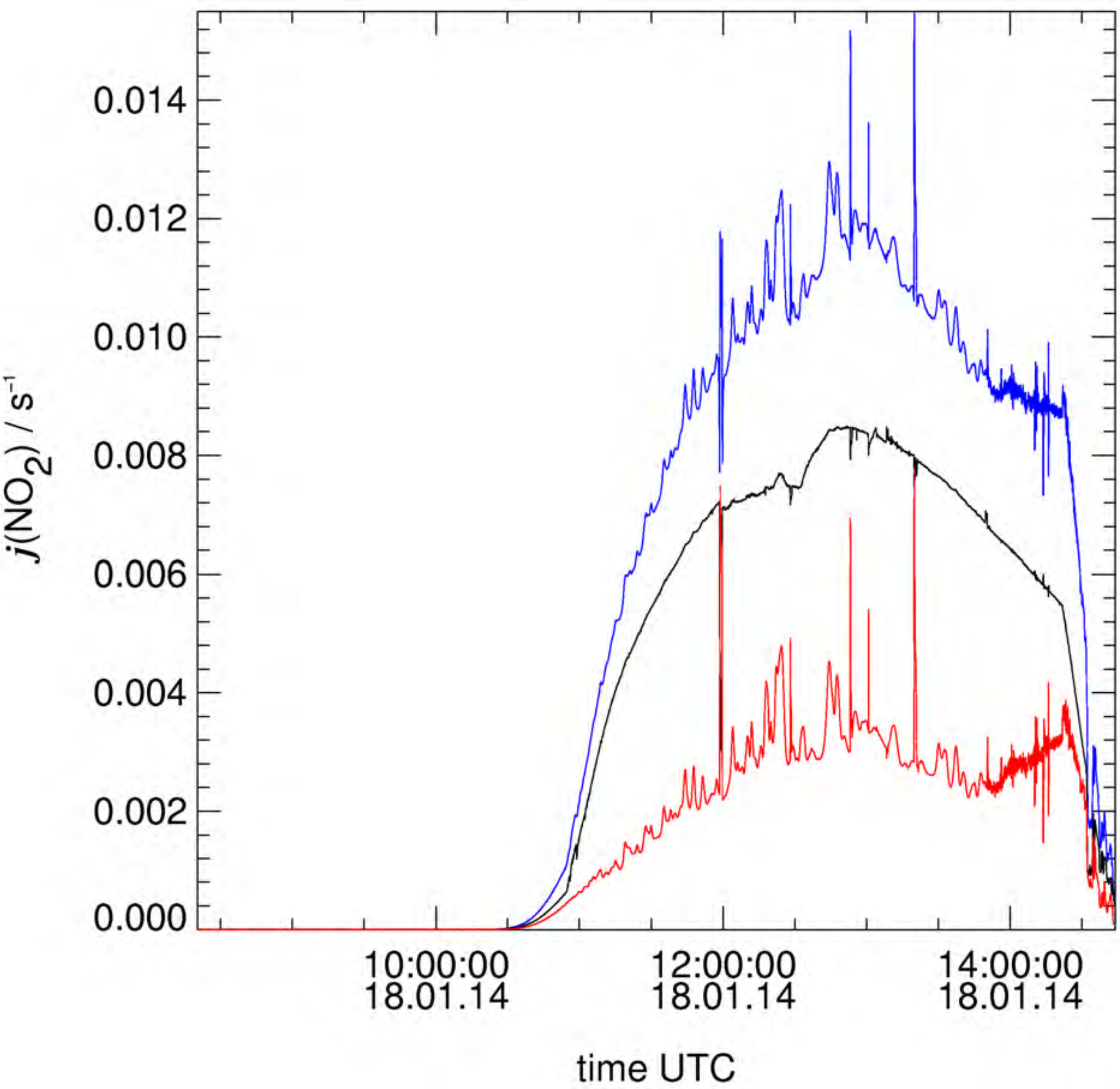

Fig RF12.20.: HALO-SR photolysis frequency $j(NO_2)$ from lower hemisphere (red), upper hemisphere (black) and combined (blue) measurements. Changes in zenith component reveal changes in flight altitude and flight latitude.

The SSMIS and CloudSat perspective:

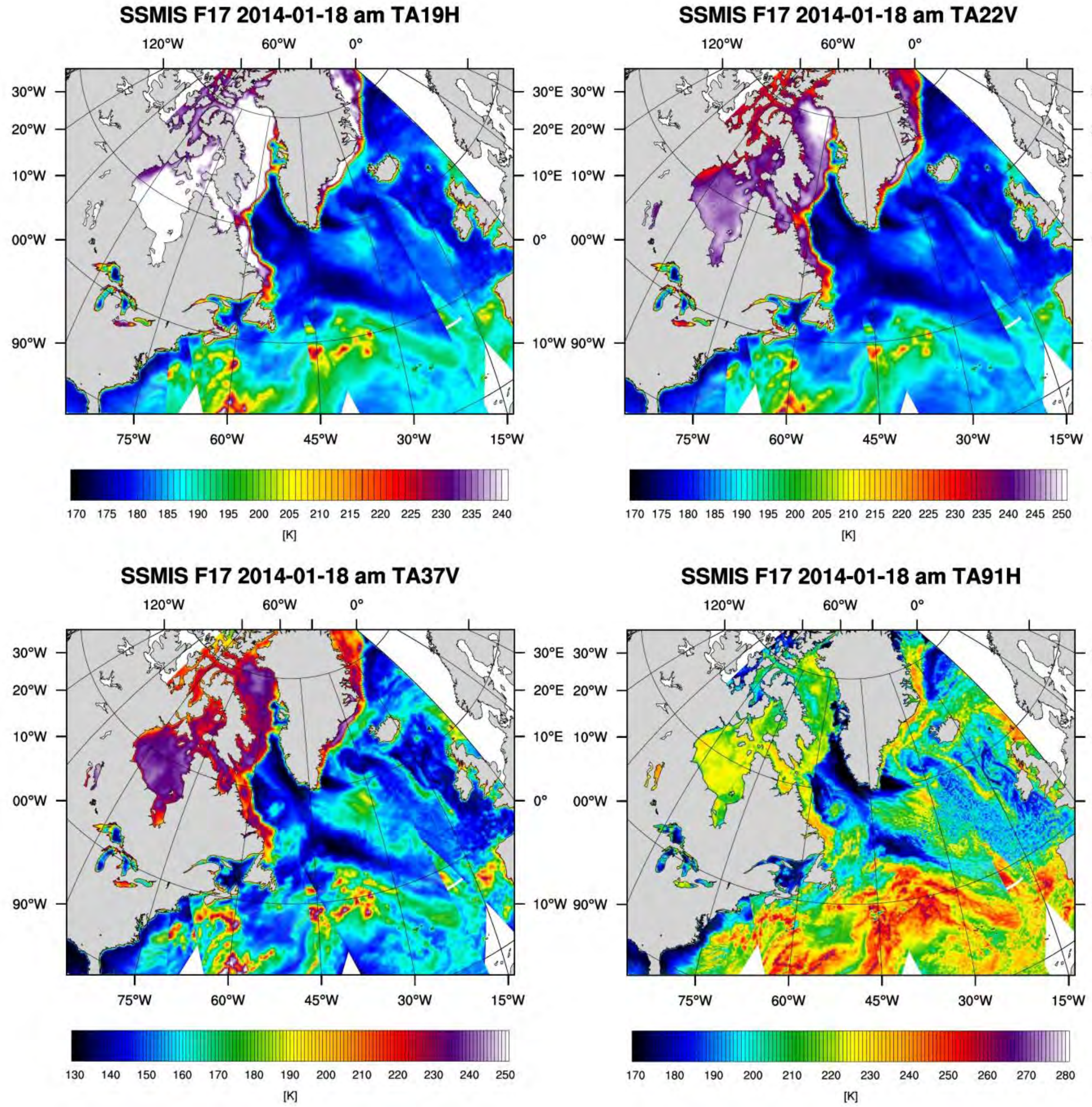

Fig. RF12.21: Preliminary HOAPS 4 fundamental climate data record (FCDR) antenna temperatures (TA) for DMSP-F17 SSMIS target area overpass at 09:40 UT. Shown are the environmental data record (EDR) emission channels 19 GHz H (sensitive to rain; top left), the water vapor channel 22 GHz V (top right), the 37 GHz V (lower left), and the 91 GHz H scattering channel (sensitive to ice; lower right) indicated for horizontal (H) and vertical (V) polarization. The multiple occlusions are easily recognized as are the dry slot in the northerly low pressure center and the cloud-free tip jet area. The great detail of the precipitating cloud structure in the antenna temperatures is promising for the forthcoming brightness temperature conversion followed by the precipitation rate retrieval. Note the resolution increase from the 50 km pixel size 19 GHz channel to the 8 km pixel size of the 91 GHz channel. Six SSMIS collocation overpasses occurred during the box pattern by DMSP-F16 (10:19 UT), DMSP-F17 (09:40, 11:19 UT), and DMSP-F18 (10:22, 12:03 and 13:42 UT).

20140118:

13:43:00	52.0058	9.7302	344.11
13:44:00	55.5402	11.4675	343.09
13:45:00	59.0509	13.4967	341.79
13:46:00	62.5299	15.9282	340.10

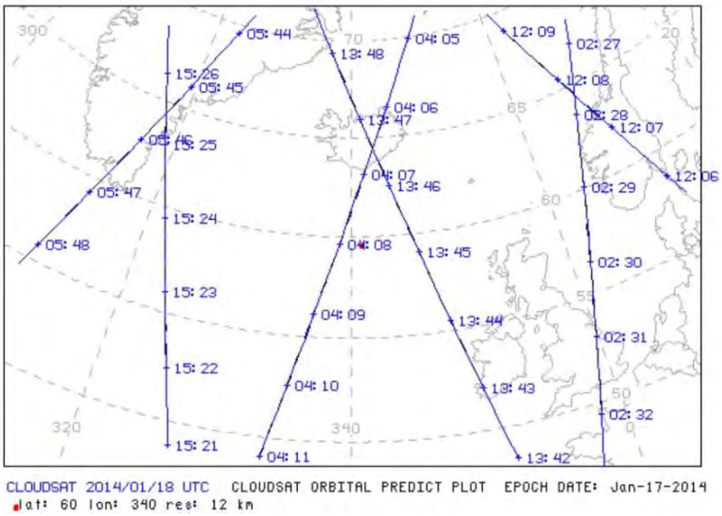

Fig. RF12.22: CloudSat ascending orbit track over the North Atlantic on 18 Jan 2014 between 13:42 UT and 13:48 UT. The collocated HALO underflight was at 13:44 UT in northwestward flight direction of CloudSat. Coordinates for 13:43 UT to 13:46 UT are given in the table above the figure.

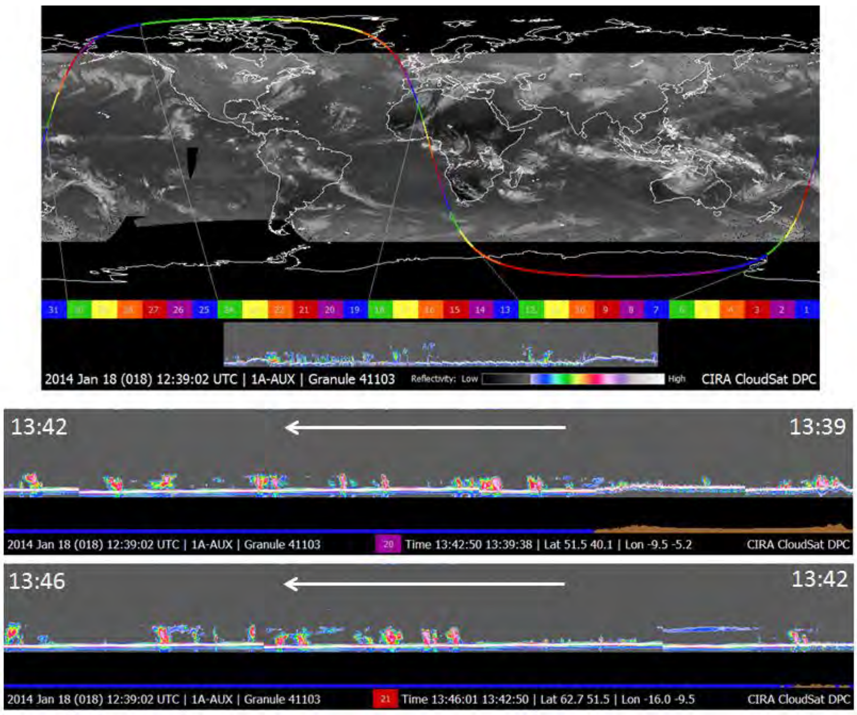

Fig. RF12.23: CloudSat quicklook track granule 41103 over the convection and occlusions bands between 13:39 UT (violet track) and 13:46 UT (red track). The northwestward flight direction is indicated by the white arrow. The collocated overpass is documented in the center of the red track. The convection and cirrus bands of the occlusions are easily recognized.

NARVAL North Research Flight 13 (RF13), Flight Report

- 20 January 2014 -

CHRISTIAN KLEPP

Crew: Roland Welser (Pilot), Stefan Grillenbeck (Pilot), Alexander Wolf (Flight engineer), Silke Groß (WALES), Andreas Schäfler (Dropsondes), Heike Konow (HALO SR & MiniDOAS), Martin Hagen (HAMP), Christian Klepp (Mission scientist)

Objective: The scientific objective of the fourth research flight was to sample the cold air convection regimes on the backside of a cyclone with less pronounced intensity. The postfrontal cold air outflow did not originate directly from polar environment. Hence, the difference in SST and air temperature was weak compared to strong cold air outbreak situations. The measurements should clarify if the overall convective activity would consequently be less pronounced compared to the research flights 1 to 3. The different regimes investigated in this cyclone comprised the passage of the main occlusion (OCC) and the tiltback occlusion (TBO). The remote sensing pattern of the cold air regimes contained shallow cumulus (SHC), enhanced cumulus (ENC), the postfrontal subsidence (PFS) and Cb's that were shielded by an overlain stratiform appearing cloud layer directly above the anvils. This resulted in a masking effect that obscured the visibility of the Cb's from the aircraft window (MCB). Consequently, satellite visible and infrared imagery may also calssify these clouds in error as stratiform. The tiltback occlusion was crossed several times including the ruptured tiltback occlusion (R-TBO) that featured a spiral shape in the cyclone center. Fig. RF13.1 shows the meteorological setting at 17 UT. The entire flight was performed at FL270 with a zigzag mattress pattern consisting out of 6 legs of 5:26 h length allowing for scanning the cold air regimes in great detail. The CloudSat overpass at 15:10 UT was not collocated with the HALO flight track. The temporal mismatch of 49 minutes may be used for cloud development investigation. During the HALO operation time six SSMIS overpasses occurred. 11 dropsondes were released along FL270.

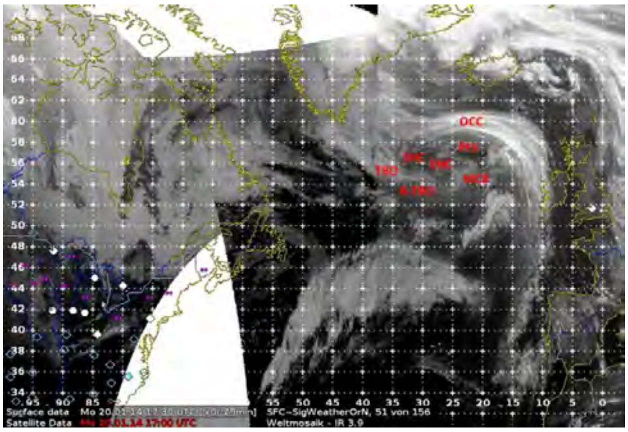

Fig. RF13.1: The widely occluded low pressure system to the south of Iceland with the main occlusion (OCC), the tiltback occlusion (TBO), the ruptured spiral shaped tiltback occlusion tail (R-TBO) and the cold air regimes of shallow convection (SHC), enhanced convection (ENC), cloud layer masked Cb's (MCB) and the cloud-free postfrontal subsidence in the satellite composite from 17:00 UT at 20 Jan 2014.

Overview:

In the course of the week after research flight 2 on 12 Jan 2014, the large scale flow further developed into the strong meridional pattern allowing the Acores High to expand northward into the region of the Labrador Sea. The high pressure ridge developed its maximum northward displacement on Fri, 19 Jan 2014 where the polar front reached the latitude of New Foundland over the North Atlantic. The corresponding narrow eastern trough was located over the Iberian Peninsula with a sustained blocking situation over Eastern Europe. This weather situation cut off the target area over the North Atlantic from the usual Arctic cold air supply while the developing low pressure systems were smaller in size and less pronounced in intensity. A pool of cold air moved in over the Northern Territories of Canada and induced cyclogenesis along the eastern Arctic Canadian continental margin that extended into the northern Labrador Sea on Sun, 20 Jan 2014. Along the polar front a fast moving low pressure system was advected with a cold core connecting to the cold air over the outflow of the Labrador Sea. However, the postfrontal activity saw no Arctic cold air inflow (Fig. RF.4.2). The cyclone developed three occlusion fronts that merged during the research flight into one major occlusion and a tiltback occlusion. The tiltback occlusion ruptured from the main system and the cold cyclone core developed weak convective activity in the west and progressively stronger convection towards the spiral shaped center and the postfrontal subsidence (Fig. RF.4.3 and Fig. RF13.1). To the east numerous occluded fronts of the previous low pressure systems were located between Iceland, Great Britain and Northern Germany as a result of the strong high pressure blocking situation over Scandinavia (Fig. RF.4.3).

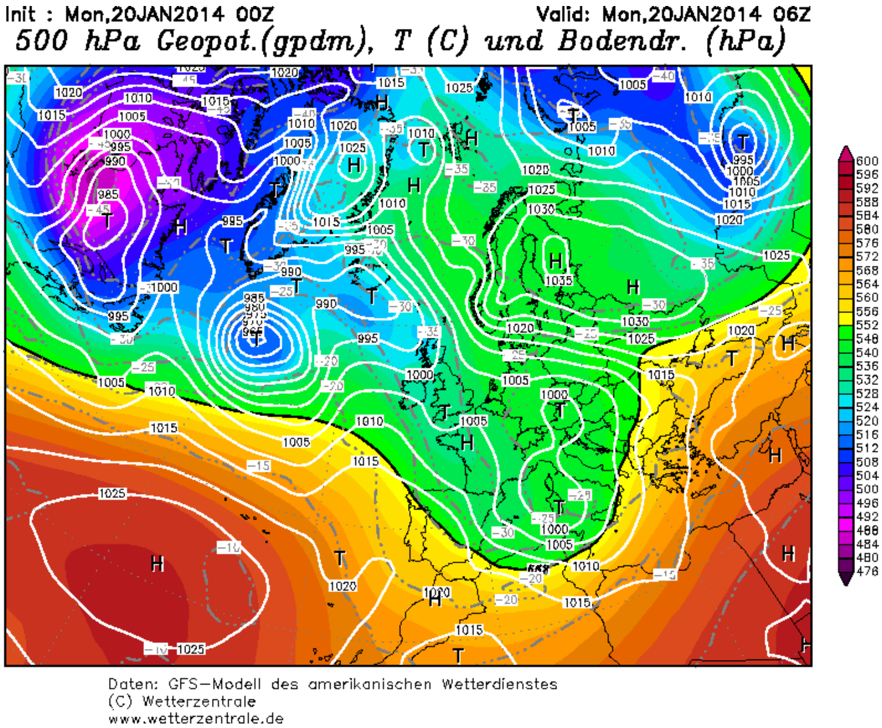

Fig. RF13.2: GFS analysis of surface pressure (white isolines), 500 hPa geopotential height (color, 552 dekameter isoline in black) and temperature (dot-dashed grey isolines and white boxes) in °C valid for Mon, 20 Jan 2014 06 UT showing the cold core low pressure system in place to the south of Greenland. The postfrontal cold air inflow into this low pressure system is fairly week compared to the climatological January conditions in this region. This is a consequence of the high pressure ridge influence over the central North Atlantic and the blocking situation over Scandinavia.

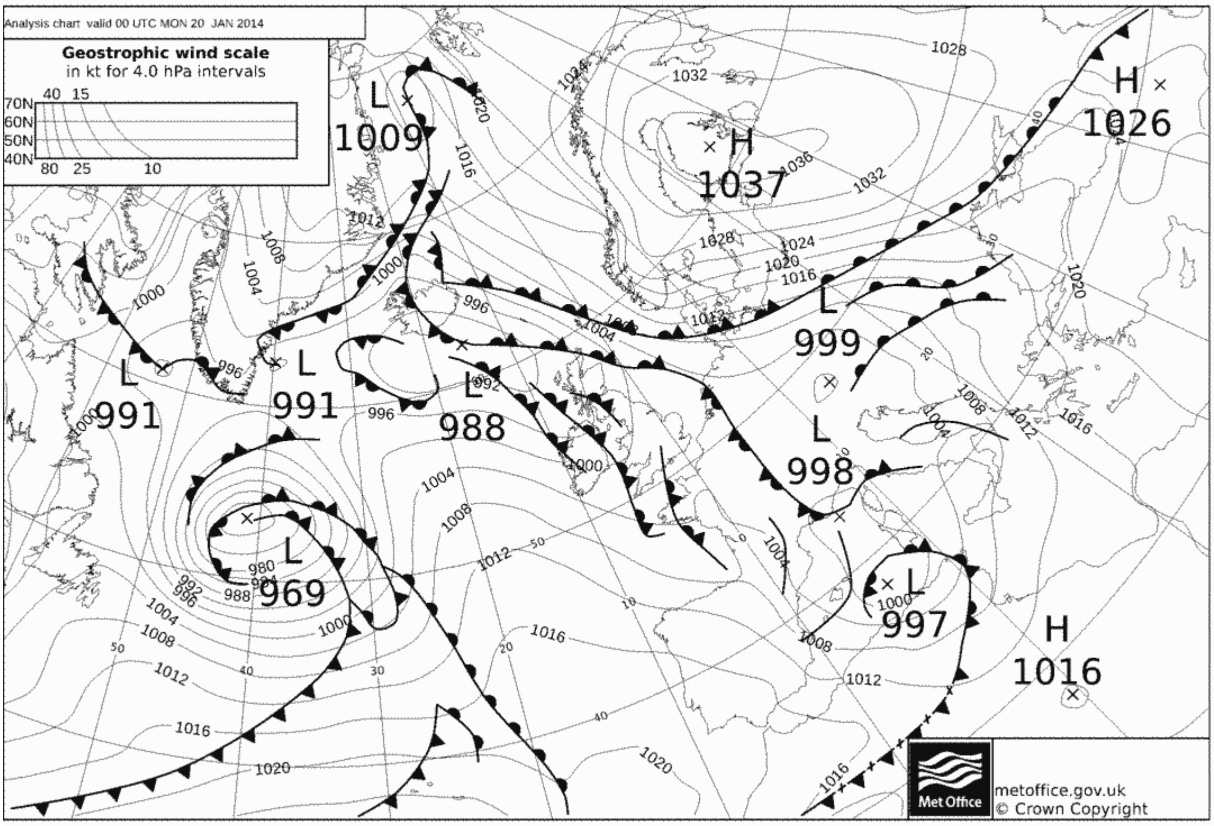

Fig. RF13.3: UK Met. Office analysis chart for 00 UTC on Mon 20 Jan 2014 with the target area being located in the area of 50°N and 40°W. At 00 UT the cyclone is in rapid development and still shows two separated occlusions which in the course of the day joined. The tiltback occlusion is forming and the cyclone center pressure is about 969 hPa. The evolution of the system is well documented in the difference between this figure and the satellite mosaic of Fig. RF.4.1.

Flight Planning: Remote sensing of the cyclone cold core was best realized by flying a zigzag mattress pattern across the system. A large bounding box area was requested in which HALO is allowed to operate freely according to the uncertainties between the cyclone's forecast position and the fast changing weather situation throughout the flight. For dropsonde allowance and ATC restriction reasons the flight altitude was requested for FL270 equivalent to approximately 8 km altitude. To reach the cold core of the cyclone with a mattress flown from west to east, a transfer leg was planned from KEF (BIKF) via the FIR boundary to the entry point of the blocked airspace area and further to waypoint 2 at 55°N, 40°W. The entry point was approved at 59°N, 30°W. The exit point was located at 59°N, 21°W. The mattress pattern and waypoint locations are given in Fig. RF13.7. The mattress was flown from west to east to account for the fast eastward moving system to allow for a maximum time over the cold core system. The 6 mattress legs of approximately 1 h duration each were planned to cover the entire cold air convection from the main occlusion to the tiltback occlusion. A CloudSat collocated overpass was estimated for 15:10 UT. However, the duration of the entire flight of 8:30 h, strong tail winds during the flight and the location of the cyclone relative to the CloudSat overpass led to a temporal mismatch of 49 minutes. CloudSat passed the cyclone to the west of HALO in the direction of WP5 to WP4 and crossed the tiltback occlusion that HALO crossed over at 14:21 UT (Fig RF13.12, right panel). The take off time was 10:15 UT and HALO touched down at 18:45 UT. 11 dropsondes were released along FL270 and six SSMIS overpasses occurred during the flight operation time.

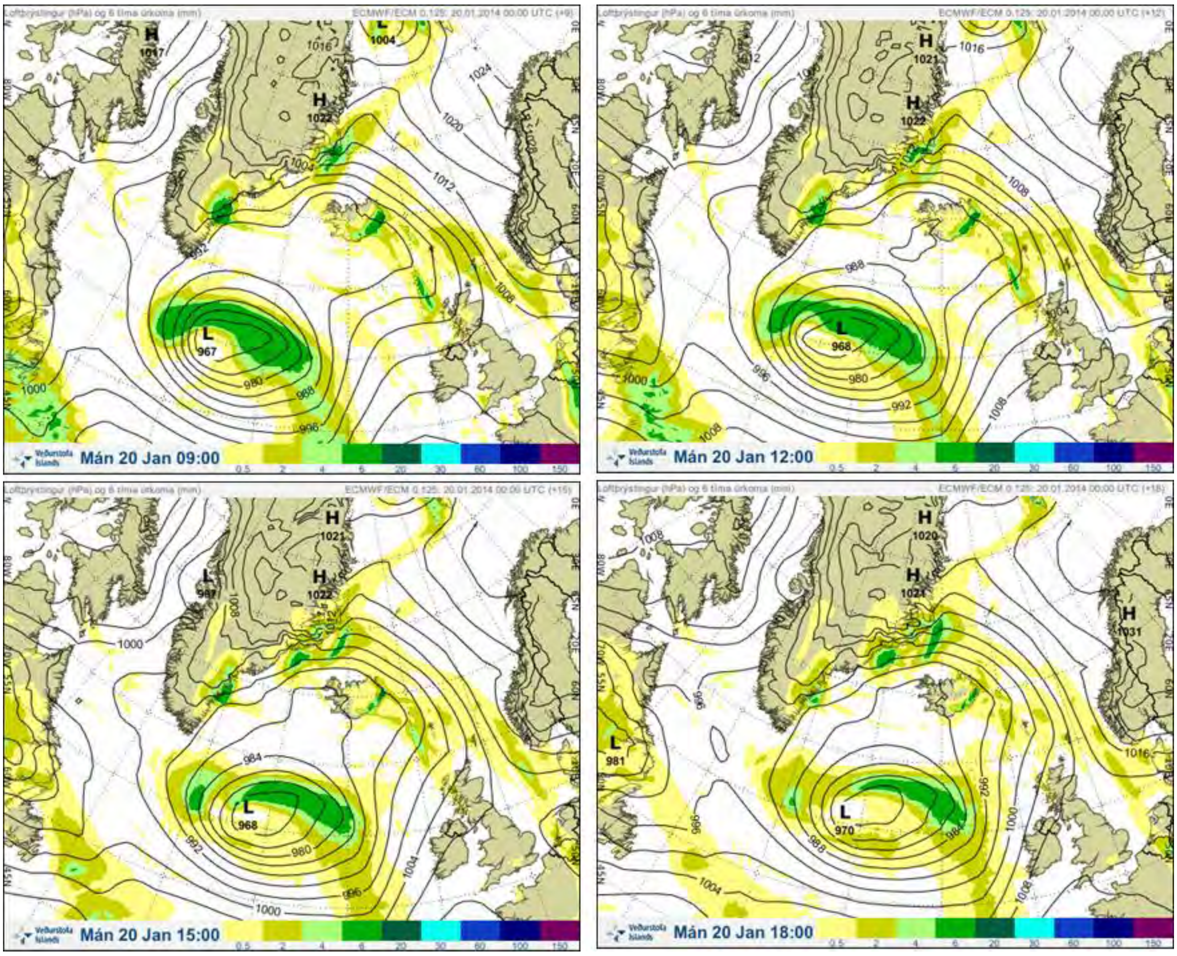

Fig. RF13.4: ECMWF forecast for 20 Jan 2014, 09, 12, 15 and 18 UT for surface pressure isobars and precipitation amount accumulated over 3 hours (mm in color). The precipitation development shows that the cold air convective activity is rapidly increasing with time and is on its maximum at 18 UT. This well coincided with the aircraft data collected and the antenna temperature record of SSMIS (Fig. RF13.25).

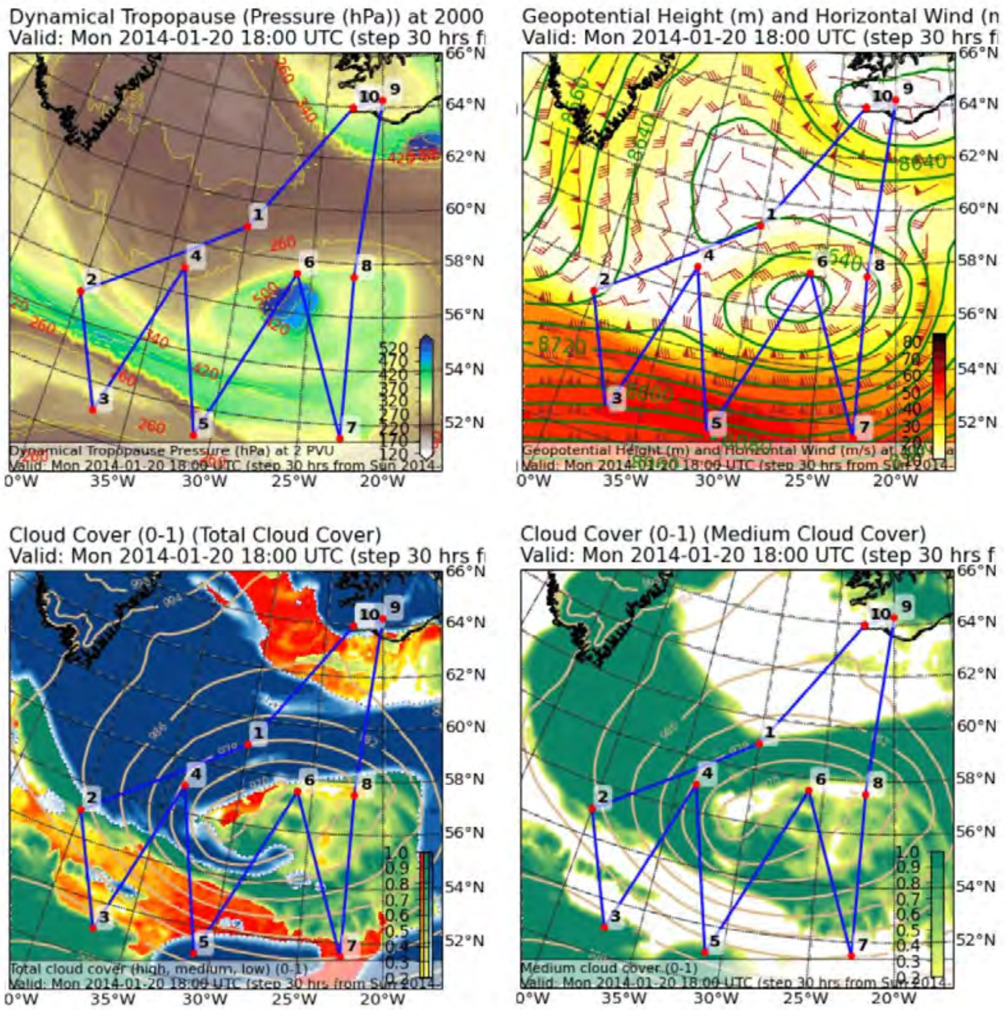

Fig. RF13.5: ECMWF based flight planning tool of DLR showing 20 Jan 2014, 18 UT forecast of dynamic tropopause pressure (hPa, in color, top left panel), the 300 hPa geopotential height (m, in color, top right panel), total cloud cover (high clouds in blue, mid-level clouds in green, low-level clouds in red) in the lower left panel and the medium cloud cover (lower right panel) including the flight pattern in blue and numbered waypoints as red dots.

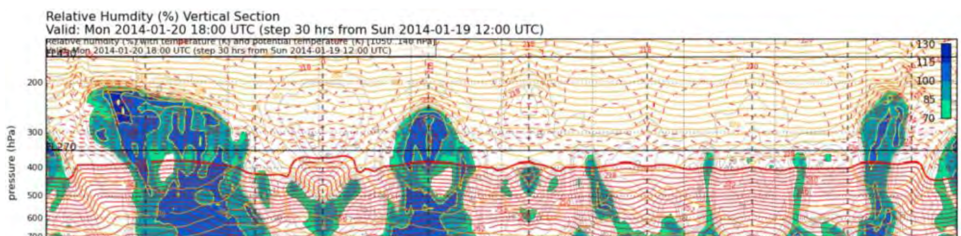

Fig. RF13.6: ECMWF based flight planning tool of DLR showing the vertical section of relative humidity (%, in color) and temperature (K, in red) forecast at 20 Jan 2014, 18 UT along the flight track from left to right. The waypoints are listed as numbers along the blue lined flight altitude of FL270.

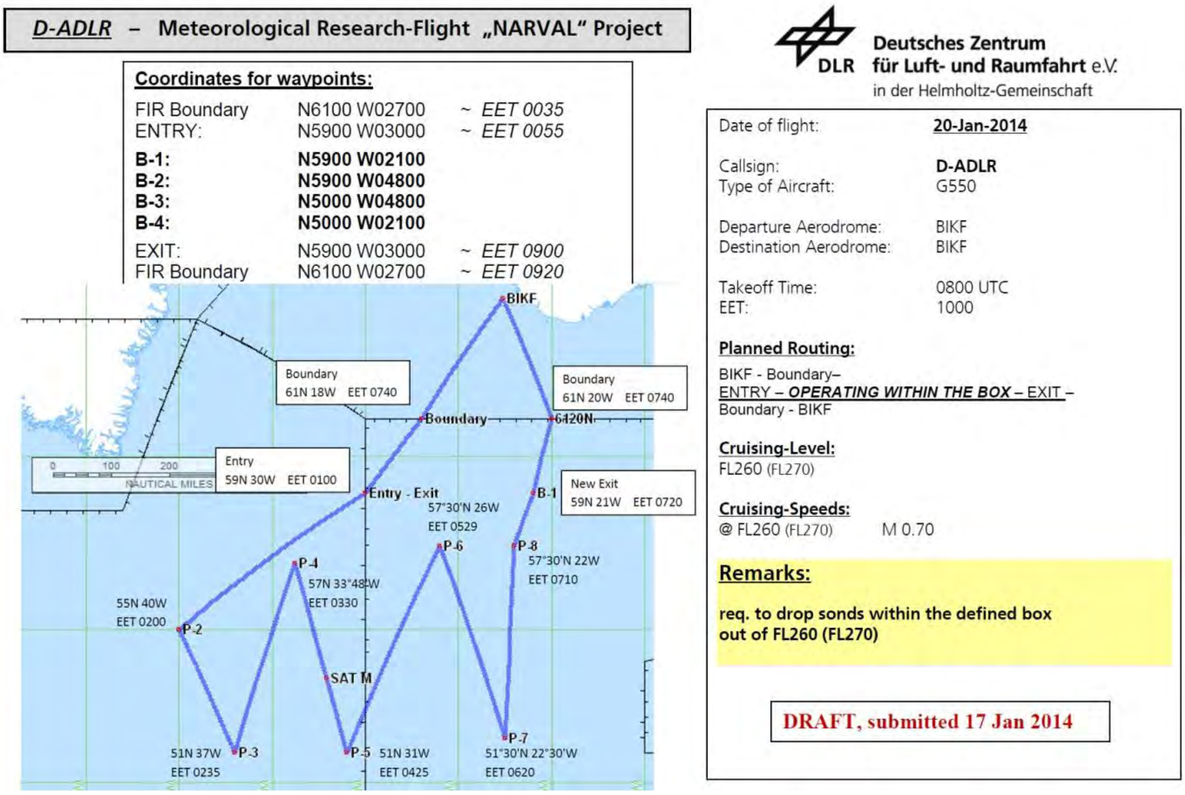

Fig. RF13.7: The ATC requested and approved flight pattern for RF4 with the flight track in blue and the waypoint WP2 to WP8 marked as P-2 to P-8. Waypoint WP1 is the entry point. The CloudSat collocated point SAT M was passed 49 minutes too early and hence could not be collocated. The flight operated at FL270 throughout the flight and 11 dropsondes were released.

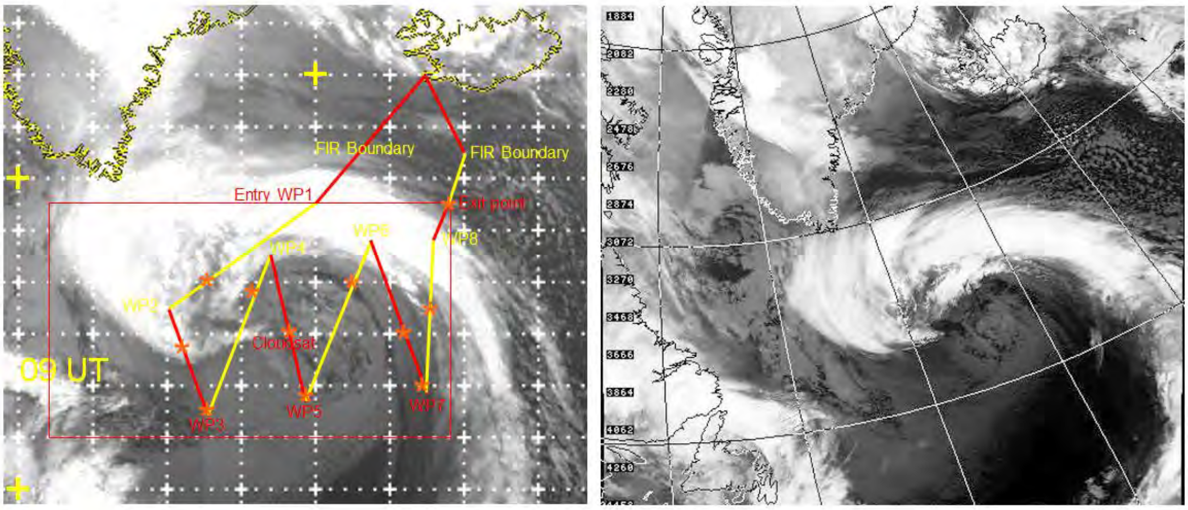

Figure RF13.8: Flight pattern on 20 January 2014 between 10:15 UT (take off) and 18:45 UT (touch down, left panel) including the waypoint tracks in different color coding and the dropsonde positions (orange stars) with the satellite image of 09 UT. The AVHRR satellite image (right panel) shows the weather development in the infrared channel 4 at 05:16 UT.

Flight Report:

Bracketed numbers refer to photo raw file number. For example (6178) refers to file IMG_6178.CR2 while CR2 is the Canon Raw Data file format.

The cold target calibration could not be carried out because no liquid nitrogen was available. Therefore, the calibration from 09 Jan was used. At 09:15 HALO was pushed back out of the hangar and the APU start up was at 09:20 UT. At 10:11 UT HALO was taxiing and took off from runway 02 at 10:15 UT.

TRANSFER LEG1 (1:59 h duration) KEF to WP2

Leg 1 comprises the straight transfer from KEF via the box entry point (WP1) to WP2. WP2 marks the entry into the matress pattern. Right after take off (10:15 UT) low level Stratocumulus was crossed and at 10:18 UT widespread Altostratus prevailed above the plane and almost closed shallow Sc decks were observed during sunrise (Fig. RF13.9, upper panel, photo 6058). FL240 was reached at 10:25 UT and the final altitude FL270 at 10:28 UT. At this time HALO was above all clouds with only broken Sc decks below (Fig. RF.4.9, lower left panel at 10:51 UT, photo 6063). With the approach of the FIR (Flight Information Region) boundary at 10:51 UT (Fig. RF13.8, left panel), first cirrus outflow of the cold front and occlusion boundary was abruptly reached. Both the radar and the lidar were operating by 10:52 UT. Since this time HALO was repeatedly in clouds or had clouds above. At 11:03 the cirrus was so thick that the visibility reduced to zero. WP1 was reached at 11:15 UT and the visibility was reduced by optically thick cirrus. The lower right panel of Fig. RF13.9 documents the cold front and occlusion boundary with multilayer cloud decks and As translucidus above (photo 6076). At 11:34 UT the radar recorded frontal rainfall and from 11:38 UT on the clouds became partly convective with scattered convection protruding the As. Consequently the rainfall intensified and inflight turbulence occurred at 57N, 35W. The transition towards the convection is also seen in the satellite flight track (Fig. RF13.13 at 12 UT) as HALO flew along the boundary between the front and the convective low pressure core. Dropsonde 1 was released at 11:53 UT in the convective occluded area (56° 2min N 37° 6min W) with only thin cirrus above. The dropsonde recorded 4°C at the surface verifying the brightband rain signal in the radar. At 12:01 UT the multilayer cloud decks and the As translucidus above merged into an undistinguishable cloud mix with rainfall. At 12:14 UT WP2 was reached and a left curve brought HALO towards the tiltback occlusion. The thick clouds prevailed but the rainfall became less while the brightband lowered.

10:24 UT Altostratus and Stratocumulus

10:51 UT broken Stratocumulus

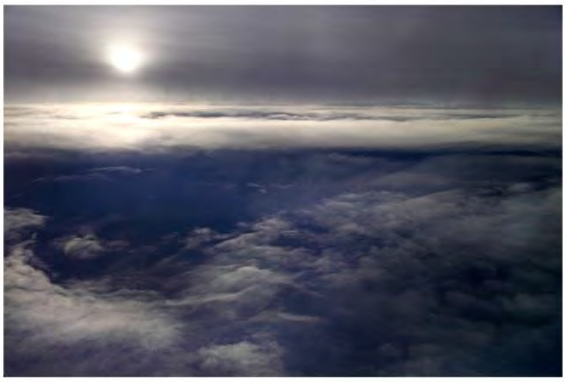

11:25 UT frontal Altostratus translucidus

Fig. RF13.9: Leg 1 inflight photo documentation of the cloud patterns showing the transfer leg 1 from KEF via WP1 to WP2. The upper panel shows Altostratus above HALO and Stratocumulus fields at sunrise (10:24 UT). Along track the Stratocumulus opened at 10:51 UT (lower left panel). The lower right panel documents the frontal passage with low clouds and frontal Altostratus translucidus above the plane at 11:25 UT towards WP2.

MATTRESS PATTERN (5:26 h duration) WP2 to WP8

LEG 2 (38 minutes) WP2 to WP3

The mattress pattern began at 12:14 UT with the left curve at WP2 heading towards south / southeast. The flight pattern started in thick clouds within the tiltback occlusion. In southward direction the precipitation got fewer and the melting layer lowered towards the surface. At 12:23 UT HALO exited the tiltback occlusion and went out of the clouds. The occlusion wall cloud spread across the flight track from west to east and subsequently the cloud tops lowered down to shallow Cumulus and Stratocumulus occurring in almost closed decks at 12:25 UT (Fig. RF13.10). The precipitation died out almost completely in these cloud types. At 12:29 UT dropsonde 2 was released at 53.5°N 38.9°W into light raining Sc decks with no gaps. From 12:39 UT on the Sc decks opened allowing views to the sea surface and braking waves (6078). At 12:49 UT cirrus bands visible in the satellite image came into sight but were not reached as WP3 led to a left return curve at 12:52 UT.

12:25 UT postfrontal shallow cloud decks

Fig. RF13.10: Leg 2 inflight photo documentation of the cloud patterns showing the distant wall cloud of the tiltback occlusion and the subsequent cold air cloudiness with stratiform shallow Sc/Cu clouds at 12:25 UT.

LEG3 (59 minutes) WP3 to WP4

After the turn into leg 3 cloud streets of broken cumulus (6079) were overflown at 12:35 UT and turbulences occurred caused by 112 kn side winds from the left. Dropsonde 3 was released at 51°N, 37°W in turbulent air over the cloud streets (6080). The left panel of Fig. RF13.11 illustrates the cloud streets at 12:56 UT. At 13:10 UT the cloud decks closed into stratiform Sc and Cu. Because leg 3 was flown in close proximity to the frontal system the tiltback occlusion was already reached again at 13:14 UT and HALO came into dense clouds with light rain below. At 13:23 UT multilayer clouds dominated (6084) partially allowing view onto the sea surface (Fig. RF13.11, right panel). By 13:30 UT HALO went into the frontal clouds again with no visibility while rain showed up in the radar data. Dropsonde 4 was released at 13:36 UT and 55.6°N within multilayer clouds (6085) with partial gaps allowing separating the cloud decks. At 13:50 UT the high frontal multilayer clouds (6087) were located to the left of the flying direction (northwest) while to the right (southeast) the cold air convection became visible (6086). HALO left the clouds and was from now on flying above all clouds. At 13:52 UT WP 4 was reached followed by a right curve into leg 4 towards WP5.

12:56 UT cloud streets

13:22 UT multilayer clouds

Fig. RF13.11: Leg 3 inflight photo documentation of the cloud patterns showing the cloud streets at 12:56 UT (left panel) and the frequently recurring multilayer clouds of the frontal system (13:22 UT) in the right panel.

LEG4 (45 minutes) WP4 to WP5
At 14:03 UT leg 4 entered the systems backside cold air starting with few Sc fields and Cu that contained no precipitation with large cloud-free areas. Partial high clouds of the last leg were still visible to right (west). The convection grew into 4 km cloud tops with intense rain and scattered iced cloud top without anvils at 14:12 UT (6089, left panel of Fig. RF13.12). Dropsonde 5 was released at 14:22 UT on 54°N (Fig. RF13.13, panel 15 UT) at the boundary to the tiltback occlusion cloud wall (6090, right panel of Fig. RF13.12). This narrow but high frontal cloud band is the very tail of the tiltback occlusion ending in a spiral cloud pattern. At 14:22 UT HALO crossed this cloud band within the clouds. The passage took only two minutes. At 14:33 UT closed low level clouds decks occurred and WP5 was reached at 14:48 UT with 110 kn winds at FL270. A left curve was flown into leg 5.

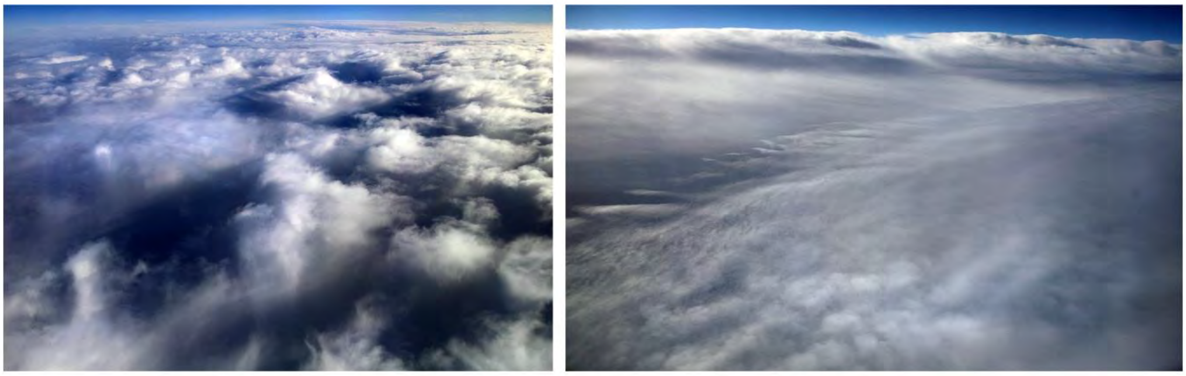

14:15 UT intense convection | 14:21 UT tiltback occlusion wall cloud

Fig. RF13.12: Leg 4 inflight photo documentation of the cloud patterns showing the intense convection at 14:15 UT up to 4 km altitude and intensive rain (left panel) and the approach of the impressive cloud wall of the tiltback occlusion tail at 14:21 UT (right panel).

LEG5 (61 minutes) WP5 to WP6
Dropsonde 6 was released right after the WP5 turn at 14:50 UT over broken Cu decks giving view on extreme wave action at the sea surface (6092). At 14:58 UT the shallow Cu decks almost closed completely. At 15:06 UT HALO reached the spiral shaped cloud fields of the tiltback occlusion core (6093 and 6094, Fig. RF13.13, top left panel) and was partly flying within clouds for a short time period. The CloudSat overpass at 15:10 could not be collocated with HALO due to the long duration of the flight and the flight pattern chosen. This may turn out being an advantage in this case as it may document the cloud development between the HALO and CloudSat overpass. CloudSat passed the scene to the west of HALO in the direction of WP5 to WP4 and crossed the tiltback occlusion that HALO crossed over at 14:21 UT (Fig RF13.12, right panel). The temporal mismatch is 49 minutes and may well be used for cloud development investigation. At 15:15 UT dense cumulus occurred that turned into multilayer clouds of Sc, Cu and As at 15:15 UT (6095, Fig. RF13.13, top right panel). Dropsonde 7 was released at 15:35 UT over a fairly cloud-free area with scattered Cu at 56°N (6096 and 6097, Fig. RF13.13, lower left panel). At 15:44 UT partly higher convection with rain showers occurred out of scattered towering Cu with cloud tops up to 5 km altitude (6098). At 15:51 UT the photo 6099 in Fig. RF13.13, lower right panel, documents this convection at WP6 including scattered Cb's. The main frontal system was visible at the horizon from the cockpit view but not reached. At WP6 a right curve brought HALO towards leg 6 with a southeasterly flight direction.

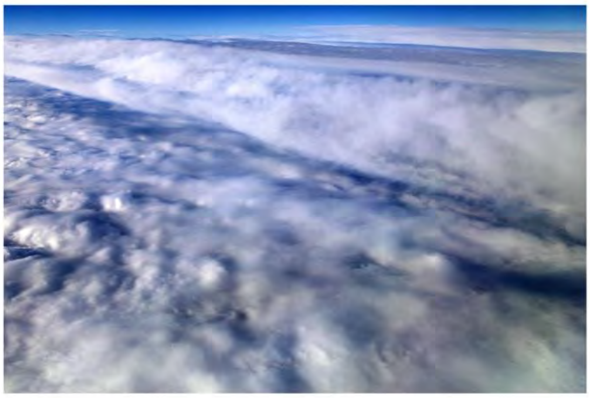

15:06 UT passage of a thick cloud band

15:20 UT multilayer clouds of Sc, Cu and As

15:34 UT partly cloud-free areas with embedded Cu

15:51 UT partly enhanced convection up to 5 km altitude

Fig. RF13.13: Leg 5 inflight photo documentation of the cloud patterns showing the passage of the spiral shaped tiltback occlusion core at 15:06 UT (top left panel), the multilayer clouds at 15:20 UT (top right panel), the partly cloud-free area at 15:34 UT (lower left panel) and the enhanced cold air convection with rain showers in front of the main frontal system at 15:51 UT (lower right panel).

LEG6 (47 minutes) WP6 to WP7

Along leg 6, thin cirrus was crossed at 16:03 UT followed by the passage of a high cloud band with closed cloud decks below at 16:05 UT. At 16:12 UT the cloud field was left and an almost cloud-free band with shallow scattered Cu was crossed (6100, Fig. RF13.14, left panel). The scenery changed at 16:20 UT with rather homogeneous closed cloud decks with numerous convective plumes containing rain showers and cloud tops of about 4 km altitude (6117, Fig. RF13.14, right panel). At 16:25 UT dropsonde 8 probed these clouds at 54°N. At 16:49 UT Sc and Cu prevailed with larger cloud-free areas. A closed cloud band ahead in flying direction was not reached because WP7 was reached at 16:50 UT and the next left turn brought HALO to the last mattress leg 7 towards WP8.

16:13UT cloud-free band with shallow Sc | 16:38 UT uniform cloud deck obscures frequent showers

Fig. RF13.14: Leg 6 inflight photo documentation of the cloud patterns showing the almost cloud-free conditions with embedded shallow Sc at 16:13 UT (left panel) and the closed cloud deck of numerous cumuli up to 4 km altitude containing rain showers at 16:38 UT (right panel).

LEG7 (43 minutes) WP7 to WP8

The last mattress leg may turn out to reveal the most interesting cloud and precipitation pattern and type of this rather weak convective cold air system. The leg began with shallow Sc and Cu fields with partial views to the sea surface. Dropsonde 9 was released into these clouds at 52°N at 16:53 UT. At 17:01 UT the cloud formation changed into a stratiform appearing type of streak-like almost completely closed Cu with straight lines and partly right angle edges resembling the appearance of a city from above (6119, Fig. RF13.15, left panel). Along track the precipitation out of these cumuli increased in number and intensity until the pattern changed at 17:16 UT into ever more uniform looking cloud tops that contained ever more intense showers. The individual shower cells could not any longer be identified from the planes window view. At 17:21 UT the radar showed a Cb cloud below the aircraft with 5 km cloud top and a perfectly shaped iced anvil. The window view however did not reveal any kind of information about the situation below as only a uniform cloud top was visible that did not appear to contain iced clouds (6120, Fig. RF13.15, right panel). Therefore, dropsonde 10 was quickly released directly into the Cb below at 55°N at 17:21 UT. Numerous Cb's and towering Cu with intense precipitation were captured in the instrumentation data of all instruments. This area contained the most intense convective precipitation of the entire flight pattern although none of these clouds could be seen from the aircraft window indication that a masking second cloud layer must have been above at even higher altitudes. Note, however, that HALO was at FL270 of approx. 8 km altitude. This significantly reduces the possibilities of cloud types that may have masked the Cb's. Consequently, the visible and infrared satellite images may have been misinterpreted the clouds as stratiform type (Fig. RF13.17, 17 and 18 UT panel). Only the active and passive microwave aircraft and satellite data show the intense convective nature of these clouds in the scattering channels. The SSMIS 91 GHz channel clearly indicates intense convective activity (RF13.21, lower right panel) and the HALO bellypod instrumentation documents these showers in Fig. RF13.19 and Fig. RF13.20. At 17:38 UT WP8 was reached ending the mattress pattern over the postfrontal subsidence area with large cloud-free areas.

17:02 UT streak-like stratiform cloud deck

17:25 UT above 5 km altitude Cb's that are obscured by high stratiform cloud layer decks, most likely As and Ac

Fig. RF13.15: Leg 7 inflight photo documentation of the cloud patterns showing the "city from above "streak-like cloud pattern at 17:02 UT (left panel) and the intense convection containing numerous Cb's that were not visible from the aircraft window at 17:25 UT. A secondary more stratiform cloud layer was masking the visibility. Hence, also the visible and infrared satellite images may have been misinterpreted the clouds as stratiform type. Only the active and passive microwave aircraft and satellite data show the intense convective nature of these clouds in the scattering channels.

TRANSFER LEG8 (65 minutes) WP8 to KEF

At 17:40 UT the dawn set in allowing for a perfect view of the Earth's shade at 8 km altitude (6124 to 6127, Fig. RF13.16, left panel). The clouds turned into a closed cloud deck at 17:45 UT with intense showers. Dropsonde 11 was released at the bounding box exit point at 59°N at 17:56 UT over the closed cloud deck and a close by convection line (6132 and 6135, Fig. RF13.16, right panel). The approaching main systems cold front already came into view. At 17:58 UT HALO went into the cold front clouds and the lidar and radar were switched off at 18:00 UT. The cold front was exited at 18:13 UT at the FIR boundary. Consequently, HALO established radar contact with ATC and started descend into KEF at 18:27 UT. Runway 02 ILS was fully established at 18:36 UT and the cleared to land was received at 18:42 UT with touch down at 18:45 UT. After taxiing to the parking position the engines were shut down at 18:50 UT.

17:40 UT Earth shade rising, intense showers

17:55 UT crossing convection line with the cold front ahead

Fig. RF13.16: Leg 8 inflight photo documentation of the cloud patterns showing the intense Earth's shade from 8 km altitude at 17:40 UT (left panel) and the passage of a convective line with the cold front ahead indicated by the dark distant cloud band at 17:55 UT (right panel).

In total 8 legs were flown with leg 1 and 8 being the transfers from and to KEF, and leg 2 to leg 7 containing the mattress pattern. The individual legs were of 1:59 h (1), 38 minutes (2), 59 minutes (3), 45 minutes (4), 61 minutes (5), 47 minutes (6), 43 minutes (7), and 65 minutes (8) duration. In total HALO was flying 8:30 h, the mattress duration was 5:26 h and 11 dropsondes were released at FL270. Six SSMIS collocation overpasses occurred during the flight pattern from 10:15 UT to 18:45 UT by DMSP-F16 (16:28 UT, 18:08 UT), DMSP-F17 (10:56 UT, 17:28 UT), and DMSP-F18 (11:40 UT, 13:20 UT). The CloudSat overpass could not be collocated at has a temporal mismatch of 49 minutes and one leg spatial difference.

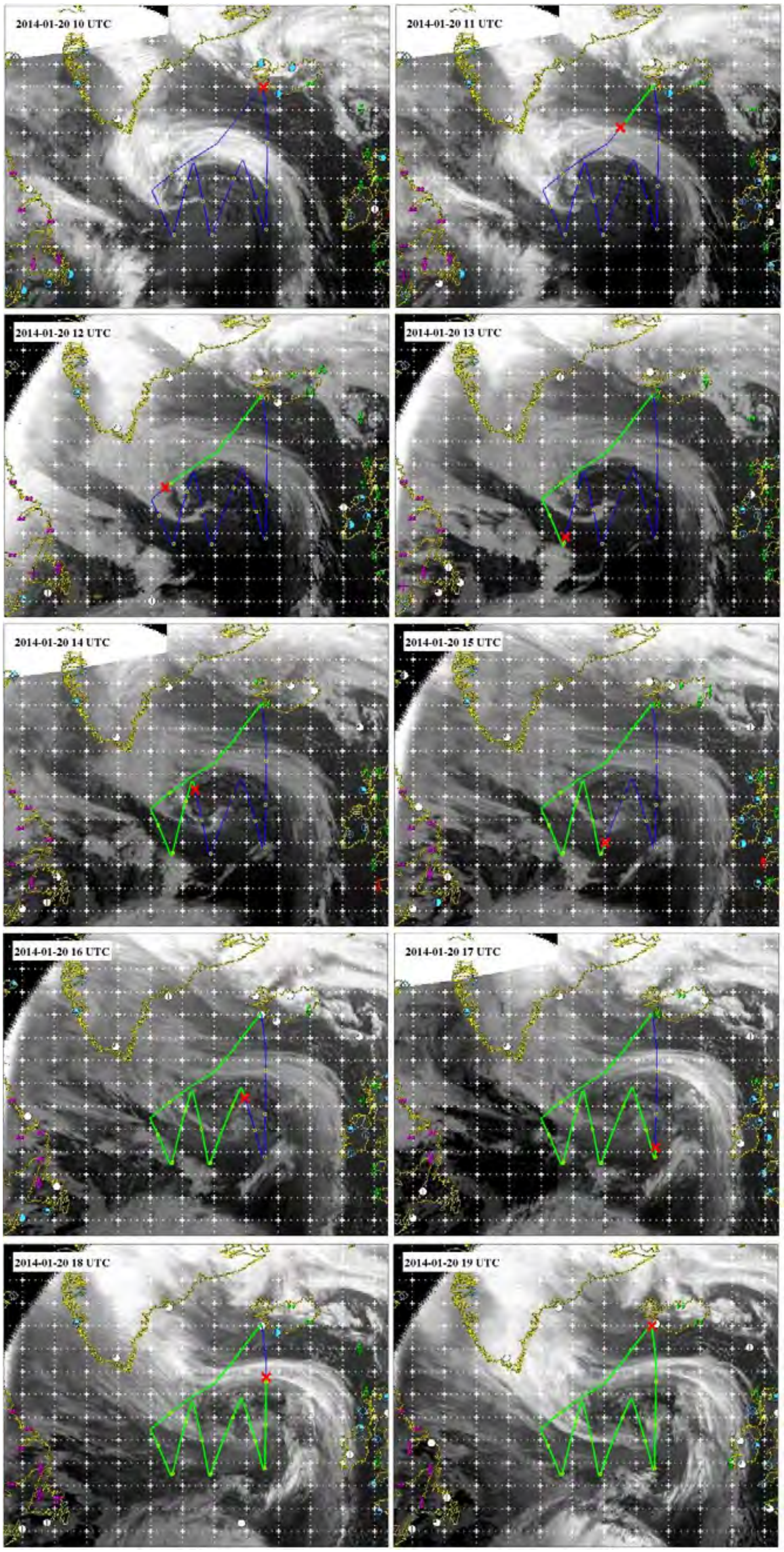

Fig. RF13.17: Hourly flight track composite in blue and infrared satellite data with elapsed flight time in green, current aircraft position as red cross and dropsondes positions as yellow circles. This composite is to be used as a reference for the flight protocol below.

Flight Protocol
All times in UT. Four digit numbers refer to Canon photo numbers in raw file format.

No liquid nitrogen
Calibration as of 09 Jan used (Emiliano)
09:15 roll out hangar
09:20 APU running
10:11 taxi
10:15 take off RWY02
10:17 into low level clouds
10:18 out of clouds, As above and Sc decks below, sunrise, 6058
10:25 FL240
10:28 FL270 above all clouds, broken Sc
10:46 broken Sc
10:50 photogenic Sc 6062- 6074
10:51 first cirrus outflow of front above HALO
10:51 FIR Boundary
10:52 radar and lidar on
10:58 cloud-free stripe, patches of dissolving Sc
10:59 flying into the cirrus outflow of the cold front, HALO in thin clouds
11:03 no visibility, in cirrus
11:15 WP1 Entry point, almost at thick cloud top with cirrus above
11:25 cold front multilayer clouds, cirrus above HALO, translucidus, As below, 6076
11:29 HALO above clouds, very thin cirrus above
11:34 flying along As cloud top, cirrus above, uniform frontal rain below
11:38 flying into cloud, appears to be convective, like a bubble protruding out of As
11:40 rain intensifies on radar, turbulence, flying in cloud, 57N 35W, convective cloud patches in satellite
11:45 in thin clouds, cirrus above, lower level clouds
11:53 DS1 in convective occluded area 56°, 2 min N 37°, 6 min W multilayer clouds, only thin cirrus above plane, 4°C at surface
12:01 in clouds, translucidus, multilayer clouds are growing together, rain below
12:14 WP2 left turn in tiltback occlusion, flying in thick cloud, fewer precipitation, melting layer low
12:23 above all clouds, exiting tiltback occlusion, wall of cloud, uniform Sc like low level clouds
12:24 radar sees two layers of low level clouds, almost no precipitation, 6077
12:29 DS2 53.5°N 38.9°W into light rain Sc decks, no gaps
12:35 turbulence, strong wind area, homogeneous closed Sc decks
12:39 Sc decks open, sea surface shows braking waves, 6078
12:49 approaching cirrus bands of high cloud field in satellite image, not reached
12:52 WP3
12:53 cloud streets of broken cumulus, 6079 turbulence, 112 kn winds from left
12:53 DS3 51N 37W after turning at WP3 in turbulent air over cloud streets, 6080
13:10 closed Sc/Cu decks
13:14 connecting to internet, not working
13:15 reaching tiltback occluded part again, in dense clouds, light rain
13:23 6084 multilayer clouds, sea surface visible
13:30 into clouds, no visibility
13:33 rain in radar

13:36 DS4 at 55.6N within multilayer cloud, 6085, partly gaps with view on cloud decks
13:50 to left high multilayer clouds 6087, to right convection starts 6086, flying above all clouds
13:52 WP4 right turn
14:03 few Sc fields und Cu, large areas cloud-free, no precipitation, high clouds of last leg visible to right
14:12 4 km cloud top convection with rain, iced top but no anvils, scattered
14:15 6089, convection grows, 4 km intense rain, icy tops,
14:22 DS5, 54N at boundary to wallcloud 6090, wallcloud is the tail of the occlusion
14:24 Into clouds
14:26 above clouds
14:33 6091 after occlusion passage closed low level clouds
14:48 WP5, 110 kn wind
14:50 DS6 shortly after WP5, broken Cu decks, extreme waves at surface, 6092
14:58 shallow cu in almost closed cloud deck
15:06 6093+6094 passage of thick cloud bands, flying partly in clouds
15:10 CloudSat overflight, not collocated in time
15:15 above clouds, dense cumulus
15:19 multilayer cloud decks, Sc, Cu, As, 6095
15:19 internet satellite image received
15:35 DS7 6096+6097 cloud-free band in satellite image at 56N
15:44 partly higher convection with rain showers, cloud tops 5 km, 6098
15:51 WP6, occlusion not reached but visible at horizon, few Cbs, 6099
16:03 flying through thin cirrus
16:05 passing through a high cloud band, underneath closed cloud deck
16:12 out of cirrus, cloud-free band passage, shallow Sc fields 6100
16:20 cloud tops appear rather homogeneous and closed but contain cells of 4 km rain showers
16:25 DS8 54N over rather uniform cloud deck containing showers, 6117
16:49 Sc with Cu, larger open areas, cloud band ahead in flying direction, not reached
16:50 WP7 left turn
16:53 DS9 52N over shallow Sc and Cu with partly open ocean
17:01 stratiform cloud deck, streak-like, few cirrus as FL270, 6119, like "city blocks from above"
17:16 uniform looking cloud tops hide intense showers below, not seen from window
17:21 DS10 55N exactly over 5 km anvil Cb that is not seen from window, uniform cloud tops, 6120
17:36 postfrontal subsidence, large cloud-free areas
17:38 WP8 reached, continuing northward flight direction
17:40 6124-6127 Earth shade rising
17:45 closed cloud deck, uniform, with intense showers beneath
17:56 DS11 at Exit Point, 59N, closed cloud deck, convection line, 6132+6135, cold front in front of plane
17:58 into clouds, cold front passage, partly visibility, clouds above and below
18:00 lidar and radar off
18:13 cold front exit at exit point 61N
18:18 broken Sc
18:27 descend into KEF
18:36 established ILS RWY02
18:42 cleared to land RWY02

18:45 touch down
18:47 taxi
18:49 parking position
18:50 engines shut down

Dropsondes:

01 11:53 DS1 in convective occluded area 56°N 37°W multilayer clouds
02 12:29 DS2 53.5°N 38.9°W into light rain Sc decks, no gaps
03 12:53 DS3 51N 37W after turning at WP3 in turbulent air over cloud streets, 6080
04 13:36 DS4 at 55.6N within multilayer cloud, 6085, partly gaps with view on cloud decks
05 14:22 DS5, 54N at boundary to wallcloud 6090, wallcloud is the tail of the occlusion, at CloudSat position 49 minutes prior to overpass
06 14:50 DS6 at WP5 broken Cu decks, extreme waves at surface, 6092
07 15:35 DS7 6096+6097 cloud-free band in satellite image at 56N
08 16:25 DS8 54N over rather uniform cloud deck containing showers
09 16:53 DS9 52N over shallow Sc and Cu with partly open ocean
10 17:21 DS10 55N exactly over 5 km anvil Cb that is not seen from window, uniform cloud tops, 6120
11 17:56 DS11 at Exit Point, 59N, closed cloud deck, convection line, 6132+6135, cold front in front of plane

Preliminary HALO instrument data: All instruments onboard recorded data without significant gaps. Displayed below are selected preliminary results with the exception of MiniDOAS. This data will be analyzed after the campaign.

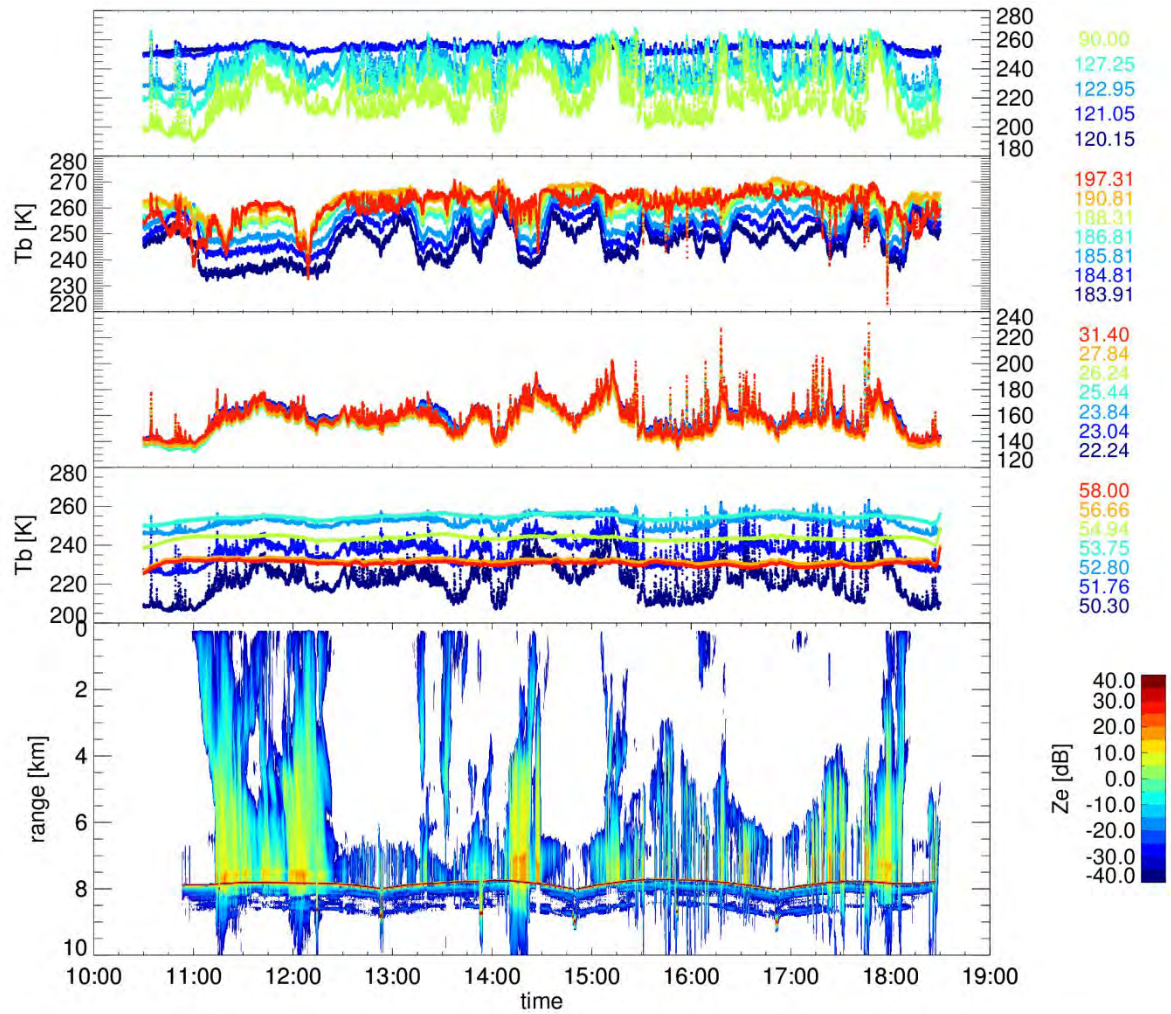

Fig. RF13.18: Time series (in UT) of the microwave radiometer brightness temperatures (top four panels) and radar reflectivity profiles (lower panel) for the entire flight RF4 for the scattering channels (first panel), the sounding channels (second panel), the emission channels (third panel) and the 50 GHz channels (fourth panel) and the range corrected radar reflectivity (lowest panel). The raw data radar reflectivity profiles still include surface signals as well as multiple scatter signals at range gates beyond the surface. Flights through clouds occurred repeatedly when crossing the tiltback occlusion and during the passage of the main cold front after take off and prior to landing.

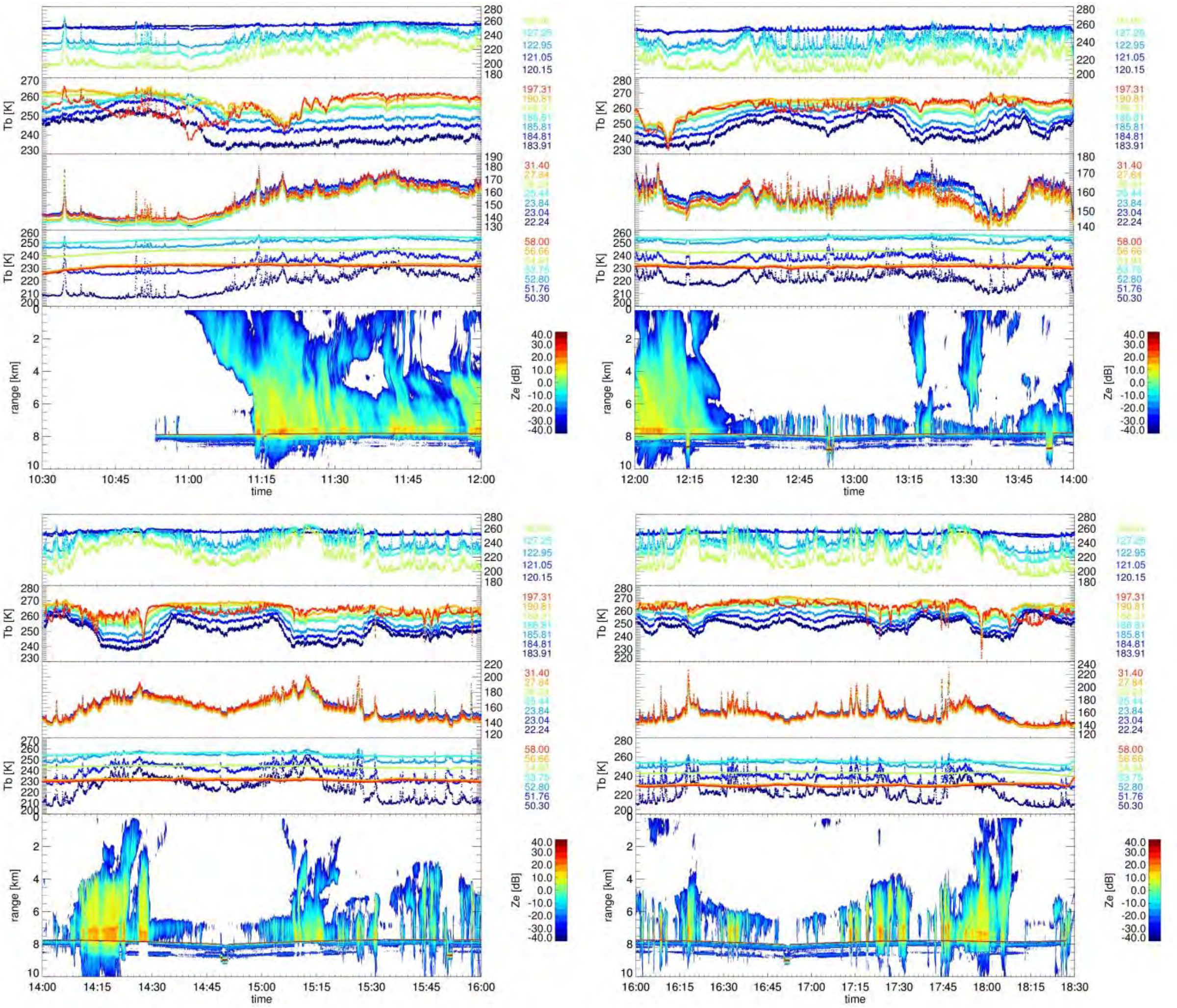

Fig. RF13.19: Time series as in RF13.14 but temporally higher resolved into 4 panels of approximately 2 hour interval length corresponding to legs 1 to 8. The flight pattern documents the main occlusion passage along leg 1 (top panels) and the postfrontal numerous shallow convective cells. Repeatedly, the tiltback occlusion and main cold front is crossed (high clouds) intersected by convective cold air cells that increase in cloud height and precipitation content with time (lower panels). Note, the Cumulonimbus rainfall between 17:20 and 17:30 UT. However, the Cb masking clouds, seen from the aircrafts window, are not obviously seen in the radar signal in this resolution. The postfrontal subsidence region was overflown followed by the cold front at 17:45 UT and the descend into KEF.

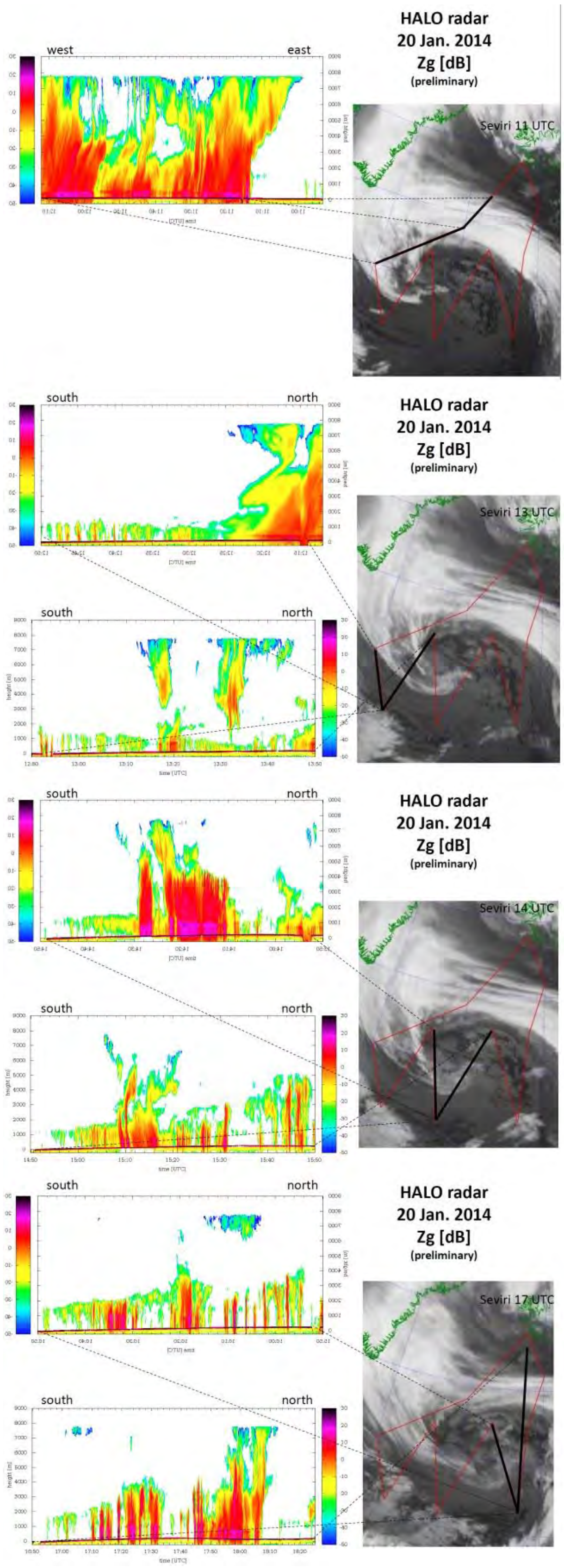

Fig. RF13.20: The complete RF4 MIRA-36 radar times series. Zg is the range gate corrected reflectivity with eliminated signals below the surface and the vertical axis is flipped to the one in Fig. RF12.18 and RF12.19. The time series is described in Fig. RF13.19. The higher resolved Cb passage (lowermost panel) indicates a fairly homogeneous cloud top without gaps that may explain the masking effect seen from the aircrafts window.

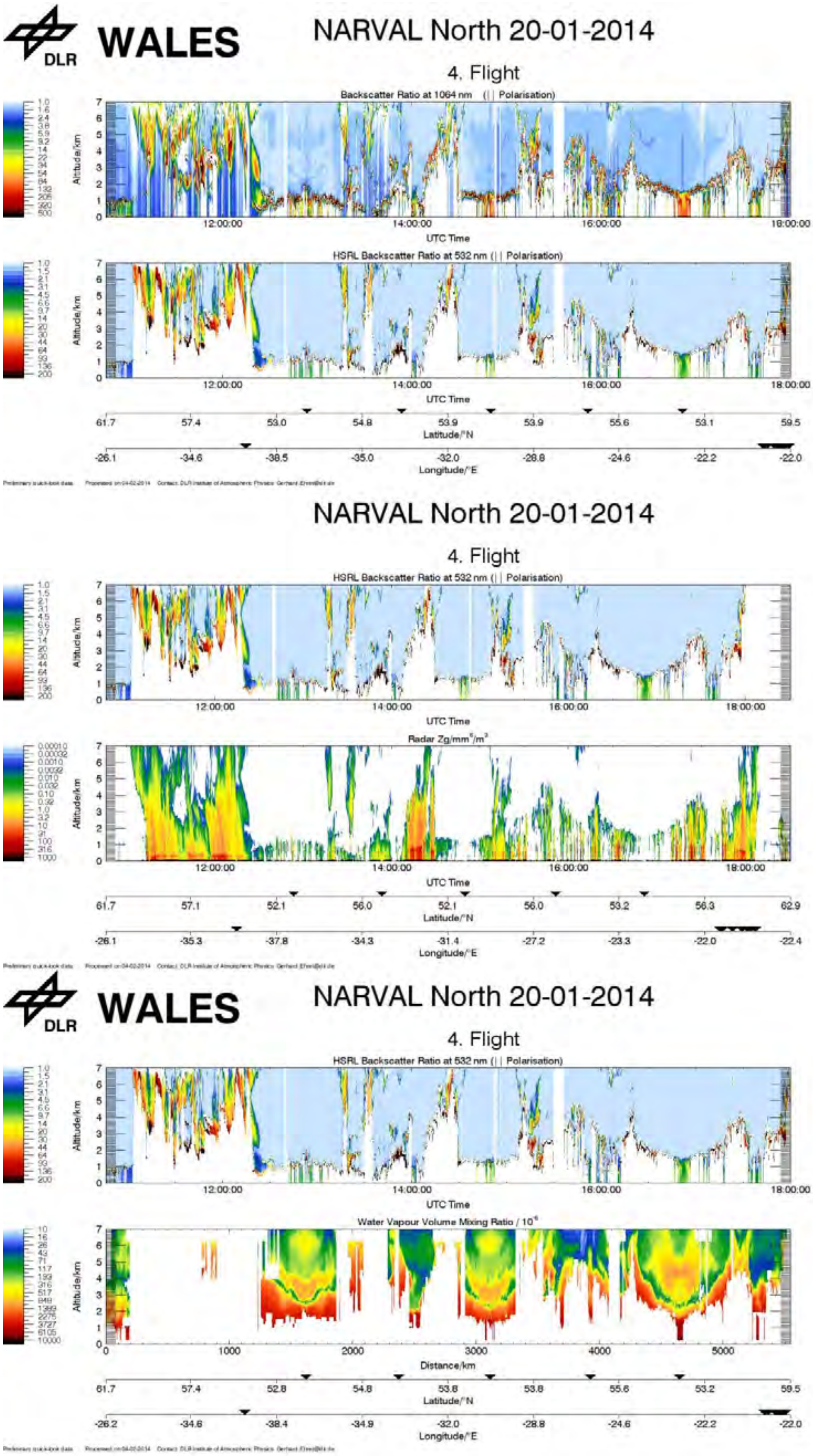

Fig. RF13.21: The top panel shows the WALES lidar backscatter ratio time series at 1064 and 532 nm compared to the MIRA36 radar data (middle panel) and the lidar water vapor mixing ration (bottom panel).

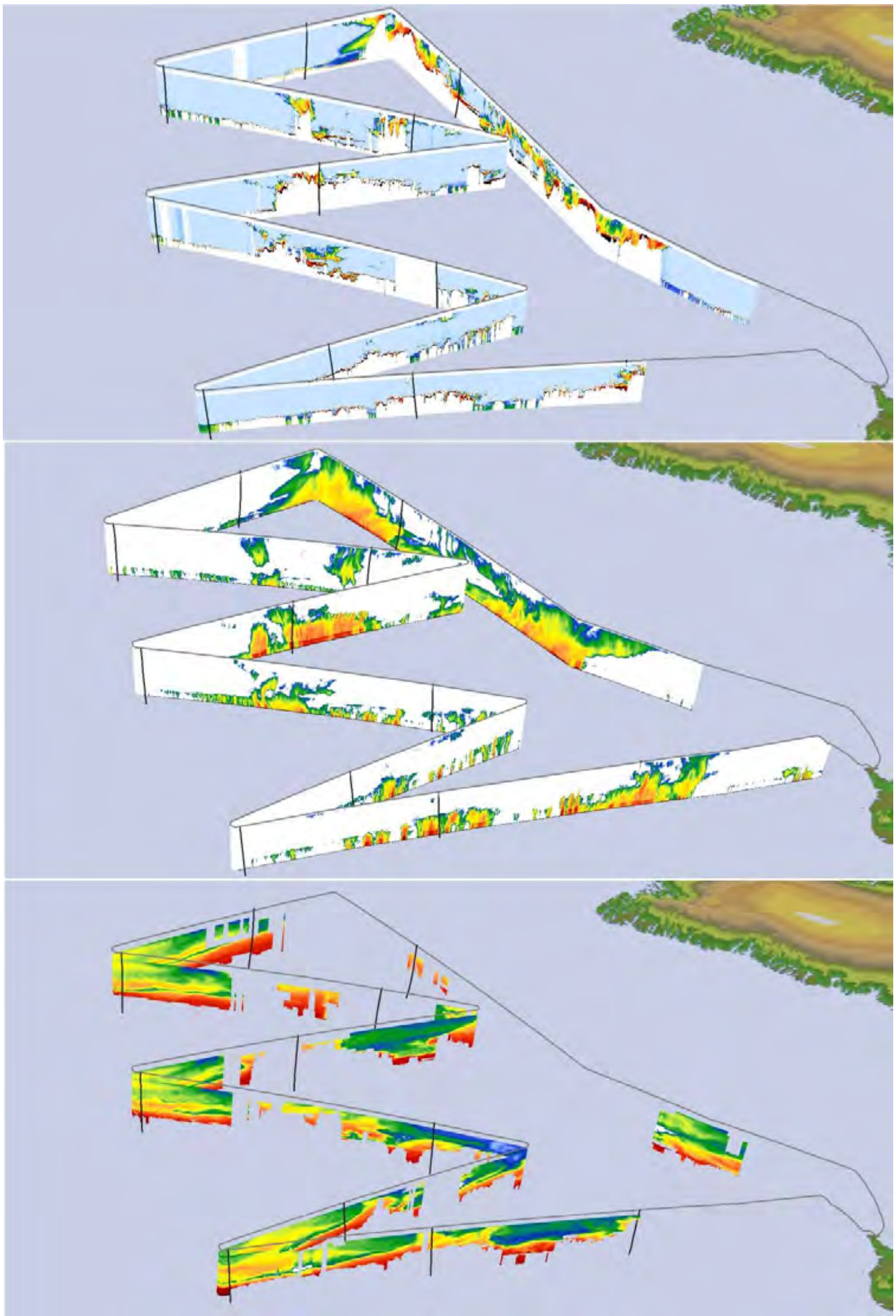

Fig. RF13.22: 3-D visualization of the lidar data for the backscatter ratio (top), the MIRA36 radar data (middle), and the water vapor mixing ratio (bottom) and along the entire flight track. Blue backscatter colors indicate clear air while white and black relate to strong extinction due to optically thick clouds. The water vapor mixing ratio exhibits dry air in green and the intrusions in yellow showing strong humidity gradients. For better visualization the atmosphere is stretched by a factor of 70 to focus on the clouds. The grey line is the plane position and data is recorded about 600 m below the aircraft down to the ground if atmospheric conditions allow. Fig. RF12.21 discusses the meteorology being valid for this viewgraph also. The 3-D flight pattern illustrates well the vertical structure of the entire low pressure system with its different cold air regimes.

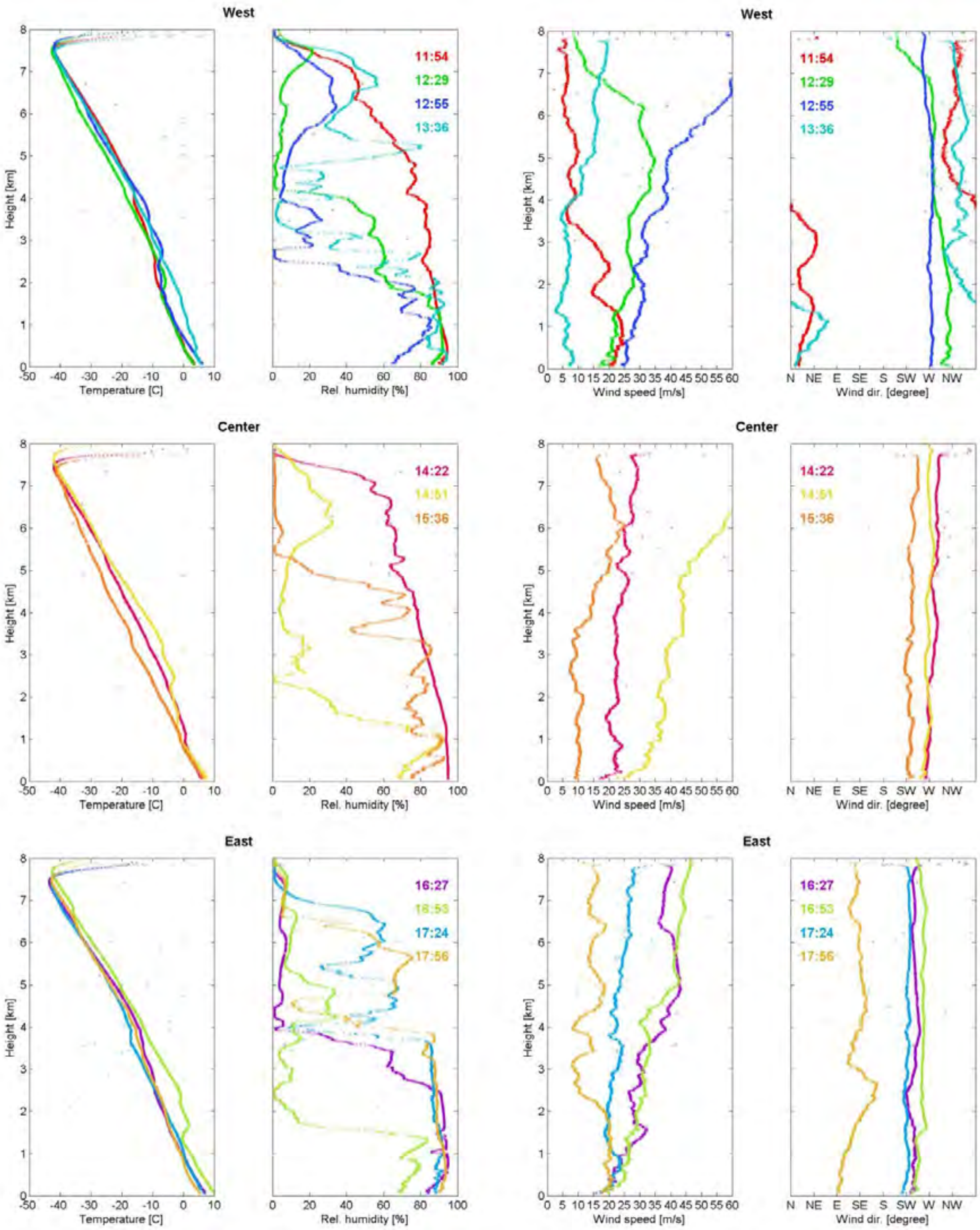

Fig. RF13.23: All 11 dropsonde profiles in chronological order released at 11:54 UT, 12:29 UT, 12:55 UT, 13:36 UT (upper panel), 14:22 UT, 14:51 UT, 15:36 UT(middle panel) and 16:27 UT, 16:53 UT, 17:24 UT, 17:56 UT (lower panel), plotted for height versus temperature (first column), humidity (second column), wind speed (third column) and wind direction (fourth column). The dropsonde at 17:24 UT went into the cloud-masked Cb. Surface temperatures remain well above the freezing levels at all times indication rain at the surface as suggested by the brightband in the radar data.

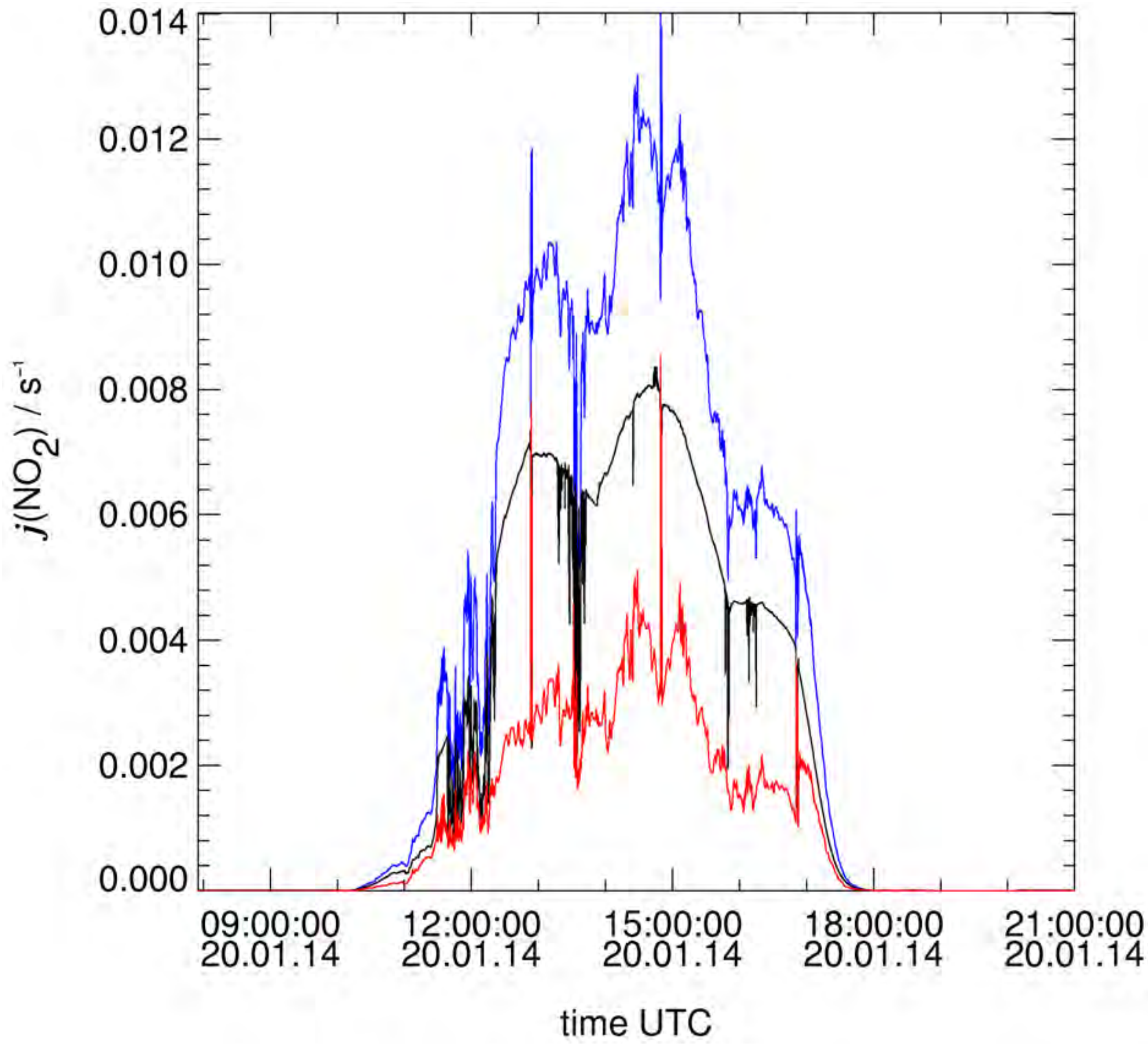

Fig RF13.24: HALO-SR photolysis frequency $j(NO_2)$ from lower hemisphere (red), upper hemisphere (black) and combined (blue) measurements. Downwelling component is partly influenced by clouds. Structures of measurement curves reveal latitudinal changes in flight track.

The SSMIS and CloudSat perspective:

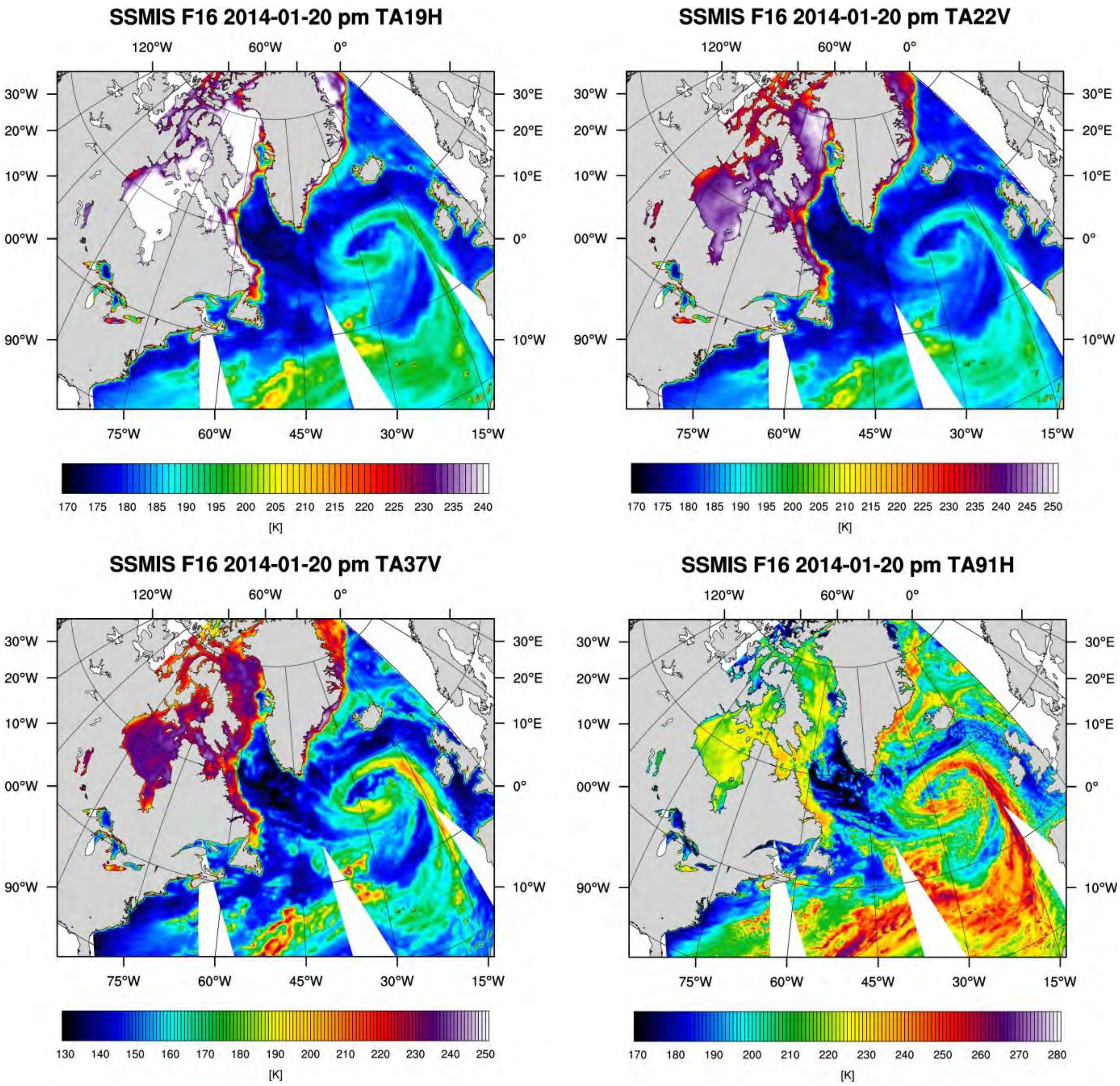

Fig. RF13.25: Preliminary HOAPS 4 fundamental climate data record (FCDR) antenna temperatures (TA) for the ascending DMSP-F16 SSMIS target area overpass at 16:28 UT. Shown are the environmental data record (EDR) emission channels 19 GHz H (sensitive to rain; top left), the water vapor channel 22 GHz V (top right), the 37 GHz V (lower left), and the 91 GHz H scattering channel (sensitive to ice; lower right) indicated for horizontal (H) and vertical (V) polarization. The dry cyclone core is well documented by the low (blue) antenna temperatures in the different channels. The tiltback occlusion is well connected to the main frontal system in the liquid water channels but show a rupture in the ice channel (lower right panel). The postfrontal cloudlayer-masked Cb's are easily identified in the 91 GHz ice column channel (lower right panel) as individual antenna temperature peaks up to values of 250 K. Six SSMIS collocation overpasses occurred during the flight pattern from 10:15 UT to 18:45 UT by DMSP-F16 (16:28 UT, 18:08 UT), DMSP-F17 (10:56 UT, 17:28 UT), and DMSP-F18 (11:40 UT, 13:20 UT).

20140120:

15:06:00 39.1863 26.6020 -999.00
15:08:00 46.3438 29.0380 345.12
15:10:00 53.4506 32.0552 343.52

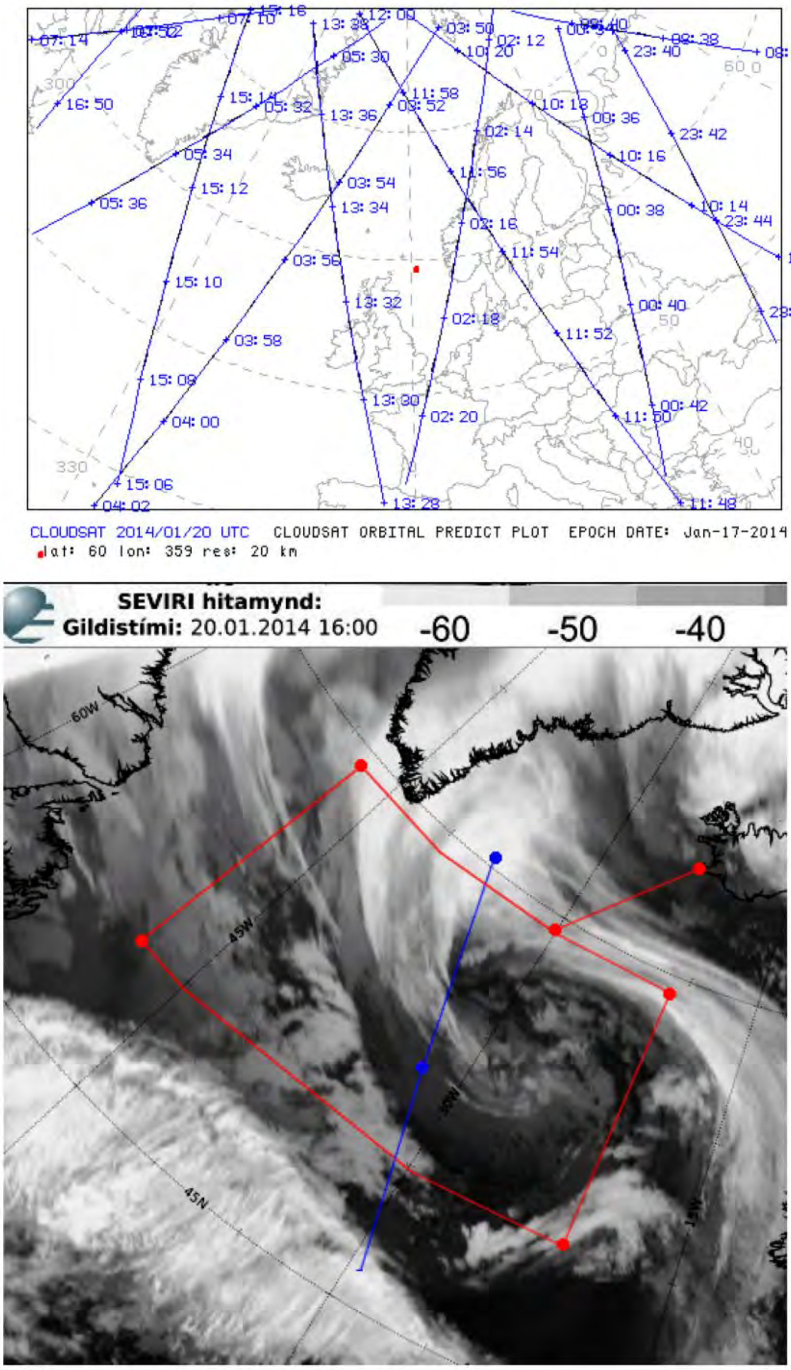

Fig. RF13.26: The CloudSat overpass at 15:10 UT could not be collocated with HALO due to the long duration of the flight and the flight pattern chosen. This may turn out being an advantage in this case as it may document the cloud development between the HALO and CloudSat overpass. CloudSat passed the scene to the west of HALO in the direction of WP5 to WP4 and crossed the tiltback occlusion that HALO crossed over at 14:21 UT (Fig RF13.12 right panel). The temporal mismatch is 49 minutes and may well be used for cloud development investigation.

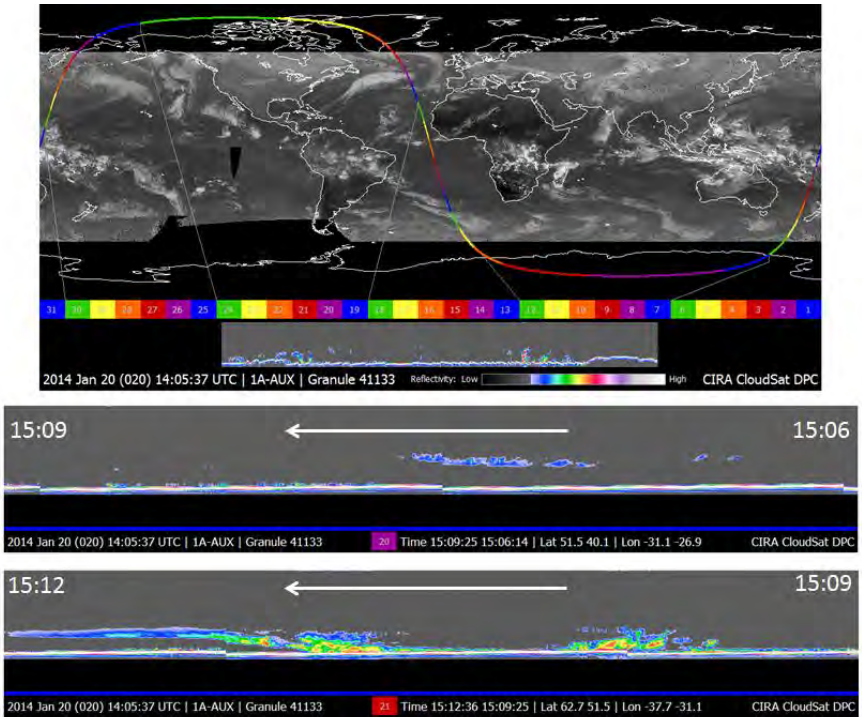

Fig. RF13.27: CloudSat quicklook track granule 41133 crossing over the convection and occlusions bands between 15:06 UT (violet track) and 15:12 UT (red track) with the cyclone center overpass at 15:10 UT. The northwestward flight direction is indicated by the white arrow. CloudSat passed from southeast to northwest first over the tiltback occlusion followed by shallow convection and the large-scale cold front and main occlusion with a broad cirrus outflow to the northwest.

NARVAL North Research Flight 14 (RF14), Flight Report

- 21 January 2014 -

STEPHAN BAKAN

Crew: Roland Welser (Pilot), Stefan Grillenbeck (Pilot), Alexander Wolf (Flight engineer), Heike Konow (HAMP radiometer, dropsondes), Martin Hagen (HAMP radar), Andreas Fix (WALES), Marcel Reichert (MiniDOAS + HaloSR), Stephan Bakan (Mission scientist)

Objective: The scientific objective of the fifth NARVAL North research flight was to sample the convective core of a considerably aged cyclone over the North Atlantic. This cold core had already been studied the day before during Research Flight 4. Therefore RF5 could help specifying the temporal development of convection in cold cores. 7 dropsondes were released and a successful CloudSat underflight has been accomplished.

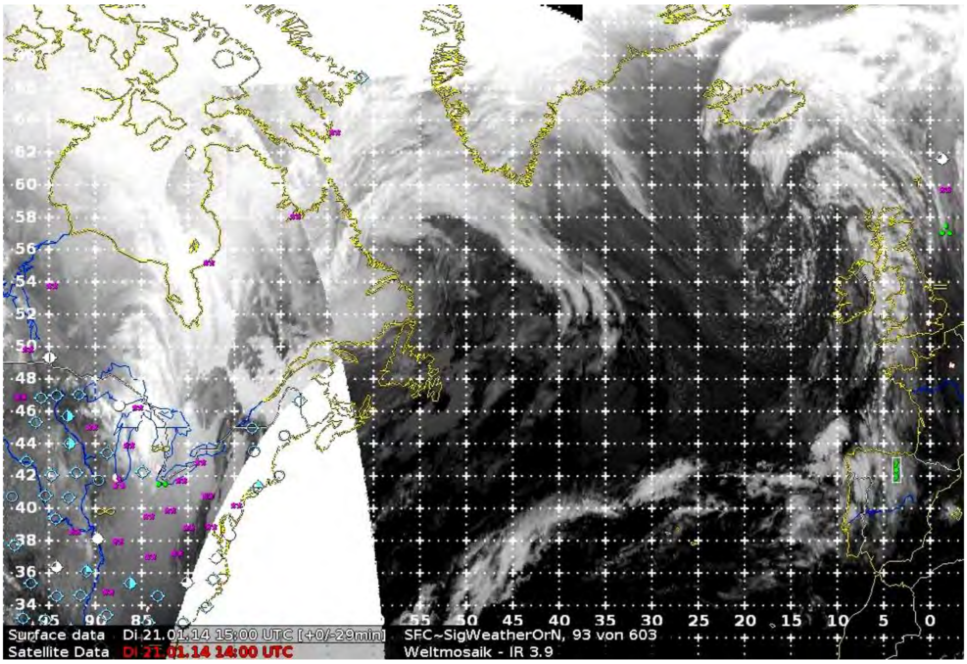

Fig. RF14.1: Infrared satellite mosaic of the North Atlantic from 21 Jan 2014, 15 UT showing the sampled re-intensified cold air convection between Southwest Iceland and Ireland.

Overview: In a strong baroclinic zone between extremely cold air over the Canadian arctic and warm air over the North Atlantic several disturbances developed in the days before RF5 along the North American East coast. While they moved eastward mostly south of the NARVAL target region, a compact cyclone with a cold core appeared as far north as New Foundland on early Sunday 19 Jan. On its way into the NARVAL target area the core pressure of this cyclone decreased rapidly and reached a minimum of about 965hPa during Monday 20 Jan. The cold air in this cyclone core developed intensive surface driven convection which was observed in detail during RF13. This cold core and its surrounding occlusion front remained much localized with slowly increasing core pressure. During Tuesday 21 Jan the pattern moved into the cold trough region over the eastern North Atlantic, which has characterized large scale circulation for quite some time before. RF5 was intended to document this aged cold air convective core which was now located to the south of Iceland and the NW of Ireland.

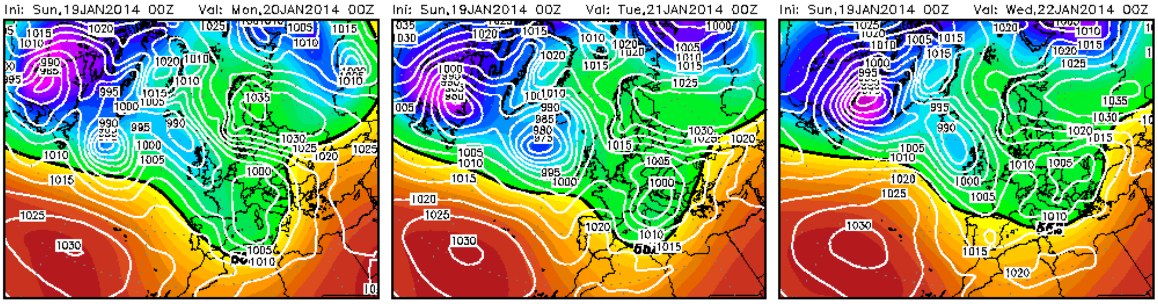

Fig. RF14.2: ECMWF 24, 48 and 72 h forecasts of surface pressure (white isolines) and 500 hPa geopotential height (color, 552 dekameter isoline in black) starting at 00 UTC on 19 Jan 2014.

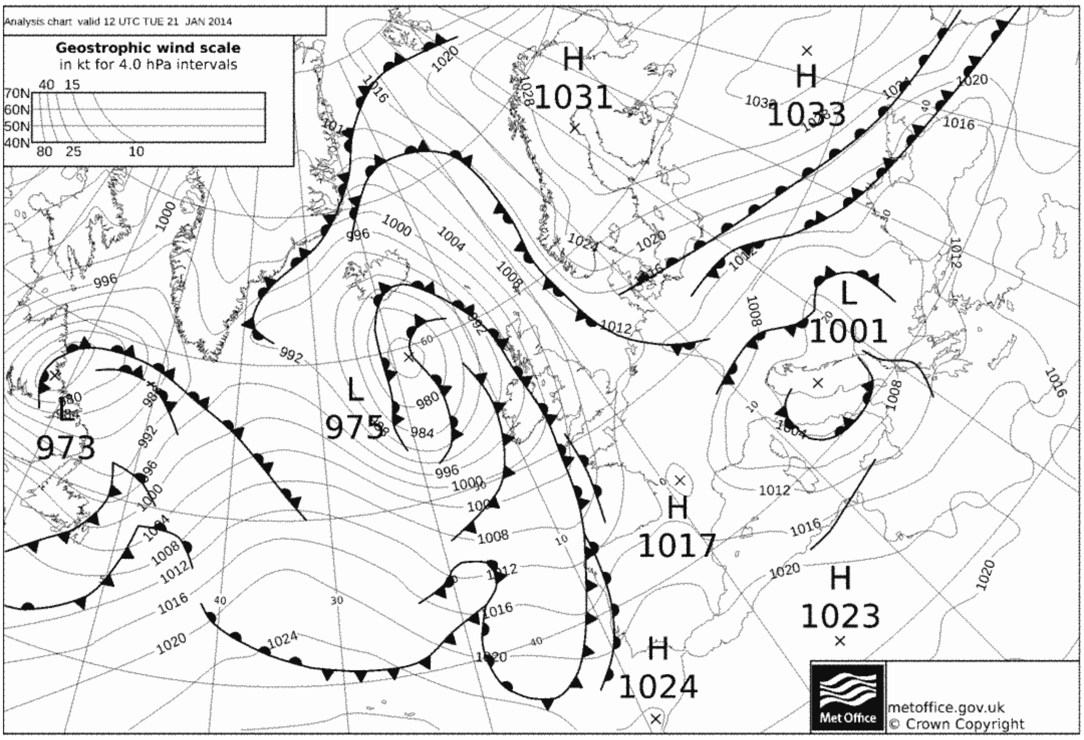

Fig. RF14.3: UK Met. Office analysis chart for 12 UTC on Tue 21 Jan 2014 with the target area of RF5 around 55N/20W.

Flight Planning: As can be seen in the right panel of Figs. RF14.2 and RF14.4, the three day forecast on Sun 19 Jan 2014 did neither prove nor exclude the Tuesday 21 Jan situation as a promising flight opportunity. Therefore it was decided during the morning briefing to secure at least the chance of a flight to study the late development of convection in an aged cold cyclone core. Due to a firm flight decision for the next day, the pilots would not be available for detailed flight planning during Monday. Therefore it was decided to draw up a preliminary flight plan on the basis of available information and turn it in to ATC for approval. The finally granted flight plan is given in Fig. RF14.5. The bounding box is limited to Shannon air space (E of 30W) and avoiding Ireland air space. The leg between waypoints SAT1 and SAT2 is chosen for CloudSat underflight which was calculated to happen at 14:15

UTC. The fit of this plan with the 24 hour ECMWF precipitation forecast is shown in Fig. RF14.6 (left panel) and with the preflight 08 UTC MSG satellite image (right panel). A careful review of this planning decision in the evening of Mon 20 Jan resulted in a GO for the flight, as the chance for sampling an aged but fairly well preserved cold convective cyclone core became clearer.

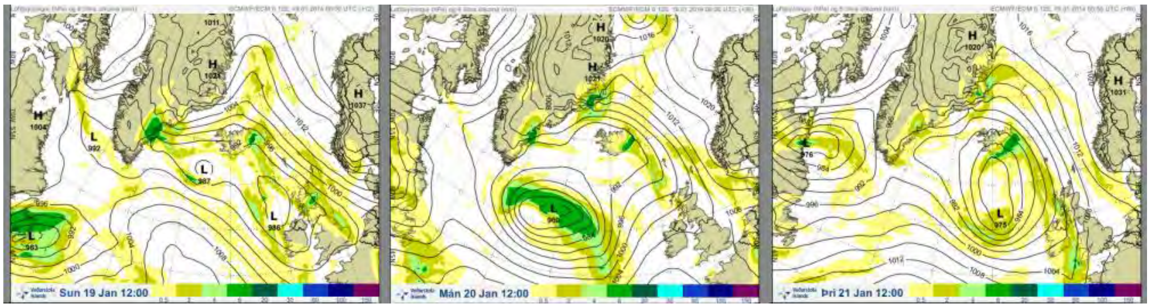

Fig. RF14.4: ECMWF 12, 36 and 60 h forecasts of surface pressure isobars and precipitation amount accumulated over 6 hours (color) starting at 00 UTC on 19 Jan 2014.

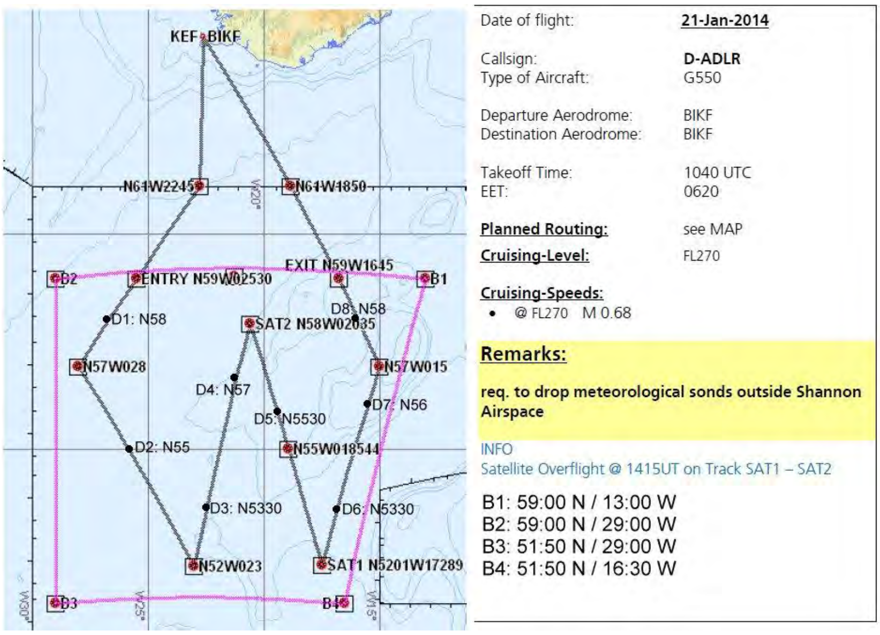

Fig. RF14.5: Flight plan for RF5 on 21 Jan 2014, including bounding box (red), flight path (black), waypoints (red dots in back square) and provisionally planned dropsonde release locations (black dots).

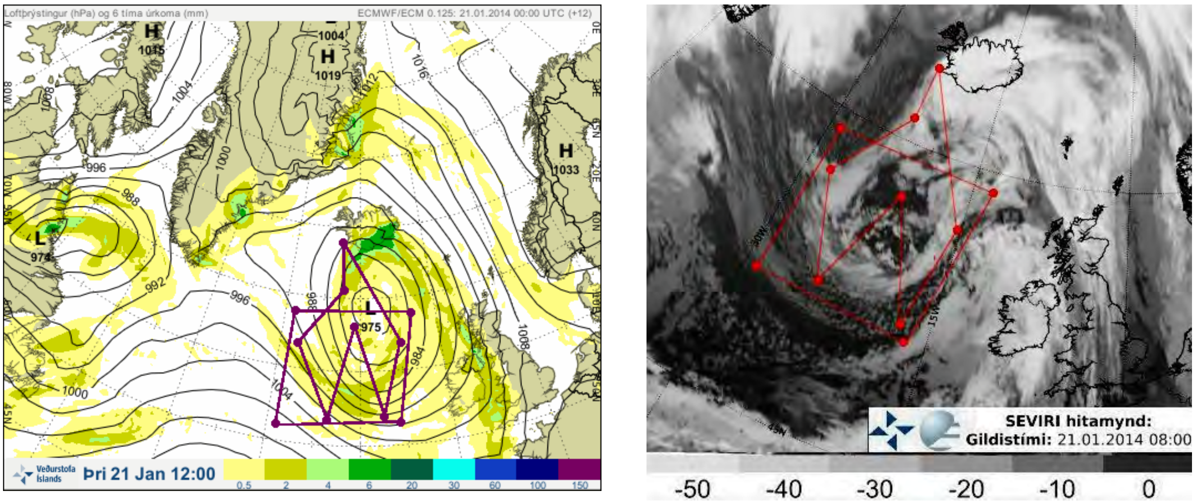

Fig. RF14.6: Bounding box and planned flight pattern in relation to the 24 hour ECMWF precipitation forecast (left panel) and with the preflight 08 UTC MSG satellite image (right panel; courtesy IMO, Reykjavik).

Flight Report: HALO took off from KEF at 1052 UT and reached the cruising altitude of FL270 after 10 minutes. Clouds prevailed in several layers from a few hundred meters all the way up to the final flight level due to the strong occlusion frontal band.

From the last minute preflight satellite images it became clear to the mission scientist that the originally planned first leg would be too far to the W for catching the cold core, which moved faster towards east than originally expected. Therefore he requested to skip the first way point within the bounding box and fly directly from the entry point towards the planned southern turning point at 52N/23W. The pilots accepted this suggestion and adjusted accordingly the first waypoint as well as the box entry point somewhat towards east. Fig. RF14.10 contains the actual flight path and provides an overview of the cloud distribution during the first phase of the flight.

At the transit level the plane was in and out of cirrus clouds until about 1115 UTC. This was about 8 minutes after the westward turn at (the adjusted) waypoint 61N/22W after which the track pointed away from the occlusion front. After leaving the cirrus cloud area on the way towards the entry point 59N/25W, HALO flew mostly above fields of Sc or Cu without much recognizable structure. At 1148 UTC the box entry point was reached and HALO turned directly towards the southern waypoint 52N/23W.

On that track it became very clear that we were flying in some distance to the west of the cold core with the higher rising convection there being visible towards the eastern horizon. Typical photos of the situation on this first leg are given in Fig. RF14.7. Nevertheless, especially the WALES crew was very happy with the good signals in this situation so that no further change of the track was considered in this phase.

Fig. RF14.7: View of cloud fields towards E (left, 1200 UTC, Sc in the forefront and convective boundary of the cold core at the horizon) and W (right, 1157 UTC , Cu and Sc).

The first dropsonde (D1) was released at 1156 UTC at 58N. The second dropsonde (D2) was scheduled for release at 55N (reached at about 1220 UTC). Due to missing GPS signal the data recording was stopped and the release was postponed. Although there was still no GPS signal, D2 was finally released as D3 at 1236 UTC (53:20N/23:20W).

After the left turn at the southernmost point 52N/23W at 1250 UTC it was decided to skip the originally planned dropsonde at 53:30N due to obviously unchanged conditions with fairly flat and weakly expressed boundary layer convection below HALO. Images in Fig. RF14.8 illustrate the subsequent approach of the higher developed convective clouds at the cold core boundary. The images in Fig. RF14.9 show impressions during the crossing of that boundary around 1330 UT with obviously considerably higher cumulus cloud tops than before.

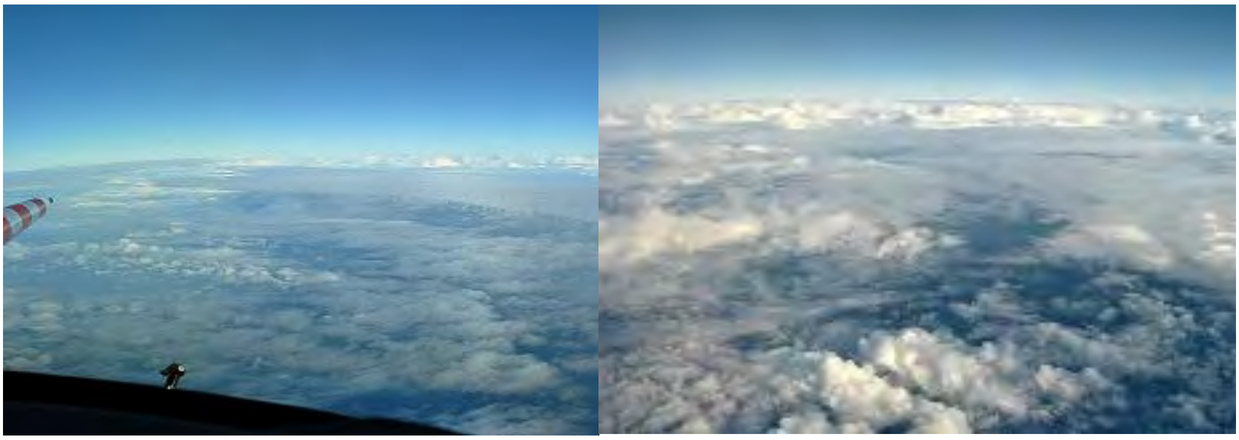

Fig. RF14.8: View of cloud fields in flight direction towards NE while approaching the cold core boundary at 1311UT (left) and at 1317 UT (right).

Fig. RF14.9: View of cloud fields at the cold core boundary towards NW (left, 1331 UT) and NE into the cold core (right, 1334 UT).

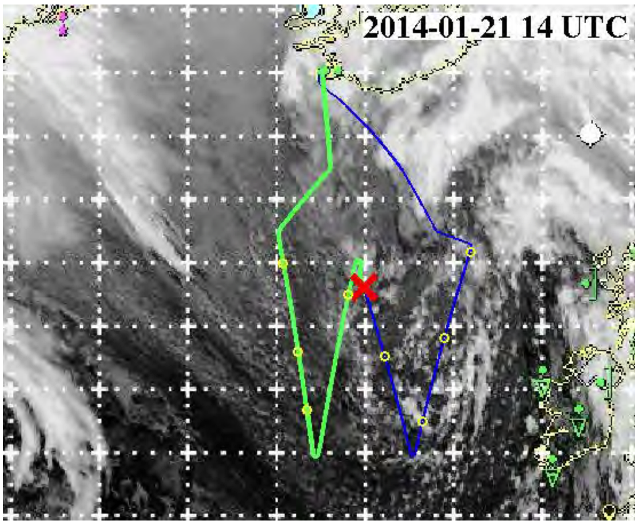

Fig. RF14.10: MSG satellite image at 14 UT with flight track (in blue), dropsondes' locations (yellow circles) and HALO inflight position (red x).

At 1341 UT the dropsonde D4 was released without complications at 57N.

Immediately after crossing the cold core boundary cloud tops were lower again (as seen in Fig. RF14.9). Around the northern turning point (SAT2 at 58N/20:35W, reached at 1351 UT) for the CloudSat underflight leg cloud tops were high and the convective towers were covered by a cirrus layer of variable thickness (Fig. RF14.11, left image). The situation from the satellite perspective is documented in Fig. RF14.10.

Heading towards south, HALO came free of the cirrus layer again and the vertical extension of the underlying convection was generally smaller with a few higher rising CBs (Fig RF14.11, right image).

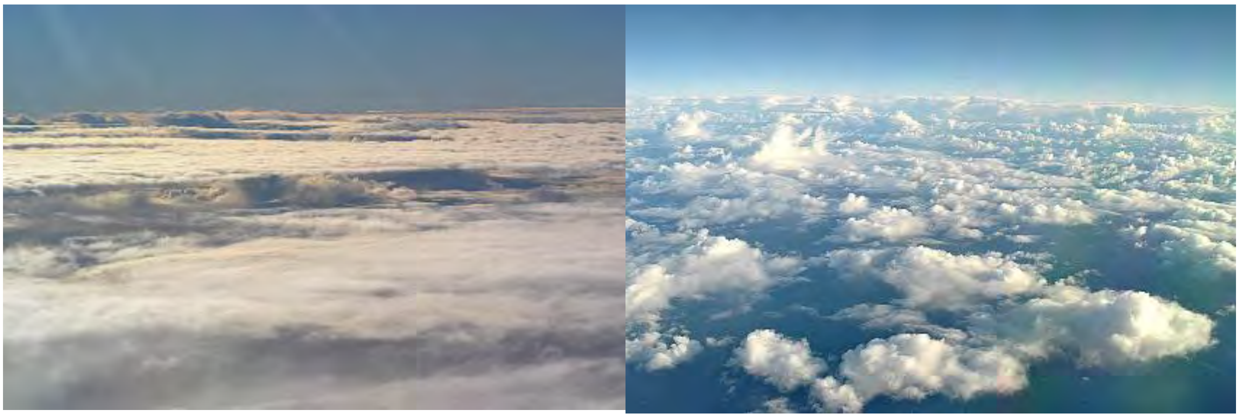

Fig. RF14.11a: View of cloud fields at the turning point SAT2 towards SW (left, 1359 UT) and on the way southward (right, 1409 UT).

At 1418 UT the dropsonde D5 was released at 55N/18W, again without GPS signal.

CloudSat overpass at 1419 UT in poleward direction.

Left turn at southern waypoint SAT1 (52N/17:30W) at 1444 UT in mostly cloudy conditions with several higher developed Cbs (Fig. RF14.12)

Fig. RF14.11b: View of cloud fields at the turning point SAT1 towards NW at 1445 UT.

A science request for some flight plan modifications due to expected higher convection in the NE part of the bounding box resulted in the following changes: Shift of waypoint 57N/15W to 58:30N/14W in order to extend the last science leg, change of planned dropsonde (D5) release location from 53:30N to 53:00N, and insertion of an additional dropsonde at 55:30N.

At 1455 UT the dropsonde D6 was released at 53N in an area with enhanced Cu and occasional Ci at cloud top level.

After a short period of less high reaching cloud tops the convective intensity increased and produced Cu cong with occasional Ci outflow anvils (Fig. RF14.12, 1518 UT).

Fig. RF14.12: Scattered Cu cong with occasional Ci anvils towards NW at 1518 UT.

At 1521 UT dropsonde D7 was released at 55:30N, again without GPS signal.

Partly flying within or not too far above Ci patches. In distance Cu cong visible under a fairly dense cirrus shield (Fig. RF14.13, 1534 UT).

At 1547 UT the last dropsonde (D8) was released at 58N, again without GPS signal.

Fig. RF14.13: Cu cong under fairly dense Ci shield towards NE at 1534 UT.

End of last science leg at 1549 UT followed by left turn towards box exit point. Right turn at exit point (1559 UT, 59N/16:45W) and heading back towards KEF airport. Flight track is initially above and later also within the Ci layer on top of the associated occlusion front. Fig. RF14.14 shows the situation as seen from Meteosat MSG. For some time HALO flew just above and near the western edge of a Ci shield allowing an overview image over a narrow postfrontal clearing, a following Sc deck and some convective towers in the far distance (Fig. RF14.15). HALO landed safely at KEF airport at 1700 UT after a very successful science flight of slightly above 6 hours duration.

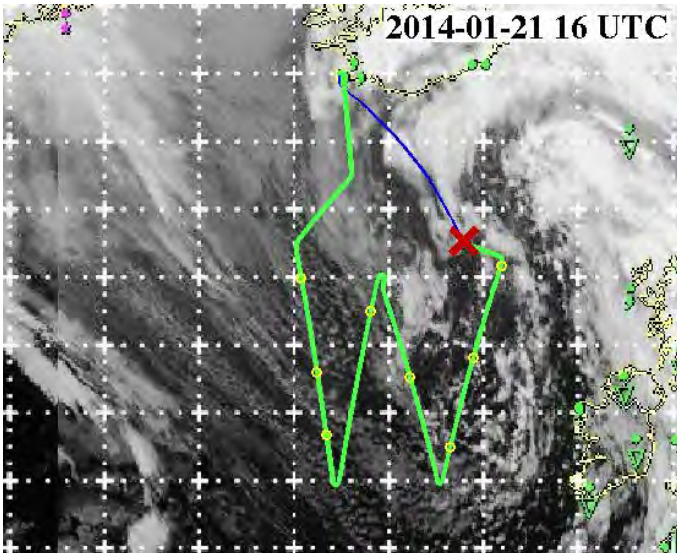

Fig. RF14.14: MSG satellite image at 16 UT with flight track (in blue), dropsondes' locations (yellow circles) and HALO inflight position (red X).

Fig. RF14.15: At 1606 UT HALO flew just above and near the western edge of a Ci shield heading northwest towards KEF airport. Behind the Ci a narrow postfrontal clearing, a following Sc deck and some convective towers in the far distance can be seen.

Flight protocol:
Two test images before take off (7810 at 10:23 and 7817 at 10:41). Camera time in UT
10:48: Weather at BIKF: Overcast with As towards NE+N, cloud-free towards SE+S
10:52 Take off
10:53 Below As/Ac, first photo (7820)
10:54 Above lower cloud level (1/8 Sc)
10:55 Level 905 (?)
10:55 Above cloud base, cloud base fairly diffuse
10:56 In horizontally homog. (?) clouds
10:59 In clouds
11:00 22000ft CT, above us Ci towards W
11:01 24000ft Wales Laser switched on
11:02 FL 270 reached
11:02 Change in flight track requested and decided: Due to eastward motion of target direct course from box entry point to south point 52N/23W
11:06 Flight almost along cloud top
11:07 Change in flight coordinates decided by pilots: Waypoint 61N/2245W > 61N/22W and box entry point 59N/2530W > 59N/25W (and further on to 52N/23W)
11:10 Flight at CT, weak structures towards E
11:14 End of high level clouds to the E, remaining 1-3/8; below that 8/8 Sc/Ac
11:16 Radar is up,
11:16 Photo (7822)
11:18 Above several cloud levels: 3-5 Ci immediately below FL, below that 7-8 Ac/Sc
11:22 Few Ci, low Sc/Ac, more Ci towards W visible
11:23 Photo (7824): Ci over Ac towards E
11:26 Reached 61N/22W, now heading towards 59N/25W
11:27 Mostly free of Ci, lower Ac/Sc. Probably being W of frontal band. Towards W rather As, higher clouds being visible towards S.
11:36 Photos in flight direction right (W, 7826, 7/8 Cu) and left (SE, 7827, Bl Sc)
11:38 We are far to the W of the frontal band in clear air above Bl Cu/Sc without recognizable ordered structure.
11:42 3 Photos towards E showing the distant frontral band Ci and occasional sun reflectance at lower Sc ice cloud particles (7828-7831).

>>> Onboard onscreen photo numbers seem to be smaller than saved DSC-numbers by a value of 6485 - i.e. e.g. Photo #1347 is saved as DSC_7832 <<< (comment inserted on 19 Feb 2014)

11:46 Photo 7832(1347) towards W shows 3/8 Cu, denser Cu (and higher clouds in distance) towards SE (7834) – not interesting but pretty.
11:48 At box entry point at 59N/25W, 9 min to dropsonde release, turn left towards 52N/23W
11:50 Above scattered Bl Cu and in places Sc, high Ci shield towards E, some convective overshooting recognizable towards SE at horizon (7835).
11:56 Dropsonde release at D1 (58N) at reduced speed. Position far outside the target area of today
11:56 Photo 7836(1351) towards E and 7837(1352) towards W show Bl Cu +Sc
11:57 Photos 7838(1353) and 7839(1354, taken with Tele) towards SE show towering Cu at the SE horizon
12:10 Flight goes more or less parallel to Ci and Cb's in the E

12:11 Trying internet access
12:18 Made proposal to shorten leg and turn already at 54N towards next WP(Sat2). Andreas Fix requests full leg for good data quality with WALES. Therefore decided to go on!
12:21 Dropsonde release at D2 (55N) delayed due to missing GPS signal! Neither has Wales, but HALO does have! Dropsonde canclled.
12:24 Flying above BL Cu with Sc patches 4-6/8. Some Cu show icy tops, some of this ice flows out in the stable layer above and shows (gravity) wave structures – Photo 7840(1355, towards SE).
12:34 Dropsonde does not yet work, difficulty with GPS-init, decided to drop anyway
12:36 Dropped as D3 at N53:20, W23:20
12:36 Stronger turbulence felt in the plane
12:38 Above fairly closed Sc while heading towards the southernmost point (52N/23W), higher clouds only visible towards NE (we passed outside the frontal wall and will hopefully enter the target object on the way back to SAT2)
12:44 Photo 7841(1356, towards SE) shows large cloud free patch with considerable amount of braking waves.
12:46 Pilot warning to MiniDOAS for turn at southern point in 3 minutes, Marcel hopes for view into sun!
12:48 Turn left at southernmost point (52N/23W)
12:49 Andreas Fix sees now more than 5 satellites, finally 9
12:51 End of turn, start of new leg heading towards SAT2
12:51 Above compact patches of BL Sc mixed with cloud free areas (Photo 7842/1357, towards N)
12:55 Decided to cancel originally intended dropsonde at N53:30 as it would only give same result as before in Sc condition (save it for later)
13:02 Sc-deck becomes denser and individual cloud turrets become visible in the layer, above these clouds (in the inversion) some ice (?) spreads out, especially towards E. At the eastern horizon Cb towers become visible
13:03 Turbulence sets in
13:06 End of turbulence.
13:10 Stephan Bakan moved up to the Cockpit to take photos of the pilot (7843/1358) and the higher cloudiness ahead (7846, 7847) to the right (E) of the course. We are still not heading into these clouds
13:18 More pictures (7849/1564-51/66) out of the right fore window to the E of our course, showing the increasing cloud heights and CBs in distance
13:22 Irregular Sc, occ. Cu, growing in height to the E of our course, partly topped by thin cloud layer somewhat above CTs.
13:30 Crossing now first patches of towering Cu, some of them with ice caps. (Photos 7852/1367 and 53/68 towards NW)
13:35 … and towards E/NE (7854/1369+55/70)
13:41 Dropsonde at 57N (D4) released
13:42 Reduced convection height again, Cu and capping ice (?) layer, denser towards E. Cb towers visible towards SE. Satellite image (NARVAL-Satpic from Hamburg server) suggests that we entered the (c)older air mass and are now in its interior.
13:46 Capping cloud deck becomes denser and covers mostly the Cu.
13:51 Arrived at SAT2 and turn for heading towards SAT 1, CloudSat underflight
13:52 Turn happened over dense AS cloud deck covering boundary layer convection. Towards NE capped convective area visible without upper cloud deck. Higher clouds visible in the distance towards SE

13:58 Upper cloud deck not as compact towards W, higher clouds visible towards NW (photos 7856-8/1371-3)
14:00 Boundary layer convection visible below cloud deck towards E (photo 7859/1374)
14:03 As over low layer Cu ends and higher developing Cu prevails
14:08 Photo 7861/1376 (towards SE) shows fairly shallow Cu in the forefront and frontal CBs in far distance. Similarly shallow Cu are visible towards NW (photo 7862/1377) and in distance towards W boundary layer Sc.
14:18 Dropsonde D5 released at 55:04N/18:56W, again no GPS signal at release time
14:19 CloudSat underflight (14:18 on board clock)
14:22 Patch of very narrow cloud streets (roughly oriented W-E) below HALO (photo 7863/1378 towards E)
14:24 Towering Cu towards E (photo 7864/1379, zoom detail from scene in image before)
14:32 Similar (7865/1380)
14:42 Science request for course change due to expected higher convection in NE part of bounding box and related dropsonde changes: Shift Point N57/W15 to N58:30/W14, change of dropsonde at N53:30 to N53:00, addition of another dropsonde at N55:30, keep dropsonde at N58
14:44 Turn left at SAT1, cloud-free areas below with breaking waves (photos 7866+7)
14:45 Flat convection with occ. higher Cu development (photos 7869/1384 and 7870/1385 towards W)
14:50 Same in photo 7872/1387
14:55 Dropsonde D6 release at 53N successful
14:57 Somewhat higher development towards E (photos 7874+5)
15:01 Higher towers towards NW (7876/1390) and N (7877/1391)
15:05 and E (7878/1392, similar to tropical towers) and SE (convection capped by cloud cushion, photo 7879)
15:10 Several memorable photos of the airplane science crew (7880-7884)
15:16 Cu with signs of wind shear in upper cloud part (photos 7885/1400+7886/1401)
15:17 Few Cu cong with sign of anvil (photos 7887/1402-7890/1405)
15:21 Dropsonde (D7) released at 5530N, again without GPS signal
15:23 Photos of towering Cu (7891) and capping cirrus layer (7892) towards E
15:29 Upper air turbulence again
15:34 View to the cockpit (photo 7893)
15:36 Higher Cu development visible ahead (photos 7894/1409-7896/1411) under capping Ci at about our FL
15:38 Entering a patch of cirrus
15:43 Above a patch of cirrus, topping further cloud layers and Cbs. Reminds me of tropical situations
15:45 At Ci cloud top again
15:46 Ci layer with some Cb activity below in reddish sunset light (no useful photo)
15:47 Dropsonde (D8) released at 58N, again without GPS signal
15:49 End of leg at 58:30N, turn left, heading for exit point.
15:56 Scattered Cu below HALO, As(?) deck visible in distance towards W (photos 7898 + 7899)
15:58 Dense Ac deck capping lower convective development. Generally very different cloud heights and developments in neighbouring patches (photos 7900+7901)
15:59 Turning right to exit point
16:07 Flight shortly above and at the western boundary of a Ci-field (opaque deck to the E) with interesting filaments in front of As fields below, distant Cbs and contrail streaks (photos 7903+7904)

16:28 Flight back now over fairly overcast Ci deck without much structure, shortly before sunset
16:30 Institute's camera battery low! Remaining photos of cloud impressions during flight back with personal camera (IMG_4658-4669, time difference to UT: 2 h)
17:00 Landing at Keflavik

In air: 6:12 h

Instrument performance:

Bahamas - board data system: Had one longer and some shorter periods of GPS unavailability. Longest was for 20 min during 1st leg shortly before reaching the southernmost point. But also at several other occasions wrong height information was given. This affected all systems that depend on position data from the Bahamas system.

Radar: worked well from successful start-up at 11:16 UTC

Radiometers: showed constantly plausible signals

WALES: worked well from 11:01 UTC, but requires good GPS-information offline

MiniDOAS + HALO SR: Worked great, but require good GPS-information offline

Dropsondes: 7 were dropped, 4 of them without initial GPS signal.

Some lessons learned and related recommendations:

- Info terminal at one or several points in HALO for online scientist information (especially mission scientist) about flight track, height, external conditions as well as the online view of the downward looking camera would be much appreciated.
- Internet connection via satellite should not be possible through individual scientist notebooks. An onboard internet connection notebook (and a data stick for transfer to and/or from individual notebooks) should be available for any necessary data transfer. A mechanism for automatic closing of the connection after some time without activity should be implemented.
- Occasionally missing GPS signal several meteorological measurements, especially several dropsonde profiles.

Preliminary HALO instrument data:

All instruments onboard recorded data without significant gaps. Displayed below are preliminary results with the exception of MiniDOAS. This data will be analyzed after the campaign.

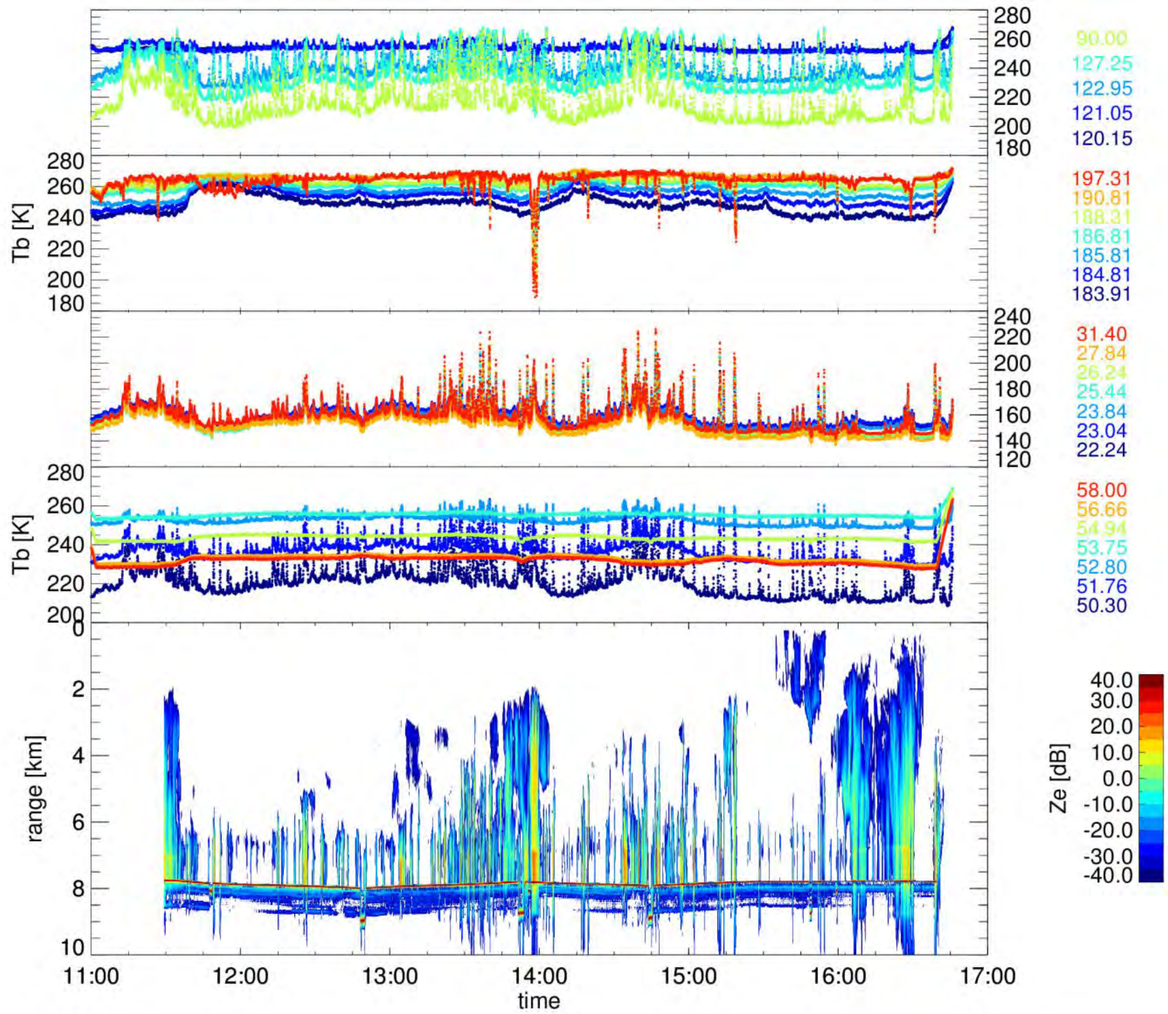

Fig. RF14.16: Radiometer brightness temperatures for the scattering channels (top panel), the sounding channels (second panel), the emission channels (third panel) and the 50 GHz channels (fourth panel). The lower panel shows the corresponding radar time series.

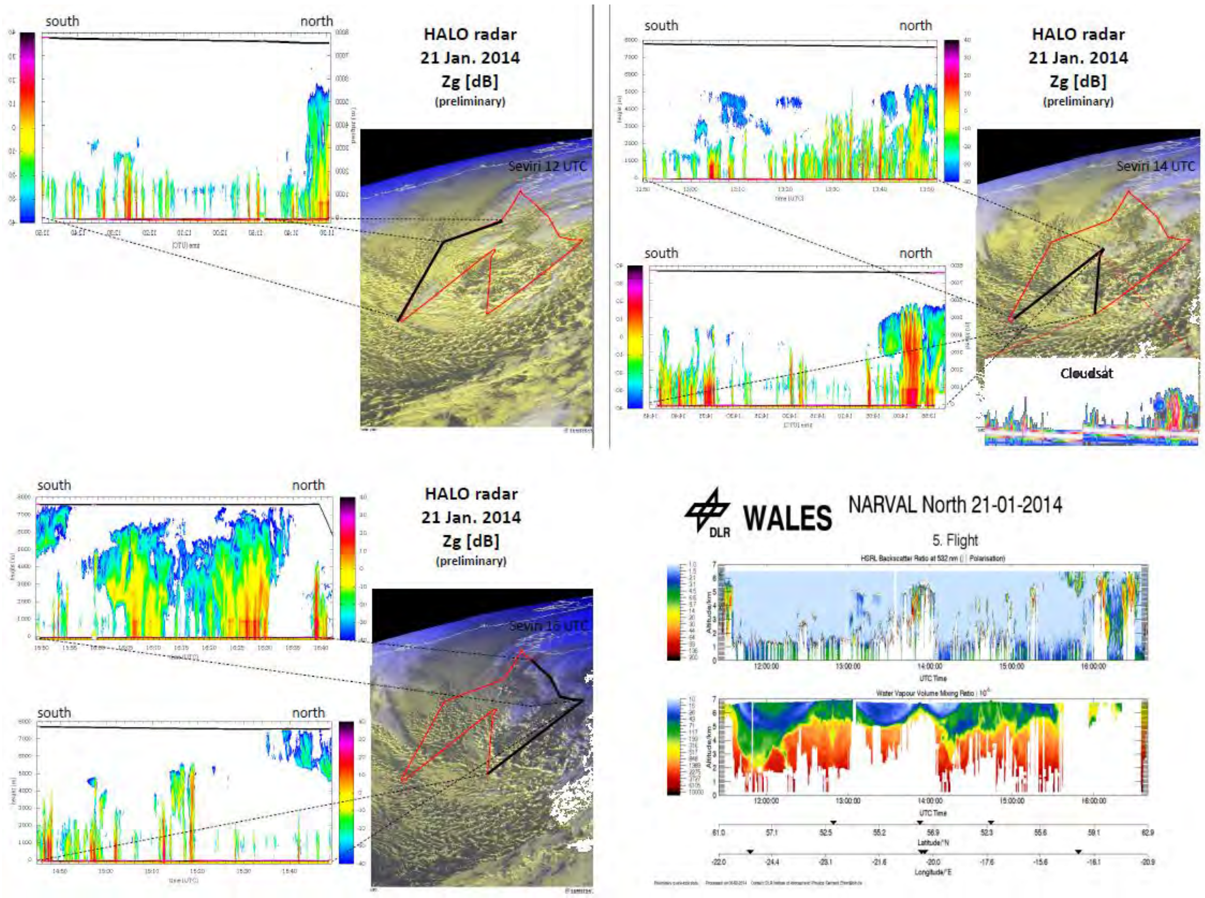

Fig. RF14.17: The two top panels and the lower left panel show selected radar time series sections along the indicated tracks. The lower right panel shows the backscatter ratio (top) and water vapor mixing ration (bottom) of the WALES lidar for the whole time series. In addition, the upper right panel contains below the satellite image the CloudSat cross section along the underflight leg at 14:19 UTC indicating convincing correlation between HALO and satellite radar profiles.

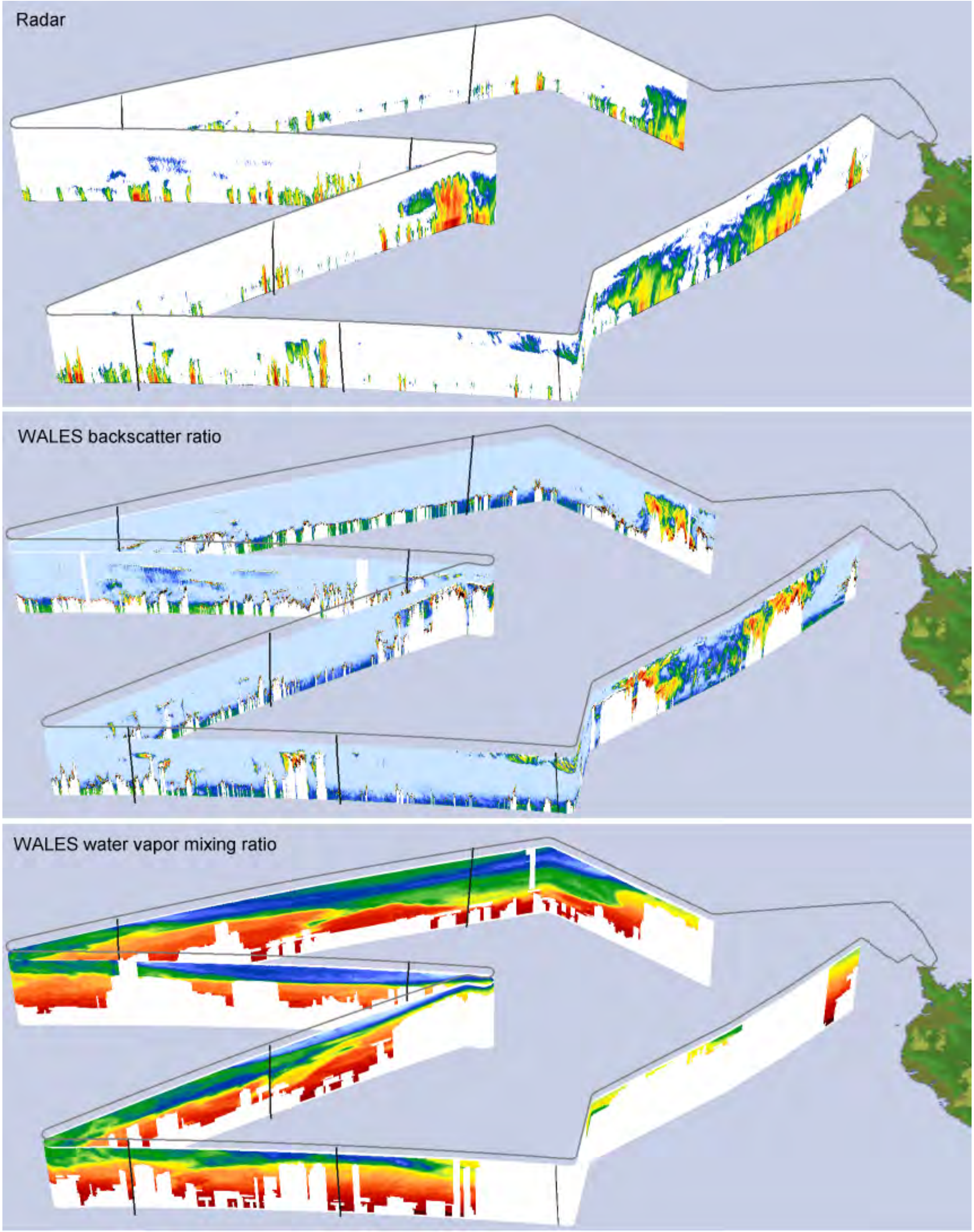

Fig. RF14.18: 3-D visualization of the radar backscattering (top panel), the lidar backscatter ratio (middle panel) and the derived water vapor mixing ration (lower panel) along the entire flight track.

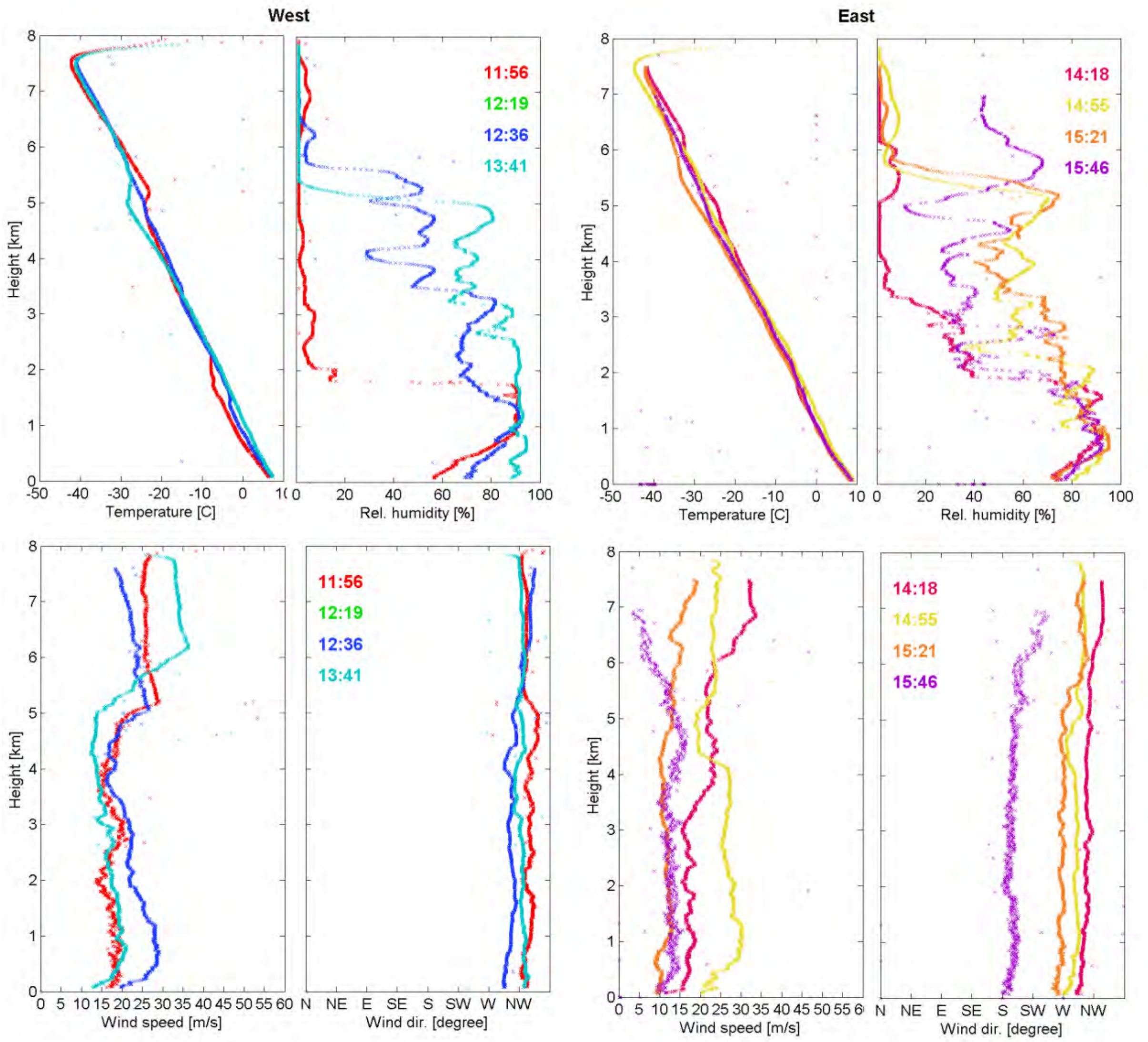

Fig. RF14.19: Quicklook dropsonde profiles of temperature, humidity, wind speed and direction. The planned dropsonde at 12:19 UTC was not released due to missing GPS signal. The data acquisition was therefore stopped and restarted later for the successful profile at 12:36 UTC. Due to repeatedly missing GPS signal upon release, several profiles start well below flight level.

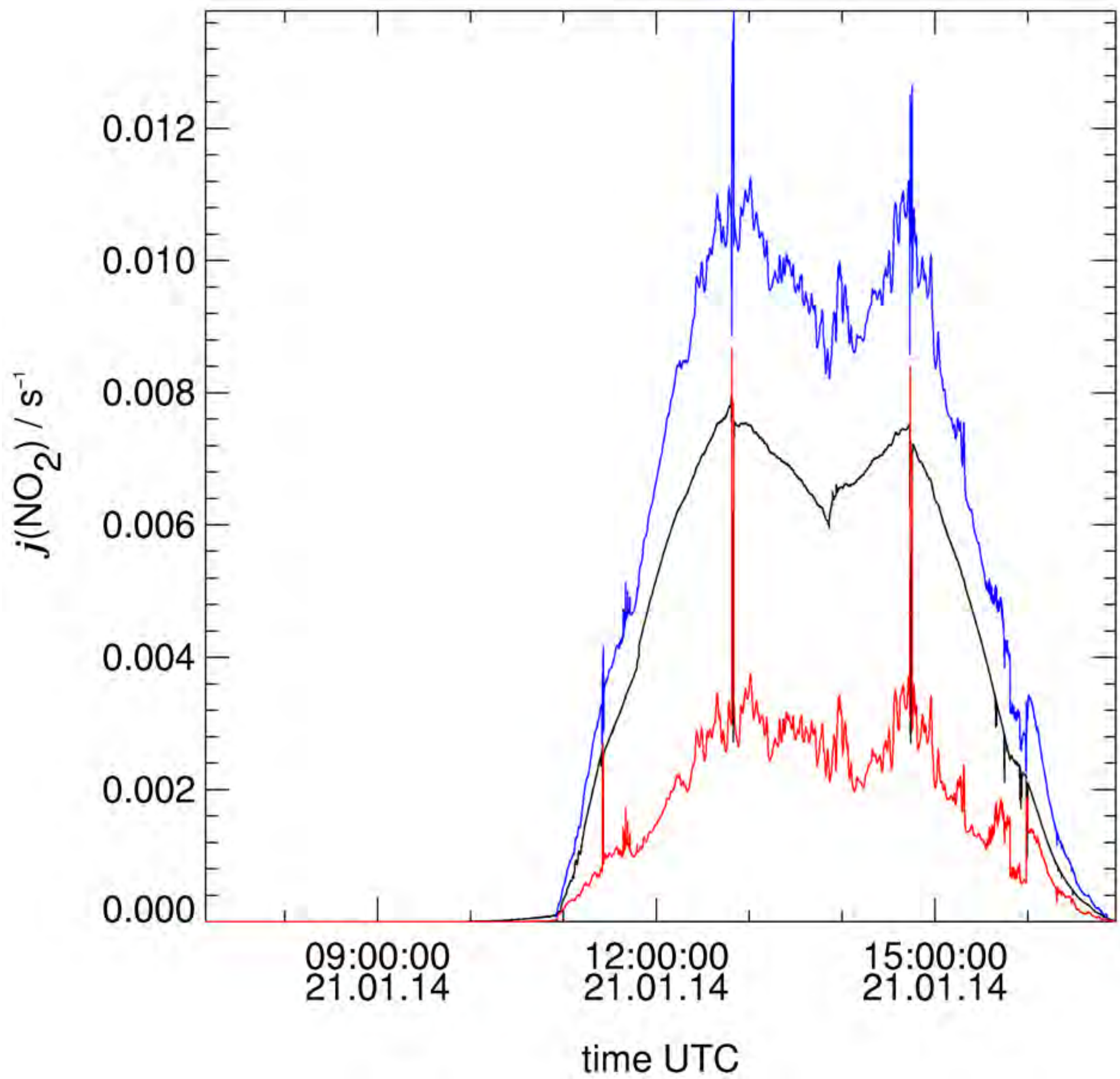

Fig. RF14.20: Photolysis frequency $j(NO_2)$ from lower hemisphere (red), upper hemisphere (black) and combined (blue) measurements. Drop in signal of zenith component between 13 and 14 UTC caused by changes in flight latitude. Strong peaks in nadir component indicate turning points in flight track.

The SSMIS and CloudSat perspective:

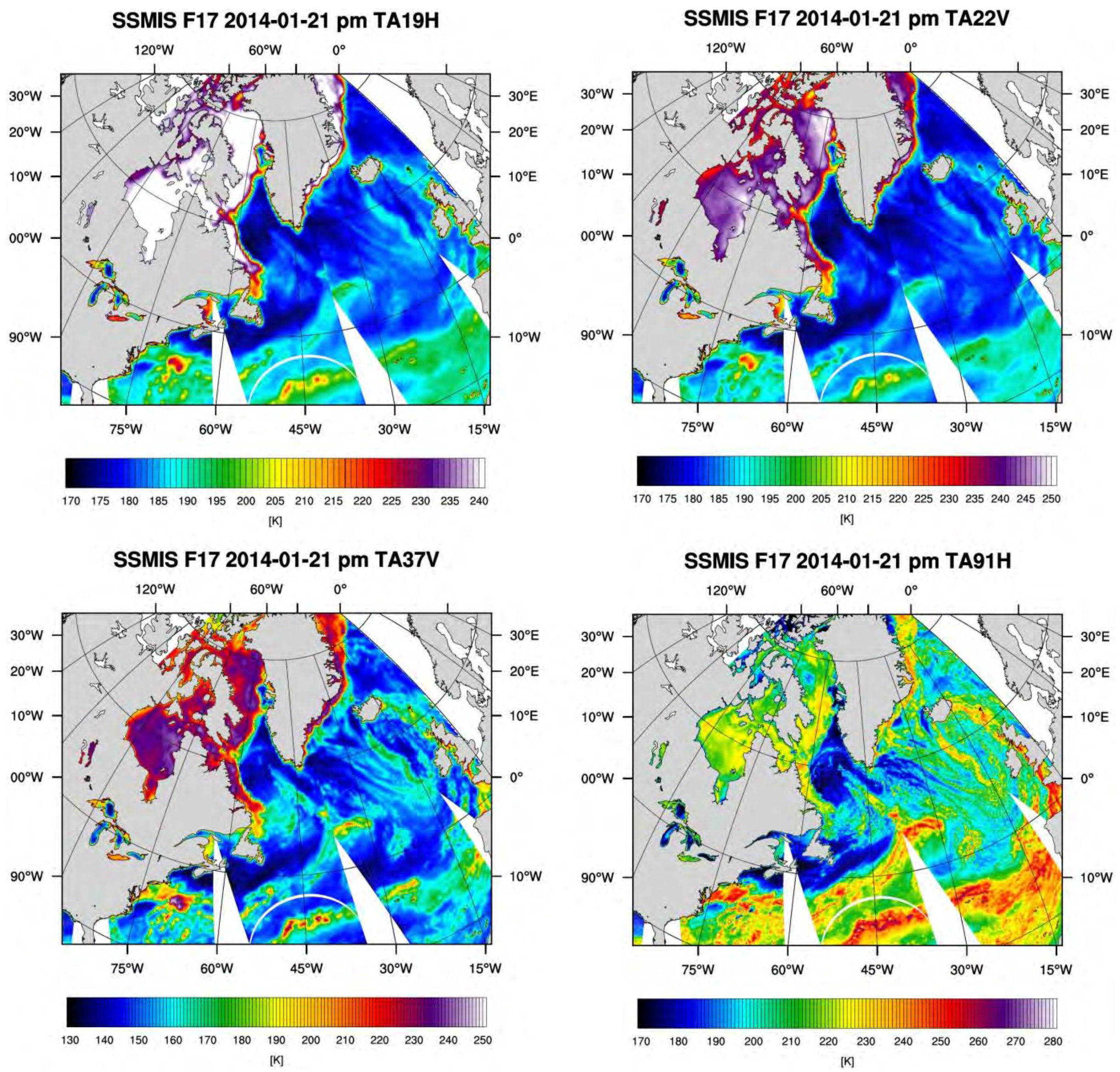

Fig. RF14.21: Preliminary HOAPS 4 fundamental climate data record (FCDR) antenna temperatures (TA) for DMSP-F17 SSMIS target area overpass at 15:35 UT. Shown are the environmental data record (EDR) emission channels 19 GHz H (sensitive to rain; top left), the water vapor channel 22 GHz V (top right), the 37 GHz V (lower left), and the 91 GHz H scattering channel (sensitive to ice; lower right) indicated for horizontal (H) and vertical (V) polarization. The frontal system is located in a band from the UK towards Iceland. The re-intensified cold air convection is well organized and exhibits rainwater content in the 19 GHz emission channel and 22 GHz water vapor channel indicated by the light blue and green colors between 185 and 200 K. The scattering channel shows intense signatures of precipitating ice clouds, with enhanced convective activity and embedded cumulonimbus clouds with values above 220 K. The great detail of the core structure in the antenna temperatures is promising for the forthcoming brightness temperature conversion followed by the precipitation rate retrieval. Note the resolution increase from the 50 km pixel size 19 GHz channel to the 8 km pixel size of the 91 GHz channel. 3 SSMIS overpasses occurred: DMSP-F16 (16:14 UT), DMSP-F17 (15:35 UT), and DMSP-F18 (11:27 UT).

14:14:00	52.0192	17.4820	343.91
14:16:00	59.0639	21.2509	341.57
14:18:00	65.9770	26.6907	337.59

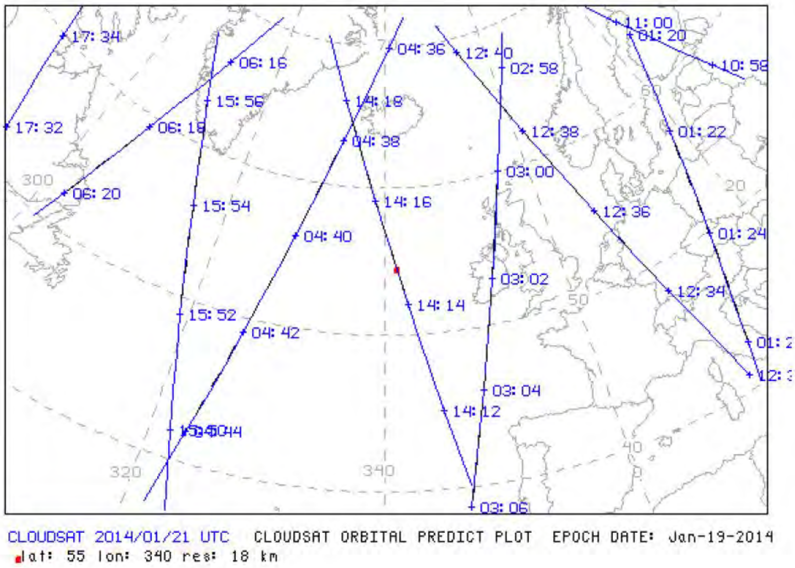

Fig. RF14.22: CloudSat ascending orbit track over the North Atlantic on 21 Jan 2014 between 14:12 UT and 14:18 UT. The collocated HALO underflight was at 14:15 UT in northwestward flight direction of CloudSat and is indicated by the red dot. Coordinates for 14:14 to 14:18 UT are given in the table above the figure.

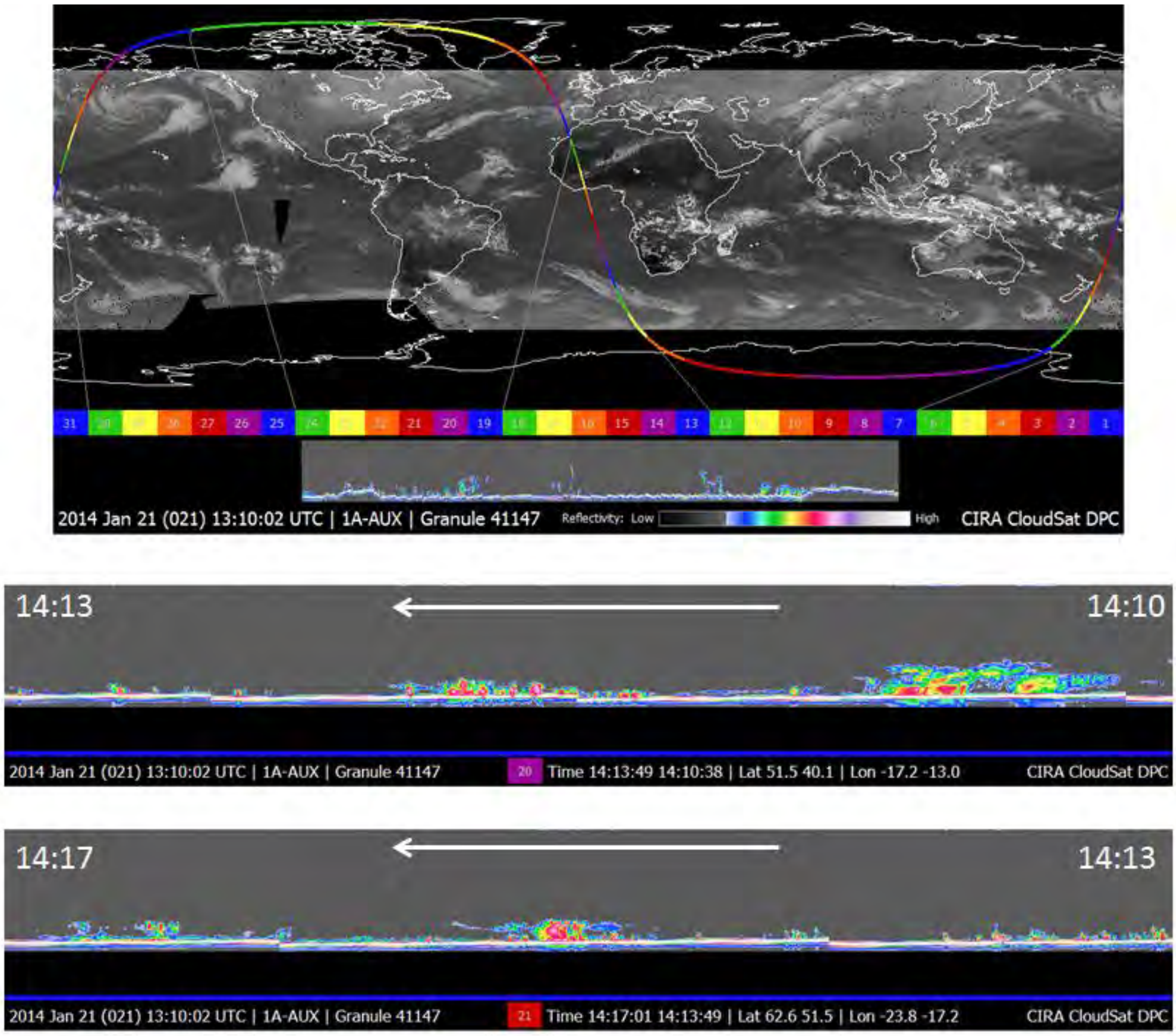

Fig. RF14.23: CloudSat quicklook track granule 41147 section 20 and 21 over the convectively active region between 14:10 UT (violet section 20) and 14:17 UT (red section 21). The collocated HALO underflight was at 14:15 UT in the area of the enhanced convection of section 21. The northwestward flight direction of CloudSat is indicated by the white arrows. CloudSat passed over an area of convective cells.

NARVAL North Transfer Flight 15 (TF15), Flight Report

- 22 January 2014 -

ANDREAS FIX

Objective: Back transfer BIKF-EDMO with overflights over Chilbolton and Jülich supersites

Cockpit Crew: Stefan Grillenbeck (Pilot), Roland Welser (Pilot), Alexander Wolf (Flight Technician)

Scientific Crew: Marcel Reichert (DOAS, HALO-SR), Heike Konow (HAMP) Lutz Hirsch (HAMP), Silke Groß (WALES), Andreas Fix (WALES, PI)

Flight Schedule:

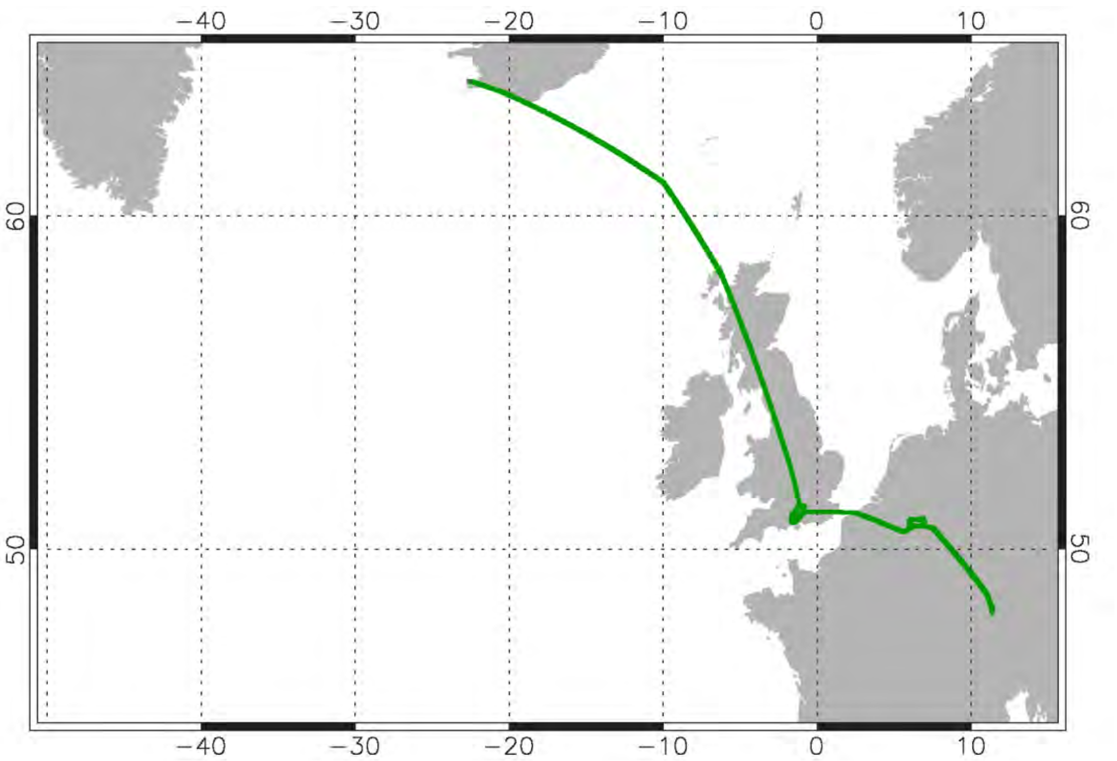

Take Off (under drizzle conditions): 10:02 UT
Cruising level: FL 410
Radar, Lidar on 10:19 UT, 10:30 UT
Over land 11:27 UT
Race track pattern over Chilbolton at FL 41012:22 UT - 12:42 UT
Race track pattern over Jülich at FL 410 13:20 UT - 13:41 UT
Closed cloud deck @ 1.5 km not seen by radar 13:52 UT

Begin of descent 13:57 UT
Landing: 14:25 UT

Instrument Performance:

- DOAS: normal operation
- HALO-SR: normal operation
- HAMP-Radar: operational at 10:15 UT , begin of processing: 10:19UT, radar off at 14:03 UT radar (due to descent below 6km agl)
- WALES: normal operation, data available between ~10:30 UT (system operational and begin of recording) till 13:55UT (switch-off due to descent)
- BAHAMAS: normal operation (no GPS drop-out, no data distortions)

Additional Remarks:

- Photos were taken over Chilbolton and Jülich.
- Only few clouds were present over Chilbolton and no clouds over Jülich
- Between Jülich and Oberpfaffenhofen high-fog like cloud structure at ~1.5km agl, which was almost not seen by radar.

11:57:54 UT: Cloud structure over Britain.

12:40:17 UT: Clouds as seen during the Chilbolton overflight. In the background the Isle of Wright and the English Channel.

14:29:15: Extended low cloud layer over Southern Germany.

13:34:51 UT: In the vicinity of Jülich; Hambach surface mine and power plants Niederaußem, Neurath and Frimmersdorf in the background

Appendix

NARVAL Mission White Paper
Next-generation Aircraft Remote-sensing for VALidation Studies

(Original version from 29.01.2010 without cost estimates)

B. Stevens[1], C. Klepp[2], L. Hirsch[1], G. Peters[2], S. Bakan[1], F. Ament[2], J. Quaas[1]
[1]Max-Planck-Institut für Meteorologie, Hamburg
[2]Meteorologisches Institut, Universität Hamburg

1. Overview

NARVAL proposes to explore the use of HALO as a remote sensing aircraft for retrieving the state of the atmosphere with particular attention placed on moist processes and composition. Our study will use a combination of airborne remote sensing, and in situ measurements to address two main questions:

1. Can HALO be configured as a remote sensing vehicle in a manner that provides new and quantitative insights into the development of moist processes in the atmosphere?

2. To what extent are shallow cloud regimes, both in the trades and in the cold, post-frontal regions of extra-tropical cyclones, precipitating?

The first question is strategic. HALO has unique features which merit the definition of a standard remote sensing configuration of the aircraft. These include its long range, and its ability to fly at high altitude with a substantial payload. By posing this question we hope to show that a standard configuration of HALO, consisting of the Hamburg Microwave Package (HAMP), the DLR lidar systems, the University of Heidelberg DOAS system, and various imagers and base instrumentation, can meaningfully constrain the composition of the underlying atmosphere (or surface). If this could be demonstrated it would open a new dimension in the use of HALO. As HALO constituted as a remote sensing aircraft, with a standard and pre-certified set of sensors, could be rapidly and flexibly deployed from its home base, for one to three day missions. So doing would complement the traditional, field deployment, use of research aircraft and optimize the usage of this unique resource.

The second question is an example of the types of measurements a remote-sensing configuration of HALO could usefully answer. Satellite climatologies and NWP data tend to severely misrepresent the amount of precipitation from shallow cloud systems. This has long been appreciated in studies of fair-weather or trade-wind convection, but recently has also been shown to be the case for post-frontal convection over the North Atlantic. Interest in how the aerosol may modify the propensity of clouds to precipitate, and the resultant effects on cloud cover, continues to grow, and shallow cloud regimes are thought to be those most susceptible to perturbations in the aerosol. Hence we proposed to use HALO to fill gaps in the satellite and surface based remote sensing record related to the formation of precipitation from shallow convection, and its relation to the ambient state (and composition, in terms of the aerosol) of the atmosphere.

To answer these questions we will be conducting a series of missions over the extra-tropical and tropical North Atlantic. During these missions we propose to deploy a full array of remote sensing instrumentation, as well as in situ sensors designed to evaluate the airborne retrievals. Each mission will consist of an outbound and return leg. Extra-tropical flights will be between Oberpfaffenhofen and Goose Bay / Gander, while tropical flights will be between Oberpfaffenhofen and Grantley Adams airport in Barbados (BGI). The tropical (Barbados) missions will also include a short flight in the vicinity of Barbados to calibrate the aircraft measurements against a suite of surface based remote sensors being maintained on an upwind promontory of the Islands.

Within the context of HALO-SPP, and the scheduling delays faced by HALO, other groups are being invited to propose variations on the NARVAL themes to advance their measurement interests. That is we wish to support additional missions that are in the spirit of NARVAL. In practical terms this means that other missions must: (i) be based out of Oberpfaffenhofen, thereby not requiring the transfer of logistical support to remote facilities; (ii) be able to work with the aircraft as configured for NARVAL, where we note that this base configuration is still flexible with respect to the amount and character of in situ instruments it will include. So doing will extend access to HALO to groups who do not currently have missions in the planning phase.

2. Barbados Flights

These missions will enable both in situ sampling and airborne remote sensing designed to relate the point measurements on Barbados to the broader trade-wind region and the developing satellite record. Each mission shall consist of 20-30 hours of flight time distributed over three legs. In the context of NARVAL the in situ sampling will help evaluate the capability of the remote sensing configuration of the aircraft to characterize the state and composition of the atmosphere.

HALO will fly above the north-east trades and measure their evolution with modern remote sensing as they move across the Atlantic Ocean. The flight strategy for each HALO mission is illustrated by Fig. 1. An outbound leg, will begin at the HALO home base in Oberpfaffenhofen, near Munich, and end at the Grantley Adams airport on Barbados. HALO will fly, at cruising altitude, along an air-mass trajectory that intersects an A-Train orbit three days upwind of Barbados. At the point (marked “1” in Fig. 1) where the air-mass, HALO, and the A-Train coincide HALO will descend to the near surface and commence a period of in situ measurements so as to characterize the air-mass, surface fluxes and cloud properties. HALO will then proceed at altitude to Barbados where, before landing, it will again characterize air-mass and cloud properties just upwind of the measurement site. The following day, time permitting, a short (2-3 h) mission will be flown in the air-mass upwind of the Island, as marked by the figure. On the third day HALO will reverse its outbound journey, this time attempting to intercept the originally sampled air-mass, where it again is intercepted by an A-train overpass, as indicated by the point marked “3” on the figure.

  

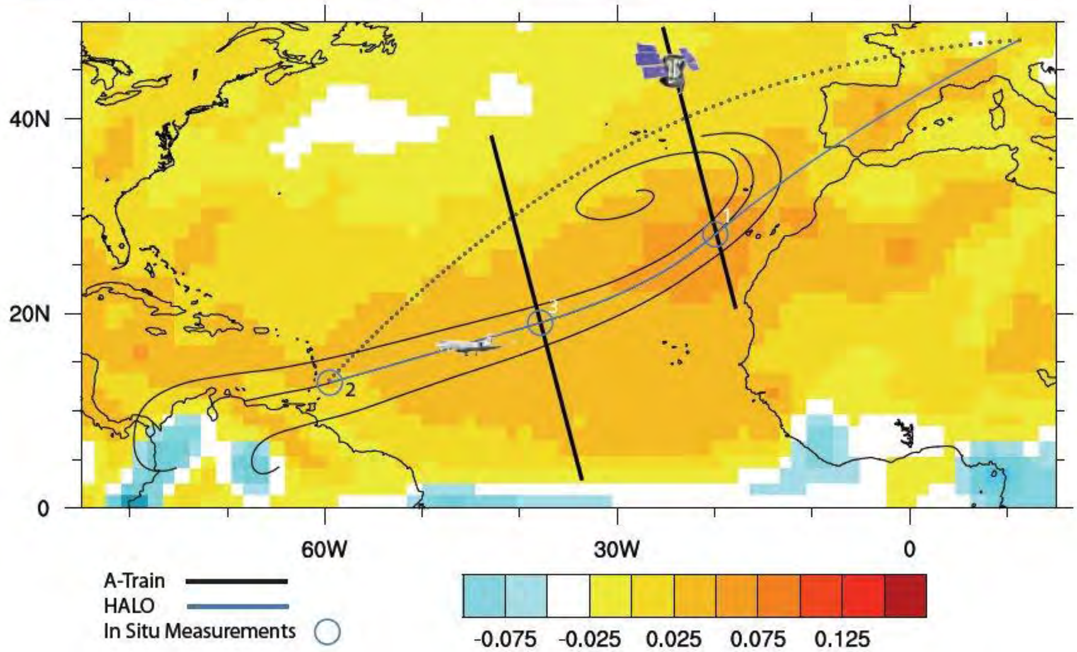

Figure 1: Sketch of proposed flight strategy, showing mean streamlines of the winter trades from ECMWF superimposed on large-scale vertical velocity. A-train orbits are shown by straight solid lines, and the dotted lines indicate a great circle between Oberpfaffenhofen and Barbados. The enumerated circles reflect in situ sampling stations at positions upwind of Barbados.

In addition to the Hamburg Microwave Package (HAMP, which contains many twins of the instruments to be deployed on the Barbados ground site) important instrumentation anticipated for the HALO include: dropsondes; microphysical sensors mounted from PMS canisters on wing-pods; aerosol measurements similar to what is being requested for ACRIDICON; as well as standard instrumentation for measuring basic state parameters, including turbulence measurements with the gust-probe and fast temperature and humidity sensors. The dropsondes will help constrain the utility of the Integrated Profiling Techniques of the Köln group for deriving atmospheric profiles from remotely sensed data only. In addition we also intend to fly the DLR-DIAL system so as to measure the profile of water vapor along the flight path, as measurements are crucial to understanding the behavior of clouds and would further complement those being made at the ground site. The backscatter measurements from the DIAL system may also be used to identify and quantify the structure of possible aerosol layers, for instance associated with the export of dust from Africa.

3. Goose Bay / Gander Flights

These missions will use the remote sensing instrumentation for the validation of convective postfrontal mesoscale precipitation to the west of mature North Atlantic low pressure systems in the outflow region of the Labrador Sea. The NARVAL remote sensing measurements shall not only be supported by the HALO in-situ measurements but through point measurements of

ships using optical disdrometers and drift buoys with rain gauges during the experiment. A corresponding coordination with the community is envisaged.
The position and orientation of the measurement area over the North Atlantic will be determined based on real-time satellite imagery and large scale flow analysis prior to take-off in Oberpfaffenhofen. The proposed flight pattern is to a large extent determined by the remote sensing based mission and will hence measure the cloud area of interest from above. The flights will be performed in two legs with a night stop in Canada (Gander / Goose Bay) or St. John due to the long range distance between the HALO home base and the measurement area off New Foundland.

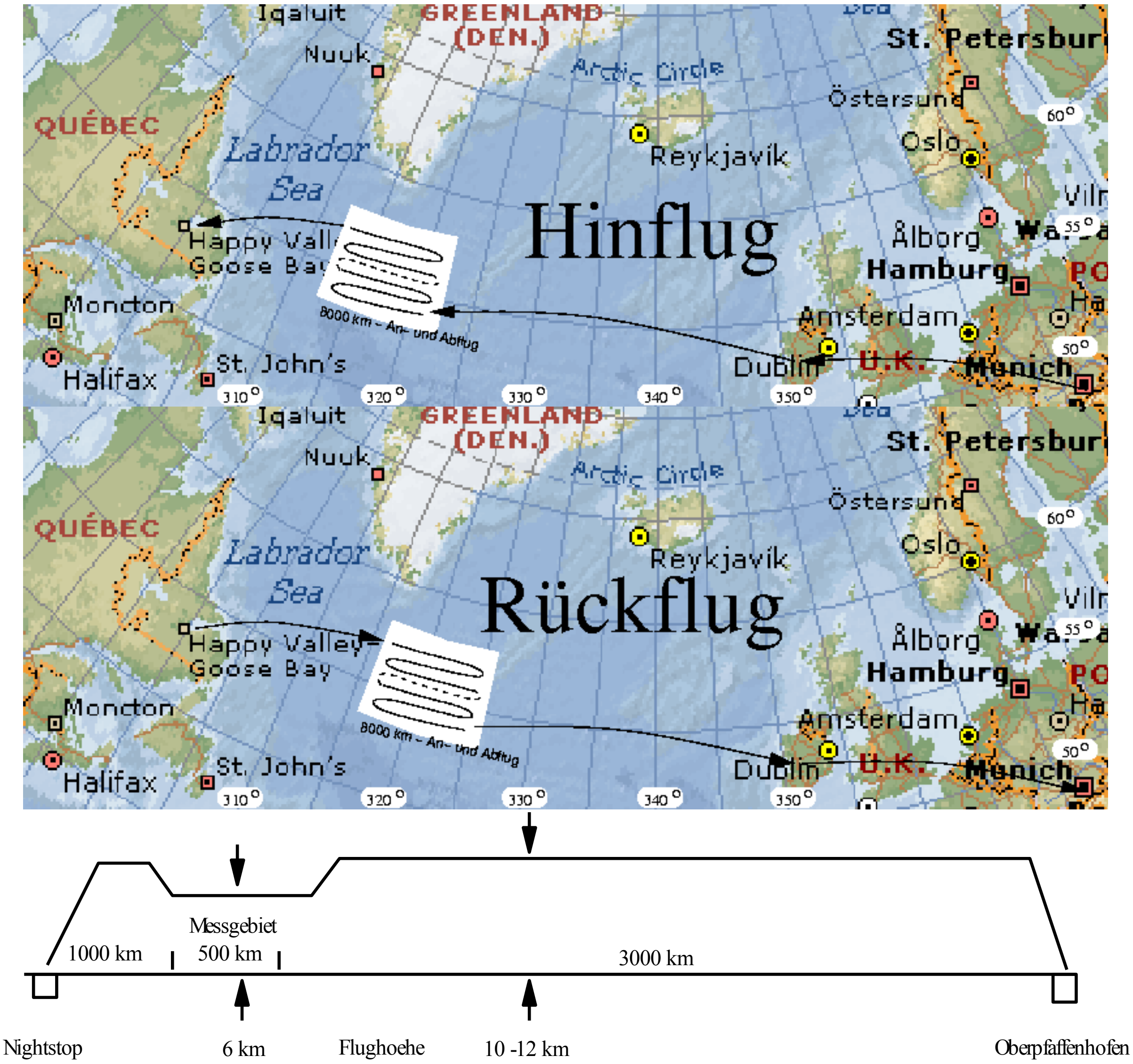

Fig. 2: Top and middle panel: Outward- and return flight along with the flight pattern in the measurement area. Bottom panel: Measurement flight levels for the approach and departure at the measurement area.

The measurement area drifting to the east is shown in Fig. 2 (top and middle panel). The corresponding flight levels are given in the lower panel. The typical cloud top height of polar type cold air outbreak convective clouds are limited to 3 to 5 km. This would allow a flight level of 6 km height. High-level cirrus is usually absent under the weather conditions due to

sinking air masses (dry intrusion). The corresponding mature low pressure system to the east will be crossed at maximum flight level.
The flight pattern resembles a mattress of maximum length in the measurement area and will be flow during both flight legs. The night stop allows flying over the post frontal low (PFL) on successive days and will hence reveal insight in the temporal development of the systems. It would be of interest to cover the development, maturity and decaying stage of such a system.
The HALO home base for the envisaged field campaign will be Oberpfaffenhofen, Germany. A minimum of two outward- and return flights within a temporal window of two months between January and February 2012 is needed to archive the mission goals. Due to the flight time a night stop in Gander / Goose Bay will be necessary. If the large scale meteorological field is prone for the development of successive PFL, an operation out of Gander / Goose Bay would be eligibly as the PFLs could be reached effectively with a minimum reaction time.
The project closely cooperates with the Universität Köln (S. Crewell) and the Max-Planck Institut für Meteorologie (B. Stevens). Cooperation with the cloud radar working group of the DLR (U. Schumann) for incorporation of the DIAL is envisaged.

Instrumentlist for NAR*VAL*

Fuselage

HAMP (MPI-M, Stevens, Hirsch; UniHH, Ament, Klepp)	***liquid water path, temperature + humidity profiles, cloud snow + rain water path, profiles of radar reflectivity, depol. ration + vertical velocity***	2 Rackspaces (RS)	450 kg		Bellypodsection A,C
WALES (DLR, Wirth, Fix, Ehret)	***Water vapor and aerosol profiles***	6 RS	500 kg	2 kW	Bellypodsection B
HALO-SR (FZ-Jülich, Uni Leipzig, Bohn, Wendisch)	***irradiance, radiance, actinic flux densities***	0.5 RS sums up to 1 RS with Snoopy	90 + 18 kg		2 Ports
miniDOAS (Uni Heidelbg. Pfeilsticker)	***H2O (g, l, s), CO2, CH4, NO2, HONO, BROx, ClOx, IOx, HCHO, SO2, O3***	0 RS	47 kg		Boiler room
Dropssondes (DLR, Busen)		0 RS			Baggage Compartment

<u>HASI inlet (2 micron) possibly MAI (10 microns)</u> (20 kg, 2 kW)

CCN (MPCH Mainz, Pöschl)	***activation spectra***	1 RS	80 kg		
C-TOF-AMS / ALABAMA (MPIC Mainz, Schneider**;** Uni Frankfurt, Curtius)	***aerosol mass spectrometer***	1 RS	185 kg		
SNOOPY (DLR, Weinzierl, Minikin)	***black carbon***	0.5 RS	68 + 18 kg		
AMETYST (DLR, Weinzierl, Minikin)	***aerosol micro physics***	1 RS	166 + 35 kg		
Tandem OPC (IfT Leipzig, Hermann)	***hygroscopic growth***	1 RS	50 + 35 kg	450 W	

<u>Wings</u> RS *requirements*

for wings covered AMETYST

UHSAS-A (DLR, Weinzierl, Minikin)	***Aerosol size distribution accumulation mode (0.07-1.0 µm)***		12 + 40 kg		
CAS-Dipol (DLR, Weinzierl, Minikin)	***Aerosol size distribution coarse mode and cloud elements (0.5-50 µm); depolarization***		17 + 40 kg		
CCP (Uni Mainz, Weigel)	***In-situ aerosol & cloud particle SD***		110 kg		
CIP (Uni Mainz, Weigel)	***In-situ aerosol & cloud particle SD***		See CCP		
FSSP(Uni Mainz, Weigel)	***In-situ aerosol & cloud particle SD***		See CCP		
MTP (DLR, Fix)	***Temperature distribution***				
SID3 (Schnaiter, KIT)	***Phase, shape, and size of cloud particles, 1–100 µm***		13 kg		
CAPS (Krämer, FZJ)	***Ice crystal size distribution***		61 kg		

Oportunities

FINCH (Uni Frankfurt, Bundke)	***IN counter***		185 kg		
CVI inlet (IfT, Mertes)			10 kg		
CVI (IfT, Mertes)	**Cloud particle residues: number concentration (CPC), number size distrib. (UHSAS), black carbon (PSAP), condensed water content (Lyman-alpha hygrometer)**	1 RS	140 + 35 kg	1.4 kW	
FSS					

Estimation and distribution of flight hours

For each Barbados mission a number of 25 flight hours is estimated:

  11 hour Oberpfaffenhofen to Barbados
\+ 3 on site flights
\+ 11 hour Barbados to Oberpfaffenhofen

For each Goose Bay /Gander mission 24 flight hours are estimated:

  12 hours Oberpfaffenhofen to Gander
\+ 12 hours Gander to Oberpfaffenhofen

For 2 Barbados missions and 2 Gander Missions this sums up to 98 hours.
2 additional hours are scheduled for test flights, so that a minimum number of 100 flight hours is necessary for the NARVAL campaign.

The MPIHH und UNIHH are contributing 50 hours each to the campaign.
Each other partner is invited to contribute additional flight hours, so that additional Barbados or Gander missions, possibly focusing on special interest of the partners in the frame of NARVAL, can be accomplished.

Mission Description for NARVAL North:

North Atlantic Rainfall Validation

C. Klepp[2], S. Bakan[1], L. Hirsch[1], G. Peters[2]
[1]Max-Planck-Institut für Meteorologie, Hamburg
[2]Meteorologisches Institut, Universität Hamburg

1. Goals

Described is the planned field campaign on validation of convective postfrontal mesoscale precipitation to the west of mature North Atlantic low pressure systems in the outflow region of the Labrador Sea. To achieve these goals, the new research aircraft HALO will be used. The main project along with the flights necessary is already accepted as a DEMO mission for HALO. The envisaged flight schedule is the time frame between January and February 2012. Another flight mission using identical instrumentation using the same time frame until May 2012 is planned to investigate the convective structures in the North Atlantic trades and is described in a second document (Bjorn Stevens, Appendix B).
The main motivation for the proposed mission arises from the obvious deficits of both satellite- and numerical weather prediction data to correctly detect intensive mesoscale precipitation anomalies over the North Atlantic Ocean. This caused forecast errors when the high impact weather associated with these weather phenomena reached the European continent with gale force winds and precipitation with flooding potential. This follows from investigations on the precipitation distribution within the North Atlantic storm track using the satellite climatology HOAPS (Hamburg Ocean Atmosphere Parameters and Fluxes from Satellite data; http://www.hoaps.org; Andersson et al., 2010) within the context of the SFB 512 on "Low pressure systems and the North Atlantic climate system".
During the cold season, intense precipitation in North Atlantic low pressure systems exists not only in the frontal systems, but in particular within the cold air outbreak sector to the west of large cold fronts. Such convective mesoscale postfrontal (PFL) lows develop from enhanced cumulus or tiltback occlusions of the main low pressure system within few hours and frequently cause high impact weather. They are shown to occasionally reach the European continent where they can cause gale force winds with precipitation up to 16 mm/h. This documents the importance to correctly detect these mesoscale PFLs to the west of mature cyclones. While the HOAPS climatology allows detecting all of these systems, the model based detection and forecast remains a challenging issue.
A voluminous data set based on voluntary observing ships (VOS) and research ships during the FASTEX field campaign in January and February 1997 was used to evaluate the precipitation of the HOAPS climatology on a case study basis. This comprised the PFL-rich region of the Labrador Sea outflow where ship observations are usually sparse. The precipitation rate was compared between various internationally accepted satellite algorithms along with model data from a regional model (REMO) and the ECMWF (European Centre for Medium-Range Weather Forecast) and the HOAPS satellite climatology. Results show, that the HOAPS precipitation patterns and intensities agree well to the VOS data, in contrast to all other satellite based precipitation algorithms (Klepp et al., 2003).
In contrast to the PFLs results, the investigated frontal systems precipitation pattern and intensities indicate a good agreement between the ECMWF and REMO model, HOAPS satellite and VOS observation data. The VOS data allows the investigation of the shipboard

measured sea-level pressure (SLP). It is shown, that the observed SLP steeply drops by values up to 16 hPa in the regions of the PFLs that usually cover areas up to 500 km in diameter, compared the surrounding SLP. The cloudiness and cloud structure associated with these mesoscale low pressure anomalies, as observed in satellite images, suggest that some PFLs are characterized by mesoscale vortices. In total more than 750 such events were identified in the HOAPS climatology between 1988 and 2006. The PFL frequency occurrence shows a sharp cold season maximum with up to 13 events per months that usually drop towards zero in the summer months with lifetimes between 12 and 48 hours. The ECMWF model detects about 7% of the systems identified in HOAPS with a longlivety of 10 to 50% compared to HOAPS. Hence, the mesoscale SLP anomalies are not contained in the model. This leads to the conclusion that the missing model precipitation in the PFL area may mainly be a consequence of the missing mesoscale low pressure anomaly (Klepp et al., 2005). The reason why the VOS observation data in the area of the PFLs is excluded from the model analysis could be related to the plausibility control of the model input data that might be too restrictive in these cases.

The proposed demo mission should contribute answering the following scientific questions:

- Estimation of the quantitative precipitation rate and its distribution in different regimes of North Atlantic cyclones.
- Can the postfrontal precipitation rates of the HOAPS climatology be verified using the high resolution of the HAMP and radar data? The HOAPS postfrontal precipitation areas in the cold air to the west of the cold fronts contain a substantial part of the total precipitation within a cyclone.
- Are the HOAPS derived and VOS observed convective PFL precipitation rates mesoscale clusters with numerous single shower cells or more or less homogeneous precipitation events with diameters up to 500 km? This question cannot be answered given the 50 km resolution of the SSM/I pixels used in HOAPS and the point measurements of the ships. The narrow swath of CloudSat reveals insight but cannot deliver the big picture. The HALO collected bellypod data will close this information gap both in space and time. This calls for scale dependent point-to-area validation statistics.
- AVHRR satellite images with a resolution up to 1.1 km resolve structures that may resemble frontal features like 100 km long cold fronts within the PFLs. Detailed HALO measurements are needed here for a better process understanding.
- What needs to be improved in the NWP model processing chain to reduce the described discrepancies between the observation and model data? What needs to be done to successfully forecast such events?
- What causes the development of the PFLs and their high impact weather? Why do some of them reach the European continent resulting in extreme weather events while most of them decay over the open ocean? (Dynamics, Dry Intrusion, etc…)

Andersson, A., C. Klepp, S. Bakan, K. Fennig, J., and J. Schulz, 2010: The Hamburg Ocean Atmosphere Parameters and Fluxes from Satellite Data - HOAPS-3, *Earth Syst. Sci. Data*, **2**, 215-234, doi:10.5194/essd-2-215-2010.

Klepp, C., S. Bakan, and H. Graßl, 2003: Improvements of satellite derived cyclonic rainfall over the North Atlantic. *J. of Climate*, 16, 657-669.

Klepp, C., S. Bakan, and H. Graßl, 2005: Missing North Atlantic Cyclonic Precipitation in the ECMWF Model detected through HOAPS II. *Met. Z., Vol. 14, No. 6, 809-821.*

2. Criteria for HALO demo missions

The project is suitable for a demo mission as it addresses a topic of overarching scientific significance

- the closure of the global water cycle, estimation and impact of cyclonic freshwater flux (up to 1 Sv) on the THC and corresponding impacts on climate modeling and is also of high socio-economic interest
- forecast improvements of extreme weather situations in Europe.

HALO is (among HIAPER) the only available measurement platform to achieve these goals. The large and remote measurement area needs to be reached in time as the lifetime of a PFL is short, too. This can only be achieved using aircrafts although existing research aircrafts usually lack the ability of long range flights.
To our knowledge there is no competitive project – for example on HIAPER, that addresses similar scientific questions.

3. Onboard instruments and staff

Cloud and precipitation data will be measured using active and passive microwave remote sensing equipment. The instruments consist of a 36 GHz cloud radar and passive radiometers working at frequencies of 22-32 GHz, 51-59 GHz, **90** GHz, 119 GHz and 183 GHz. This configuration is referred to as HAMP (HALO Microwave Package) of the MPG and the Universität Hamburg**.** The instrumentation is already completed. Adaptation for the HALO bellypod installation is well advanced, the certification process is progress and testing of the system is almost finished. The radar antenna is mounted outside of the pressurized cabin and is housed inside a bellypod below the fuselage in front of the wing. The construction is made by DLR in close cooperation with the users. The workshop results at IAP at DLR on 3 May 2005 defined the configuration of the bellypod instruments along with future proceedings.

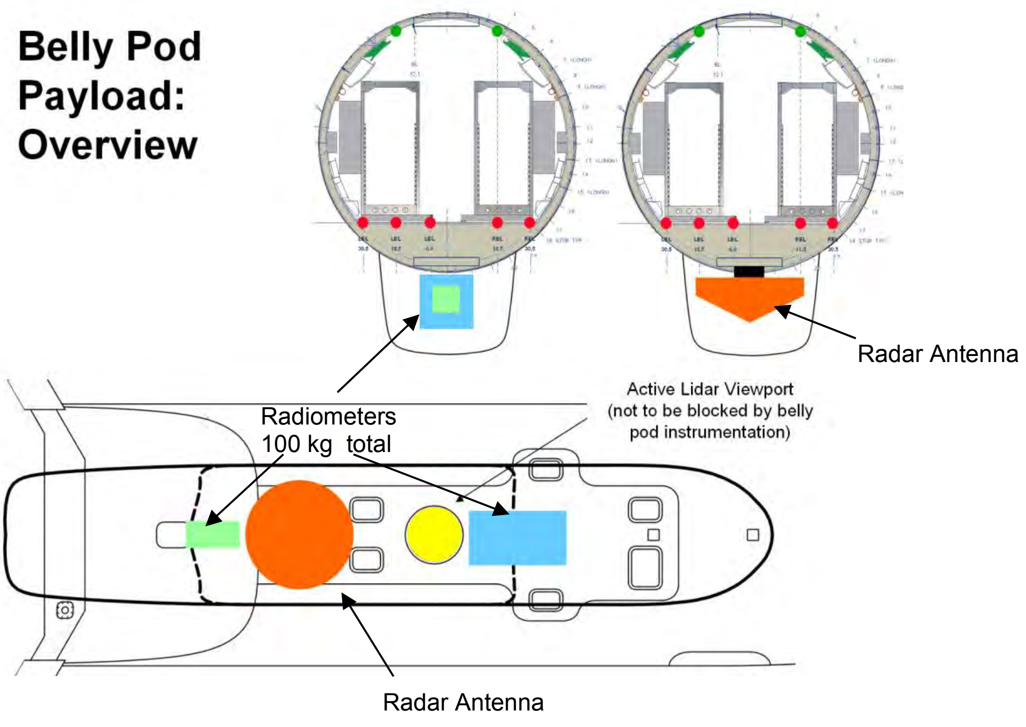

Fig. 1: Cross-section through the fuselage and the bellypod. Left: Radiometer, right: Cloud radar antenna (After A. Giez, cloud radar, workshop 3 May 2005)

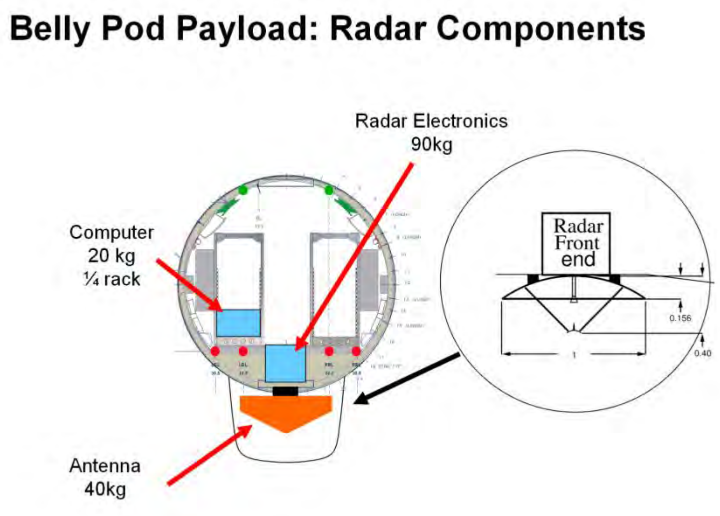

Fig. 2: Cross-section through the fuselage and the bellypod showing the radar antenna and radar electronics.

(After A. Giez, cloud radar workshop 3 May 2005)

Weights:

Radar antenna	40 kg
Radar electronics	90 kg
Radiometer	300 kg (total sum)
Data acquisition	20 kg + ¼ rack

Testing of the interference-free usage of the HAMP instrumentation is in progress at MPI, Hamburg using a trailer installation.

Staff: 2 scientists for the HAMP core program

In the interest of a comprehensive description of the cloud scenario and thermodynamics simultaneous lidar and radiation flux measurements in the visual and near infrared are envisaged. Another useful addition is the usage of drop sondes to validate the remote sensing products. Potential partners bringing such instrumentation into the measurement campaign are welcome to participate.

4. Schedule

Analysis of the HOAPS time series, covering 18 years from 1988 to 2006, reveals that the temporal window, containing the most intense precipitation in the storm track over the North Atlantic, is between December, January and February. The probability for PFL developments is also highest within these three months. Such high impact weather events develop every two to three days given that the large scale flow pattern allows large cyclones to develop and pass over the North Atlantic. In these cases the PFLs develop to the west of the mature cold fronts. The cold air outbreaks, with temperatures as low as –40°C, originate from the Canadian continent. This air mass passes over the Labrador Sea and crosses the region of the warm

Gulfstream waters off the coast of New Foundland. This area is known to have the strongest horizontal SST gradients on Earth. This is the region where most of the PFLs form (320°W and 50°N).

Take-off Criteria:
The flight decision will be made on combined information of NWP forecasts of the large scale flow patterns and real-time satellite imagery (GOES-E, AVHRR and others). First, the analysis of the Rossby wave pattern and its corresponding developing low pressure systems to the east of the U.S. coast need to show favorable conditions. Second, a detailed satellite imagery based cloud analysis on PFL precursor clouds will be carried out. This comprises analysis of enhanced cumulus within the cold air outbreak channels along with observations of possible tiltback occlusion behavior in the wake of the mature cyclone center.

Frequency occurrence:
The HOAPS climatology shows that during DJF PFLs develop every two to three days if mature cyclones traverse the North Atlantic. These estimates are based on a statistical analysis comprising more than 750 North Atlantic PFLs between 1988 and 2006. The early warning time is relatively short as these systems usually develop within 6 to 12 hours. The lifetime varies between 12 and 48 hours.

Mission Description for NARVAL South:

Flights in support of the Aerosols, Clouds, Precipitation and Climate: Barbados Field Study

Bjorn Stevens
Max Planck Institute for Meteorology, Hamburg Germany

December 16, 2009

Figure 1: Shallow precipitating cumulus cloud as observed during the Rain in Cumulus Over the Ocean Field Study (Rauber et al., 2007). Such clouds have come to iconize the role of clouds, precipitation and the aerosol in climate.

Executive Summary

We describe a planned field study of the structure of convection in the winter-trades. In this study we propose to incorporate flights from the new German HALO research aircraft. The requested flights are to be supported out of an allocation made available to the Max Planck Society (and in particular this PI, through the course of his starting negotiations) in the context of the NARVAL mission, and potentially as an addition to the proposed ACRIDICON measurements. The request entails a shift prolongation in the requested window for NARVAL (January to May 2011) as well as additional flights being added to the proposed ACRIDICON project. In the context of NARVAL the missions described herein compose one of two sets of missions to be flown, the other set: "Validation of convective mesoscale precipitation in North Atlantic Cyclones" by Klepp et al. is described in an accompanying document. Proposed flight plans are described, with all flights based out of the DLR facility in Oberpfaffenhofen.

Background

Climate science, particularly climate prediction, has been stymied by difficult and longstanding problems— mostly related to clouds. Long ago Langmuir (1948) recognized that:

> since cumulus clouds often develop rain within less than thirty minutes after their formation, we see that some mechanism other than that assumed in evaporation-condensation theory most be involved in rain formation.

Langmuir's "mechanism" turned out to be collision-coalescence, but a quantitative understanding of the factors that initiate the coalescence process remains elusive. Dating back to the work of Squires (1956) Warner and Twomey (1967) and Twomey and Wojciechowski (1969) the idea that the aerosol may be key has underlain many attempts to understand warm rain formation. Initially such connections motivated research into cloud seeding. More recently the emphasis has been on aerosol effects on climate, as a number of studies continue to suggest that the role of the aerosol in setting the precipitation rate (particularly for shallow clouds) may control cloud radiative properties as well (e.g., Albrecht, 1989; Denman et al., 2007).

If only we understood clouds better—irrespective of the aerosol. Indeed, long after Langmuir, but still more than thirty years ago, (Arakawa, 1975) wrote that

> the modelling of time dependent clouds is perhaps the weakest aspect of the existing general circulation models and may be the most difficult task in constructing any reliable climate model.

It was a prescient comment. Four years later the National Research Council published the report of the Ad Hoc Study Group on Carbon Dioxide and Climate, (otherwise known as the Charney Report Charney et al., 1979) which concluded that we

> cannot predict the location and intensities of regional climate change with confidence [in part because] existing parameterizations of cloud amounts in general circulation models are physically very crude ...[and are] one of the weakest links in the general circulation modeling efforts.

Through to the present day, cloud effects "remain the largest source of uncertainty" in model based estimates of climate sensitivity (IPCC, 2007), with "low clouds making the largest contribution" (Randall et al., 2007, emphasis added).

This confluence of problems: Clouds, the Aerosol, Precipitation and Climate, remain among the most difficult and important problems in the field and motivate, in broad terms, our study.

To elevate the empirical basis for addressing this problem, the Max-Planck-Institute for Meteorology has initiated a project to study the structure of tropical cloud regimes using a combination of long-term active remote sensing, in situ observations, and analysis of satellite observations.

Objective

Our specific focus will center on the question:

> What controls the distribution and structure of trade-wind convection?

The initiative will have both a modeling and an observational component. The observational component is described herein.

The specific point of focus, trade-wind convection, is motivated by a number of studies (e.g., Bony and Dufresne, 2006; Medeiros et al., 2008), which have argued that the divergent changes in cloudiness in the trade-wind regimes is the single largest contributor to divergent cloud-feedbacks in model based estimates of climate sensitivity. Likewise, rain in the trades is not necessary, as the water budget can be balanced simply by enhanced transport of dry-air to the surface. Hence many of the questions as to the possible role of the aerosol in modulating rain and cloud amount are most relevant to trade-wind cloud regimes. Further, a recent intensive period of observations, with extensive in situ and ground- based remote sensing (Rauber et al., 2007) in such a regime, provides a rich framework for longer-term, more statistically oriented, measurements—particularly of (non-precipitating) clouds which were poorly characterized in previous studies.

Experimental Strategy

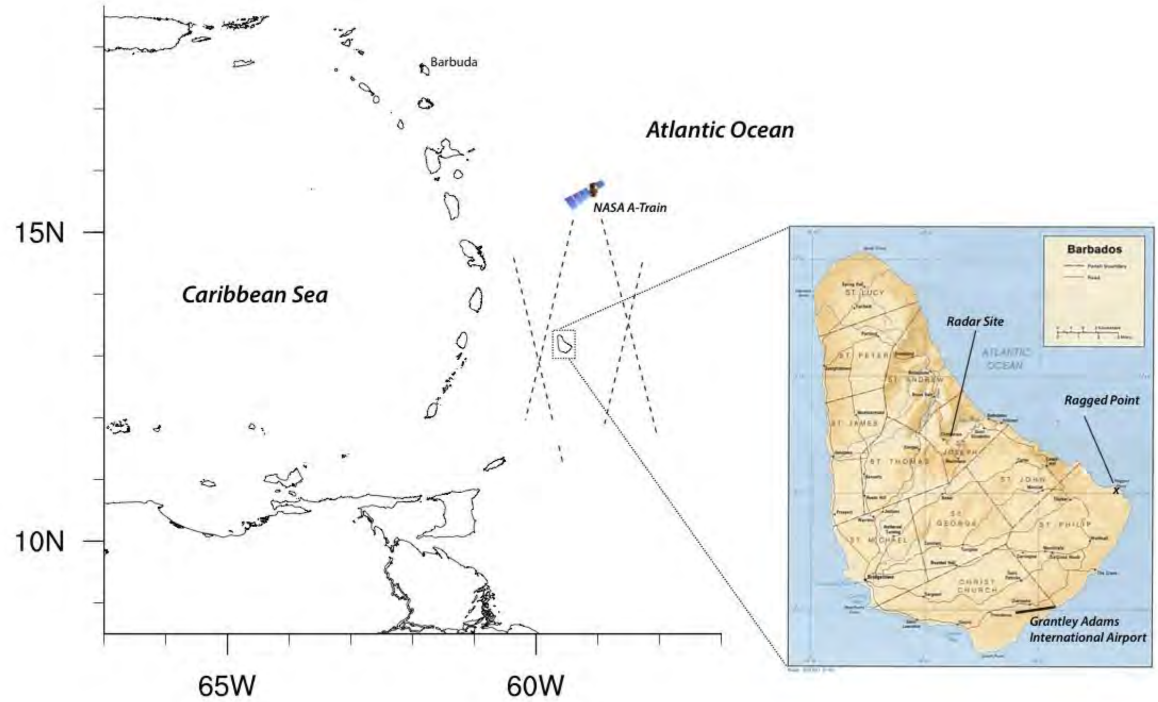

Figure 2: Barbados, including inset map of Island showing airport (which indicates prevailing wind direction) and measurement site at Ragged point. The point marked radar site refers to the location of the CMO precipitation radar. Also indicated is the Island of Barbuda where the radar measurements during the recent RICO field study were made, and approximate location of nearest CALIOP (CALIPSO Lidar) swaths.

Field work will be centered around observations to be collected at Ragged Point on the Island of Barbados. As shown in Fig. 2 the measurement site is ideally suited to sample a variety of cloud regimes, not least the downstream regime of the winter trades. In early 2010 we plan to install:

- A highly sensitive scanning K-band cloud radar
- A DIAL water vapor Lidar
- An advanced multi-channel Raman Lidar.
- A JENOPTIK CHM 15K Ceilometer
- A Micro-rain Radar to measure drop size distribution, liquid water and drop fall speed distributions.
- An all sky imager.
- Time-lapse photography (perhaps stereo).

We anticipate maintaining the instruments on this site for at least two years, thereby spanning two sea- sons. The instrument suite will be complemented by: (i) the University of Miami Aerosol measurement station, which has been operative for more than forty years; (ii) the AGAGE site, which measures 40 trace gases; and (iii) daily soundings and S-Band Caribbean Meteorological Organization radar measurements made continuously. In addition we hope to augment our measurements with the help of a second, portable, cloud radar, and through the participation of other institutes as discussed briefly below.

The long-term measurements will be complemented by in situ sampling through the use of the HALO aircraft, operated by the DLR. It is proposed that in the second year of measurements, two to four missions be flown. Each mission shall consist of 20-30 hours of flight time distributed over three legs. It is proposed that the missions be flown in the context of the NARVAL and ACRIDICON demonstration projects, as a core component of the former and as a supplement to the latter.

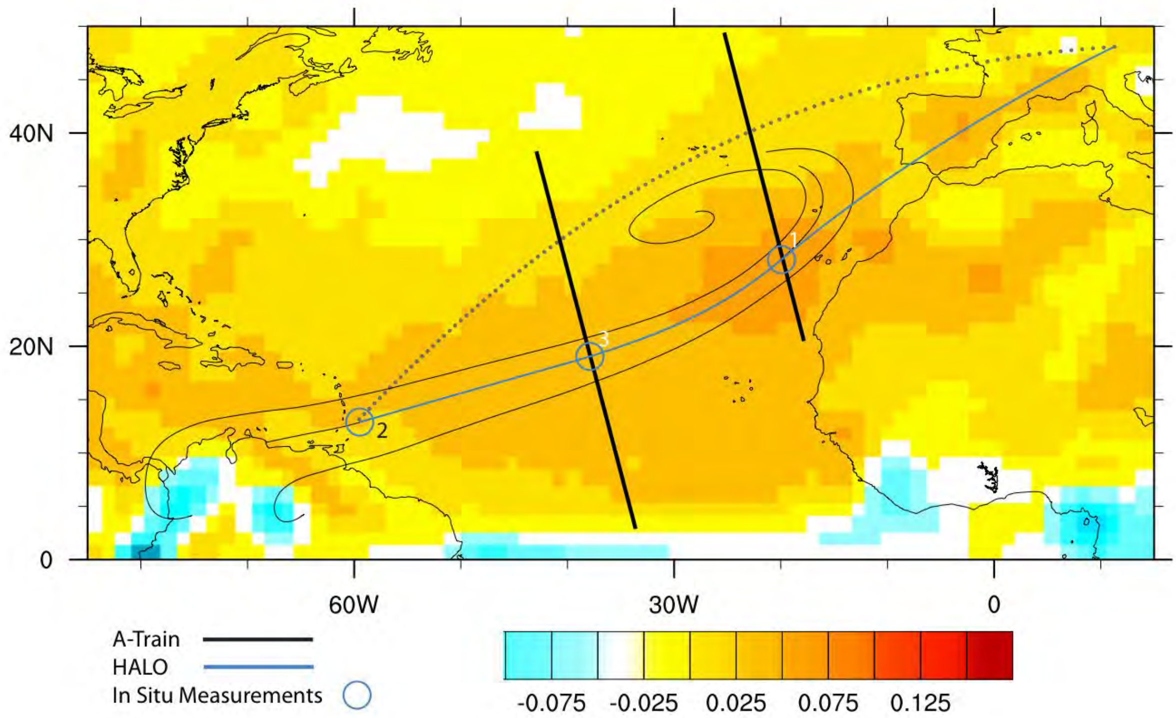

Figure 3: Sketch of proposed flight strategy, showing mean streamlines of the winter trades from ECMWF superimposed on large-scale vertical velocity. A-train orbits are shown by straight solid lines, and the dotted lines indicates a great circle between Oberpfaffenhofen and Barbados. The enumerated circles reflect in situ sampling stations at positions upwind of Barbados.

The flight strategy for each HALO mission is described with the help of Fig. 3. The first, outgoing leg, will be between the HALO home base in Oberpfaffenhofen, near Munich, and Grantley Adams airport on Barbados. Our idea is for HALO to fly, at cruising altitude, along an air mass trajectory that intersects an A-Train orbit three days upwind of Barbados. At the point (marked “1” in Fig. 3) where the air mass, HALO, and the A-Train coincide HALO will descend to the near surface and commence a period of in situ measurements so as to characterize the air mass, surface fluxes and cloud properties. HALO will then proceed at altitude to Barbados where, before landing, it will again characterize air mass and cloud properties just upwind of the measurement site. The following day, time permitting, a short (2-3 hr) mission will be flown in the air mass upwind of the Island, as marked by the figure. On the third day HALO will reverse its outbound journey, this time attempting to intercept

the original air mass where it again is intercepted by an A-train overpass, as indicated on the figure.
Additional instrumentation, other than HAMP as was originally requested for NARVAL, include: dropsondes, if the dropsonde facility is available; microphysical sensors mounted from PMS canisters on wing pods; (iii) aerosol measurements similar to what is being requested for ACRIDCRON; and (iv) and basic state parameters, including turbulence measurements with the gust-probe and fast temperature and humidity sensors. In addition if it is possible to also fly the DLR-DIAL system during this flights such measurements would greatly complement those we already are planning to make.
Ideally HALO would be flown during the period of active winter trades, which are best sampled in the time-frame between January and May 2011. This entails a slight change in the requested NARVAL time-slot, with a preferred period some months later than what is currently planned. To the extent the originally planned NARVAL missions are still flown such a delay would not interfere with the originally planned NARVAL flights, as both types of missions favor winter conditions over the North Atlantic.

Flight Planning and Coordination

During the first year of remote sensing measurements, in 2010, we will work through the flight planning and coordination to estimate how reasonably we can predict the position of upstream air-masses three days ahead of time, and how well this positioning can be coordinated with A-Train overpasses. That is the 2010 period provides an opportunity for a year of virtual flight planning. In addition to the PI's interest in the project, one full-time scientist and a scientific support person will be devoted full time to project planning, preparation and subsequent data analysis and integration. Current planning for the project with the MPI-M is being coordinated by Dr. Lutz Hirsch, and a PhD student has recently been invited to join the project in the context of the International Max Planck Research School. More students and post-doctoral researchers can be anticipated to join the project as it develops and grows.

Synergy with ACRIDICON

To the extent to which instrumentation from other missions (primarily ACRIDICON) might usefully fly as part of the NARVAL missions, and the other way around, some degree of coordination may be beneficial. In addition to the possibility of adding NARVAL flights to the ACRIDICON mission, it may well be possible to accommodate objectives from each of these missions within the other. Toward this end we have begun initial discussions with the group at Mainz and others involved in the ACRIDICON project.

External Partners

In addition to collaborations with the measurements groups at the University of Miami and the Caribbean Institute for Meteorology and Hydrology, we look to partner with a variety of national institutions. In particular we have been in close contact with investigators the Leipzig Institute for Tropospheric Research (Stratmann, Siebert), Karlsruhe Institute for Technology (Beheng), the University of Köln (Crewell), the Max Planck Institute for Chemistry in Mainz (Andrea, Pöschl), and at the Universities in Hamburg (Peters), Mainz and eventually Leipzig (Wendisch). We are hoping to have support for in situ analysis and measurements by collaborators in Leipzig and Mainz. The Karlsruhe group has tentatively made their state of the art cloud radar available for this study, which may make it possible to have two cloud radars for part of the observational period. Last, but certainly not least, the cloud-radar facility is partly established through the cooperation with DLR (U. Schumann) whose DIAL facility would also naturally complement the objectives of this project.

References

Albrecht, B. A., 1989: Aerosols, cloud microphysics and fractional cloudiness. Science, 245, 1227–1230.

Arakawa, A., 1975: Modelling clouds and cloud processes for use in climate models. in GARP, number 16 in series, pp. 100–120. WMO, Geneva, Switzerland.

Bony, S. and J.-L. Dufresne, 2006: Marine boundary layer clouds at the heart of tropical cloud feedback uncertainties in climate models. Geophy. Res. Let., 32, L20806.

Charney, J., A. Arakawa, D. Baker, B.Bolin, R. Dickinson, R. Goody, C. E. Leith, H. Stommel and C. Wunch, 1979: Carbon dioxide and climate: A scientific assessment. Technical report, National Research Council, Washington, DC.

Denman, K. L., G. Brasseur, A. Chidthaisong, P. Ciais, P. M. Cox, R. E. Dickinson, D. Hauglustaine, C. Heinze, E. Holland, D. Jacob, U. Lohmann, S. Ramachandran, P. da Silva Dias, S. C. Wofsy and X.Zhang, 2007: Couplings between changes in the climate system and biogeochemistry. in S. Solomon, D. Qin, M. Manning, Z. Chen, M. Marquis, K. B. Averyt, M. Tignor and H. Miller, editors, Climate Change 2007: The physical sicence basis. Contributsion of Working Group I to the Fourth Assessment Report of the Intergovernmental Panel on Climate Change. Cambridge University Press, Cambridge, United Kingdom and New York, NY, USA.

IPCC, 2007: Summary for policymakers. in S. Solomon, D. Qin, M. Manning, Z. Chen, M. Marquis, K. B. Averyt, M. Tignor and H. Miller, editors, Climate Change 2007: The physical sicence basis. Contributsion of Working Group I to the Fourth Assessment Report of the Intergovernmental Panel on Climate Change. Cambridge University Press, Cambridge, United Kingdom and New York, NY, USA.

Langmuir, I., 1948: Production of rain by a chain reaction in cumulus clouds at temperatures above freezing. J. Meteor., 5(5), 175–192.

Medeiros, B., B. Stevens, I. Held, M. Zhao, D. Williamson, J. Olson and C. S. Bretherton, 2008: Aqua- planets, climate sensitivity, and cloud feedbacks. J. Climate, 21, 4974–4991.

Randall, D., R. Wood, S. Bony, R. Colman, T. Fichefet, J. Fyfe, V. Kattsov, A. Pitman, J. Shukla, J. Srini- vasan, R. Stouffer, A. Sumi and K. Taylor, 2007: Climate models and their evaluation. in S. Solomon, D. Qin, M. Manning, Z. Chen, M. Marquis, K. B. Averyt, M. Tignor and H. Miller, editors, Climate Change 2007: The physical sicence basis. Contributsion of Working Group I to the Fourth Assess- ment Report of the

Intergovernmental Panel on Climate Change, pp. 589–662. Cambridge University Press, Cambridge, United Kingdom and New York, NY USA.

Rauber, R., B. Stevens, H. T. O. III, C. Knight, B. A. Albrecht, A. Blyth, C. Fairall, J. B. Jensen, S. G. Lasher-Trapp, O. L. Mayol-Bracero, G. Vali, J. R. Anderson, B. A. Baker, A. R. Bandy, F. Burnet, J.-L. Brenguier, W. A. Brewer, P. R. A. Brown, P. Chuang, W. R. Cotton, L. D. Girolamo, B. Geerts, H. Gerber, S. Go˙ke, L. Gomes, B. G. Heikes, J. G. Hudson, P. Kollias, R. P. Lawson, S. K. Krueger, D. H. Lenschow, L. Nuijens, D. W. O'Sullivan, R. A. Rilling, D. C. Rogers, A. P. Siebesma, E. Snod- grass, J. L. Stith, D. Thornton, S. Tucker, C. H. Twohy and P. Zuidema, 2007: Rain in (shallow) cumulus over the ocean–the RICO campaign. Bull. Amer. Meteor. Soc., 88, 1912–1928.

Squires, P., 1956: The microstructure of cumuli in maritime and continental air. Tellus, 8, 443–444. Twomey, S. and T. A. Wojciechowski, 1969: Observations of the geographical variation of cloud nuclei. J. Atmos. Sci., 26, 684–688.

Warner, J. and S. Twomey, 1967: The production of cloud nuclei by cane fires and the effect on cloud droplet concentrations. J. Atmos. Sci., 24, 704–706.